

Imperial College
London

**Exploration of neuronal ensembles
responsible for sleep and body
temperature regulation**

Ying Ma

Supervised by *Prof.* William Wisden
and *Prof.* Nicholas Franks

Imperial College London
Department of Life Sciences

September 2019

A thesis submitted for the degree of Doctor of Philosophy

Declaration of Originality

I hereby declare that all work presented in this thesis is my own. The data included in were collected during my PhD study, under the supervision of Prof. William Wisden and Prof. Nicholas Franks. Any work presented from published literature is fully referenced and any collaborated work is properly acknowledged. Figures that rely on published sources are attributed in the Figure legends.

Copyright Declaration

The copyright of this thesis rests with the author and is made available under a Creative Commons Attribution Non-Commercial No Derivatives licence. Researchers are free to copy, distribute or transmit the thesis on the condition that they attribute it, that they do not use it for commercial purposes and that they do not alter, transform or build upon it. For any reuse or redistribution, researchers must make clear to others the licence terms of this work.

Acknowledgements

This thesis becomes a reality with the great help and support from many individuals. Here, I would like to extend my sincere thanks to all of them.

Foremost, I would like to thank Professors Bill Wisden and Nick Franks for having me as a PhD student in their group, giving me the most unforgettable four years of study. My interest towards neuroscience first developed when I was doing my last Master rotation in their lab. During my PhD study, they provided years of supervision, guidance, and brilliant insights into my research and writing. The same thanks go to Dr. Xiao Yu, who introduced me into the field of neuroscience at the first place. His expertise and constant support for my experiments would be a key to the success of this thesis.

I would also like to express my special gratitude and thanks to all the members in our group, especially for Dr. Edward Harding, Dr. Wei Ba, Mr. David Miao and Ms. Raquel Yustos. Not only did they help me through my academic difficulties, but also brought plenty of joy and laugh to my life. They treated me as family and the warmth and encouragement from them made London my second home. Without them in my PhD study, my life would be less colourful.

None of this would be possible without the funding of Imperial College London and the China Scholarship Council. The scholarship they kindly provided gave me the opportunity to pursue my scientific career in such an extraordinary establishment.

最后，我想对我的父母及男友表达我最真挚的感谢。谢谢你们陪伴与照顾。尤其是在博士期间的最后一年，你们给予我的鼓励与包容是我可以顺利完成学业的关键。我所有的成长与取得的成绩都少不了你们对我的关心和帮助。感谢你们出现在我生命中！

Thesis Abstract

Sleep is a behaviour we experience every day but the fundamental function(s) and the neuronal circuitry underlying it remain mystery. Previous study from our laboratory suggests the lateral preoptic (LPO) area of the hypothalamus plays an important role in recovery sleep (RS) after sleep deprivation (SD) as well as α 2-adrenergic agonist (dexmedetomidine)-induced sedation and hypothermia.

Preliminary data of whole-brain mapping of the neuronal activity of 5-hr SD mice and 2-hr RS (followed 5-hr SD) mice by cFos expression confirmed that the LPO shows higher neuronal activity in RS mice compared to SD mice. Cell-type specific ablation of galaninergic neurons in the LPO abolished sleep homeostasis in mice, in terms of the amount of RS as well as the increased slow wave activity (SWA) of RS after SD which is a hallmark of sleep homeostasis. In addition, mice with ablation of LPO^{Gal} neurons have a permanent elevation in their body temperature compared to control mice. LPO^{Gal} neurons are also involved in mediating dexmedetomidine (DEX)-induced sedation and hypothermia. Mice without LPO^{Gal} neurons have reduced effects: administration of DEX cannot induce high-power δ oscillations or sustained hypothermia. Together, LPO^{Gal} neurons unite sleep homeostasis and α 2-adrenergic sedation.

Preliminary whole-brain cFos mapping also revealed a few other potential brain regions that might be involved in sleep/wake regulation, including the ventral tegmental area (VTA). Chemogenetic activation and inactivation increase the neuronal activity of VTA^{Vglut2} and VTA^{Vgat} neurons, respectively, and both increase wakefulness. VTA^{Vglut2/Nos1} neurons promote wakefulness by sending excitatory projections to both the lateral hypothalamus (LH) and nucleus accumbens (NAc), whereas the wake-inhibiting effect of VTA^{Vgat} neurons is achieved by sending inhibitory projections to local VTA^{Vglut2} and VTA^{DA} neurons as well as to the orexin neurons in the LH, implying the significance of the VTA in sleep/wake regulation.

Table of Contents

Declaration of Originality	2
Copyright Declaration	2
Acknowledgements	3
Thesis Abstract	4
List of Figures.....	8
List of Abbreviations	10
Chapter 1.....	13
<i>The urge to sleep.....</i>	13
An evolutionary and historical view	13
The neurotransmitters and neural circuits involving in sleep/wake regulation	20
Regulation of arousal systems	20
Regulation of NREM sleep	26
Regulation of REM sleep	32
The switch of wakefulness and sleep transitions	37
The homeostatic regulation.....	37
The circadian regulation	40
The crosstalk between homeostatic and circadian regulations	41
<i>The need to keep warm.....</i>	43
Thermoregulation by the central nervous system	43
Sleep with thermoregulation.....	46
<i>Does sedation share a common circuitry with sleep?.....</i>	49
Chapter 2.....	53
<i>Galaninergic neurons in the lateral preoptic area (LPO) contribute to sleep homeostasis and body temperature regulation in mice</i>	53
Abstract.....	53
Introduction.....	55
Aims and objectives	58
Results.....	59
Selective genetic ablation of galaninergic neurons in the lateral preoptic area (LPO) of the hypothalamus using <i>Cre</i> recombinase	59
Galaninergic neurons in the LPO area are needed for consolidated NREM sleep	66
Ablation of LPO ^{Gal} neurons caused chronic elevation of body temperature	74
Galaninergic neurons in the LPO contribute to sleep homeostasis	78
Chemogenetic activation of LPO ^{Gal} neurons promotes sleep and reduces core body temperature.....	84

Discussion	96
Chapter 3.....	100
<i>Galaninergic neurons in the LPO are required for α2 adrenergic agonist (dexmedetomidine)-induced sedation and hypothermia.....</i>	100
Abstract.....	100
Introduction.....	101
Aims and objectives	103
Results.....	104
Ablation of LPO ^{Gal} neurons strongly reduced DEX-induced hypothermia.....	104
DEX requires LPO ^{Gal} neurons to induce NREM-like δ power	107
Discussion	113
Conclusion (Chapter 2 and Chapter 3)	116
Future work.....	118
Chapter 4.....	121
<i>Exploration of whole brain neuronal connections of wake-promoting VTA^{Vglut2} and wake-inhibiting VTA^{Vgat} neurons using chemogenetics and anterograde tracing techniques</i>	121
Abstract.....	121
Introduction.....	123
Aims and objectives	126
Results.....	127
Wake-promoting VTA ^{Vglut2} neurons induce cFos protein expression in different brain regions followed by chemogenetic activation and send axonal projections to these target areas	127
Wake-inhibiting VTA ^{Vgat} neurons induce strong cFos protein expression in the LH and VTA followed by chemogenetic inhibition and send axonal projections to brain areas different with VTA ^{Vglut2} neurons.....	134
Discussion	142
Chapter 5.....	147
<i>Materials and Methods.....</i>	147
Chapter 2 and Chapter 3	147
Mice	147
AAV transgene plasmids	148
Generation of recombinant AAV particles.....	148
Genotyping.....	148
Surgery and Stereotaxic injection of AAV	150

<i>In vivo</i> EEG and EMG recording and vigilance states scoring	151
Core body temperature recording.....	154
Sleep deprivation and recovery sleep	154
Chemogenetic treatments	154
DEX experiments.....	155
Transcardial perfusion	155
Immunohistochemistry.....	156
Quantification and statistical analysis	157
Chapter 4	158
Mice	158
AAV transgene plasmids	158
Surgery and stereotaxic injections of AAV.....	158
Chemogenetic treatments	158
Immunohistochemistry.....	159
Quantification and statistical analysis	159
Preliminary Result Chapter (Appendix).....	160
Mice	160
Sleep deprivation and recovery sleep	160
Transcardial perfusion	160
Immunohistochemistry.....	160
Quantification and statistical analysis	161
References.....	162
Appendices.....	178
<i>Preliminary Result Chapter: Exploration of brain regions regulating sleep/wake behaviours by expression of immediate early gene, cFos.....</i>	<i>178</i>
Abstract.....	178
Introduction.....	180
Aims and objectives	182
Results.....	183
Discussion	201
<i>List of publications.....</i>	<i>205</i>

List of Figures

Figure 1.1 An original drawing of human brain structure involving in sleep/wake regulation from von Economo.....	16
Figure 1.2 Physiology of sleep.....	19
Figure 1.3 Arousal-promoting circuitry.....	21
Figure 1.4 Wake-promoting orexinergic/glutamatergic circuitry.....	25
Figure 1.5 NREM sleep-promoting circuitry.....	27
Figure 1.6 Newly identified Wake/NREM-promoting neuronal populations.....	31
Figure 1.7 Example of 1 hr (ZT3-ZT4, “lights-on”) of raw EEG and EMG spectra data and vigilance-state scoring for C57bl6 mouse.....	33
Figure 1.8 REM-promoting circuitry.....	36
Figure 1.9 Classical two-process regulation of sleep.....	37
Figure 1.10 Functional neuroanatomical model of the efferent thermoeffector pathway for BAT thermogenesis.....	46
Figure 2.1 Selective ablation using <i>Cre</i> recombinase specifically reduced the number of galaninergic neurons of the lateral preoptic area (LPO) in the hypothalamus.....	61
Figure 2.2 Immunohistochemical mapping of galaninergic neurons across the LPO both in <i>LPO-ΔGal</i> and <i>LPO-Gal-GFP</i> mice.....	63
Figure 2.3 Neural ablation by <i>AAV-DIO-CASP3</i> was restricted to galaninergic neurons in the LPO, and did not affect other neuronal types, e.g. parvalbumin neurons.....	65
Figure 2.4 Ablation of LPO^{Gal} neuron increased WAKE and NREM episode numbers and reduced WAKE and NREM durations.....	67
Figure 2.5 Ablation of galaninergic neurons in the LPO caused a modest change in sleep time during “lights-off” period.....	69
Figure 2.6 Ablation of LPO^{Gal} did not affect EEG power either in WAKE or NREM state.....	71
Figure 2.7 Ablation of LPO^{Gal} caused profound fragmentation in sleep architecture.....	73
Figure 2.8 Chronic ablation of LPO^{Gal} markedly elevated core body temperature.....	75
Figure 2.9 Locomotion activity was not affected by ablation of LPO^{Gal} neurons.....	77
Figure 2.10 The increase of percentage of total SLEEP (NREM+REM sleep) was not observed in the <i>LPO-ΔGal</i> mice after 5 hrs SD (ZT0-ZT5) over a full circadian cycle (24 hrs).....	79
Figure 2.11 Sleep rebound after 5 hrs SD was nearly abolished in the <i>LPO-ΔGal</i> mice over a full circadian cycle (24 hrs).....	81
Figure 2.12 The increase of δ power after SD, one of the hallmarks of sleep homeostasis, was significantly reduced in <i>LPO-ΔGal</i> mice.....	83
Figure 2.13 Selective activation of LPO^{Gal} by chemogenetics.....	85
Figure 2.14 Selective chemogenetic activation of LPO^{Gal} neurons by CNO increased NREM sleep and reduced core body temperature.....	87

Figure 2.15 Selective chemogenetic activation of LPO^{Gal} neurons by CNO promoted NREM sleep and the effects lasted for 3 hrs.....89

Figure 2.16 NREM sleep induced by chemogenetic activation of LPO^{Gal} neurons by CNO had higher δ power (0.5-4 Hz) than natural NREM sleep.....91

Figure 2.17 CNO injection did not induce NREM sleep in control mice without hM₃D_q receptor compared with saline injection.....93

Figure 2.18 CNO induced hypothermia was only produced by activation of LPO^{Gal} neurons with hM₃D_q receptor but not in control mice that did not express hM₃D_q receptor.....95

Figure 3.1 DEX-induced hypothermia was strongly reduced in *LPO-ΔGal* mice.....106

Figure 3.2 Examples of 6 hrs recording of EEG/EMG raw data with vigilance states scoring after DEX injection.....108

Figure 3.3 DEX-induced increase in the power of the δ wave band in NREM-like state requires LPO^{Gal} neurons.....110

Figure 3.4 Ablation of LPO^{Gal} neurons caused an absence of δ power rebound after emergence from DEX-induced effects.....112

Figure 3.5 Whole brain mapping of axonal projections from LPO^{Gal} neurons.....119

Figure 4.1 Chemogenetic activation of VTA^{Vglut2} neurons induced elevated cFos protein expression in local VTA.....128

Figure 4.2 cFos-based activity mapping of brain areas after chemogenetic activation of VTA^{Vglut2} neurons.....130

Figure 4.3 Whole brain mapping of axonal projections from VTA^{Vglut2} neurons.....133

Figure 4.4 Chemogenetic inhibition of VTA^{Vgat} neurons induced elevated cFos protein expression in local VTA.....136

Figure 4.5 cFos-based activity mapping of brain areas after chemogenetic inhibition of VTA^{Vgat} neurons.....138

Figure 4.6 Whole brain mapping of axonal projections from VTA^{Vgat} neurons.....141

Figure 4.7 Conceptual circuit diagrams illustrating a hypothesis of how VTA^{Vglut2}, VTA^{Vgat} and VTA^{DA} neurons contribute to the natural sleep/wake regulation.....143

Figure 5.1 An example of *Gal-Cre* genotyping gel of *Gal-Cre* mice.....149

Figure 5.2 Illustration of the head-stage implantation.....152

Figure 5.3 Detailed criteria for vigilance states scoring and example of EEG and EMG signals.....153

Figure 6.1 Examples of whole-brain cFos expression mapping of 5-hour sleep deprived mice and 2-hour sleep recovered (after 5-hour SD) mice.....184

Figure 6.2 Robust expression of cFos has been found in the brain of SD mice compared with the one of RS mice, except for the LPO of the hypothalamus.....197

List of Abbreviations

3V	the third ventricle
5-HT	serotonin
AAV	adeno-associated virus
ACh	acetylcholine
Bar	Barrington's nucleus
BF	basal forebrain
CALCA	calcitonin gene-related peptide alpha
CeA	central nucleus of amygdala
ChR2	channelrhodopsin
CLi	caudal linear nucleus
CPu	striatum
D3V	dorsal 3 rd ventricle
DA	dopamine
DEX	dexmedetomidine
DG	dentate gyrus
DIO	double-floxed inverted orientation
dIPAG	dorsolateral periaqueductal gray
DM	dorsomedial nucleus of hypothalamus
DMH	dorsomedial nucleus of hypothalamus
DMSO	dimethyl sulfoxide
DP	dorsal peduncular cortex
DR	dorsal raphe
DREADD	designer receptors exclusively activated by designer drugs
DRG	dorsal root ganglia
EDTA	ethylenediaminetetraacetic acid
EEG	electroencephalogram
EMG	electromyography
f	fornix
GABA	γ -aminobutyric acid
HDB	magnocellular preoptic nucleus
HEK	human embryonic kidney
IF	interfascicular nucleus
IL	infralimbic cortex
i.p.	intraperitoneal
IPN	interpeduncular nucleus
IPR	interpeduncular nucleus
LC	locus ceruleus
LDTg	laterodorsal tegmental nucleus
LH	lateral hypothalamus
LHb	lateral habenula

IPAG	lateral periaqueductal gray
LPB	lateral parabrachial nucleus
LPO	lateral preoptic nucleus
MCLH	magnocellular nucleus of lateral hypothalamus
mfb	medial forebrain bundle
MHb	medial habenular nucleus
MO	medial orbital cortex
MPO	medial preoptic nucleus
MSNs	medium spiny neurons
MTu	medial tuberal nucleus
NA	noradrenaline
NAC	nucleus accumbens
NGS	normal goat serum
NMDA	N-methyl-D-aspartate
NO	nitric oxide
NOS1	nitric oxide synthase 1
NREM	non-rapid eye movement
PAG	periaqueductal gray
PB	parabrachial nucleus
PBP	parabrachial pigmented nucleus
PBS	phosphate buffered saline
PeF	perifornical nucleus
PFC	prefrontal cortex
pIII	perioloculomotor region
PL	paralemniscal nucleus
PN	paranigral nucleus
POA	preoptic area
PPT	
PV	paraventricular thalamus
PVN	paraventricular nucleus
PZ	paraventricular zone
REM	rapid eye movement
RF	reticular formation
RLi	rostral linear nucleus
RS	recovery sleep
RT	room temperature
SCN	suprachiasmatic nucleus
SD	sleep deprivation
SLD	sublaterodorsal nucleus
SNc	substantia nigra pars compacta
SPZ	subparaventricular zone
SWA	slow wave activity
TAE	Tris-acetate EDTA
TMN	tuberomammillary nucleus

TRN	reticular thalamus nucleus
VGAT	vesicular GABA transporter
vIPAG	ventrolateral periaqueductal gray
vLPO	ventrolateral preoptic nucleus
VMH	ventromedial nucleus
VP	ventral pallidum
VTA	ventral tegmental area
ZT	zeitgeber time

Chapter 1

The urge to sleep

An evolutionary and historical view

Sleep is one of the most common behaviours we experience every day. Three behavioural criteria are often used to define sleep: inactivity, reduction in responsiveness to external stimuli and rapid reversibility[1, 2]. Like all the other fundamental physiological needs such as hunger, thirst and sexual arousal, sleep is inevitable in our daily life. Infants and toddler sleep 16-20 hours per day; adults sleep 7-8 hours; and elder people sleep around 6.5 hours[3]. Although the total time spent in sleep shortens with ageing[4], human spend one third of our lives in sleep on average. Actually, we are not the only species that need sleep. At least based on the criteria of immobility and being harder to arouse, sleep is a ubiquitous state that seems to be conserved across animal species[5]. Besides those non-human mammals we commonly see in our life, such as primates, dogs and cats, small animals like cockroaches, honey bees, coral reef fishes and even nematode worms were found to have sleep or sleep-like behaviours[6-9]. Scientists have spent many years in searching for animals that do not sleep, but, so far, no animals with a central nervous system have been found to live without sleep or sleep-like states, except for a few basic animals having no brain or an extremely simple one[10].

Poor quality of sleep, or lack of sleep will cause various unhealthy outcomes in humans. One night of bad sleep causes stress and fatigue in the following day; short-term sleep deprivation (SD) increases the risks of obesity, diabetes and heart disease[11, 12]. The

most dramatically, prolonged sleep deprivation leads to death[13]. These harmful consequences can also be observed in animal models[14-16]. All of these evidence suggested that sleep is indispensable and plays a vital role in maintaining regular physiological functions in life. On the other hand, from an evolutionary aspect, sleep seems to be incompatible with the survival of animals. When animals are asleep, not only can they not feed, but also this frozen state exposes them to dangerous situations of being attacked by predators. Therefore, sleep must confer some essential advantages to animals to outweigh these negative effects[17, 18].

The first documented theory about sleep can be tracked way back to 500-450 B.C.. Alcmaeon of Croton, the Greek philosopher/physician, proposed that the phenomenon of loss of consciousness when blood drains from the vessels on the surface of the body is sleep[19]. Later on, around 350 B.C., Aristotle stated another theory of sleep: he believed that the consciousness resides in the heart and the onset of sleep results from warm vapours rising from the stomach during digestion. In 1729, the French scientist Jean-Jacques d'Ortous de Mariran discovered plants have endogenous circadian rhythms, whereby he observed that they opened and closed their leaves in an approximate 24 hours rhythm in free-running conditions of constant darkness. Not until the 19th century were theories on sleep based on experimental findings in animals and humans. In 1875, more than fifty years before the invention of the modern electroencephalogram (EEG), English scientist Richard Caton detected electrical signals on the surface of the brain using a voltmeter; in 1880, French neuropsychiatrist Jean-Baptiste-Edouard Gelineau identified

the condition of narcolepsy in his patients who fell asleep uncontrollably often at inappropriate times during the day.

The beginning of the modern approach to sleep research was the book entitled “Le probleme physiologique du sommeil” by French psychologist Henri Pieron in 1913, which was the first text addressing sleep from its physiological characteristics. Three years later during the encephalitis lethargica world epidemic, Romanian neurologist Constantin von Economo made one of the most influential discoveries in sleep research by pinpointing the origin of wake and sleep signals in the hypothalamic area of the brain[20] (**Fig. 1.1**). In 1929, the early descriptions of the differences between “brainwaves” in asleep and awake human beings were identified by German psychiatrist Hans Berger with his development of EEG[21]. EEG records the electrical activity generated by the synchronization of thousands of neurons in a physiological approach[22]. Neurons are interconnected densely via synapses that act as gateways of excitatory or inhibitory activity. A subtle electrical impulse known as a postsynaptic potential can be generated by any synaptic activity, which is difficult to detect reliably. However, an electrical field can be generated when thousands of neurons fire in sync[23]. This electrical signal is strong enough to be measured on the head surface via electrodes placed on the scalp. The voltage fluctuations recorded by the electrodes are mild, therefore the recorded data is then digitized and sent to an amplifier. The data can be subsequently presented as a sequence of voltage value after amplification[24]. With the help of the EEG technique, non-rapid eye movement (NREM) sleep and rapid eye movement (REM) sleep were discovered in 1937 and 1953 respectively[25, 26].

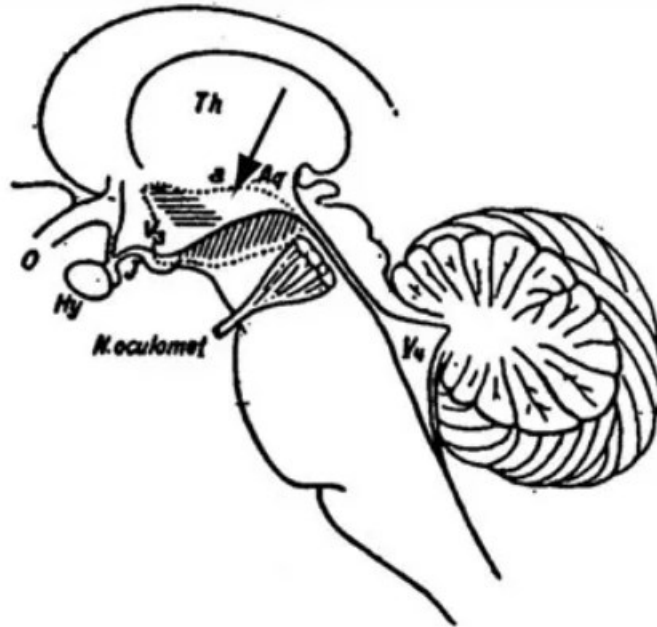


Figure 1.1 An original drawing of human brain structure involving in sleep/wake regulation from von Economo. During the encephalitis lethargica world epidemic, von Economo found that if the patients had lesions (diagonal hatching) at the junction of the forebrain and brainstem, he/she suffered with prolonged sleepiness; if the lesion (horizontal hatching) was in the anterior hypothalamus, insomnia occurred. The lesion in the site between the two regions, including the posterior lateral hypothalamus, indicated by the arrow was the region that von Economo suggested caused narcolepsy[27].

NREM sleep is defined as a high-amplitude, low-frequency pattern in the δ range (0.5 to 4 Hz) in EEG (**Fig. 1.2 A**) accompanying with low muscle electromyography (EMG), which is different from the low-amplitude, high frequency EEG pattern with high muscle EMG of the waking state. In humans, there are four stages of NREM sleep depending on the degree to which the EEG is progressively synchronized[28]. The δ rhythm of neuronal firing in the neocortex during NREM sleep has been speculated to serve various functions including memory consolidation[29], sensory transmission and synaptic plasticity for individual neurons. During NREM sleep, body temperature, breathing and heart rate fall and become more regular.


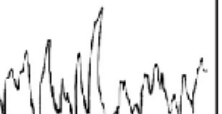
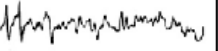
A hallmark of NREM sleep is sleep spindles. Sleep spindles are bursts of neural oscillatory activity and they are generated within the reticular thalamic nucleus (TRN) as well as other thalamic nuclei during NREM sleep[30]. Many evidence has suggested sleep spindles are strongly correlated with learning[31, 32], cognition[33] and memory[34]. The patterns of spindle activities change with ageing and people with neuronal disorders often lack the normal pattern of sleep spindles[35]. Although little is known about the function of sleep spindles in sleep/wake regulation, study has suggested that the spindle activities during NREM sleep is possibly involved in sleep maintenance and REM sleep initiation[36].

After NREM sleep, REM sleep typically follows. REM sleep is physiologically distinct from NREM sleep (**Fig. 1.2A**) and it might serve special functions, for example in reducing the aversive or emotional effects of stress[37-39], as well as promoting memory formation[40]. REM is also the vigilance state from which we commonly wake up. Unlike NREM sleep, REM sleep in humans is characterized by the presence of fast EEG activity of low voltage (**Fig. 1.2 A**), loss of skeletal muscle tone (atonia-but not breathing muscles) and, of course, the occurrence of rapid eye movements. Body temperature is not regulated in REM sleep and there is often enhanced sympathetic neural activity. This stage of sleep is usually associated with a high level of brain activity and vivid dreaming[41], although dreams do often occur in NREM sleep as well. NREM and REM sleep keep alternating through the night in a cyclical fashion in humans as shown in **Fig. 1.2 B**, and mammals mostly wake up from REM sleep rather than NREM (**Fig. 1.2 C**). The different stages of NREM sleep are possibly a unique feature of mammals with a larger neocortex and is not present in rats and mice. Recently, different sleep-like states in

zebrafish were identified using calcium imaging, which could approximately correspond to NREM and REM sleep[42]. Mice and rats are polyphasic in sleep pattern, *i.e.* sleep with lots of short NREM-REM cycles throughout the whole day (**Fig. 1.2 C**).

Within the last few decades, sleep research advanced rapidly with newly developed technology and tools. Several different theories have been brought to explain why we sleep but these explanations are not consistently supported by empirical evidence. There is still a long way for sleep scientists to go to uncover the molecular and cellular mechanisms of the transition between wake and sleep.

A

	Wake	NREM sleep	REM sleep
Psychological features	Varying amounts of alertness and attentiveness	Unconscious, or bland thoughts	Vivid, story-like dreams
Physiological features	Sympathetic tone variable	Sympathetic tone low; roving eye movements in light NREM sleep	Sympathetic tone variable; bursts of fast saccadic eye movements
EEG pattern (5 sec)			
Developmental changes	Short wake bouts in infants and young children	Deep NREM sleep abundant in children, but gradually decreases across adulthood	Abundant in infants, steady levels across adulthood; NREM-REM cycle short in infants

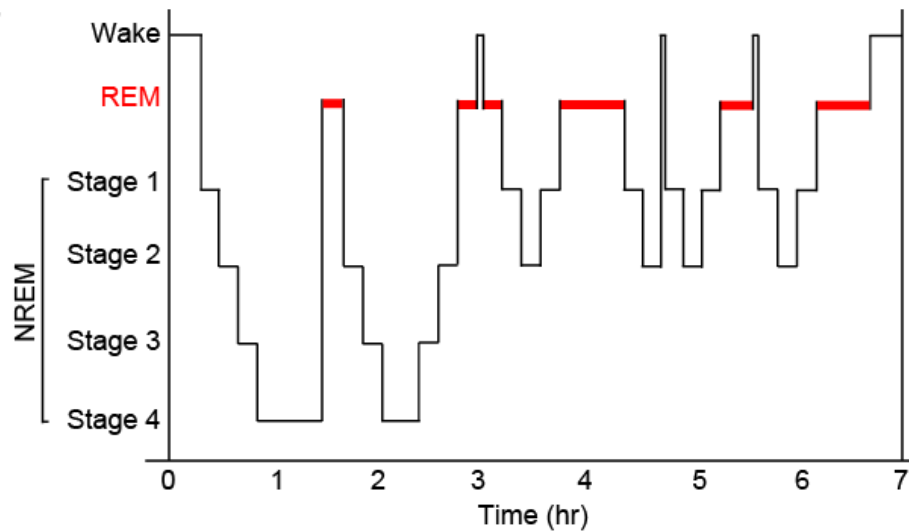
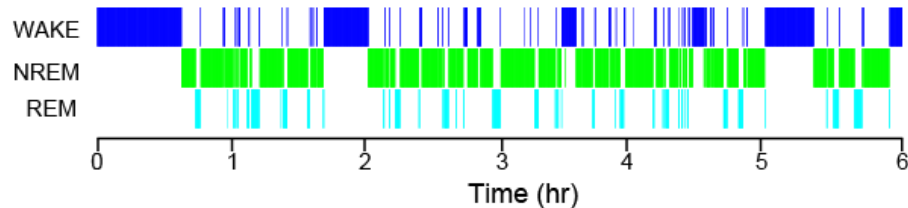
B**C**

Figure 1.2 Physiology of sleep. (A) Different features for each vigilance state in human beings. Reproduced from [43]. (B) A typical healthy young adult first enters deep NREM sleep (N3) quickly and then alternates between NREM sleep and REM sleep several cycles throughout the night. NREM sleep becomes lighter and REM sleep episodes become longer as homeostatic sleep pressure dissipates with increase of sleep time. (C) A typical sleep structure of a C57Bl6 mouse (ZT2-ZT8, “lights-on”). Mice are polyphasic in sleep pattern and there is always a short REM sleep following a NREM sleep.

The neurotransmitters and neural circuits involving in sleep/wake regulation

Despite the fundamental mechanisms and purpose(s) for sleep remaining a mystery, the advent of chemogenetic and optogenetic methods enabled sleep researchers to manipulate specific neuronal populations using synthetic ligands or light, respectively, has led to great breakthroughs on specific neurotransmitters and neural circuitry regulating sleep/wake behaviours in the past decades.

Regulation of arousal systems

During the epidemic of encephalitis lethargica in 1916, von Economo discovered that patients suffered prolonged sleepiness if they had lesions at the junction of the brainstem and forebrain and thus he speculated that vital wake-promoting circuitry was located in this region[20] (**Fig. 1.1**). Later on, the work done by Moruzzi and Magoun also confirmed the reticular formation (RF) in the brainstem is crucial for generating cortical activation and behavioural arousal of waking[44]. Taking the advantages of new tools and methodologies, we now know that there are several neuronal systems maintaining wakefulness by different chemical neurotransmitters including glutamate, gamma-aminobutyric acid (GABA), serotonin (5-HT), dopamine (DA), histamine, noradrenaline (NA), orexin (also known as hypocretin) and acetylcholine (ACh) (**Fig. 1.3**). They share some similar characteristics in driving arousal. For example, they either project in a widespread manner or innervate diffusely the cerebral cortex, basal forebrain, or lateral hypothalamus (LH) and other regions and use volume transmission whereby transmitter diffuses extrasynaptically[45]. Most of these neurons release multiple transmitters, e.g.

orexin/glutamate, acetylcholine/GABA, histamine/GABA, noradrenaline/galanin and also release gases such as nitric oxide (NO)[45]. It used to be believed, and still sometimes cited by even recent reviews[43], that the majority of neurons in these arousal systems have their highest discharge rates during waking, diminished activity during NREM sleep and ceased firing during REM sleep, although more recent work from multiple laboratories using cell type-selective calcium imaging or photometry have discovered that this not always true, e.g. dopamine neurons are selectively wake and REM active[46], and ventral tegmental area (VTA) glutamate cells are selective wake and REM active etc.[47]. Each system has its unique contribution to the generation and maintenance of wakefulness, but no single system seems to be absolutely necessary[48].

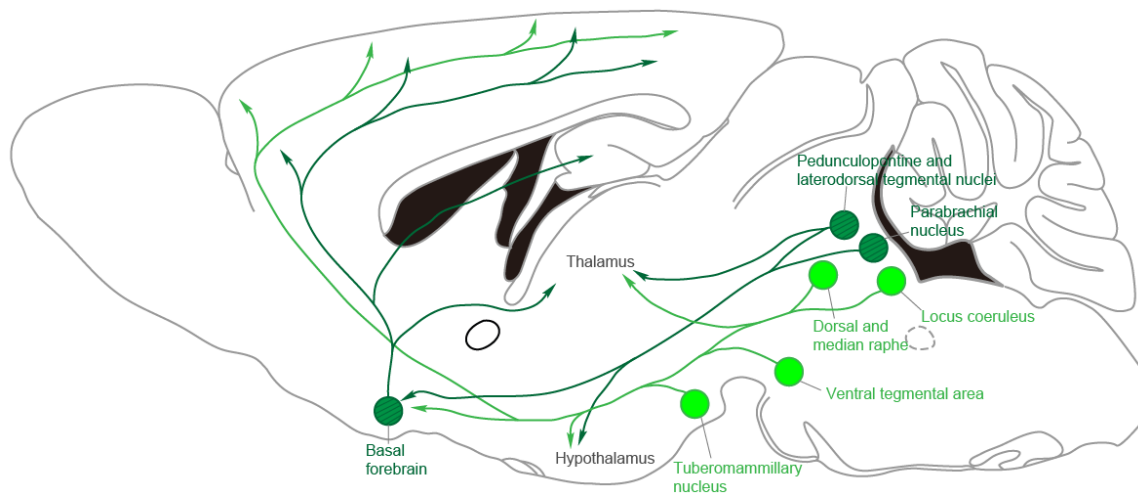


Figure 1.3 Arousal-promoting circuitry. Wakefulness and the typical fast cortical activity in wakefulness are promoted by multiple neuronal systems. Monoaminergic neurons including NA-, 5HT-, DA- and histamine-containing neurons in the LC, DR, VTA and TMN, respectively (light green) direct innervated the cortex, hypothalamus and thalamus. The parabrachial nucleus, pedunclopontine and laterodorsal tegmental nuclei and basal forebrain also send signals to promote wakefulness by cholinergic, glutamatergic and GABAergic neurons (dark green with hatching). Reproduced from [43].

NA-containing locus coeruleus (LC) sends wide projections to excite neurons in the forebrain, brainstem and spinal cord to promote arousal[48]. LC neurons are especially essential in driving high levels of arousal with salient stimuli and stressors[49]. NA-containing neurons also act to inhibit neurons involving in sleep in the brain like the basal forebrain and preoptic area through α 2-adrenoceptors, and drugs such as α 2 agonists, e.g. dexmedetomidine (DEX) and xylazine that reduce the release of NA are sedating[50] (note: work from my lab[51] and my own work presented later in **Chapter 3** in this thesis challenge this mechanism of how DEX induces sedation).

The DA-containing neurons in the substantia nigra and ventral tegmental area are confirmed to be involved in promoting arousal in recent years[46]. VTA DAergic neurons are active during wake and REM sleep and mice can be reanimated from general anaesthesia by activation of DA-containing neurons in the VTA[52, 53]. These neurons send projections to the cortex, basal forebrain and striatum. Additionally, a small population of DA-containing neurons in the ventral periaqueductal gray just lateral to the DR showed cFos expression during wake state, and the percentage of wakefulness would be reduced by 20% if lesioning these neurons[54].

The feature that brainstem raphe (dorsal raphe and median raphe) serotonin containing neurons discharge maximally during wake, reducing during NREM sleep and ceasing firing during REM sleep[55] indicates they are wake-promoting. However, recent study of zebrafish and mice has found the serotonergic raphe also promote sleep in some way[56]. The consequences to sleep/wake behaviours of activation of serotonergic raphe depend on their firing pattern, bursting or continuity. The DR and median raphe nuclei project

and receive reciprocal inputs from many sleep/wake regulating regions as well as the prefrontal cortex, insula, and extended amygdala[57]. Optogenetic activation of serotonergic neurons in the DR doubles the amount of time spent in wakefulness and causes fragmentation in NREM sleep[58]; the wakefulness of both humans and rodents is increased by drugs working to increase the tone of serotonergic neurons[43].

Histaminergic neurons are exclusively located in the tuberomammillary nucleus (TMN) in the posterior hypothalamus and they innervate wake-promoting neurons in the cortex, thalamus and other regions during wakefulness[59]. The level of histamine is consistently high when mice are awake and chemogenetic activation of TMN histaminergic neurons increases locomotion activity[60]; wakefulness and cortical activation are synergistically promoted by co-release of GABA from TMN neurons[59]. Moreover, antihistamine drugs (*i.e.* H1 receptor antagonists) acting mainly on H1 receptors often have somnolence as side-effects[61], indicating the arousal-promoting effect of histaminergic neurons.

Glutamatergic neurons have widespread locations across the whole brain. For example, the majority of neurons in the neocortex, and the pyramidal neurons, are glutamatergic, as well as thalamic relay cells. Selective activation of glutamatergic neurons in several brain regions causes strong promotion of wakefulness. Chemogenetic activation of the glutamatergic VTA neurons remarkably induces wakefulness lasting for several hours[47] and the same effect is observed with the activation of the glutamatergic PPT neurons[62]. Glutamatergic basal forebrain (BF) neurons also appear to promote arousal as optogenetic activation of them consistently wakes mice from NREM sleep[63]. In addition, glutamatergic parabrachial nucleus (PB) neurons heavily innervate the BF and lesion of

medial PB neurons or destruction of the transport of glutamate reduces the time spent in wakefulness[64], suggesting the importance of these neurons in wake-promotion.

There is strong evidence indicating the GABAergic BF neurons are wake-promoting. Chemogenetic activation of these neurons markedly promotes wakefulness and fast EEG activity lasting for several hours while NREM sleep increases for approximately 3 hrs by chemogenetic inhibition of GABAergic BF neurons[65]. Wake-promoting GABAergic neuron populations are also found in the lateral hypothalamus by innervating either the reticular nucleus[66] or some sleep-promoting brain areas[67].

The main locations of cholinergic neurons are the basal forebrain, pedunculo-pontine tegmental nucleus and laterodorsal tegmental nucleus [43]. Although selective manipulations of these cholinergic neurons have minor effects on vigilance states and it remains unclear whether these cholinergic neurons are necessary for wakefulness itself, strong evidence shows that they are essential for cortical activity during wake[68]. Cholinergic neurons may promote wake in an indirect way by coordinating with other neural types such as glutamatergic and GABAergic neurons.

Orexin-containing neurons, which co-release glutamate[69], are located in the lateral hypothalamus (in the posterior hypothalamus) which has been known as a key centre for the generation and maintenance of wake since 1916[20]. Optogenetic and chemogenetic activation of orexinergic neurons awaken mice from sleep[70] and increase wakefulness[71], respectively. Relative to wake-promotion, orexin is especially vital for the maintenance of wakefulness in long periods. The most obvious evidence for this is

that narcolepsy caused by spontaneous mutations lacking orexin or orexin receptors, happened in both mice and dogs[72, 73]. Acute loss of orexinergic neurons in mice also induces fragmentation of waking bouts without hugely affecting the total time spent in wakefulness[74]. Orexin/glutamate-containing neurons send strong excitatory projections from the posterior hypothalamus to all wake-promoting brain areas plus the cortex and midline thalamus[43] (**Fig. 1.4**) but it seems they do not send projections to the sleep-promoting preoptic region[48].

In summary, for this section, it is not clear why the brain uses so many types of wake-promoting neurons. There may be different types of wakefulness, e.g. associated with memory, or cognition, or physical action, and the different transmitter systems support these different modalities.

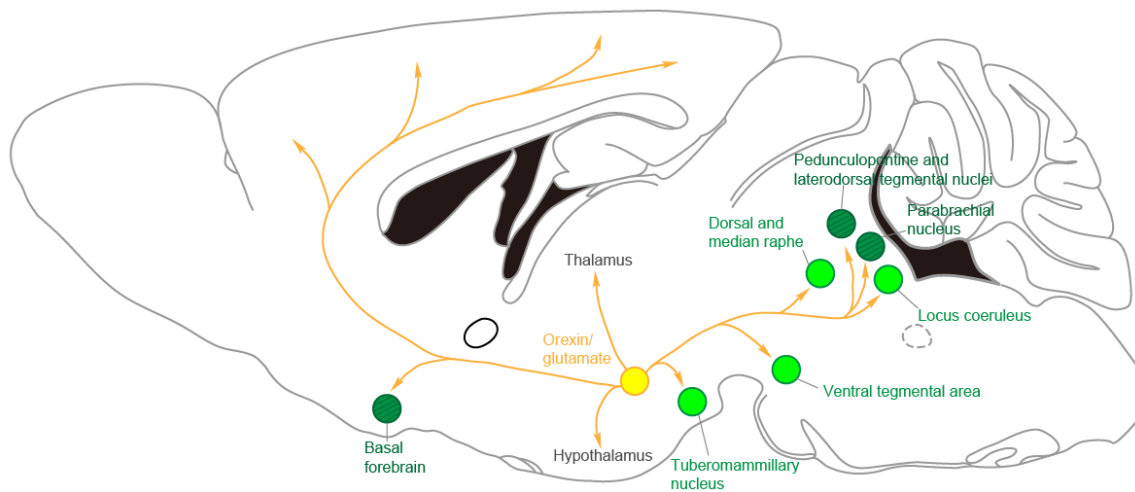


Figure 1.4 Wake-promoting orexinergic/glutamatergic circuitry. Orexinergic/glutamatergic neurons are located in the lateral hypothalamus and send excitatory projections to all wake-promoting brain areas as well as the cortex and midline thalamus. Reproduced from [43].

Regulation of NREM sleep

Unlike wakefulness, it might be anticipated that sleep is a vigilance state that is relatively straight-forward for the brain to regulate. But this seems far from the case, and the circuits that induce and maintain NREM and REM sleep are as diffuse and widespread as those regulating wakefulness. A key characteristic of NREM sleep are the δ oscillations recorded in the neocortical EEG. In other words, pyramidal neurons in the neocortex fire at a δ frequency[17]. It seems that withdrawing a range of neuromodulators (e.g. histamine and noradrenaline) from the neocortical circuitry is enough to set the neocortex into δ oscillations. (During wakefulness, these modulators are causing manifold depolarizations of neocortical pyramidal and GABA interneurons, leading to a desynchronized EEG.) If this NREM δ oscillations are produced by permitting the firing of certain types of GABAergic interneurons in the neocortex or by triggering the pyramidal cells to thalamic relay cell δ oscillation, or both mechanisms, is not clear[75].

To switch off the wake-active neuromodulators, and trigger the thalamic-neocortex δ oscillations of NREM sleep involves activating both GABAergic and glutamatergic neurons[76, 77] (**Fig. 1.5**). Also known from the work by von Economo, lesions in the basal forebrain and preoptic area (POA) cause insomnia[20]. Indeed, there are neurons selectively active during sleep in the adjacent BF and POA[78]. cFos expression shows a significant proportion of GABAergic neurons in the BF are sleep-active: the number of cFos positive GABAergic neurons increased following recovery sleep induced by sleep deprivation[79], and similarly with GABAergic neurons in the adjacent POA, especially in the vLPO and MnPO[80, 81]. The classical idea is that the GABAergic LPO/MnPO

hypothalamic neurons promote sleep by sending strong inhibitory projections to wake-promoting brain areas widespread the brain, including the cholinergic-containing BF, orexin-containing LH, TMN, DR and median raphe, PB and LC[82-84]. Conversely, the GABAergic BF neurons that produce somatostatin may promote sleep by local inhibition, *i.e.* sending inhibitory projections to wake-active BF neurons[63]. Given now that there are so many more new sleep-promoting centres discovered (see below), the simple classical model shown in **Figure 1.5** seems unlikely to be true, or at least is far from the full picture.

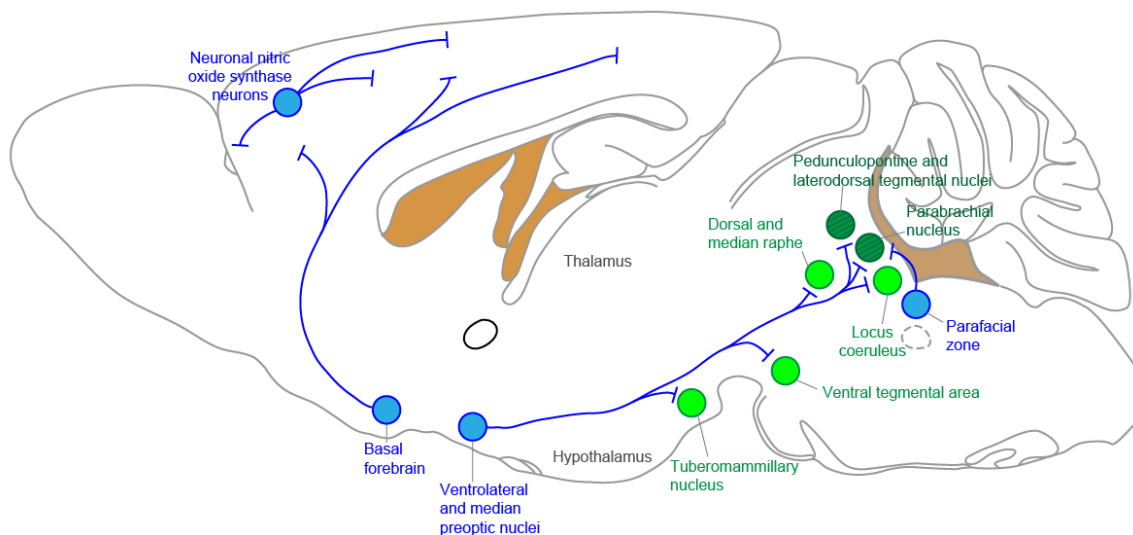


Figure 1.5 NREM sleep-promoting circuitry. GABAergic neurons in the POA send inhibitory projections to wake-promoting brain areas to promote sleep while the sleep-active BF neurons inhibit the cortex and BF locally. GABAergic PZ neurons inhibit the PB to promote NREM sleep. Some GABA/nNOS-containing cortical neurons are sleep-active as well. NREM sleep-promoting nuclei are represented by blue circles. Reproduced from [43].

There are some putative NREM-active GABAergic populations locating in the brainstem, including the RF, LC, and paraventricular zone (PZ). GABAergic neurons in the RF and LC show neuronal activity during sleep by expression of cFos[48], although cFos is too slow

to use as a precise measure of which vigilance state a neuron is active in. Similarly, chemogenetic activation of GABAergic/glycinergic PZ neurons also shows cFos expression as well as inducing NREM sleep, and wakefulness increases with disrupted GABA/glycine transmission or cell-specific lesions in this brain region[85]. GABAergic PZ neurons are necessary for generating NREM sleep as chemogenetic activation of GABAergic PZ neurons quickly triggers sustainable NREM sleep while chemogenetic inhibition of these neurons strongly reduces NREM sleep even with a high sleep drive. These GABAergic neurons promote sleep by sending inhibitory projections to wake-promoting PB neurons, including neurons projecting to the BF[43].

A subpopulation of GABAergic neuron producing neuronal nitric oxide synthase (nNOS) located in the cerebral cortex shows their activity during NREM sleep which are correlated with the time spent in NREM sleep[86]. Constitutive loss of nNOS shortens NREM sleep bouts in mice as well as reducing total NREM sleep time and homeostatic response after sleep deprivation[87], supporting the role of GABA (and possibly NO) in responding to sleep homeostasis and synchronizing slow cortical rhythms (note: nNOS is also expressed in multiple types of wake-promoting neurons, e.g. Vglut2/NOS1[47, 76]), and so NO *per se*, just like glutamate and GABA, can be deployed in both sleep-promoting and wake-promoting circuits.

This year, sleep scientists have identified multiple new sleep-promoting neuron populations in a cell type-, brain region- and time-specific manner, and it is fair to say that new sleep-promoting populations are seemingly published every month. Several neuronal groups that strongly promote wakefulness or NREM sleep have been discovered. Our

laboratory has found that the GABAergic neurons in the VTA produce remarkable increase NREM sleep after chemogenetic activation and mice consistently spend over 80% of the time in NREM sleep for the next 5 hrs[47]. Although these GABAergic neurons have strong capability in inducing NREM sleep, they are actually selective wake- and REM sleep-active, indicating they might promote NREM sleep by inhibiting wakefulness and REM sleep (**Fig. 1.6 A**). Other study also found a GABAergic subpopulation expressing GAD67 in the VTA is more active during NREM sleep, although in that particular study the calcium transitions between vigilance states were not particularly compelling[88]. Detailed discussion regarding GABAergic VTA neurons regulating sleep/wake behaviours will be presented in **Chapter 4**.

A glutamatergic population located in the paraventricular thalamus (PVT) strongly promotes wakefulness. Optogenetic activation of PVT^{Vglut2} neurons induces wakefulness from sleep and an acceleration of emergence from general anaesthesia by isoflurane, whereas suppression of these neurons reduces wakefulness[89]. The PVT^{Vglut2} neurons are activated by orexin neurons in the lateral hypothalamus and then send projections to the nucleus accumbens to promote wakefulness (**Fig. 1.6 B**)[89].

A new thalamo-amygdala circuit for sleep promotion has also been discovered (**Fig. 1.6 C**). A group of neurotensin (NTS)-positive GABAergic neurons in the central nucleus of amygdala (CeA) are NREM sleep-active. Activation and inactivation of these NTS neurons promote and suppress NREM sleep, respectively[90]. Another population of NTS-positive, but glutamatergic neurons locating in the posterior thalamus (pTh) promotes NREM sleep by innervating and exciting those CeA NTS neurons[90].

Apart from NREM sleep-promoting GABAergic neurons, a newly defined subpopulation of glutamatergic neuron expressing calcitonin gene-related peptide alpha (CALCA) located in the periolomotor region (pIII) are NREM-sleep active[91]. These neurons strongly promote NREM sleep under both optogenetic and chemogenetic activation. Another subpopulation of glutamatergic neurons in the same region promotes NREM sleep after optogenetic activation[91]. These neurons express the peptide cholecystokinin (CCK) and are distinct from the CALCA neurons. Both pIII CALCA and CCK neurons innervate and excite POA GABAergic neurons and optogenetic activation of their axonal terminals in the POA induces NREM sleep. Besides the POA, CALCA neurons also send projections to the ventromedial medulla. The increase in NREM sleep is also observed after local chemogenetic activation of CALCA neuron terminals in the medulla[91] (**Fig. 1.6 D**).

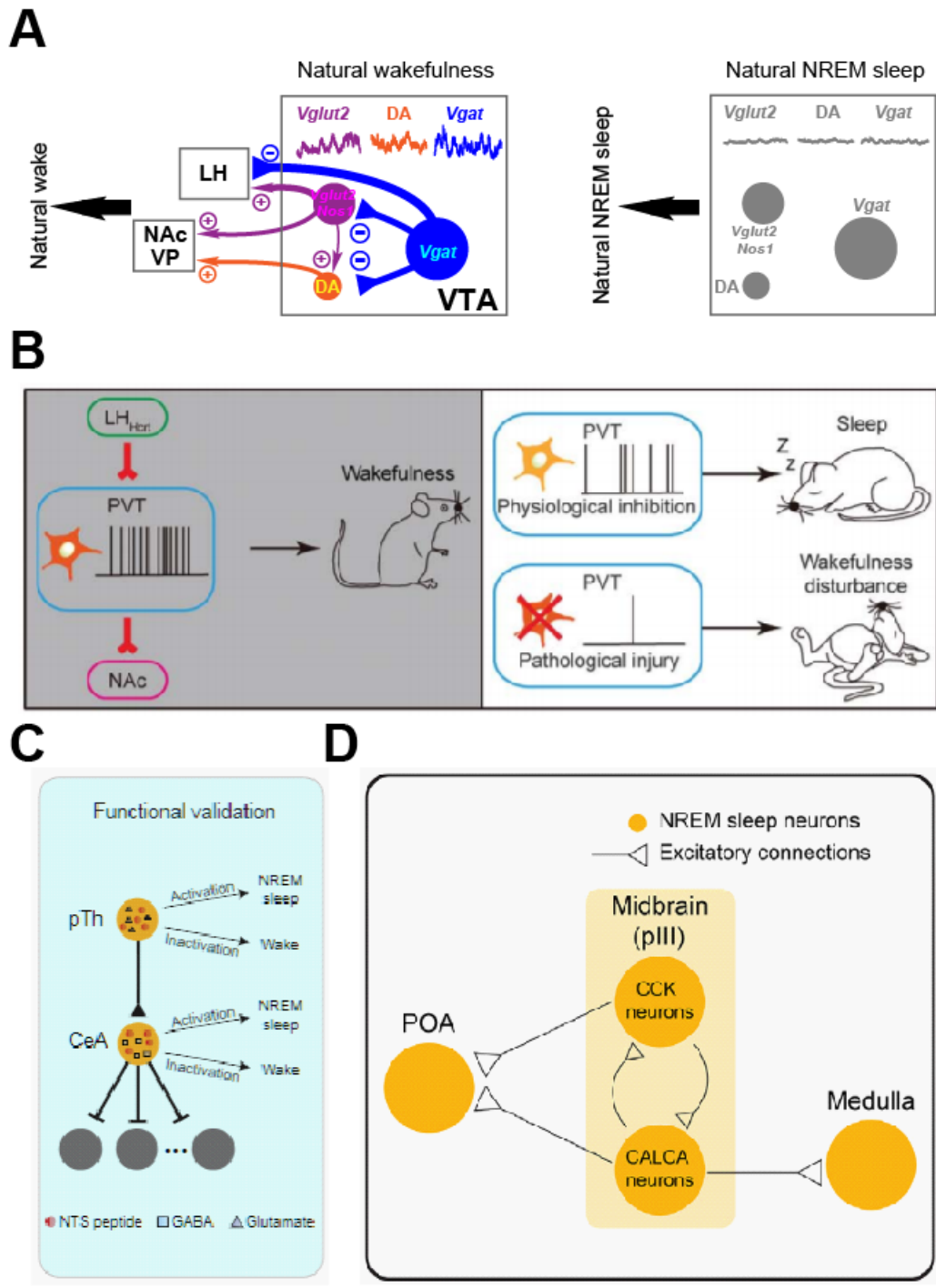


Figure 1.6 Newly identified Wake/NREM-promoting neuronal populations. (A) GABAergic VTA neurons promote NREM sleep by limiting wakefulness in the way of inhibiting the wake-promoting glutamatergic and/or dopaminergic VTA neurons locally and through projections to the LH[47]. **(B)** Activated orexin inputs from the lateral hypothalamus excite PVT neurons projecting to the NAc to promote wakefulness whereas inhibition of the PVT neuron activity

causes sleep. **(C)** Both NTS-positive GABAergic CeA neurons and NTS-positive glutamatergic pTh neurons promote NREM sleep. NTS-positive GABAergic CeA neurons receive excitatory projections from NTS-positive glutamatergic pTh neurons and subsequently inhibit other wake-promoting brain regions[90]. **(D)** Glutamatergic CALCA- and CCK-containing neurons in the pIII are NREM-active and they promote NREM sleep by sending excitatory projections reciprocally as well as to the famous sleep-promoting POA. CALCA neurons also promote NREM sleep by projecting to medulla[91].

We seem a long way from the classical view of sleep-promoting centres advanced even in the recent review promoted by Scammell and colleagues[43], and which I have used here as it provided a helpful framework to review the classical literature. Are all these new centres regulating vigilance states relevant, or have the new chemogenetic and optogenetic approaches overemphasized the importance of these circuits? We simply do not know yet. A big challenge will be to understand the larger “connectome” of these NREM sleep-promoting circuit, and how they interact with the wake-promoting and REM promoting circuitry.

Regulation of REM sleep

After NREM sleep, the animals frequently pass into the REM sleep vigilance state. In the mouse, there is typically about 4 minutes of NREM sleep followed by about 1 minute of REM sleep (**Fig. 1.7**). It is unknown how the NREM-promoting circuitry, or perhaps other timing circuitry “decides to”, initiate the REM circuit. Compared to the studies on wake- and NREM sleep-regulation, the molecular mechanism and neural circuitry of REM sleep is less understood[92]. Thus, the investigation of the REM sleep regulation would provide us with a different angle of sleep study.

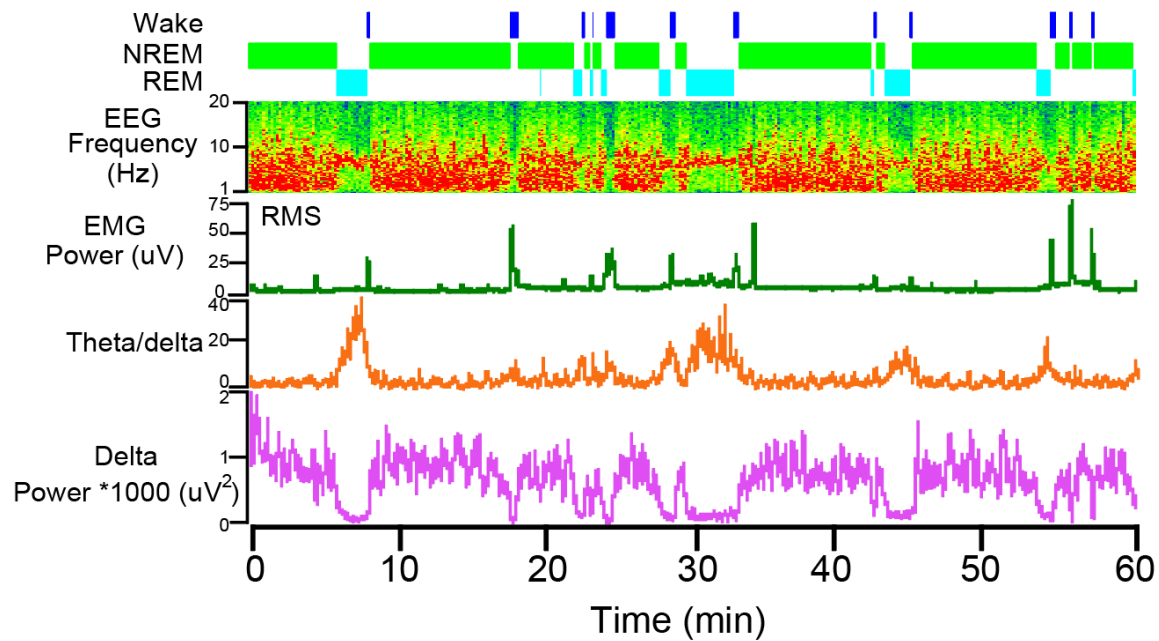


Figure 1.7 Example of 1 hr (ZT3-ZT4, “lights-on”) of raw EEG and EMG spectra data and vigilance-state scoring for C57bl6 mouse. Typically, there is usually a few minutes of REM sleep following NREM sleep.

The circuitry involved in the REM sleep regulation is widespread throughout the brainstem, including the midbrain, pons and medulla, and also the hypothalamus by a variety of neurotransmitters and neuropeptides (**Fig. 1.8**). The sublateral nucleus (SLD) located in the brainstem is vital for REM sleep regulation. Glutamatergic SLD neurons are more active in REM sleep state compared to wakefulness and NREM sleep. During wake state and NREM sleep, the SLD is inhibited by GABAergic ventrolateral periaqueductal gray (vlPAG) neurons and monoaminergic neurons in the LC and DR[43]. After a prolonged REM sleep, the glutamatergic SLD neurons show strong cFos expression[93].

In the pedunclopontine tegmental nucleus (PPT) and laterodorsal tegmental nucleus, there are dense populations of REM-on neurons, including cholinergic, GABAergic and

glutamatergic neurons[94-96]. Optogenetic activation of cholinergic PPT/LDT neurons induces REM sleep from NREM sleep[97]. During REM sleep, cholinergic PPT/LDT neurons may promote REM sleep by innervating the REM-promoting SLD.

Besides the heavy involvement of REM sleep regulation in the brainstem, researchers have identified neurons in the hypothalamus regulating REM sleep recently (**Fig. 1.8**). The orexin-containing neurons located in the lateral and posterior hypothalamus is crucial for regulating REM sleep physiologically by stabilizing wake bouts as mentioned before. Orexinergic/glutamatergic LH neurons send heavy innervation to REM sleep-suppressing brainstem regions, such as the vIPAG, DR, and LC[98, 99]. Deficiency in this circuitry causes cataplexy which has pathologically sudden intrusion of REM sleep. In contrast to orexinergic neurons, melanin-concentrating hormone-containing LH neurons are strongly active during REM sleep[100] and innervate the REM-promoting SLD[101]. Optogenetic activation of LH^{MCH} neurons increases the probability of NREM-to-REM sleep transitions if at the onset of NREM sleep and extends the duration REM sleep if at the onset of REM sleep[102-104]. A newly identified galaninergic neuron group located in the dorsomedial hypothalamus also promotes REM sleep: a subpopulation of galanin-expressing GABAergic dorsal medial hypothalamus (DMH) neurons projecting to raphe pallidus in the ventral medulla is REM-on and induces REM sleep after optogenetic activation[105]. In addition to those neuron populations mentioned above, a small cluster of GABAergic/galaninergic POA neurons are also REM-active, and lesions of the area containing these neurons reduce the time spent in REM sleep[106].

Muscle atonia is probably the best understood feature of REM sleep and is suggested in REM sleep behaviour disorder[107]. Muscle atonia during REM sleep may be mediated by the projections from glutamatergic SLD neurons to GABAergic/glycinergic neurons in the ventral medulla, which in turn send inhibitory projections to spinal motor neurons[108].

However, the circuitry underlying the wake-like activation of the neocortex during REM and the dysregulation of brain and body temperature is complex[109]. It is unclear if there is one key centre which initiates or maintains REM sleep. Acetylcholine seems essential because no REM sleep occurs when muscarinic receptors Chrm1 and Chrm3 are genetically deleted[110]. There are also quite a few types of neurons which are selectively wake and REM active (e.g. VTA glutamate neurons[47] and VTA dopamine neurons[46]), but it is unknown if they are simply responding passively to REM, as artificially activating them produces wakefulness rather than REM. However, it does suggest that during REM sleep, many of the wake-promoting chemicals are present in the neocortex, for example, acetylcholine, glutamate, and dopamine[28]. Overall, we are not yet in a position to say which are the primary REM centres.

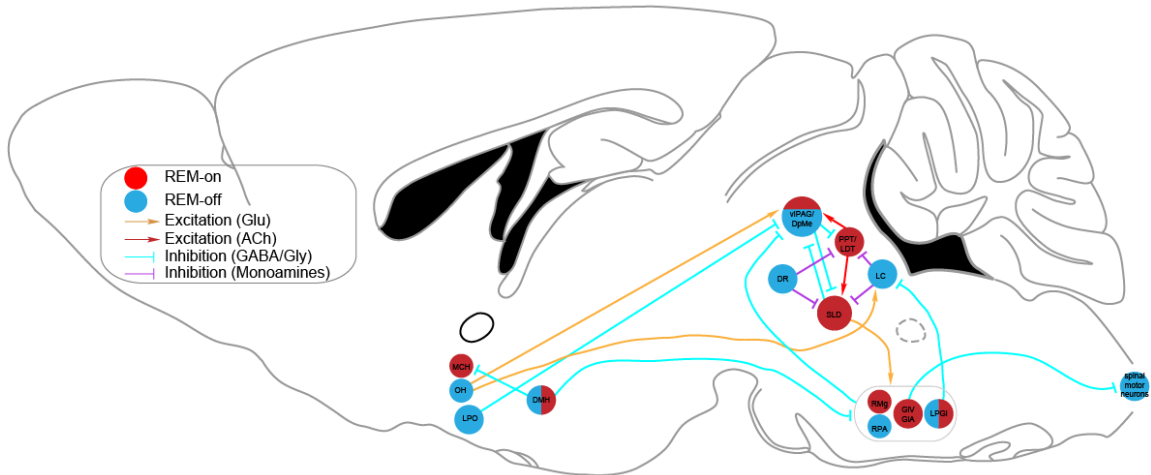


Figure 1.8 REM-promoting circuitry. The regulation of REM sleep involves both the brainstem and hypothalamus. The sublateralodorsal nucleus plays a central function in generating REM sleep. It receives inhibitory projections from the vIPAG, DR and LC during wakefulness and excitatory projections from PPT/LDT during REM sleep. During REM sleep, glutamatergic SLD neurons excites VM to produce muscle atonia. Several neuronal groups in the hypothalamus are involved in REM sleep regulation as well, including orexinergic, MCH, galanergic and GABAergic neurons. Reproduced from [111].

The switch of wakefulness and sleep transitions

At the EEG level, the switch between behavioural states is rapid and complete. Numerous external influencers and internal physiological mechanisms are involved in the transitions of sleep and wakefulness[112]. Two of the basic determinants of when we sleep are believed to be circadian and time we have spent awake. A two-process model of sleep-wake regulation was first proposed by the Swiss sleep researcher Alexander Borbely and his colleagues in the early 1980s[113]. In this model, two separated biological mechanisms, *i.e.* the homeostatic drive (Process S) and the circadian rhythm (Process C), interact together, resulting in a 24-hr sleep/wake cycle (**Fig. 1.9**).

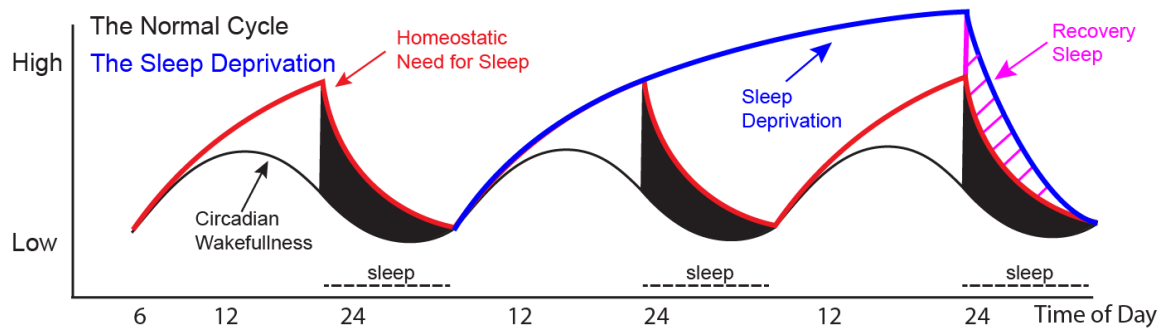


Figure 1.9 Classical two-process regulation of sleep. The interaction between homeostatic need for sleep and circadian rhythm determines the onset and amount of sleep. Sleep occurs when the difference between the two processes is at its highest. Sleep deprivation forcefully increases the homeostatic need for sleep and results in longer and deeper sleep.

The homeostatic regulation

Sleep and wakefulness are homeostatically regulated. The need for sleep accumulates during wakefulness, *i.e.* as the time of preceding wakefulness increases, the need and propensity to initiate sleep increase accordingly, and then decrease in the presence of sleep. If humans or rats are sleep deprived for some period of time, they have recovery

sleep with an increase in sleep time and a reduction in waking time subsequently to compensate the loss of sleep[114, 115]. In addition, the slow wave activity (SWA), a feature of NREM sleep, is also homeostatically controlled and reflects sleep need[116]. Long bouts of wakefulness induces more intense slow wave activity in EEG during NREM sleep, which decreases with sleep[117]. The extent of sleep homeostasis is typically measured by SWA, or δ power (0.5-4 Hz), which can be thought of as reflecting the depth of NREM sleep following sleep deprivation. The larger the δ power, the more synchronized neocortical firing. Actually, the neuronal excitability is independent of the current vigilance state but is homeostatically regulated[116]. Cortical neurons fire at higher frequencies after sustained wakefulness and their spontaneous firing rates increase systematically with the duration of preceding wakefulness. After NREM sleep, they also decrease with the duration of preceding sleep in a systematic manner[116]. This homeostatic relationship is also applied to the neuronal synchronization[116], suggesting an intrinsic function of sleep and sleep homeostasis.

Although any neurochemical factors and neuronal mechanisms driving this homeostatic regulation have not been fully understood, much work has focused on adenosine. It has been found that adenosine increases in the extracellular space following sleep deprivation[118, 119]. Adenosine increases with time spent awake in just two brain nuclei: the basal forebrain and the thalamic nucleus[120]. Increased extracellular adenosine promotes SWA and NREM sleep by its inhibitory A1 receptors locating on wake-promoting neurons, including ACh, serotonin, histamine and orexin-containing neurons. The expression of adenosine inhibitory receptors also increase on those neurons with sleep

deprivation[121]. During sleep deprivation, the production of increased adenosine on its inhibitory receptors would inhibit the wake-promoting circuitry and at the mean time excite its another receptor, A_{2A} , locating on sleep-promoting neurons[122, 123]. Together, the effects enhance sleep drive and promote sleep homeostasis. However, the adenosine hypothesis has various weakness. It has been proven difficult to get reliable measurements of extracellular adenosine[124]. Furthermore, it is unlikely that adenosine is responsible, if at all, for the entire process of homeostasis because homeostatic sleep drive persists even without adenosine receptors[125]. Another mechanism that could drive sleep homeostasis is changing synaptic strength with time spent awake[126]. For example, the longer the time spent awake, the stronger an input might be onto sleep-promoting neurons.

There is evidence that particular neuronal types can regulate sleep homeostasis globally. Across the sleep-wake cycle, the firing rates of LPO neurons increase with slow wave firing in the EEG, but themselves do not increase during prolonged wakefulness[127], suggesting with the accumulation of homeostatic sleep need, LPO hypothalamic neurons may interact with other neurons sending inputs to them, such as the POA. Indeed, I have recently identified that the galaninergic neurons in the LPO help regulate sleep homeostasis. Lesions of galaninergic LPO neurons abolished recovery sleep after sleep deprivation and hugely reduced the response in the δ power elevation. More details regarding how LPO^{Gal} neurons functioning in sleep homeostasis will be presented in **Chapter 2**.

The circadian regulation

The circadian rhythm is a body's built-in clock controlling the timing of internal biological processes and alertness levels, such as hormone production, feeding patterns, core body temperature, and sleep cycles[117]. The suprachiasmatic nucleus (SCN) located in the hypothalamus is the key pacemaker in mammals[128]. The firing patterns of SCN neurons are intrinsically rhythmic under transcriptional control and lead to biological responses based on a 24-hr cycle and SCN neurons would still maintain their rhythms even in complete darkness. Astrocytes in the SCN can drive the rhythm by releasing glutamate onto SCN neurons[129]. Lesions of the SCN, or disruption of expression of vital clock genes, causes severe loss of circadian rhythms[60, 130]. Interestingly, the SCN itself does not control the total time spent in sleep/wake[131], nor has outputs to sleep/wake regulatory regions[132]. The main projecting-targets of the SCN are the subparaventricular zone (SPZ), paraventricular nucleus (PVN), dorsomedial nucleus (DMH), ventromedial nucleus (VMH), LH and MPO[133, 134]. The SPZ is a major relay for circadian regulation of sleep/wake cycle by the SCN. It receives dense efferents from the SCN and cell-specific lesions of the ventral SPZ result in remarkable disruption of sleep/wake circadian rhythm[135]. The role of the SPZ in regulating sleep/wake rhythms is probably achieved via its heavy projections to the wake-promoting DMH. Cell-specific lesions of the DMH also abolish sleep/wake circadian rhythms[136], and reduce total time spent in wakefulness, suggesting that the DMH possibly integrates circadian inputs from the SCN and SPZ and then innervates other brain areas to promote either wakefulness or sleep at certain times.

Despite that the SCN circadian clock has its intrinsic rhythm, it is also synchronized by the external environment. One of the most potent influencers to the circadian clock is light. The light information received by retina is conveyed to the SCN by the retinohypothalamic tract[137, 138] and the SCN synchronizes its autonomous oscillation with the external timing cue. In addition, the hormone melatonin releasing from the pineal gland during dark period is also used for synchronization of the circadian clock. Although the secretion of melatonin is driven by the circadian clock, melatonin acts on the SCN, forming a feedback loop to help regularize sleep onset by entraining circadian rhythms.

The crosstalk between homeostatic and circadian regulations

Sleep homeostasis and the circadian processes are suggested to both contribute to the regulation of sleep/wake transitions. The sleep homeostasis tracks the sleep need over 24-hr cycle while circadian system determines the sleep time. These two systems are generated apparently independently but the interactions between these two processes determine the timing, duration and quality of sleep and wakefulness. Based on the two-process model, sleep occurs when the homeostatic sleep need is high and the onset of circadian clock; During sleep, the homeostatic sleep need dissipates as the increase of sleep time; After a whole-night of sleep in humans, the homeostatic sleep need reaches its lowest level and the circadian arousal system begins. This process cycles roughly every 24 hours, regulating the 24-hr sleep/wake cycle (**Fig. 1.9**).

Although the two-process model has shed some insights on the regulation and transitions between sleep and wake states, it is still an overly simplified assumption based on existing

evidence. There are also many controversial phenomena that cannot be explained by this model. For instance, in the two-process model, Process S and Process C are assumed to be independent. However, raising evidence shows that there is an interplay between them. Sleep deprivation suppresses certain circadian genes. In hamsters, sleep deprivation phase-shifts the circadian clock under constant darkness[139]. In humans, the circadian rhythm varies in the level of performance and alertness, and many sleep variables are dependent on the status of sleep homeostasis[140-142].

Apart from the homeostatic and circadian processes, sleep/wake states are influenced by environmental and physiological conditions. The sleep/wake behaviours can be adjusted under environmental factors, like seasonal changes, mating, migration, food availability, etc[143, 144]. One of the common physiological cues affecting sleep/wake states is stress. Stress-induced arousal can be found both in animals and humans[145, 146].

In conclusion, sleep is a complicated process involving different neurotransmitters, neuropeptides, neuronal circuitry, and environmental cues. Although much progress has been made by numerous sleep researchers and scientists, the fundamental function(s) and molecular mechanisms remain unanswered. For example, we know little about the mechanisms by which homeostatic sleep need is either accumulated or dissipated. There is still a long way for us to resolve this mystery neuroatomically, physiologically and comprehensively.

The need to keep warm

Like sleep/wake regulation, it is crucial for the survival of mammals to control their body temperature homeostatically. Environmental temperature has a broad range and mammals need to maintain their body temperature within a narrow range to optimize the tissue and cellular functions in a proper physiological range. Homeothermic animals utilize both physiologic (autonomic) and conscious (behavioural) reactions to regulate their body temperature in response to environmental temperature stimuli[147]. Failure to do so will eventually result in death of the animal.

Thermoregulation by the central nervous system

The central nervous system processes thermal afferent inputs from the peripheral skin and the body core to regulate the core body temperature by multiple thermoeffectors which include cutaneous vasomotion, thermogenesis and evaporative heat loss[148]. Vital thermoeffector systems have evolved to control core temperature at a proper level a bit higher than the surroundings to optimize cellular functions and enzymatic reactions. Meanwhile, they also prevent fatal changes in body temperature that might cause protein denaturation leading to cellular dysfunction.

Sensory neurons that measure the body temperature send primary inputs into the thermoregulatory system. While located their cell bodies in peripheral ganglia, sensory neurons extend their axons to sense the temperature in the skin, abdominal viscera and spinal cord. Classic neurophysiological studies showed there are distinct classes of sensory neurons that respond to either heat (around 34-42 °C), or cold (around 14-

30 °C)[149]. These neurons are pseudounipolar and located their cell bodies either in trigeminal ganglion to innervate the face and head, or in dorsal root ganglia (DRG) to innervate the rest of the body.

In vitro experiments showed that the transient receptor potential cation channel subfamily M member 8 (TRPM8) can be activated by mild cooling (<26-28 °C)[150, 151]. Indeed, *in vivo* cold perception requires the expression of TRPM8, as ablation of TRPM8-positive cells diminished both neural and behavioural responses to cooling[152]. Consistent with TRPM8's role in thermoregulation, TRPM8 agonist treatment induces hyperthermia, whereas TRPM8 antagonists induces hypothermia as well as abolishing the capability of environmental cold-inducing cFos expression in brain areas mediating thermoregulation [153, 154], suggesting TRPM8-expressing neurons convey cold information to the CNS from the periphery.

For the peripheral warm sensor, there is conflicting experimental evidence for several neuronal candidates. The transient receptor potential cation channel subfamily V member 1 (TRPV1) has received the most extensive attention. In contrast with the role of TRPM8 in thermoregulation, although counter evidence exists[155], several studies show TRPV1 agonist treatment causes hypothermia whereas TRPV1 antagonists cause hyperthermia[156-159]. But indeed, there is evidence indicating some other compensatory systems involving in the thermoregulation of TRPV1, as ablation of TRPV1 in mice does not affect regulation of normal body temperature[160-162].

The cold- and warmth-sensitive sensory neurons that have cell bodies located in the dorsal root ganglia provide the input temperature information received from the peripheral to the superficial lamina of the spinal dorsal horn[163, 164]. Dorsal horn glutamatergic neurons then project to the lateral parabrachial nucleus (LPB), which subsequently relays the inputs to the POA hypothalamus[148]. The importance of the ascending inputs to the LPB for the activation of thermoregulatory responses to environmental temperature has been demonstrated by lesioning the LPB[165].

The POA hypothalamus is a crucial integratory centre for thermoregulation. Local temperature changes in the POA elicit thermoregulatory responses[166] and there are directly thermosensitive neurons in the POA[167]. In addition, the POA sends dense projections to brain regions controlling thermoregulatory effectors[148]. Involuntary responses that generate or dissipate heat when encountering temperature changes are called physiologic effectors, including thermogenesis, cutaneous vasomotion, and evaporative heat loss. Despite that there are distinctive central circuits controlling different responses, all these thermogenic efferent pathways involve afferents from the POA, which then relays the information to the DMH, which in return innervates the raphe pallidus area (RPa)[168, 169], the primary brain region driving BAT thermogenesis (**Fig. 1.10**). The cutaneous vasoconstriction is mediated directly by the POA projections to the raphe. Mice also evaporate their heat through salivation, which has a similar pathway. The POA sends inhibitory projections to the lateral hypothalamus (LH) which subsequently activates the superior salivatory nucleus, driving the ganglion cells for salivation. Furthermore, the POA also participates in motivated behavioural

thermoregulation[170]. Cold- and warmth-seeking, such as nest-building and huddling, is the most common thermoregulatory behaviour observed in mammals[147]. Activation of POA neurons or direct change in POA temperature induces thermoregulatory behaviours[171-173].

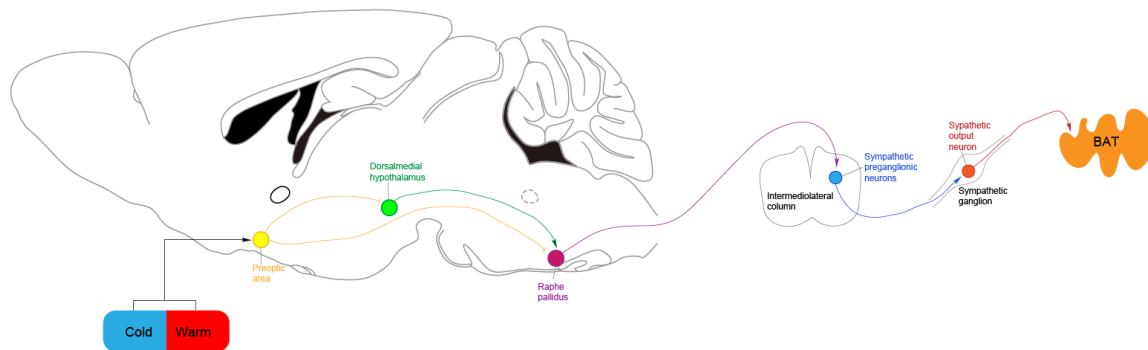


Figure 1.10 Functional neuroanatomical model of the efferent thermoeffector pathway for BAT thermogenesis. The temperature input from ambient conditions increases the activity of a subset neurons in the POA that provides an inhibitory output to BAT thermogenesis-promoting neurons in the DMH and the RPa.

In summary for this section, the POA is central for regulating in thermoregulation and thermos-homeostasis, but the circuit and molecular basis for this has not been fully-determined. Both POA^{GABA} and POA^{Vglut2} pathways to the DMH contribute to thermoregulation of mice[174, 175], as well as the POA^{Gal} neurons[176, 177] (**see details in Chapter 2**).

Sleep with thermoregulation

Thermoregulatory systems fluctuate in response to both internal and external factors that reflect the interactions between thermoregulatory and other physiologic systems. Sleep is one of the physiologic systems modulating with the thermoregulatory system and vice versa. In mammals, sleep seems to coincide with the circadian temperature rhythm.

Before sleep, the “Warm Bath Effect” that immerses humans in hot water prior to sleep shortens sleep latency and enhances sleep quality[178-180]. The onset of sleep relates closely with the maximum rate of body temperature decline[181]. During sleep, mammals tend to choose warmer environments similar to thermoneutrality to minimize their energy expenditure[182, 183] and this thermoregulatory behaviour is conserved across species, including rodents and large primates[147]. All this evidence indicates there might be a strong link between sleep and thermoregulation. Although sleep regulation involves several different brain regions, the POA has long been recognized as a sleep regulatory centre[20], as well as thermoregulatory centre. The POA contains mechanistic connections between sleep induction and whole body warming, as the activity of sleep-promoting neurons in the POA can be induced by warming[184]. Similarly, both warm-defence behaviour and total sleep reduction appear in cats after lesions in the POA[185]. δ power in the EEG during sleep is also increased by local warming of the POA using a “thermode”[186]. In the rat, inhibitory projections from the POA to arousal-promoting nuclei, such as the histamine neurons in the posterior hypothalamus and serotonin neurons in the dorsal raphe, can be activated by warming[187, 188].

A further link between sleep and thermoregulation converging in the POA was found in our laboratory by Zhang et al.[51]: both NREM sleep and hypothermia can be recapitulated by activation of POA neuronal ensembles previously tagged by cFos-dependent activity-tagging technique by either recovery sleep after sleep deprivation or sedation induced by the α 2 adrenergic agonist DEX (see later sections of this **Introduction** about sedatives). Work from Harding et al. raises the possibility that thermoregulatory

circuits themselves facilitate sleep: POA neuronal ensembles receiving warm sensory information were activity-tagged, and reactivation the same group of neurons induces body cooling and NREM sleep simultaneously[76]. Additionally, I and another group found that chemogenetic activation of galaninergic POA neurons induced both NREM sleep and hypothermia in mice[176, 177] (see details in **Chapter 2**).

Another indication of the interaction between sleep regulation and thermoregulation is that sleep deprivation disrupts thermoregulation. Rats with chronic total-sleep deprivation have increased body temperature at early stages and then progressively develop hypothermia and prefer warmer environments[189, 190]. Additionally, UCP-1 knockout mice that lack a key component of BAT thermogenesis have reduced homeostatic rebound following sleep deprivation. Compared to control mice, these mice also have blunted reactions in initiating sleep to warmer temperatures, suggesting that UCP-1 mediated BAT thermogenesis aids NREM sleep initiation and recovery sleep[191].

In summary for this section, based on our results and work from other studies, we hypothesize the POA in the anterior of the hypothalamus integrates sleep/wake regulation and thermoregulation. Considering the neuronal heterogeneity and multiple functions of the POA, further work focusing on the cell-type specific study and neural circuitry are required. This will provide us with vital knowledge of thermoregulation and metabolism central to understanding our own physiology.

Does sedation share a common circuitry with sleep?

Millions of people experience general anaesthetics every year. Anaesthesiologists use anaesthetic drugs in their day to day practice to help patients reduce the pain from clinical surgery[192, 193]. There are several types of general anaesthetics including intravenous, inhaled, and gaseous anaesthetics. Although different anaesthetics have their distinct chemical and physical properties, they all can induce a reversible state satisfying the conditions of loss of consciousness, analgesia, muscle relaxation and suppression of autonomic nervous reflexes[194]. It is still baffling scientists that how such a structurally diverse group of drugs can produce a common end point and what are the neuronal mechanisms of this phenomenon.

Although the full picture of how can general anaesthetics cause reversible loss of consciousness is not clear, a few molecular targets have emerged from anaesthesiological studies. The potential importance of GABA type A (GABA_A) receptors as an anaesthetic target has been appreciated for more than a few decades[195-197]. Various mutations in the α subunit affect the sensitivity of GABA_A receptor to volatile anaesthetics, for example, substitution at Ser270 decrease potentiation by isoflurane[198-201]. Another potential molecular target of anaesthetics is the TASK two-pore-domain K⁺ channels. Its linker region between the large carboxy-terminal cytoplasmic domain and transmembrane domain 4 (TM4) is essential for activation by the anaesthetic halothane[202]. A third target is the N-methyl-D-aspartate (NMDA) receptors whose sensitivity to inhalational anaesthetics is affected by mutations in its membrane domain 3 (M3) and M4[203]. Apart from the three targets mentioned above, there are a few other possible molecular targets

for anaesthetics, such as glycine receptors, cyclic-nucleotide-gated (HCN) channels and certain Na⁺ channel subtypes[192].

When some anaesthetic drugs are used at low doses, they induce sedation, a state highly resembling natural sleep. Sedation and sleep share many similarities, such as reduced response to external stimuli. In last a few decades, an extensive research was carried out sleep and the neuronal circuitry regulating sleep (see earlier sections of this **Introduction**).

Sedative drugs are often used to treat insomnia[204-206], a sleep disorder that causes the patients have difficulties falling and/or staying asleep. They induce a state usually with a reduced movement, an increase in slow δ power oscillation (0.5-4 Hz) in the EEG, reduced breathing rate and body temperature, and closed eyes in humans[193], which are typical features observed in natural sleep. In the sedative state, the subjects still have functional brainstem circuitry and respiratory systems, as well as slow cognitive responsiveness, and it is usually possible to arouse them from sedation[193]. Although the chemically-induced sedation is not identical with natural NREM sleep, several sedative drugs do employ some selective sleep/wake circuitry to induce the NREM sleep-like sedative state[192, 193].

GABA as an inhibitory neurotransmitter plays an important role in sleep/wake regulatory circuitry. In general, GABAergic neurons in the POA send inhibitory projections to the arousal-promoting nuclei in the posterior brain regions. But the POA is not the only GABA-positive region that regulate sleep/wake behaviour. Recent discovered GABAergic VTA neurons and GABAergic midbrain neurons also promote sleep as well [47, 91] (see earlier

sections of this **Introduction**). Several sedative drugs, such as zolpidem, potentiate GABA_A receptors. Zolpidem is a positive allosteric modulator at GABA_A receptors and *in vivo* probably works on $\alpha 1\beta\gamma 2$, $\alpha 2\beta\gamma 2$ and $\alpha 3\beta\gamma 2$ GABA_A receptors[193]. The net effect of zolpidem is to shorten the latency to NREM sleep in humans[205]. Although the zolpidem-induced sedation is lighter than natural NREM sleep, it generates synchronization in the 2-4 Hz range of frequencies as seen in natural NREM sleep[193]. Zolpidem probably partially works through suppression of the wake-promoting histamine system to induce its NREM-like sleep in both humans and animals. When the histamine neurons in the mouse TMN are manipulated to be selectively sensitive to zolpidem, the latency to NREM sleep is strikingly reduced when systemically given zolpidem[207].

Similar to the histaminergic TMN, the noradrenalinergic LC is also a wake-promoting centre. Through the $\alpha 2$ adrenergic receptors, NA acts across the whole brain as a modulator working on neurons in excitatory and inhibitory ways simultaneously. The intravenous dexmedetomidine (DEX) is a popular clinical sedative drug working as an $\alpha 2$ adrenergic agonist. DEX induces a NREM stage2-like sleep in humans[208-210] and a NREM sleep-like state in rodents[211-213]. The sleep-promoting centre POA contains neuronal ensembles can be activated during recovery sleep after sleep deprivation and DEX-induced sedation[51]. More details of DEX-induced sedation will be presented in **Chapter 3**.

In summary, it appears that sedative drugs achieve their sedative effects through the neuronal circuitry that is commonly used by sleep/wake regulation, partially if not entirely. We are still far from understanding how we fall asleep. It is always beneficial to learn how

we sleep regarding to anaesthesiology. Further studies, especially involving cell-type specific technique, are needed and will help us reveal the function of sleep and perhaps develop the next generation of sedatives with less side-effects.

Chapter 2

Galaninergic neurons in the lateral preoptic area (LPO) contribute to sleep homeostasis and body temperature regulation in mice

Abstract

Sleep homeostasis is the phenomenon that the urge to sleep increases with time spent awake and the sleep following prolonged wakefulness becomes longer and deeper, accompanying with an increased EEG power in the δ wave band (0.5-4 Hz)[119, 214-216]. Widely-expressed genes have been demonstrated to regulate sleep homeostasis[119, 216-222] and some somnogens and phosphorylation track the process of sleep homeostasis[118, 119, 124, 215, 219, 223, 224]. However, sleep homeostasis has remained mysterious at the circuit level. Previously our lab found that the preoptic area (POA) in the hypothalamus might be a candidate involving in homeostatic regulation of sleep[51, 225]. The POA has long been considered as a sleep-regulating centre as well as thermoregulation. For example, within the POA, various neuronal subtypes, such as neurons expressing glutamate/NOS1 and GABA/galanin, induce NREM sleep[76, 80, 176, 177] and accompanying with body cooling[76, 176, 177]. It is possible that the restorative effects of NREM sleep depend on lower body temperature[226, 227]. In this **Chapter**, I demonstrate that mice with lesioned LPO^{Gal} neurons have reduced sleep homeostasis: (1) there is a diminished increase in EEG δ power of the recovery sleep following sleep deprivation; (2) the mice are unable to compensate their lost sleep during sleep deprivation. Besides, lesions of LPO^{Gal} neurons in mice cause a permanent elevation in core

body temperature while keeping the diurnal rhythm. Chemogenetic activation of LPO^{Gal} neurons induces NREM sleep and hypothermia, suggesting the importance of LPO^{Gal} neurons in both sleep-wake regulation and thermoregulation.

The results of this **Chapter** have been published as Ma et al. (2019) *Curr Biol.*[177].

Introduction

Sleep plays important roles in many physiological processes, such as stress reduction[37], protection of the heart[228], synaptic down-scaling[229, 230] and metabolite clearance[231]. Many adverse changes will occur in the blood plasma metabolome and brain gene expression if one's sleep gets disrupted[232-234], which might reflect the fundamental restorative purpose(s) of sleep, *i.e.* the urge to sleep.

Sleep scientists call this urge to sleep the sleep homeostatic drive and it typically increases with the time spent in awake and dissipates during sleep[214]. Sleep deprivation induces strong homeostatic drive and is followed by a characteristic recovery sleep with an immediate increase in δ power (0.5-4 Hz) oscillations in the EEG[119, 214]. The amount of subsequent NREM sleep is proportional to the previous time spent in awake during the sleep deprivation[215, 216]. In addition to the amount of sleep as well as the slow wave activity, previous study has shown that the patterns of cortical firing are also associated with sleep homeostasis. The neuronal firing rates change in a homeostatic way: the spontaneous cortical firing rates increase with the duration of prior wakefulness and decrease with the duration of prior sleep[116].

Sleep homeostasis has been found to be modulated by various genes expressed widely, such as *clock*, *per3*, *Sik3*, *mGluR5*, *Adora1*, *homer 1A* and *reverbA*[119, 216-222, 230]. The molecular substrate of this homeostatic drive is speculated to be the cumulative phosphorylation of selected synaptic proteins[224]. Messengers released from astrocytes and skeletal muscle are also suggested to modulate the process[223, 235]. However, little

is known about the neuronal circuit involved in the sleep homeostasis, or even whether the prime homeostatic drive is determined locally or globally.

The preoptic area (POA) in the hypothalamus has been strongly suggested in regulating sleep homeostasis[236]. The PO, together with their neighbouring bed nuclei of the stria terminalis become excited during sleep deprivation and the following recovery sleep[51, 81, 237, 238]. As mentioned in **Chapter 1**, the POA is involved in the homeostatic regulation of body temperature as well[239-241]. Using cFos-dependent activity-TetTagging techniques, the neuronal ensembles in the POA that are active during the recovery sleep after sleep deprivation can be reactivated to induce both NREM sleep and hypothermia[51]. Further study shows there is common circuitry linking NREM sleep induction and core body cooling in the POA[76]. Besides, approximately 80% of brain neocortex temperature variance associates with sleep/wake states[242]. The neocortical temperature of mice and rats drops quickly upon entering NREM sleep[227, 243].

Within the POA, the majority of the neurons contains the inhibitory neurotransmitters galanin (Gal) and GABA[82, 244]. Galanin is a neuropeptide consisting of 29 amino acids[245] and has been found to regulate sleep/wake states[82, 246]. General lesions in the POA where the galaninergic neurons are concentrated reduce sleep time by nearly half in rodents[246, 247]. In humans, loss of vLPO^{Gal} neurons causes sleep fragmentation and reduces consolidated sleep bouts[248]. On the other hand, although hypothalamic galanin-positive neurons are mainly GABAergic and seem to promote sleep, a small proportion of galaninergic neurons are active during wake[244]. Furthermore, a recent study identified that the POA^{Gal} neurons co-express 13 different neuronal markers

including the vesicular glutamate transporter[249] and optogenetic activation of POA^{Gal} neurons at 10 Hz increases wakefulness in mice[250], implicating a possibility of galaninergic neurons being involved in arousal.

Aims and objectives

Previous researches showed evidences of sleep/wake states and body temperature regulation by POA^{Gal} neurons, which blur the exact role of POA^{Gal} neurons. In this **Chapter**, to determine the exact role(s) of POA^{Gal} neurons in sleep and thermoregulation, a cell type- and brain region-specific study is applied, and I will

- Use recombinant AAV containing caspase-3 to ablate LPO^{Gal} neurons.
- Investigate the effect(s) of LPO^{Gal} ablation on sleep time and sleep structure in baseline 24-hr sleep/wake cycle in mice.
- Examine the role(s) of LPO^{Gal} in thermoregulation using the core body temperature as the parameter.
- Investigate the effect(s) of LPO^{Gal} ablation on sleep homeostasis after 5-hr sleep deprivation depending on both recovery sleep and immediate increase in δ power in EEG.
- Use chemogenetic activation of LPO^{Gal} neurons to determine their acute effects on sleep and thermoregulation.

Results

Selective genetic ablation of galaninergic neurons in the lateral preoptic area (LPO) of the hypothalamus using Cre recombinase

To selectively ablate LPO^{Gal} neurons, a Cre-activatable AAV expressing Caspase 3 virus (AAV-DIO-CASP3) was bilaterally injected into the LPO area of *Gal-Cre* mice to generate *LPO-ΔGal* mice (**Fig. 2.1 A**). AAV-DIO-GFP virus was also injected by mixing with AAV-DIO-CASP3 virus (1:1 ratio) to confirm the ablation of LPO^{Gal} neurons (**Fig. 2.1 A**). As controls, *Gal-Cre* gene-positive littermates were injected only with AAV-DIO-GFP virus to generate *LPO-Gal-GFP* mice (**Fig. 2.1 A**). The injection coordinates targeted galaninergic neurons in the LPO area and mice with successfully AAV-DIO-CASP3 virus injections would show no GFP expression whereas GFP would label LPO^{Gal} neurons in the control mice (**Fig. 2.1 A**). Four weeks after viral injection, the mice in both groups were transcardially perfused for GFP-positive cell quantification. AAV-DIO-CASP3 virus injection eliminated about 98% of LPO^{Gal} neurons in the LPO area of *LPO-ΔGal* mice compared with that in *LPO-Gal-GFP* mice (**Fig. 2.1 B**). In *LPO-Gal-GFP* mice, the total number of LPO^{Gal} neurons was 264 ± 28 whereas there was only 5 ± 2 LPO^{Gal} neurons in *LPO-ΔGal* mice (**Fig. 2.1 B**). The distribution of galaninergic neurons across the LPO was also different between *LPO-Gal-GFP* and *LPO-ΔGal* mice (**Fig. 2.1 C**). 40 μm thick brain sections between bregma 0.62 to -0.38 were selected for mapping galaninergic neurons in the LPO (**Fig. 2.1 C**). In *LPO-Gal-GFP* mice, LPO^{Gal} neurons were concentrated between bregma 0.26 to -0.22. The LPO^{Gal} neurons were most concentrated in Bregma 0.02 with approximately 80 galaninergic neurons in each brain section and the number of galaninergic neurons gradually reduced in the caudal LPO area (**Fig. 2.1 C**). The galaninergic (GFP-positive) neurons were hardly

observed in the *LPO-ΔGal* mice and there were far fewer LPO^{Gal} neurons in the caudal LPO area compared to that in *LPO-Gal-GFP* mice (**Fig. 2.1 C**).

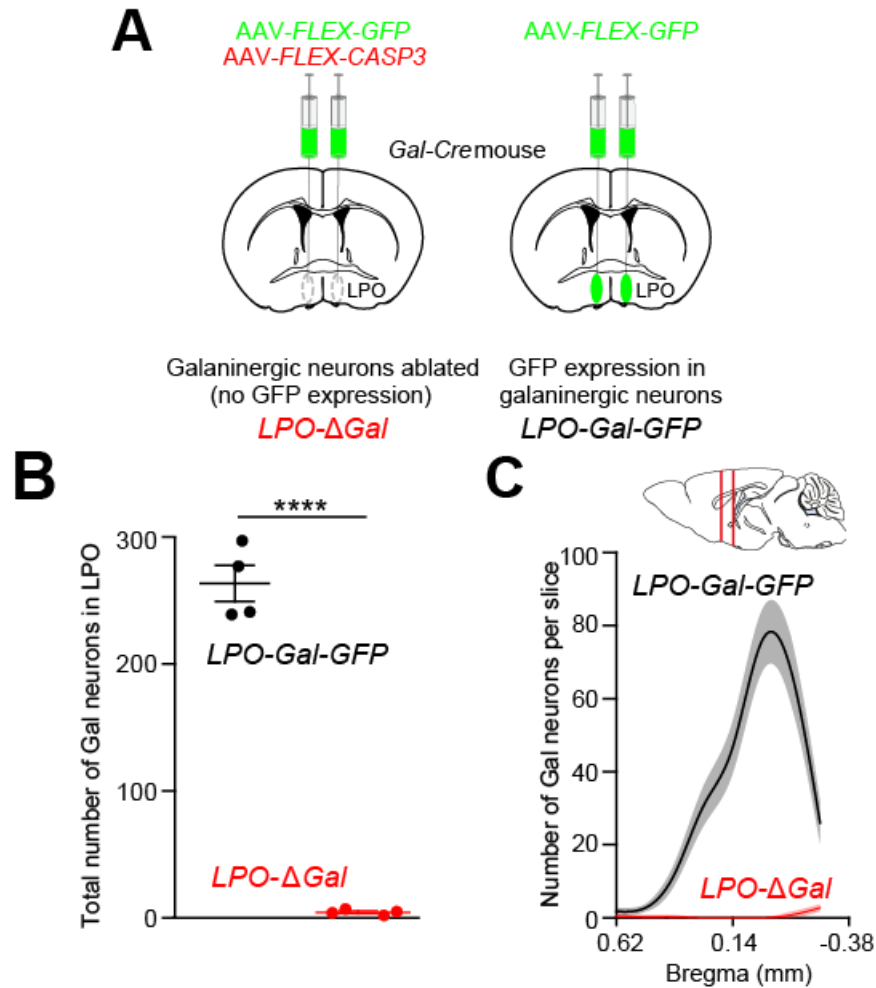


Figure 2.1 Selective ablation using Cre recombinase specifically reduced the number of galanergic neurons in the lateral preoptic area (LPO) of the hypothalamus. (A) Illustration of selective ablation of galanergic neurons in the LPO by AAV-DIO-CASP3 virus (together with AAV-DIO-GFP virus) injection in the LPO of Gal-Cre mice to generate LPO-ΔGal animal. Control mice (LPO-Gal-GFP) were injected with AAV-DIO-GFP virus alone. **(B)** Viral injection successfully ablated galanergic neurons (~98%) in the LPO (**** $P < 0.0001$; paired two-tailed t -test). **(C)** Rostral-caudal distribution of galanergic neurons in cell number in the LPO before and after selective ablation. (LPO-ΔGal, red; $n=4$. LPO-Gal-GFP, black; $n=4$.) For the data in (B) and (C), brain sections containing the LPO area from 4 individual mice were selected for each group, *i.e.* 4 coronal brain slices for each coordinate for the quantification of one group. All error bars represent the S.E.M..

Brain sections between Bregma 0.26 to -0.22, covering most of the LPO area according to the Mouse Brain Atlas (The Allen Brain Atlas, <http://www.brain-map.org>), were selected for immunohistochemistry against GFP expression (**Fig. 2.2 A**). In *LPO-Gal-GFP* mice, there was strong GFP expression focused in the LPO area (partially on the edge of the MPO area) with densest signal around Bregma 0.02 (**Fig. 2.2 B**). In contrast, there was barely any GFP expression observed in the LPO area in *LPO-ΔGal* mice, indicating successful ablation of LPO^{Gal} neurons (**Fig. 2.2 C**). Corresponding DAPI staining, which marks DNA, of brain sections from *LPO-ΔGal* mice showed there was no overt tissue damage in the brain, implying the AAV-*DIO-CASP3* virus selectively ablating LPO^{Gal} neurons (**Fig. 2.2 D**).

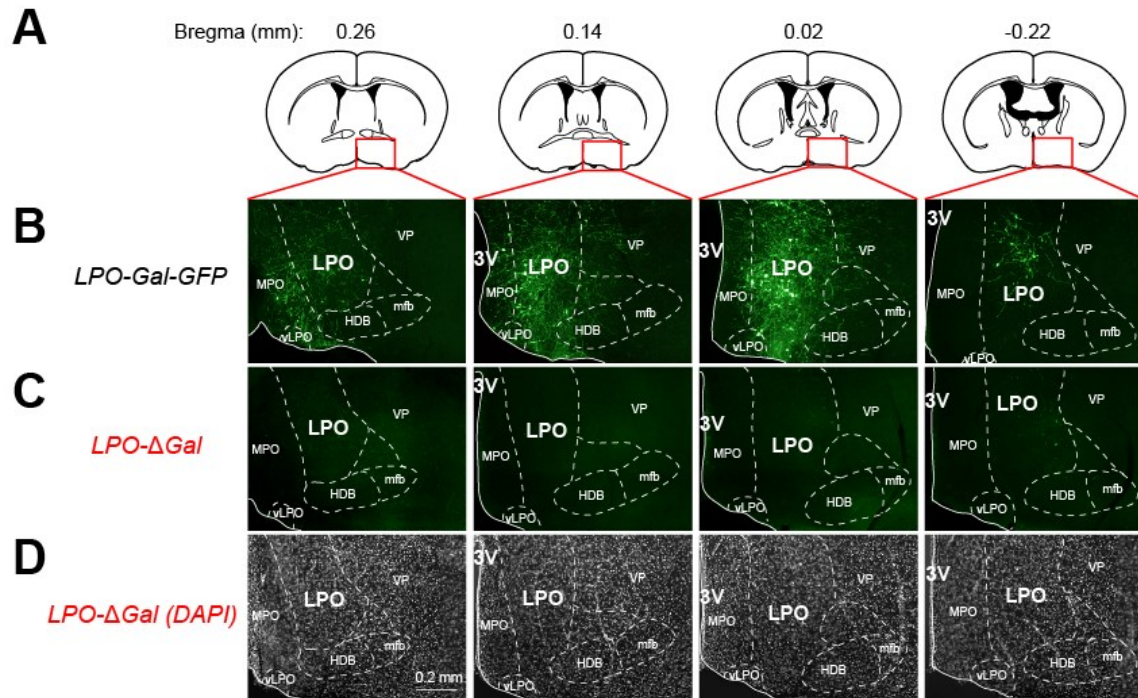


Figure 2.2 Immunohistochemical mapping of galanergic neurons across the LPO both in *LPO-ΔGal* and *LPO-Gal-GFP* mice. **(A)** The LPO area covered sections from Bregma 0.26 to -0.22 according to the Mouse Brain Atlas (The Allen Brain Atlas, <http://www.brain-map.org>). **(B)** Example images showing galanergic neurons in the LPO area by GFP expression of *LPO-Gal-GFP* mice. **(C)** Example images showing galanergic neurons in the LPO area by GFP expression of *LPO-ΔGal* mice. **(D)** Corresponding images of DAPI staining in (C) of *LPO-ΔGal* mice. 3V, the third ventricle; HDB, magnocellular preoptic nucleus; LPO, lateral preoptic nucleus; mfb, medial forebrain bundle; MPO, medial preoptic nucleus; vLPO, ventrolateral preoptic nucleus; VP, ventral pallidum.

To further confirm *AAV-DIO-CASP3* virus selectively targeting LPO^{Gal} neurons, parvalbumin neurons, an independent neuronal population not expressing galanin[249], was selected for immunohistochemistry. For this particular experiment, *AAV-DIO-mCherry* virus was injected to both mouse groups instead of *AAV-DIO-GFP* virus to avoid antibody species cross reactivity. Immunohistochemistry against mCherry showed dense galanergic neurons expressed restrictedly in the LPO in control mice (**Fig. 2.3 A**), similar to the pattern in **Fig. 2.2 B**. Same brain section was stained against parvalbumin antibody as well (**Fig. 2.3 A**). A similar expression pattern of parvalbumin was observed in the *LPO-ΔGal* mice without mCherry-positive neurons in the LPO (**Fig. 2.3 A**), indicating LPO^{Gal} neurons were selectively ablated by *AAV-DIO-CASP3* virus. Quantification of parvalbumin-positive neurons in the LPO area demonstrated there was no significant difference of the total number of LPO^{Parv} neurons between *LPO-ΔGal* mice and control mice, with approximate 350 LPO^{Parv} neurons in both mouse groups (**Fig. 2.3 B**).

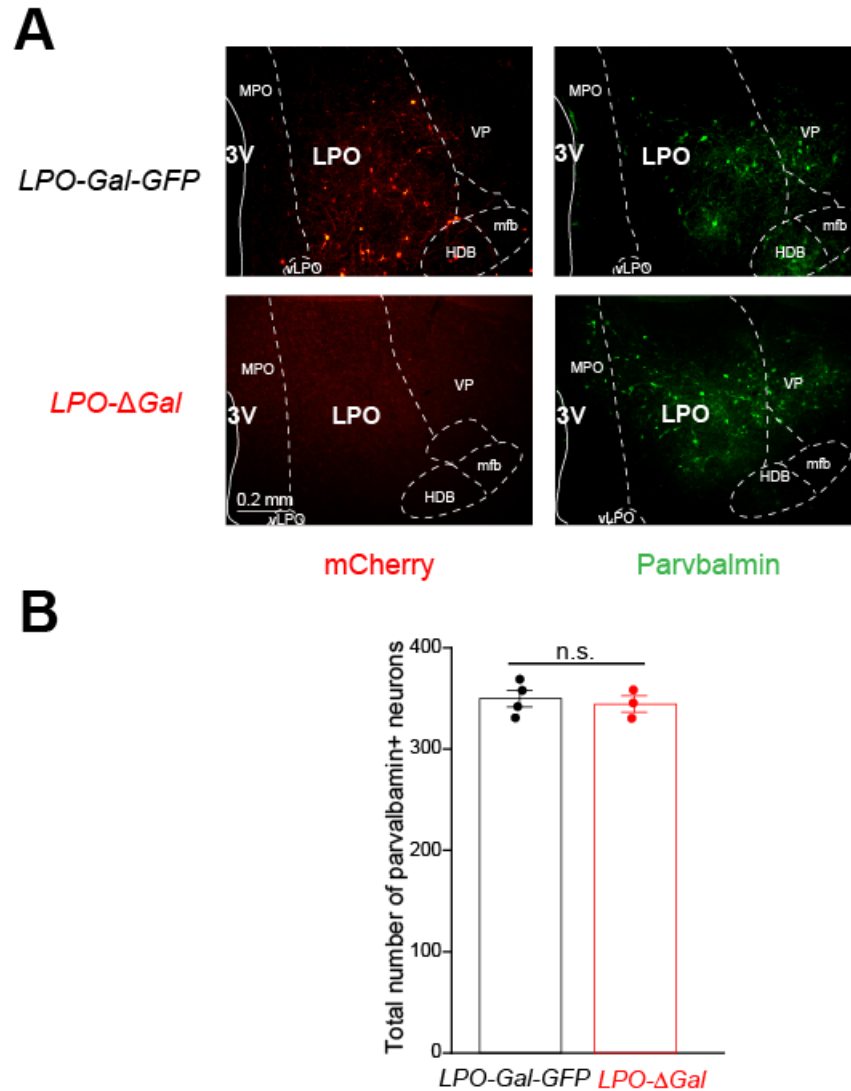


Figure 2.3 Neural ablation by AAV-DIO-CASP3 was restricted to galanergic neurons in the LPO, and did not affect other neuronal types, e.g. parvalbumin neurons. (A) Example images of galanergic neurons (in red) and parvalbumin neurons (in green) from both *LPO-Gal-GFP* and *LPO-ΔGal* mice. **(B)** Quantification of total parvalbumin neurons in the LPO area. (*LPO-Gal-GFP*, black; $n=4$. *LPO-ΔGal*, red; $n=3$.) 3V, the third ventricle; HDB, magnocellular preoptic nucleus; LPO, lateral preoptic nucleus; mfb, medial forebrain bundle; MPO, medial preoptic nucleus; vLPO, ventrolateral preoptic nucleus; VP, ventral pallidum. All error bars represent the S.E.M..

Galaninergic neurons in the LPO area are needed for consolidated NREM sleep

To investigate the role of LPO^{Gal} neurons involved in sleep regulation, sleep data were recorded using Neurologger 2A devices. The devices recorded raw electroencephalogram (EEG) and electromyography (EMG) spectra data. Mice were given at least 2 hrs to adapt to the fitted devices before recordings started. Examples of the first 6 hr segment of baseline recordings from both *LPO-Gal-GFP* and *LPO-ΔGal* mice were extracted and investigated in detail (**Fig. 2.4 A and B**). Vigilance states were auto scored (with manual corrections) into WAKE, NREM, and REM states based on real-time EEG and EMG data, which are shown in indigo, green and sky blue, respectively (**Fig. 2.4 A and B**). High EMG periods were considered as wake if accompanied by low EEG δ power (0.5-4 Hz); high δ power periods were considered as NREM if accompanied by low EMG tone; Within sleep, periods of exclusively high EEG θ (6-10 Hz)/ δ power ratio were considered as REM if accompanied by low EMG tone. Frequency composition characteristic of each vigilance state, *i.e.* WAKE, NREM and REM, would be distinctively presented after Fast Fourier Transforms (FFT) (**Fig. 2.4 A and B**).

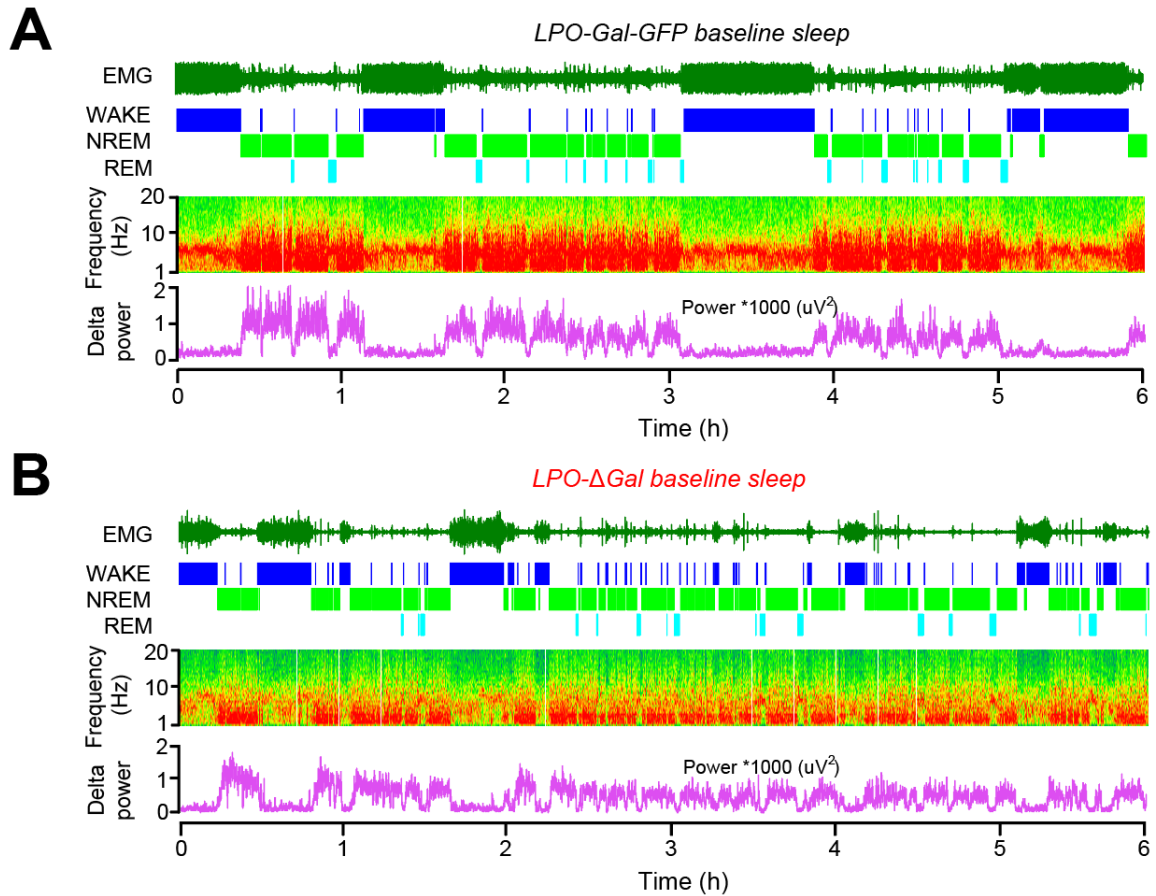


Figure. 2.4 Ablation of LPO^{Gal} neuron increased WAKE and NREM episode numbers and reduced WAKE and NREM durations. (A) Example of 6 hrs (ZT0-ZT6) of raw EEG and EMG spectra data and vigilance-state scoring for *LPO-Gal-GFP* mouse. **(B)** Example of 6 hrs (ZT0-ZT6) of raw EEG and EMG spectra data and vigilance-state scoring for *LPO-ΔGal* mouse.

The 24-hour sleep/wake cycle (12 hrs “lights-on”: 12 hrs “lights-off”) was first examined to reveal how LPO^{Gal} neuron ablation influenced natural sleep/wake cycle. A full cycle of 24 hr natural sleep was recorded starting from ZT0 (the start of “lights-on”) and took place in the home cages. Hourly vigilance state analysis showed both *LPO-Gal-GFP* and *LPO-ΔGal* mice had a normal circadian sleep pattern over 24 hrs recording with a higher percentage of sleep (NREM+REM) during “lights-on” period (inactive phase) and lower percentage of sleep during “lights-off” period (active phase) (**Fig. 2.5 A**). However, *LPO-Gal-GFP* mice had a higher percentage of wakefulness compared with *LPO-ΔGal* mice during “lights-off” period (**Fig. 2.5 A**). Indeed, when total time in WAKE, NREM and REM was calculated, there was a modest but significant increase of time spent in NREM sleep of *LPO-ΔGal* mice than *LPO-Gal-GFP* mice during “lights-off” period and correspondingly reduction of time spent in WAKE (**Fig. 2.5 B**). This effect only presented in the “lights-off” period, not in the “lights-on” period, and there was no change of the time spent in REM sleep either in “lights-off” or “lights-on” period (**Fig. 2.5 A and B**).

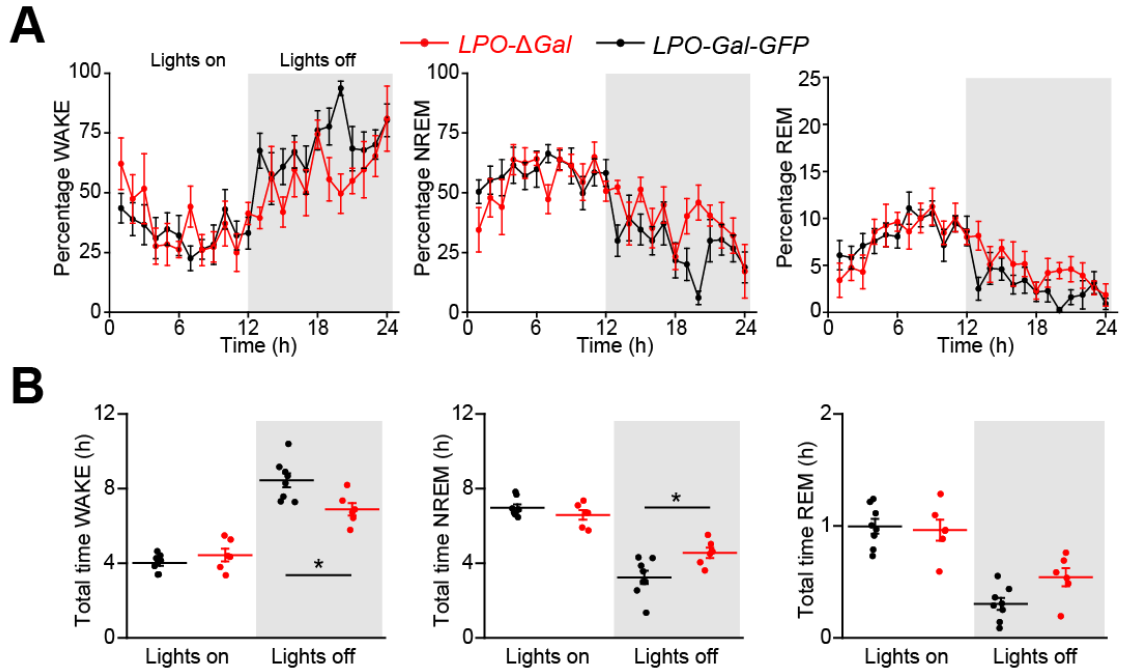


Figure 2.5 Ablation of galanergic neurons in the LPO caused a modest change in sleep time during “lights-off” period. (A) Percentage of WAKE, NREM and REM from baseline recordings across 24 hrs (one circadian cycle) of both $LPO-\Delta Gal$ and $LPO-Gal-GFP$ mice. **(B)** Total time spent in WAKE, NREM, and REM in “lights-on” and “lights-off” periods. Total WAKE time was slightly reduced ($*P < 0.05$; unpaired two-tailed t -test) and total NREM time was slightly increased ($*P < 0.05$; unpaired two-tailed t -test) during “lights-off” period, not “lights-on” period. ($LPO-\Delta Gal$, red; $n=6$. $LPO-Gal-GFP$, black; $n=8$.) All error bars represent the S.E.M..

The EEG is an important parameter for recording the electrical activity of the brain during WAKE and sleep. Although there was only a modest change of NREM sleep amount during “lights-off” period, I was interested in whether the ablation of LPO^{Gal} affected the EEG power of $LPO-\Delta Gal$ mice. As for the analysis of sleep amount, the EEG power was also analysed separately in “lights-on” and “lights-off” (**Fig. 2.6 A and B**). The EEG power of the WAKE state across whole 12 hrs was normalised to 1 in both periods respectively and the corresponding power of the NREM state was further normalised. There were no significant differences in the baseline EEG power in either the WAKE state or NREM state between $LPO-Gal-GFP$ and $LPO-\Delta Gal$ mice (**Fig. 2.6 A and B**).

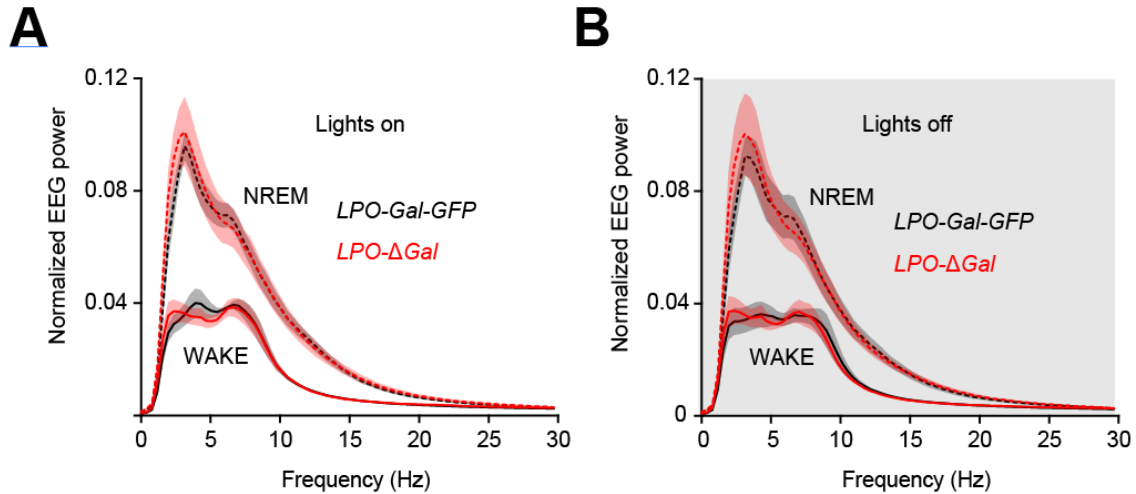


Figure. 2.6 Ablation of LPO^{Gal} did not affect EEG power either in WAKE or NREM state. (A) EEG power normalized such that the area under the curve was unity during WAKE state of *LPO-Gal-GFP* and *LPO-ΔGal* mice in “lights-on” period. **(B)** EEG power normalized such that the area under the curve was unity during WAKE state of *LPO-Gal-GFP* and *LPO-ΔGal* mice in “lights-off” period. (*LPO-ΔGal*, red; $n=6$. *LPO-Gal-GFP*, black; $n=6$.) All error bars represent the S.E.M..

Mice shift between NREM and REM sleep, as well as WAKE. The sleep durations and the number of sleep episodes are important for defining sleep architecture. The raw sleep data of the first 6 hrs of 24-hr baseline natural sleep recording showed that *LPO-ΔGal* mice appeared to have more NREM sleep episodes and the duration of these NREM episodes were shorter compared to the ones of *LPO-Gal-GFP* mice (**Fig. 2.5 A and B**). The number of NREM episodes was increased from 127 ± 7 of *LPO-Gal-GFP* mice to 160 ± 11 of *LPO-ΔGal* mice during “lights-on” period and this increase was more remarkable during the “lights-off” period (*LPO-Gal-GFP*: 68 ± 9 ; *LPO-ΔGal*: 132 ± 8) (**Fig. 2.7 A**). By contrast, as the total time spent in NREM sleep of *LPO-ΔGal* mice was just slightly increased and only during “lights-off” period (**Fig. 2.5 B**), the NREM episode duration of *LPO-ΔGal* mice was significantly shortened in both “lights-on” and “lights-off” periods (**Fig. 2.7 B**). The raw sleep recordings also showed the fragmented and shorter NREM episodes of *LPO-ΔGal* mice were majorly interrupted by WAKE episodes (**Fig. 2.4 B**). As a result, the corresponding WAKE episodes number of *LPO-ΔGal* mice was significantly elevated in both periods, especially during the “lights-off” period (**Fig. 2.7 A**). Furthermore, compared to *LPO-Gal-GFP* mice, the WAKE episode duration was also shortened in *LPO-ΔGal* mice during “lights-off” period (**Fig. 2.7 B**). The continuous interruption of NREM sleep by WAKE caused a marked increase of the transitions between these two vigilance states in both periods (**Fig. 2.7 C**). However, the ablation of LPO^{Gal} only affected WAKE and NREM states, not the REM state. Neither the episode number nor the episode duration of REM sleep was changed in *LPO-ΔGal* mice compared with the control mice and transitions between REM and other vigilance states did not change neither (**Fig. 2.7 A, B and C**).

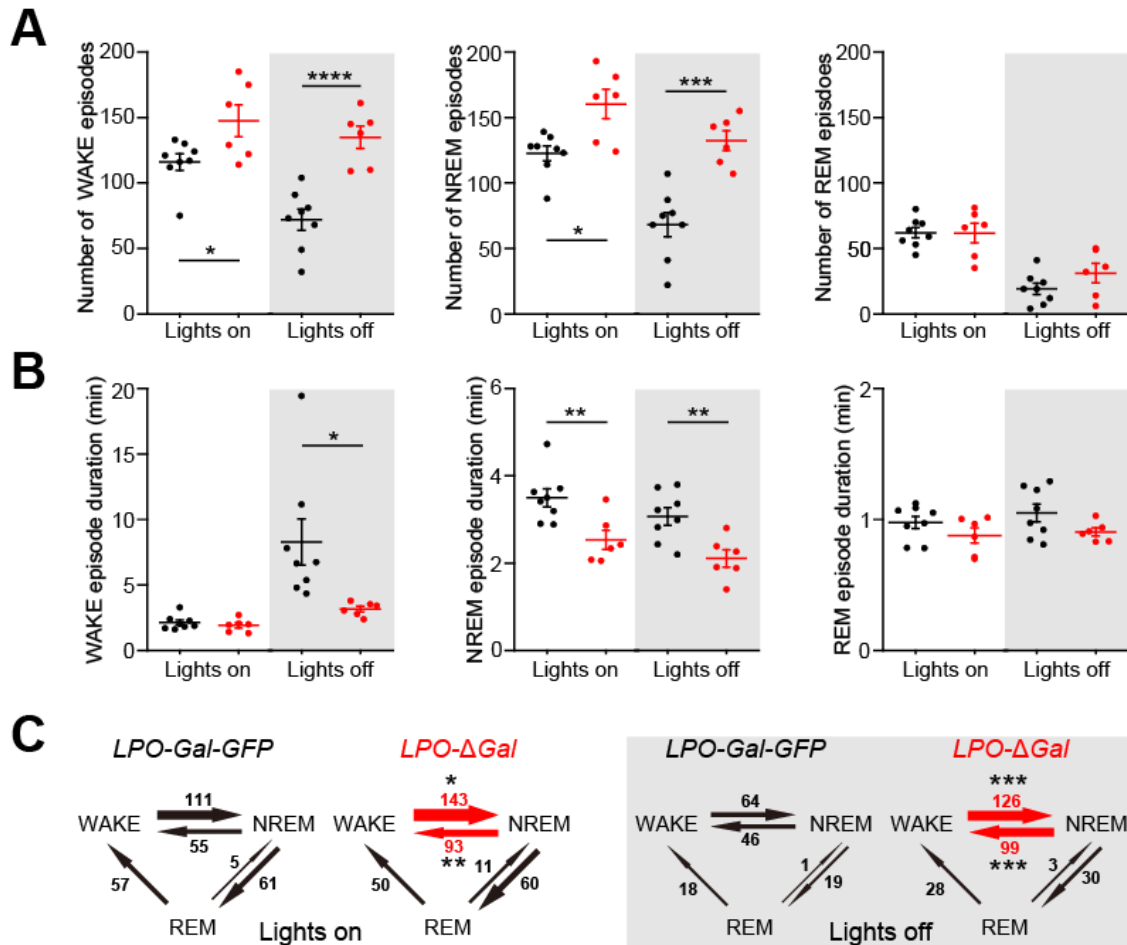


Figure 2.7 Ablation of LPO^{Gal} caused profound fragmentation in sleep architecture. (A) Ablation of LPO^{Gal} increased number of episodes of both WAKE and NREM, but not REM. **(B)** The episode duration of NREM was strikingly reduced in both “lights-on” and “lights-off” periods and the episode duration of WAKE was reduced only in “lights-off” period. **(C)** The number of WAKE to NREM and NREM to WAKE transitions were significantly increased in both “lights-on” and “lights-off” periods, but transitions between other vigilance states did not change. (*LPO-ΔGal*, red; *n*=6. *LPO-Gal-GFP*, black; *n*=8.) **P*<0.05, ***P*<0.01, ****P*<0.001, *****P*<0.0001. All error bars represent the S.E.M..

Ablation of LPO^{Gal} neurons caused chronic elevation of body temperature

Five weeks after ablation of galaninergic neurons in the LPO area, *LPO-ΔGal* mice had a striking increase in their average core body temperatures compared with *LPO-Gal-GFP* mice (**Fig. 2.8 A and B**). In a continuous recording of body temperature over 5 days (120 hrs), the *LPO-ΔGal* mice still retained a normal diurnal variation of their body temperature with a lower temperature during “lights-on” period (inactive phase) and a higher temperature during “lights-off” period (active phase), the same as the controls (**Fig. 2.8 A and B**). However, the average body temperature of the *LPO-ΔGal* mice was raised to 36.9 °C, compared with the average 35.4 °C of the *LPO-Gal-GFP* controls (**Fig. 2.8 A and B**). In addition, the range of daily core body temperature changes during the 24-hr diurnal cycle increased from 1 °C (*LPO-Gal-GFP*) to 2 °C (*LPO-ΔGal*). In the *LPO-Gal-GFP* control group, the average body temperature during the “lights-on” and “lights-off” period was around 35 °C and 36 °C respectively, whereas the *LPO-ΔGal* group had their average “lights-on” and “lights-off” body temperature around 36 °C and 38 °C respectively (**Fig. 2.8 C**). Thus, LPO^{Gal} neurons must be acting chronically to induce body cooling.

A new feature also emerged in the diurnal temperature variation of the *LPO-ΔGal* mice. In *LPO-ΔGal* mice, a pronounced spike in body temperature appeared just prior to the transition from “lights-off” to “lights-on” at ZT24 (see red bars in **Fig. 2.7 A and B**), which was not evident in the *LPO-Gal-GFP* control mice.

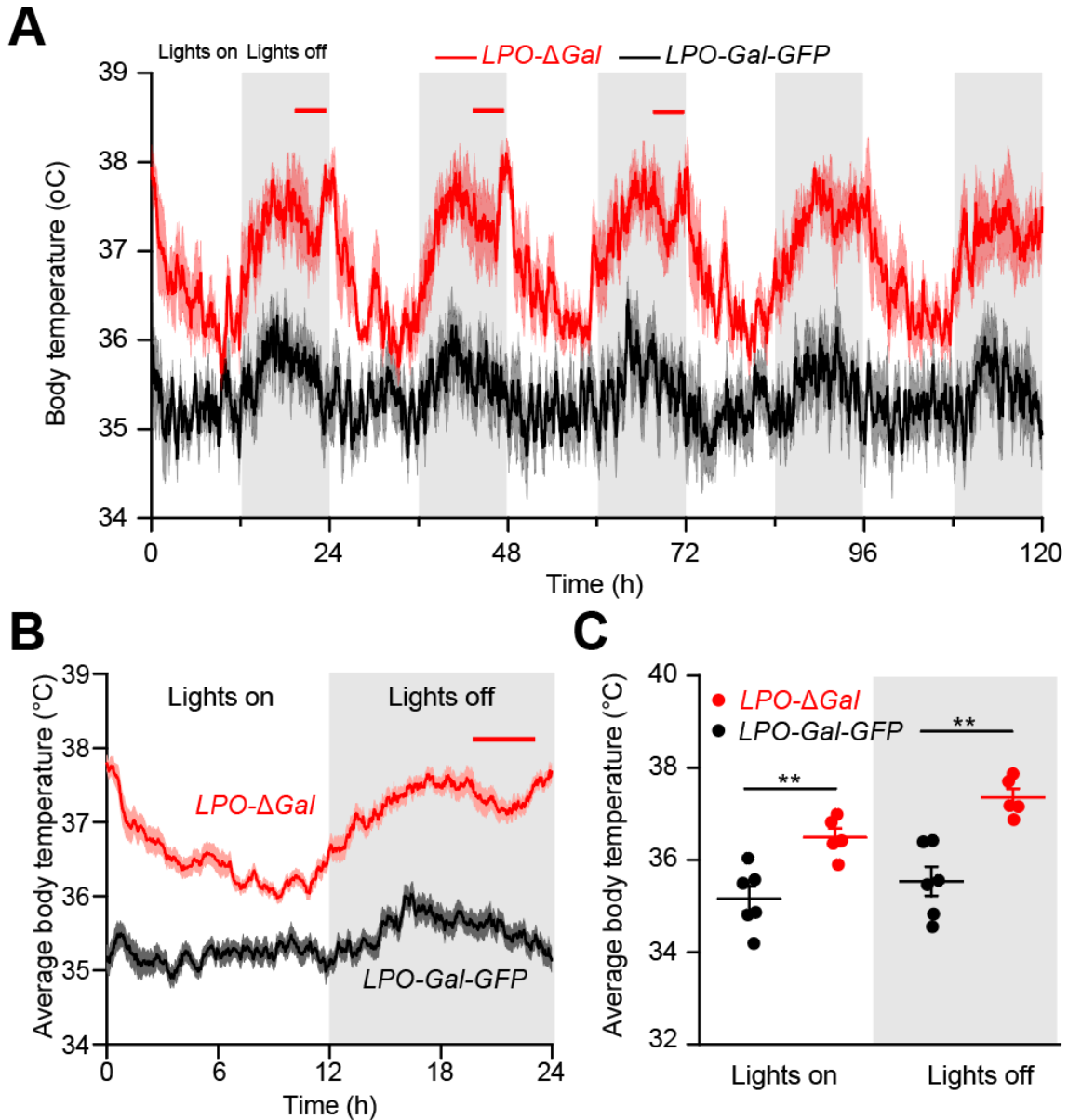


Figure. 2.8 Chronic ablation of LPO^{Gal} markedly elevated core body temperature. **(A)** Ablation of LPO^{Gal} neurons caused increases in both the average core body temperature and its diurnal variation. The record shows typical recordings over five days for both *LPO-ΔGal* mice and control *LPO-Gal-GFP* mice. **(B)** Average core body temperature over 24 hours also shows an abrupt and transient increase in body temperature around the transition from “lights-off” to “lights-on” in the *LPO-ΔGal* mice but not the control *LPO-Gal-GFP* mice. **(C)** Average core body temperature

increased in *LPO-ΔGal* mice in both “lights on” and “lights off” (** $P < 0.01$, unpaired two-tailed t -test). (*LPO-Gal-GFP*, black; $n=6$. *LPO-ΔGal*, red; $n=5$). All error bars represent the S.E.M..

When mice are in their high activity state, they have higher body temperatures. As shown in **Fig. 2.8**. In “lights-off” period (active phase), the mice had higher average body temperature while they had relative lower average body temperature when they were in the “lights-on” period (inactive phase) (**Fig. 2.8 A, B and C**). To determine whether this hyperthermia after LPO^{Gal} ablation was caused by hyperactivity of *LPO-ΔGal* mice, both *LPO-Gal-GFP* and *LPO-ΔGal* mice were tested for locomotor activity in an open-field (30*30 cm). Mice were allowed to run freely in the open-field for 30 mins in “lights-off” period (around ZT18) when they had their highest body temperature during the day. Both speed and distance of travel of the mice were recorded. There was no significant difference in locomotor activity between *LPO-Gal-GFP* controls and *LPO-ΔGal* mice, either in the speed of running or the total distance travelled in 30 mins (**Fig. 2.9 A and B**). This indicated that the raised body temperature of *LPO-ΔGal* mice was not explained by raised motor activity.

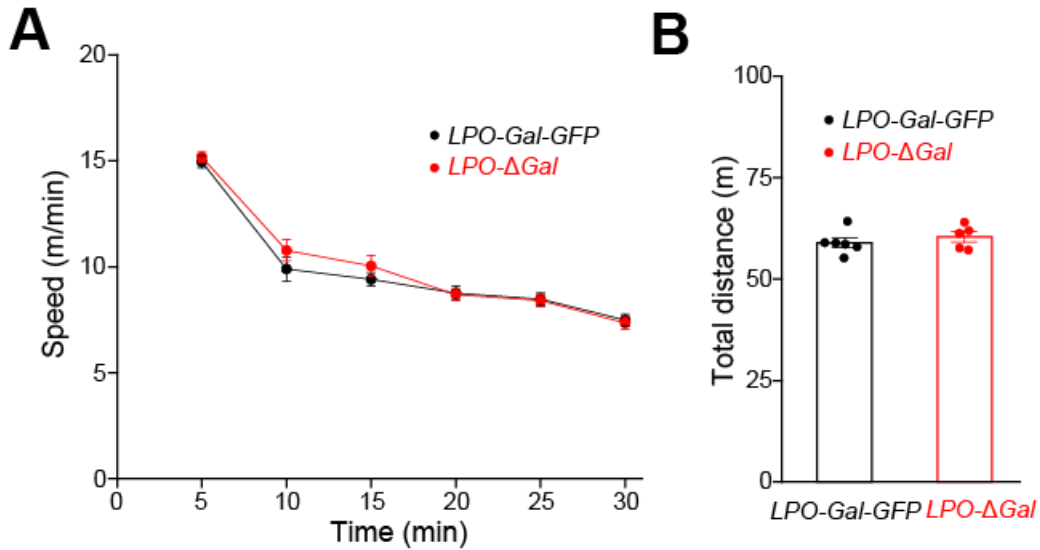


Figure. 2.9 Locomotion activity was not affected by ablation of LPO^{Gal} neurons. (A) The locomotion activity with an open field test over 30 mins in the “lights-off” period showed no difference between *LPO-Gal-GFP* and *LPO-ΔGal* mice ($P>0.93$, repeated measures one-way ANOVA with post hoc test). **(B)** Total distance of 30 mins open field locomotion activity showed no difference between *LPO-Gal-GFP* and *LPO-ΔGal* mice either ($P>0.98$, unpaired two-tailed *t*-test). (*LPO-Gal-GFP*, black; $n=6$. *LPO-ΔGal*, red; $n=6$.) All error bars represent the S.E.M..

Galaninergic neurons in the LPO contribute to sleep homeostasis

Besides sleep time, sleep architecture and core body temperature, I next examined how ablation of galaninergic neurons in the LPO affected sleep homeostasis of mice. The phenomenon of sleep homeostasis is that the sleep following sleep deprivation is longer and deeper and has an increased power of δ oscillations[119, 214-216], and the mice also try to catch up on their lost sleep. Therefore, both *LPO-Gal-GFP* and *LPO- Δ Gal* mice underwent a 5-hr sleep deprivation. The sleep deprivation started at ZT0 (the beginning of “lights-on” period) when the mice had their strongest sleep drive. Mice were sleep deprived by introducing novel objects in new cages and gentle tapping on the cages. Handling was kept at the minimum to avoid bringing any stress to the mice. Mice were transferred back to their original home cages for recovery sleep after sleep deprivation. Their EEG/EMG signals were recorded from the beginning of the sleep deprivation continuing until the end of a full 24-hr circadian cycle. Mice from both groups experienced a full 5-hr sleep deprivation and had a strong reduction in WAKE compared to their own baseline sleep (**Fig. 2.10 A and B**). However, in *LPO-Gal-GFP* control mice, there was an increase in total sleep (NREM + REM sleep) and the main effect occurred during the “lights-off” period following sleep deprivation (which was carried out during the “lights-on” period) compared to their baseline diurnal variation in WAKE and sleep times (**Fig. 2.10 A**). This recovery sleep following sleep deprivation was almost abolished in *LPO- Δ Gal* mice. Compared to their own baseline wake and sleep times, there was no obvious increase in total SLEEP (NREM + REM sleep) time after 5-hr sleep deprivation (**Fig. 2.10 B**).

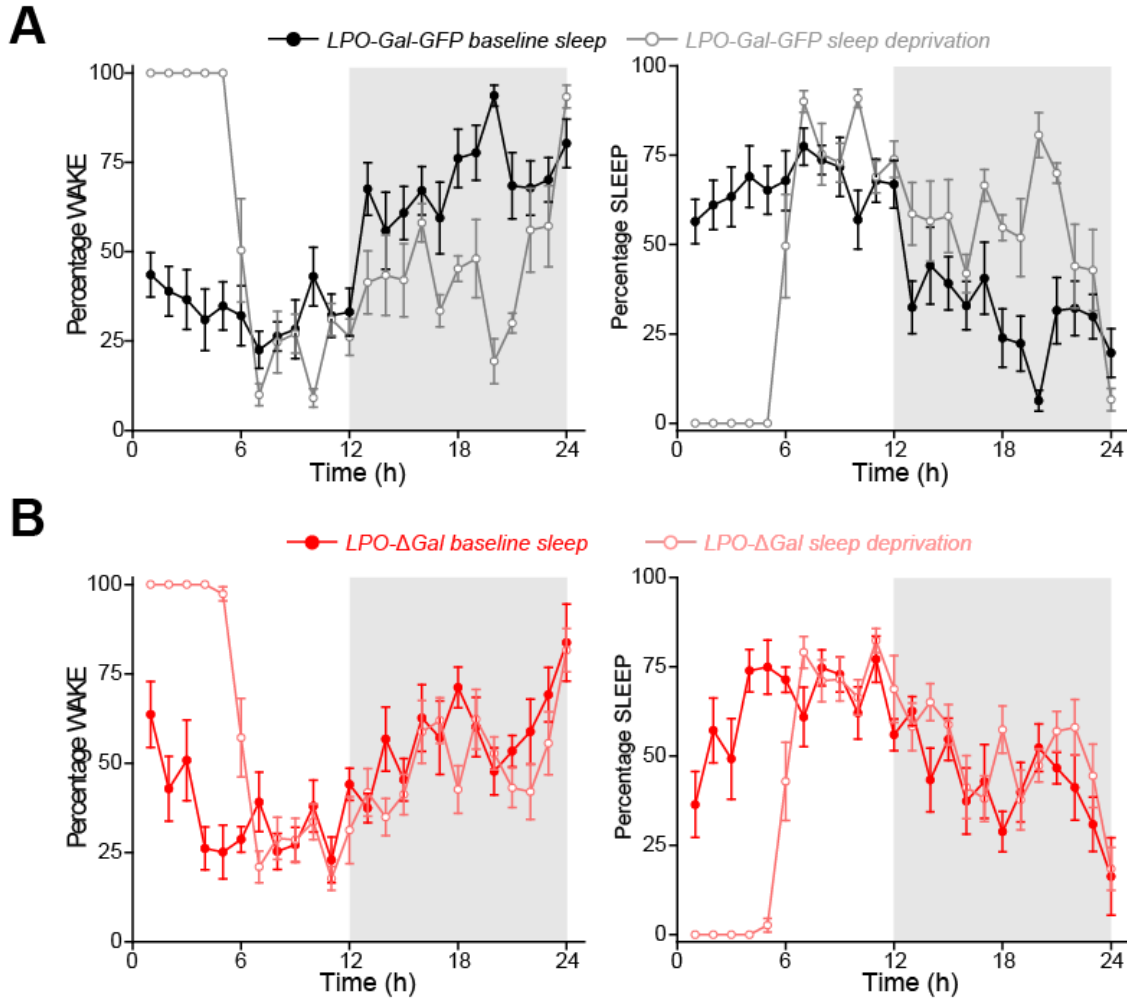


Figure 2.10 The increase of percentage of total SLEEP (NREM+REM sleep) was not observed in the *LPO-ΔGal* mice after 5 hrs SD (ZT0-ZT5) over a full circadian cycle (24 hrs). **(A)** The percentage of total SLEEP was increased in the *LPO-Gal-GFP* mice after 5 hrs sleep deprivation. **(B)** The percentage of total SLEEP remains unchanged in the *LPO-ΔGal* mice after 5 hrs sleep deprivation. (*LPO-Gal-GFP*, black/grey; $n=6$. *LPO-ΔGal*, red/light red; $n=5$). All error bars represent the S.E.M..

Statistical analysis revealed mice from both groups lost over 3 hrs of total sleep by 5-hr sleep deprivation (**Fig. 2.11 A**). In the next 19 hrs following sleep deprivation, *LPO-Gal-GFP* control started catching up their lost sleep and at the end of the day, approximately 80% of lost sleep due to sleep deprivation was recovered (**Fig. 2.11 A**). By contrast, *LPO-ΔGal* mice only caught up about 22% of lost sleep after 19 hrs (**Fig. 2.11 A**). Moreover, the sleep recovery rate after sleep deprivation of *LPO-ΔGal* mice was significant reduced (**Fig. 2.11 B**). On average, after sleep deprivation, the *LPO-Gal-GFP* control mice could recover about 0.15 hr of lost sleep every hour while there was barely any recovery sleep observed in *LPO-ΔGal* mice-indeed, one mouse kept losing sleep even when forced sleep deprivation was finished (**Fig. 2.11 B**).

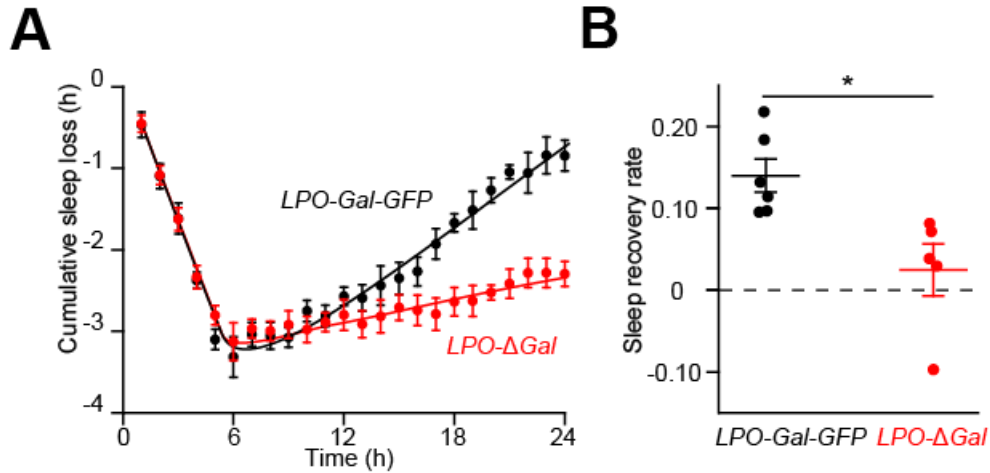


Figure. 2.11 Sleep rebound after 5 hrs SD was nearly abolished in the *LPO-ΔGal* mice over a full circadian cycle (24 hrs). **(A)** Most (~80%) of the sleep lost as a result of 5 hrs of sleep deprivation was recovered after 19 hrs in *LPO-Gal-GFP* mice whereas only ~22% of the sleep loss was recovered in *LPO-ΔGal* mice. **(B)** The sleep recovery rate after sleep deprivation is significantly reduced in *LPO-ΔGal* mice compared with *LPO-Gal-GFP* (* $P < 0.05$, unpaired two-tailed *t*-test). (*LPO-Gal-GFP*, black; $n = 6$. *LPO-ΔGal*, red; $n = 5$). All error bars represent the S.E.M..

One of the features of sleep homeostasis is the δ power increase in the recovery sleep following sleep deprivation [214]. Although the δ power of baseline NREM sleep characteristically varies over 24 hrs, this variation is within a certain range (**Fig. 2.12 A**, also see mouse data in [251]). This δ power baseline was similar between non-sleep deprived *LPO-Gal-GFP* and *LPO- Δ Gal* mice (**Fig. 2.12 A**). After 5-hr sleep deprivation, during the first part of the recovery sleep of *LPO-Gal-GFP* control mice, as expected, the δ wave power was significantly increased compared to the power of δ wave band during natural NREM sleep at the equivalent zeitgeber time (**Fig. 2.12 A**). At the first hour of rebound sleep, the intensity of δ wave power doubled in the *LPO-Gal-GFP* mice (**Fig. 2.12 B**). This increase of δ power later decayed over the next 6 hours after sleep deprivation as the mice gained more recovery sleep, leading it back to the baseline by the start of “lights-off” period (**Fig. 2.12 A**). Although there was still a significant increase in the δ power of recovery sleep in the *LPO- Δ Gal* mice, this effect was strongly reduced (**Fig. 2.12 A**). The δ power intensity of the first hour recovery sleep after sleep deprivation only increased 1.4 folds compared to the δ power of natural NREM sleep at the equivalent zeitgeber time (**Fig. 2.12 B**). Similar to that found in *LPO-Gal-GFP* control mice, the increased δ power of recovery sleep in *LPO- Δ Gal* mice decayed over time and reached the level of baseline at the beginning of “lights-off” (**Fig. 2.12 A**), but this degree of increase was significantly different between *LPO-Gal-GFP* control mice and *LPO- Δ Gal* mice (**Fig. 2.12 B**).

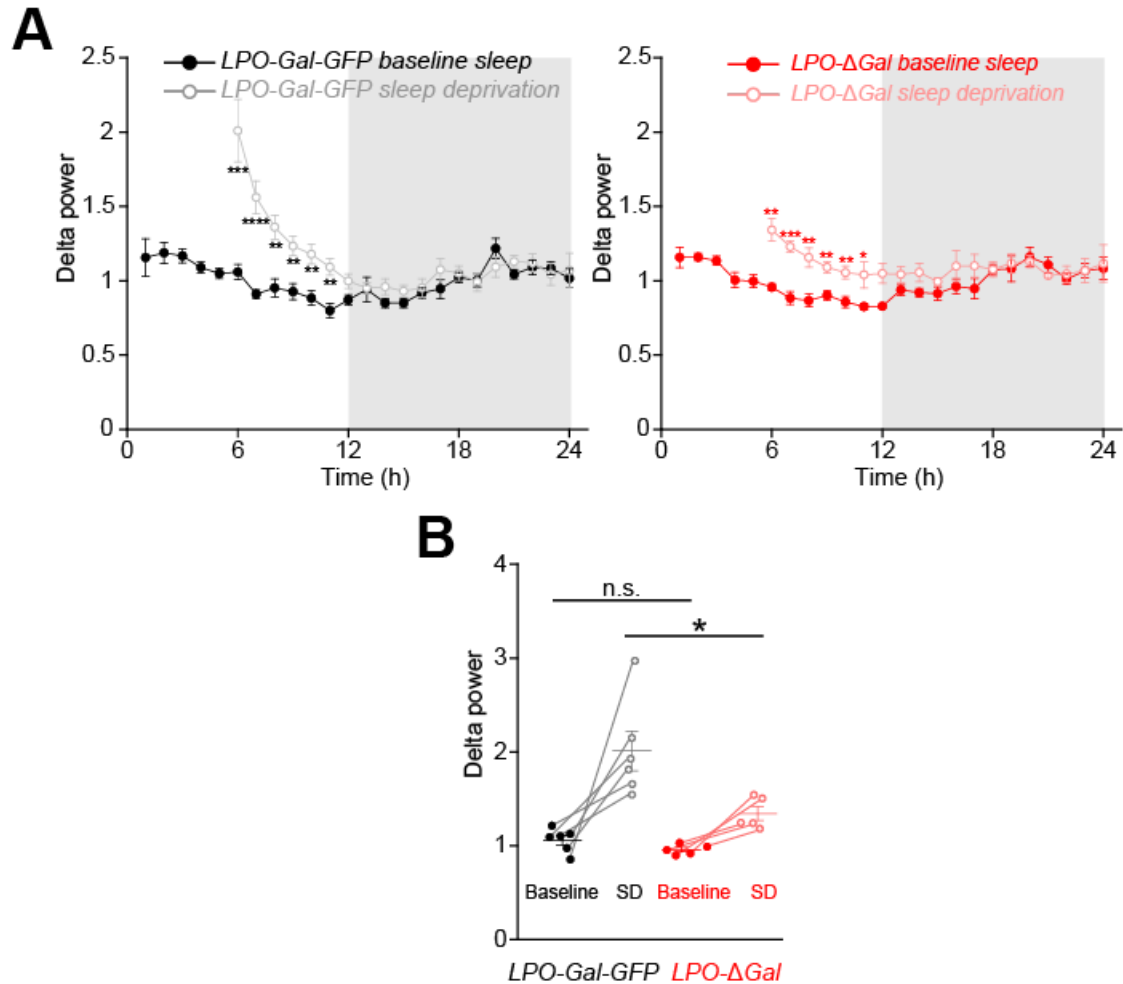


Figure. 2.12 The increase of δ power after SD, one of the hallmarks of sleep homeostasis, was significantly reduced in *LPO-ΔGal* mice. **(A)** Time course of the δ power (0.5 - 4 Hz) after 5 hrs of sleep deprivation in *LPO-Gal-GFP* and *LPO-ΔGal* mice. In *LPO-Gal-GFP*, there was a large increase in δ power after sleep deprivation that decayed over 6 hrs back to baseline. By contrast there was a lower increase in δ power after sleep deprivation in *LPO-ΔGal* mice (* P <0.05, ** P <0.01, *** P <0.001, **** P <0.0001, repeated measures one-way analysis of variance (ANOVA) with post hoc test). **(B)** δ power (0.5 – 4 Hz) in the first hour of recovery sleep compared with baseline sleep in ZT6 for both *LPO-Gal-GFP* and *LPO-ΔGal* mice. *LPO-Gal-GFP* and *LPO-ΔGal* mice had similar δ power in their baseline sleep, but after 5 hrs sleep deprivation, *LPO-Gal-GFP* mice had a larger increase in δ power compared with *LPO-ΔGal* mice (* P <0.05, unpaired two-tailed t -test). (*LPO-Gal-GFP*, black/grey; n =6. *LPO-ΔGal*, red/light red; n =5). All error bars represent the S.E.M..

Chemogenetic activation of LPO^{Gal} neurons promotes sleep and reduces core body temperature

So far, we have seen that selective ablation of LPO^{Gal} neurons caused fragmented sleep structure, chronically increased body temperature and reduced sleep homeostasis (see sections above). To comprehensively investigate the role of LPO^{Gal} neurons in sleep regulation and body temperature control, chemogenetic manipulation was used to activate galaninergic neurons in the LPO acutely. A “designer receptors exclusively activated by designer drugs (DREADD)” receptor, hM₃D_q-mCherry, was selectively expressed in the LPO^{Gal} neurons (**Fig. 2.13 A**). The DREADD receptor was fused with mCherry protein which visualized the expression of the receptor. Immunohistochemistry with mCherry antisera confirmed that the expression of hM₃D_q-mCherry was mainly confined in the LPO area (**Fig. 2.13 B**).

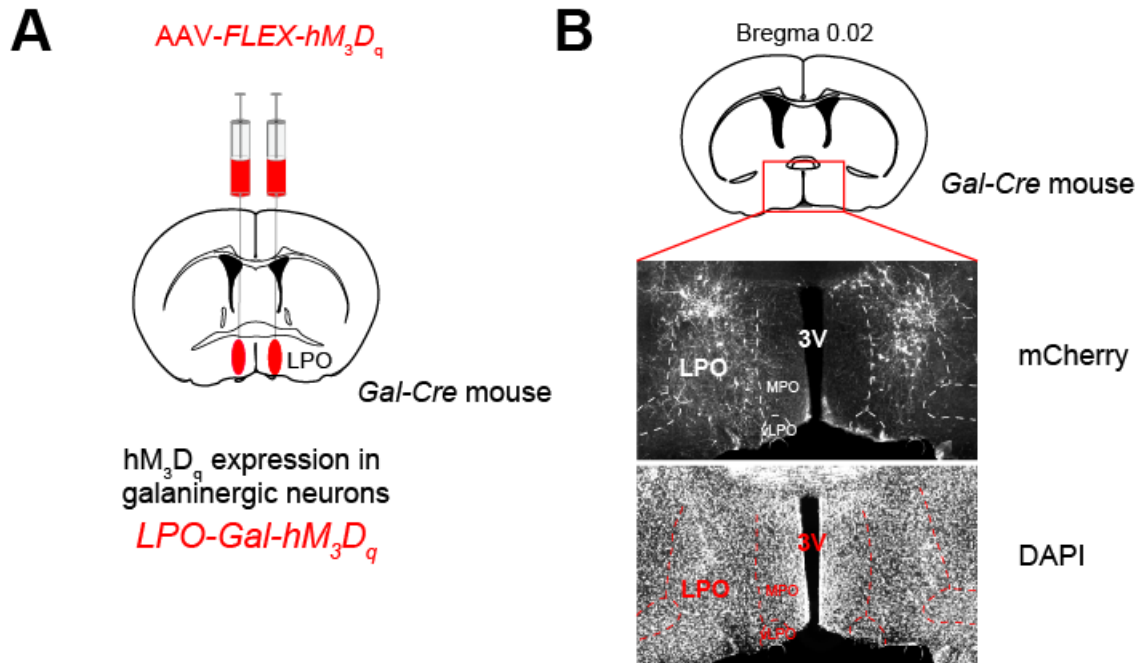


Figure. 2.13 Selective activation of LPO^{Gal} by chemogenetics. (A) Galanin neurons in the LPO of *Gal-Cre* mice were made selectively sensitive to CNO by bilateral injecting *AAV-DIO-hM₃D_q* to generate *LPO-Gal-hM₃D_q* mice. The hM₃D_q receptor is fused to the mCherry protein. (B) Immunohistochemistry against mCherry indicated the hM₃D_q receptor expression was largely restricted to the LPO area. The corresponding DAPI staining is shown below.

The DREADD receptor can be selectively activated by clozapine N-oxide (CNO). 1mg/kg of CNO was injected (*i.p.*) to *LPO-Gal-hM₃D_q* mice to chemogenetic activate LPO^{Gal} neurons at ZT18 (“lights-off” period) when animals were in their highest activity during the day. *LPO-Gal-hM₃D_q* mice were randomly divided into groups either receiving CNO or saline injection. Raw EEG/EMG data showed mice received CNO injection had marked increased NREM sleep 20 mins post-injection, accompanied by hypothermia and these effects lasted for several hours (**Fig. 2.14 A**). By the contrary, saline-injected animals remained their normal activity and body temperature (**Fig. 2.14 B**).

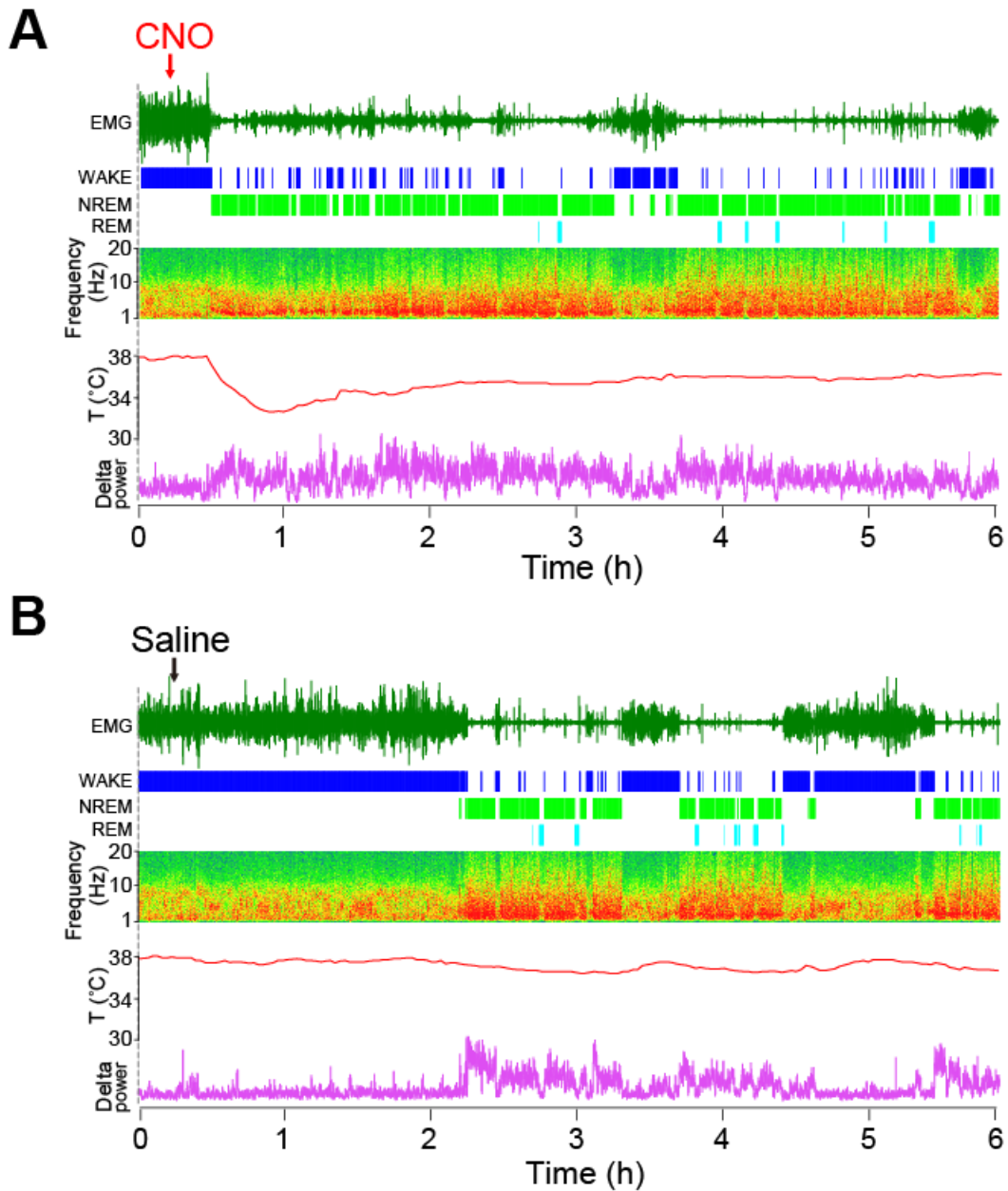


Figure 2.14 Selective chemogenetic activation of LPO^{Gal} neurons by CNO increased NREM sleep and reduced core body temperature. (A) Example of 6 hrs (ZT18-ZT24) of raw EEG and EMG spectra data and vigilance-state scoring for $LPO-Gal-hM_3D_q$ mouse with CNO (1mg/kg, *i.p.*) injection. **(B)** Example of 6 hrs (ZT18-ZT24) of raw EEG and EMG spectra data and vigilance-state scoring for $LPO-Gal-hM_3D_q$ mouse with saline injection.

Indeed, the percentage of WAKE was largely reduced and the percentage of NREM sleep increased remarkably in the first a few hours after 1mg/kg CNO injection compared with mice receiving saline injection (**Fig. 2.15 A**). For the first three hours post-injection, the time spent in WAKE and NREM sleep of CNO-injected mice was significantly different with saline-injected control mice (**Fig. 2.16 B**). But CNO injection did not affect REM sleep (**Fig. 2.15 A and B**).

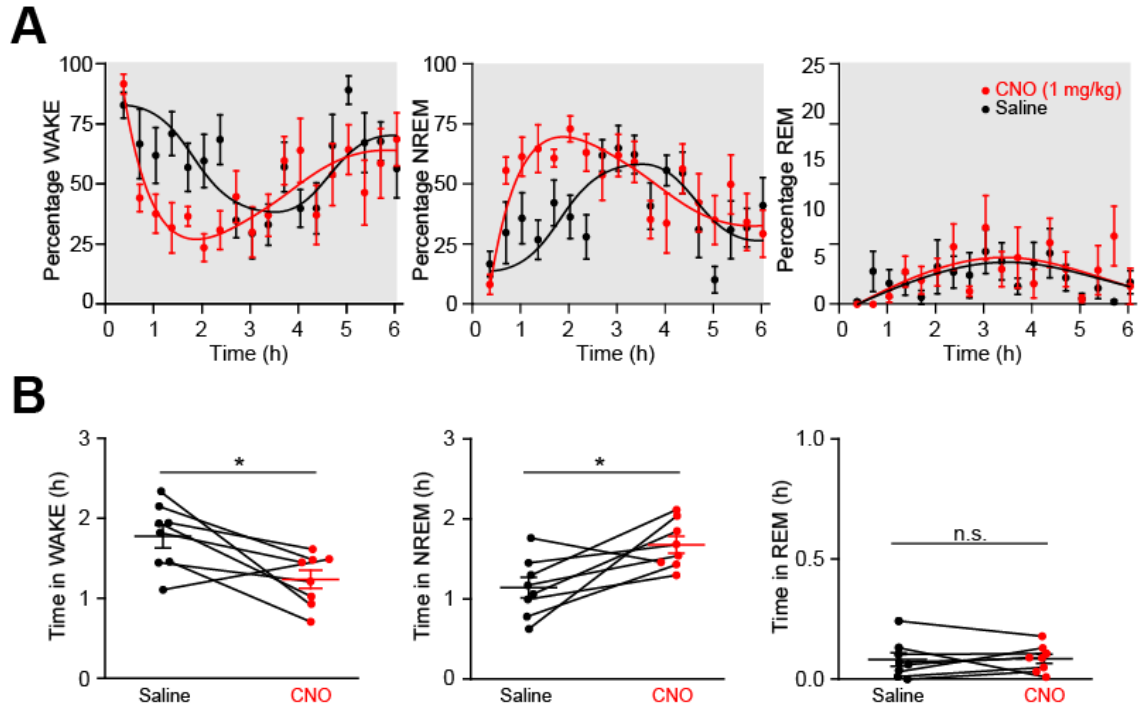


Figure. 2.15 Selective chemogenetic activation of LPO^{Gal} neurons by CNO promoted NREM sleep and the effects lasted for 3 hrs. **(A)** Percentage of WAKE, NREM and REM of $LPO-Gal-hM_3D_q$ mice with CNO (1mg/kg, i.p.) and saline injection of 6 hrs (ZT18-ZT24) recording. **(B)** Total time in WAKE, NREM and REM of $LPO-Gal-hM_3D_q$ mice with CNO (1mg/kg, i.p.) and saline injection over the first 3 hrs post injection. LPO^{Gal} neurons activated by CNO increased time spent in NREM sleep and time in WAKE reduced correspondingly. (* $P < 0.05$, paired two-tailed t -test) (CNO, red; $n=8$. Saline, black; $n=8$). All error bars represent the S.E.M..

Chemogenetic activation of LPO^{Gal} neurons induced NREM sleep (**Fig. 2.14 and 2.15**). The δ power band of CNO-induced NREM sleep in the first three hours post-injection was significantly higher than the natural NREM sleep generated after saline control injections (**Fig. 2.16 A**). The individual δ power band matching comparison showed the majority of mice had elevated δ power of CNO-induced NREM sleep compared with natural NREM sleep after saline injection and this power intensity difference was significant between groups (**Fig. 2.16 B**).

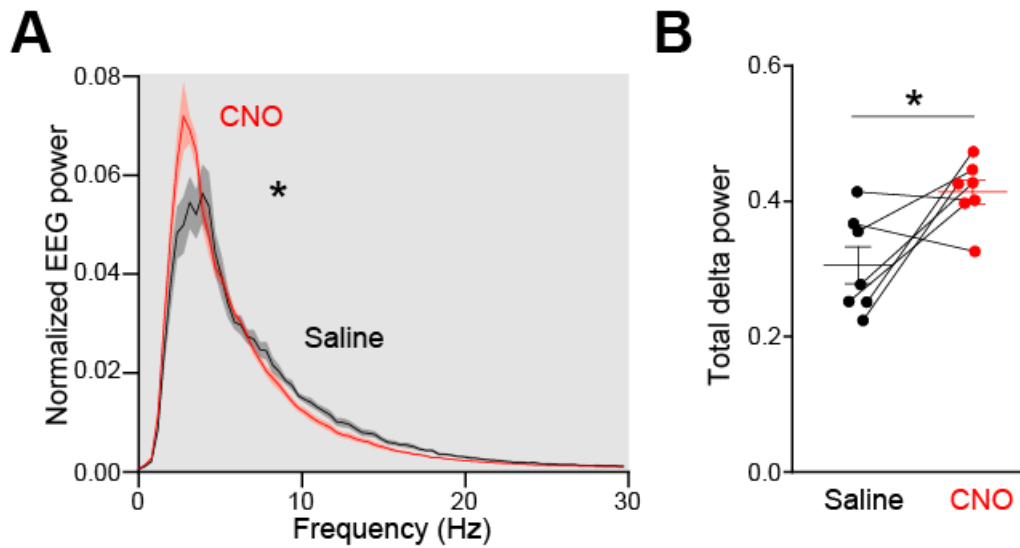


Figure 2.16 NREM sleep induced by chemogenetic activation of LPO^{Gal} neurons by CNO had higher δ power (0.5-4 Hz) than natural NREM sleep. **(A)** Normalized EEG power traces over the first 3 hours post injection showed a significantly higher power around δ power band than that of NREM sleep after saline injection (at the same time of injection at ZT18). **(B)** Statistical analysis of total δ power of the CNO-induced NREM-like sleep and the natural NREM sleep after saline injection. (* $P < 0.05$, paired two-tailed t -test). (CNO, red; $n=7$. Saline, black; $n=7$). All error bars represent the S.E.M..

To confirm the specificity of CNO activation on DREADD receptors, *Gal-Cre* mice were injected with AAV-*DIO-mCherry* virus in the LPO area to generate *LPO-Gal-mCherry* mice which had no DREADD receptor expression on LPO^{Gal} neurons. Similar to *LPO-Gal-hM₃D_q* mice, *LPO-Gal-mCherry* mice were randomly given either 1mg/kg of CNO or saline injection (*i.p.*) at ZT18 (“lights-off” period). There were no obvious changes to the percentage of WAKE, NREM or REM sleep after CNO injection compared with saline injection (**Fig. 2.17 A, B and C**). Detailed analysis on the total time spent on WAKE, NREM and REM sleep of the whole 6 hrs post-injection confirmed there were no differences between CNO injection and saline injection groups of *LPO-Gal-mCherry* mice (**Fig. 2.17 D**).

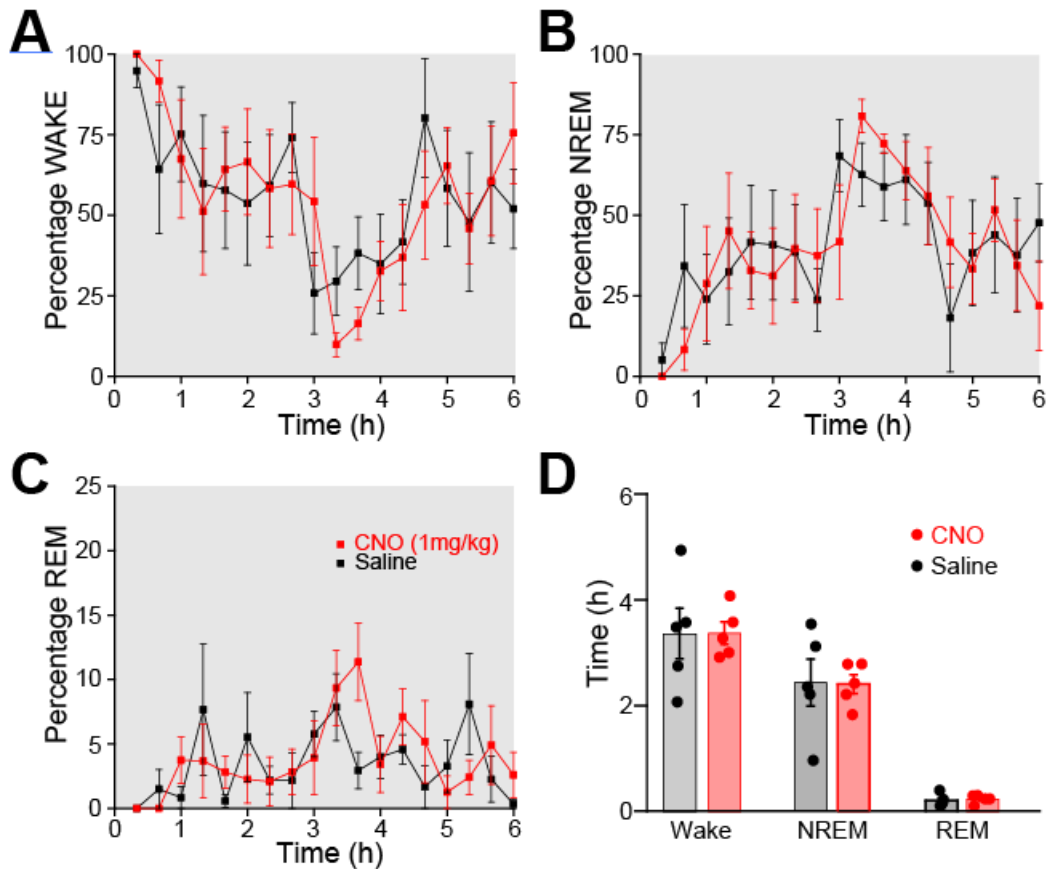


Figure 2.17 CNO injection did not induce NREM sleep in control mice without hM₃D_q receptor compared with saline injection. (A) Percentage of WAKE of *LPO-Gal-mCherry* mice with CNO (1mg/kg, i.p.) and saline injection of 6 hrs (ZT18-ZT24) recording. **(B)** Percentage of NREM. CNO injection did not induce NREM sleep above normally occurring amounts compared with saline injection. **(C)** Percentage of REM. **(D)** Total time in WAKE, NREM and REM of *LPO-Gal-mCherry* mice with CNO (1mg/kg, i.p.) and saline injection over 6 hrs post injection. There was no significant difference between CNO and saline injection. (CNO, red; *n*=5. Saline, black; *n*=5). All error bars represent the S.E.M..

Activating LPO^{Gal} neurons with CNO also induced hypothermia in *LPO-Gal-hM₃D_q* mice (**Fig. 2.14 A, 2.18 A and B**). 20 mins after receiving 1mg/kg of CNO injection (*i.p.*), the body temperature of *LPO-Gal-hM₃D_q* mice started dropping and reached the nadir, around 32 °C, at 1 hr post-injection (**Fig. 2.14 A and 2.18 A**). The CNO-induced hypothermia slowly recovered in the next a few hours and the body temperature of CNO-injected *LPO-Gal-hM₃D_q* mice went back to the same baseline as saline-injected control at 5 hrs post-injection (**Fig. 2.14 A and 2.18 A**). This hypothermic effect was not present in saline-injected *LPO-Gal-hM₃D_q* mice (**Fig. 2.18 A and B**), or *LPO-Gal-mCherry* mice either with CNO or saline injection (**Fig. 2.18 B**).

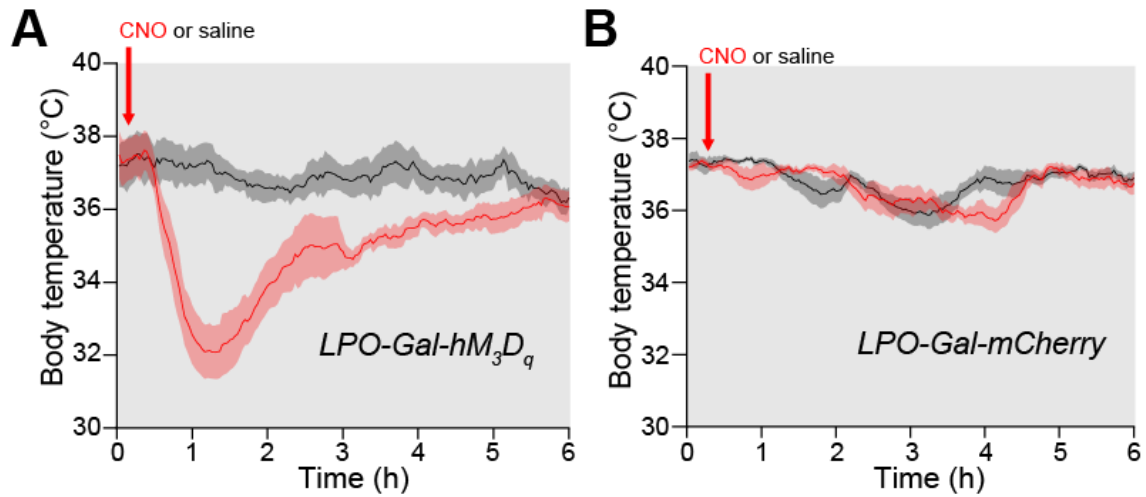


Figure 2.18 CNO induced hypothermia was only produced by activation of LPO^{Gal} neurons with hM₃D_q receptor but not in control mice that did not express hM₃D_q receptor. (A) CNO (1mg/kg, *i.p.*) but not saline injection induced a strong acute hypothermia in *LPO-Gal-hM₃D_q* mice lasting several hours. **(B)** Control for off-target effects. CNO injection to *LPO-Gal-mCherry* mice (without hM₃D_q receptor) did not induce hypothermia compared with mice received saline injections. (CNO, red; *n*=5. Saline, black; *n*=5). All error bars represent the S.E.M..

Discussion

The POA has long been indicated to play a role in sleep/wake regulation, but the neurochemical identity of cell-specific neuronal types remains uncertain. Although previous studies have shown neurons in the LPO area are sufficient to recapitulate NREM-like sleep and hypothermia after sleep deprivation by using cFos-dependent activity-tagging, the cell type involved has not been identified[51]. In this **Chapter**, by cell-specific lesioning, I have demonstrated that those neurons are likely to be galaninergic. With no LPO^{Gal} neurons, the sleep/wake structure becomes highly fragmented, and the sleep homeostasis (*i.e.* the recovery sleep and enhanced δ power in EEG after sleep deprivation) is significantly reduced, indicating that LPO^{Gal} neurons play a role in tracking the time mice spent awake. Although many genes have been demonstrated to modulate sleep homeostasis (see **Introduction**), it is the first time that a specific neuronal cell type is suggested in regulation of sleep homeostasis.

Across the animal kingdom, homeostatic sleep drive is reflected by changing neuronal activity with the time previously spent awake[51, 236, 252]. However, at the circuit level, sleep homeostasis has remained mysterious in mammals. The adenosine[119, 219] released by astrocytes[223] seems to mediate sleep homeostasis partially. As the increased level of adenosine during wakefulness can only be observed in the basal forebrain and not the POA[118, 124], then adenosine cannot directly trigger LPO^{Gal} neurons to induce NREM sleep. It possible that LPO^{Gal} neurons are activated by an unknown messenger released in skeletal muscle that regulated sleep homeostasis[235].

The circuitry regulating body temperature in the POA is complex[239, 241]. Body heating or cooling can be acutely initiated by certain POA neurons including Glut/NOS1-, GABA/galanin-, PACAP/BDNF- and TRPM2-expressing cells, which respond to immediate external or internal thermal challenges[76, 174-176, 239-241, 253]. But there is no information available for how POA neurons regulate body temperature chronically in a genetically-specific way. In this **Chapter**, I demonstrated with LPO^{Gal} lesioning, that the diurnal body temperature rhythms are shifted permanently by a few degrees higher (**Fig. 2.8**). Thus, LPO^{Gal} neurons are responsible for cooling of the body chronically, linked to the sleep/wake fragmentation in *LPO-ΔGal* mice. An extremely focal lesion in the vLPO area of rats produces chronically less NREM sleep with decreased δ power in EEG along with decreased REM sleep, but the lesion does not affect body temperature[246], implicating that at least in rats, the extreme ventral part of the POA does not have cells regulating body temperature.

The so far unexplained active link between NREM sleep induction and body cooling appears intriguing. Three decades ago, it was proposed that restorative effects of sleep homeostasis depended on body cooling[226]. There might be an active link between lower body temperature and sleep as cooling during sleep increases the expression of cold-induced genes which could remodel synapses or serve some other restorative functions[227]. In humans, when the rate of core body temperature drop is at its maximum, NREM sleep induction appears[254]. There is a new feature emerging in the diurnal core body temperature variation in *LPO-ΔGal* mice, *i.e.* around the transition from “lights-off” to “lights-on” at ZT24, there is a pronounced positive spike in their core body

temperature (**Fig. 2.8 A and B**). This indicates that LPO^{Gal} neurons might normally be particularly active in lowering body temperature at the point in diurnal cycle when the homeostatic sleep drive is highest at the beginning of the “lights-on” period, fitting their role in sleep homeostasis regulation. During the “lights-off” active period, the sleep pressure increases and causes LPO^{Gal} neurons would become active at the transition to “lights-on”, inducing both sleep and cooling of the body. This could explain why compared with *LPO-Gal-GFP* mice, *LPO-ΔGal* mice are actually more awake at the beginning of “lights-on” period (see the red bar in **Fig. 2.8 A and B**), further emphasizing the correlation between body cooling and NREM sleep induction.

It is established that POA^{GABA} neurons induce baseline NREM sleep by inhibiting the wake-promoting histamine neurons in the posterior hypothalamus[27, 80, 250]. Immunocytochemistry suggested that a majority of rat preoptic GABAergic neurons that projects to the posterior hypothalamic histaminergic neurons co-released neuropeptide galanin[82]. Indeed, galanin directly reduces the firing rate of histaminergic neurons[255]. NREM sleep can be produced by optogenetic activation of non-galanin GABAergic neuron terminals from the POA in the area where the histaminergic neurons are located while direct optogenetic activation of POA^{Gal} neuron soma induced wakefulness[250]. Different galanin neuron subtypes might be involved[249]. The results on chronic lesioning shown in this **Chapter** are consistent with a similar study by others demonstrating that optogenetic and chemogenetic activation of LPO^{Gal} neurons induces NREM sleep accompanied with hypothermia[176]. It seems that LPO^{Gal} neurons are dispensable to achieve baseline NREM sleep even though the sleep/wake structure is highly fragmented.

Actually, it is not surprising considering there are mixed subtypes of POA^{GABA} neurons (galanin and other neuronal markers) that produce NREM sleep[176, 250]; besides, glutamate/NOS1 neurons in the MnPO /MPO induce both NREM sleep and hypothermia[76].

In summary, based on specific lesioning, LPO^{Gal} neurons actively link NREM sleep induction and body cooling. LPO^{Gal} neurons are needed for chronic cooling to maintain a normal body temperature even though they are dispensable for generating NREM sleep. In addition, they are also necessary for sleep homeostasis which has also been confirmed in a recent study on zebrafish[256], implicating a primary function of POA^{Gal} neurons in sleep homeostasis.

Chapter 3

Galaninergic neurons in the LPO are required for α 2 adrenergic agonist (dexmedetomidine)-induced sedation and hypothermia

Abstract

Dexmedetomidine (DEX), one of the α 2 adrenergic agonists, has been used increasingly in intensive care units for its long-term sedative effect. However, one undesirable side-effect of DEX is dramatic body cooling. Previous study in our lab has shown that both sedation induced by DEX and sleep homeostasis depend on the POA[51]. As I have demonstrated that the LPO^{Gal} neurons play an important role in sleep homeostasis and thermoregulation in **Chapter 2**, by analogy, it is highly possible that LPO^{Gal} neurons are also involved in DEX-induced sedation and hypothermia. Here in this **Chapter**, I find that DEX cannot induce high-power δ oscillations or sustained hypothermia in mice without LPO^{Gal} neurons. Furthermore, lesioning of LPO^{Gal} neurons diminishes the effects that in wild-type mice, there is a rebound in EEG δ power when they enter normal NREM some hours after DEX administration, resembling emergence from torpor state. Together with the results in **Chapter 2**, LPO^{Gal} neurons are required for sleep homeostasis, thermoregulation and DEX-induced sedation, indicating that sleep and α 2 adrenergic agonist-induced sedation likely share common neuronal mechanisms.

The results of this **Chapter** have been published as Ma et al. (2019) *Curr Biol.*[177].

Introduction

LPO^{Gal} neurons link NREM sleep induction and body cooling (see details in **Chapter 2**). Certain pharmacological methods could also bring NREM sleep and low body temperature together, for example, $\alpha 2$ adrenergic agonists induce an arousable NREM sleep-like state with sustained hypothermia[51, 193, 211, 213, 257]. In hospital intensive care clinics, the $\alpha 2$ adrenergic agonist dexmedetomidine (DEX) is favoured over benzodiazepines increasingly for its long-term sedation effect[258] and patients who received sedation with DEX have reduced risk of developing delirium[259]. DEX induces a NREM sleep-like state in rodents accompanying with hypothermia[211-213] and in human research, it induced NREM sleep-like state resembling stage 2/3 NREM sleep[210, 260, 261].

For DEX, its sedative and hypothermic actions are only mediated through $\alpha 2A$ receptors. Mice with a dysfunctional $\alpha 2A$ receptors can neither be sedated nor cool their body temperature with DEX[212, 262, 263]. It used to be considered that $\alpha 2A$ autoreceptors on the neurons in the LC are involved in DEX-induced sedation by inhibiting noradrenaline release from neurons in the LC [264-266]. It is true that DEX inhibit the LC neurons through $\alpha 2$ receptors[51, 264] but evidence is against the proposed model as both sedation and hypothermia can be induced even under the circumstance that noradrenaline release from the LC is genetically abolished[51, 193, 267], suggesting that $\alpha 2$ drugs work somewhere else in the brain to induce sedation and hypothermia other than the LC.

Direct injection of $\alpha 2$ agonist drugs into the POA produces both NREM sleep and hypothermia[268, 269]. Thus, it appears that there are also some neurons expressing the

α 2A receptors within the POA. Indeed, neurons in the POA express cFos protein after administration of DEX[51, 225], and cFos-dependent activity-tagging technique shows that neurons in the LPO are sufficient for both sedative and hypothermic responses of DEX[51].

As similar effects are observed following sleep deprivation (see details in **Chapter 2**), it is reasonable to assume that the same neurons activated during sleep deprivation/recovery sleep in the LPO are probably involved in the process of DEX-induced NREM sleep-like state and hypothermia. In **Chapter 2**, I have demonstrated that LPO^{Gal} neurons mediate both sleep homeostasis and body cooling by selective lesioning and chemogenetic activation of the LPO^{Gal} neurons. Given the potential overlap mentioned above, it is highly possible that LPO^{Gal} neurons are also involve in the DEX-induced NREM sleep-like state and hypothermia.

Aims and objectives

In this **Chapter**, to solve the problem whether LPO^{Gal} neurons are responsible for DEX-induced NREM sleep-like state and hypothermia, I will

- Examine the effect of DEX-induced hypothermia on *LPO-ΔGal* mice.
- Investigate the effect of DEX-induced NREM sleep-like state on mice with LPO^{Gal} ablation (*LPO-ΔGal* mice) from two aspects: increased δ power in EEG and sedation time.

Results

Ablation of LPO^{Gal} neurons strongly reduced DEX-induced hypothermia

Previous work in our lab has demonstrated neuronal ensembles in the LPO marked by TetTag pharmacogenetics after DEX-induced sedation can be selectively reactivated by chemogenetics and recapitulate NREM sleep with the accompanying drop in body temperature[51]. To test whether LPO^{Gal} neurons are part of these neuronal ensembles and are involved in this DEX-induced NREM sleep and body temperature regulation, mice with LPO^{Gal} neuron ablation (*LPO-ΔGal* mice) received 50 μg/kg of DEX injection at ZT19 (12:00, “lights-off” period) when the mice were in their most active phase and highest body temperature of their circadian cycle. *LPO-Gal-GFP* control mice were given the same dose of DEX injection at the same circadian time as controls. One hour of baseline body temperature was also recorded for the comparison of pre- and post-injection of DEX. As shown in **Fig. 2.8** in the previous **Chapter**, during the 1 hr baseline recording, *LPO-ΔGal* mice had slightly higher body temperatures than that of *LPO-Gal-GFP* mice (**Fig. 3.1 A**). Within 20 mins of DEX administration, there was a striking drop in the body temperature in both groups as expected (**Fig. 3.1 A**). One-hour post-DEX injection, *LPO-ΔGal* mice reached their lowest body temperature at around 29 °C, whereas the body temperature of *LPO-Gal-GFP* kept dropping for another 2 hrs (3 hrs post-injection) and reached their lowest point at around 25 °C (**Fig. 3.1 A**). After reaching the lowest point, the *LPO-ΔGal* mice started recovering their body temperature rapidly and almost returned to their starting level within the next hour (**Fig. 3.1 A**). However, in *LPO-Gal-GFP* control mice, their body temperature recovery began until 3-hr post-injection of DEX and the recovery

rate was much slower than that of *LPO-ΔGal* mice, *i.e.* approximately 2 °C increase in 2 hrs (**Fig. 3.1 A**). Although the decrease in body temperature after injection of DEX caused significant differences in both groups, this hypothermic effect induced by DEX was largely reduced in *LPO-ΔGal* mice and they never reached the same nadir as in *LPO-Gal-GFP* control mice (**Fig. 3.1 B**).

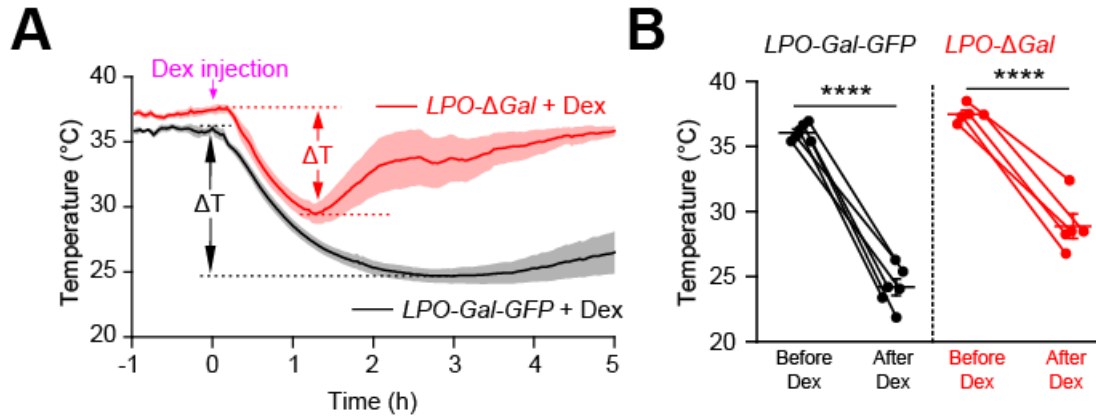


Figure 3.1 DEX-induced hypothermia was strongly reduced in *LPO-ΔGal* mice. (A) DEX was injected (*i.p.*) at ZT19 (“lights-off” period) when mice were in their most active phase. In control *LPO-Gal-GFP* mice, there was a strong decrease in body temperature from about 36 °C to approximate 25 °C over the course of 75 mins post-DEX injection. This hypothermic effect lasted beyond 4 hrs. However, in *LPO-ΔGal* mice, the initial decrease in body temperature commenced after DEX injection lasted only for the first hour, and did not reach the same nadir as in *LPO-Gal-GFP* control mice, and the body temperature almost returned to starting levels (33 ± 1.5 °C) over the next hour post-DEX injection. **(B)** Although the body temperature did not reach the same nadir as in *LPO-Gal-GFP*, the change in body temperature still had a significant difference after injection of DEX (**** $P < 0.0001$, paired two-tailed *t*-test) (*LPO-Gal-GFP*, black, $n = 6$; *LPO-ΔGal*, red, $n = 5$). All error bars represent the S.E.M..

DEX requires LPO^{Gal} neurons to induce NREM-like δ power

One of the features of DEX-induced sedation is elevation in the power of the δ wave band. An example of a 6-hr recording of raw EEG/EMG data from a *LPO-Gal-GFP* mouse with 50 $\mu\text{g}/\text{kg}$ of DEX injection (*i.p.*) shows this (**Fig. 3.2 A**). Shortly after administration of DEX, the mouse entered a NREM-like state with a large increase in its δ power compared with the natural NREM sleep generated during the first hour baseline recording (**Fig. 3.2 A**). This elevated δ power lasted about 30 mins before it suddenly dropped below the baseline and then returned to its normal level 3-hr post-injection (**Fig. 3.2 A**). The variation in δ power was similar in the *LPO- Δ Gal* mouse after DEX injection, *i.e.* δ power started increasing after injection; then dropped below baseline; and finally returned to normal (**Fig. 3.2 B**). But the initial increase in power appeared milder in the *LPO- Δ Gal* mouse compared with the one in the *LPO-Gal-GFP* mouse (**Fig. 3.2 A and B**): the same dose of DEX only induced a slight increase in the δ power in *LPO- Δ Gal* mice compared with its own baseline δ power in NREM sleep (**Fig. 3.2 B**).

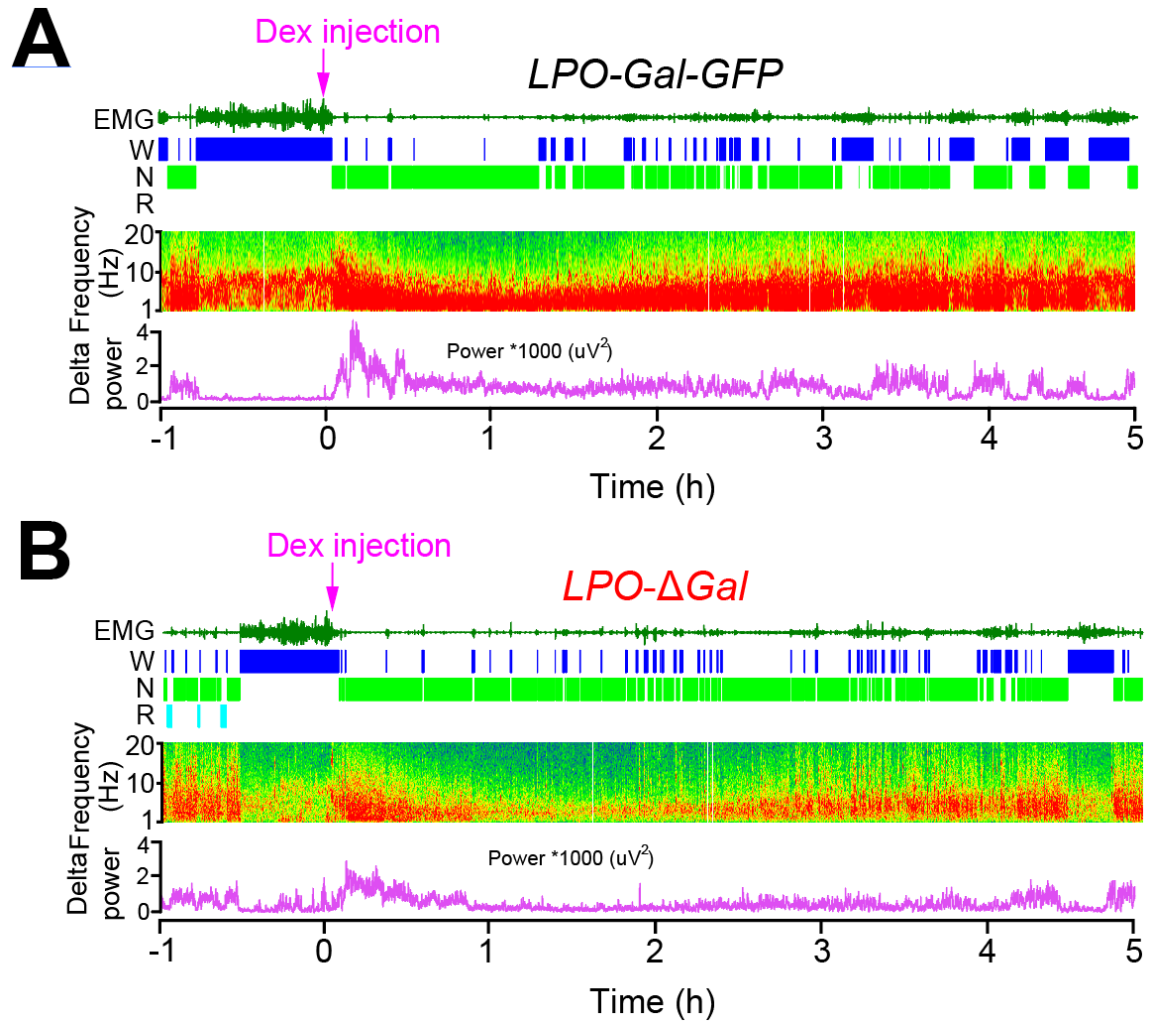


Figure 3.2 Examples of 6 hrs recording of EEG/EMG raw data with vigilance states scoring after DEX injection. **(A)** In *LPO-Gal-GFP* mice, straight after injection of DEX mice started to enter a NREM-like state and there was a large increase in the power of the δ wave band compared with its baseline. **(B)** In *LPO- Δ Gal* mice, as for *LPO-Gal-GFP* control mice, they also started a NREM-like sleep after DEX injection, but the increase in the power of the δ wave band was less dominant than the one that appeared in control mice.

Indeed, analysis of the EEG power of the first 30 mins after DEX injection demonstrated there was a striking increase in the power of the δ wave band (0.5-4 Hz) in *LPO-Gal-GFP* control mice compared with that in their natural sleep in the equivalent circadian time, but this effect was much reduced in *LPO- Δ Gal* mice (**Fig. 3.3 A**). When the power of the δ wave band was plotted across the whole 5 hrs post-DEX injection, it showed significant differences between *LPO-Gal-GFP* and *LPO- Δ Gal* mice (**Fig. 3.3 B**). The δ power in the NREM sleep generated in the first hour baseline recording from both groups was normalized to 1 respectively. The δ power of the next 5 hrs following DEX injection indicated that in *LPO-Gal-GFP* mice, the DEX-induced increase in the δ power was 2-fold larger than that in their baseline, whereas in the *LPO- Δ Gal* mice, the δ power after DEX injection remained similar with their own baseline (**Fig. 2.4 B**). However, 3 hrs post-injection, when the δ power recovered back to normal level, the difference in δ power between the two groups disappeared (**Fig. 2.4 B**). Compared with the total δ power in the first 30 mins after injection of DEX, the power was significantly weaker in *LPO- Δ Gal* mice than that in the *LPO-Gal-GFP* control mice (**Fig. 2.4 C**).

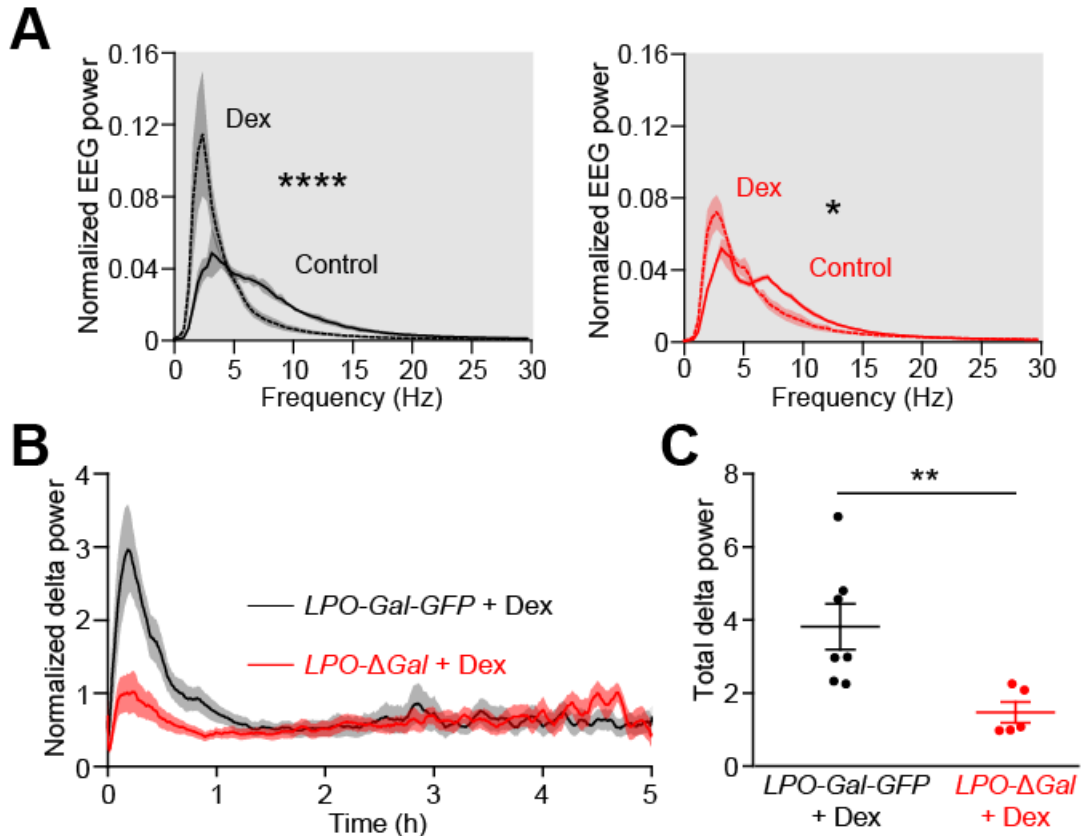


Figure 3.3 DEX-induced increase in the power of the δ wave band in NREM-like state requires LPO^{Gal} neurons. (A) The EEG power of the NREM-like state in the first 30 mins after DEX injection (*i.p.*) was significantly increased in both groups compared to the baseline in their equivalent Zeitgeber Time, but the degree of increase differed between *LPO-Gal-GFP* control mice and *LPO-ΔGal* mice ($*P<0.05$, $****P<0.0001$, paired two-tailed *t*-test). **(B)** Time courses of evoked NREM-like δ power following administration of DEX at ZT19 to *LPO-Gal-GFP* and *LPO-ΔGal* mice. **(C)** The DEX-induced increase in the total power of δ wave band in *LPO-Gal-GFP* mice was significantly larger than that in *LPO-ΔGal* mice in the first 30 mins post-injection. (*LPO-Gal-GFP*, black, $n=6$; *LPO-ΔGal*, red, $n=5$). All error bars represent the S.E.M..

Torpor is a state triggered in the wild by food shortages, which causes a metabolic suppression, leading to hypothermia and changes in the EEG. It could be argued that DEX induces an artificial torpor like state (NREM sleep with hypothermia). In some species, following torpor there is a rebound of δ power during subsequent NREM sleep [270, 271]. A Reviewer for my manuscript [177] was wondering by analogy if DEX also induced a δ power rebound, and so I carried out this analysis. As shown in **Fig. 3.3 B**, the δ power returned to the baseline level at 3 hrs post-DEX injection in both groups. The EEG power in the window between 3.5-4 hrs post-DEX injection was compared with the one in baseline NREM sleep at the corresponding zeitgeber time. There was indeed a rebound in δ power after emergence of DEX induced effect in *LPO-Gal-GFP* control mice, but this was not present in *LPO- Δ Gal* mice (**Fig. 3.4 A and B**). Although there was no difference observed in the δ power of baseline NREM sleep between two groups (**Fig. 2.6 A and B**), *LPO-Gal-GFP* mice had significantly higher total δ power 3.5 hrs post-DEX injection compared with that of *LPO- Δ Gal* mice (**Fig. 3.4 B**).

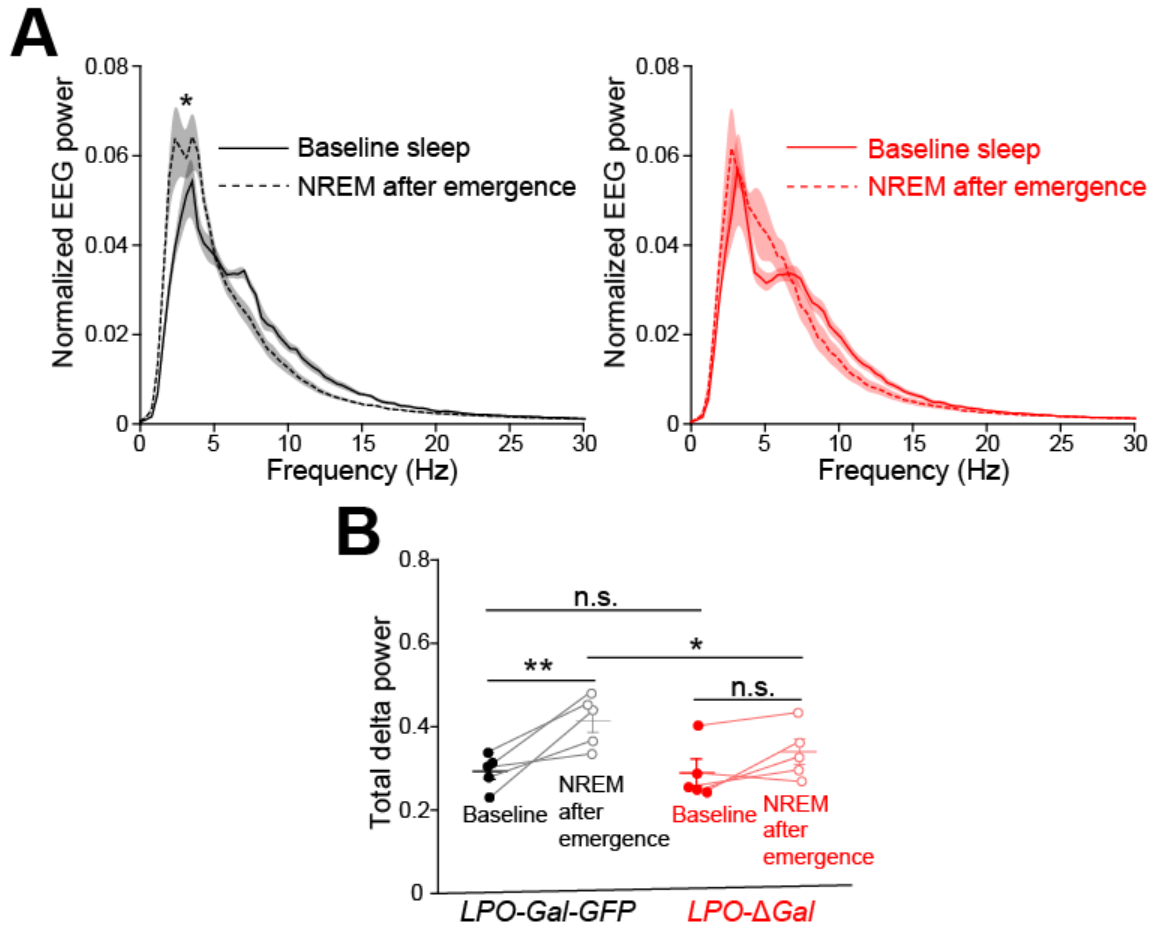


Figure 3.4 Ablation of LPO^{Gal} neurons caused an absence of δ power rebound after emergence from DEX-induced effects. (A) 3.5 hrs post-DEX injection, the *LPO-Gal-GFP* mice showed a rebound of δ power in NREM sleep compared with that in their baseline NREM sleep at the corresponding circadian time. But this effect was absent in *LPO-ΔGal* mice. **(B)** There was a significant difference in the power of the δ wave band of NREM sleep 3.5 hrs after DEX injection between *LPO-Gal-GFP* control mice and *LPO-ΔGal* mice, even though they had similar δ power in their baseline NREM sleep. * $P < 0.05$, ** $P < 0.01$; two-way ANOVA and Bonferroni-Holm post-hoc test. (*LPO-Gal-GFP*, black, $n = 5$; *LPO-ΔGal*, red, $n = 5$). All error bars represent the S.E.M..

Discussion

Previous work showed that the neurons in the LPO hypothalamus are sufficient to recapitulate the sedative and hypothermic responses[51]. Here, in this **Chapter**, I have demonstrated that those neurons involved are producing the inhibitory neuropeptide galanin. Genetically selective lesioning of LPO^{Gal} neuron strongly reduces the DEX-induced hypothermic effect in mice. Also, mice do not have an increase of δ power in their EEG after DEX injection nor rebound δ power when they emerge from DEX as we normally observe in control mice.

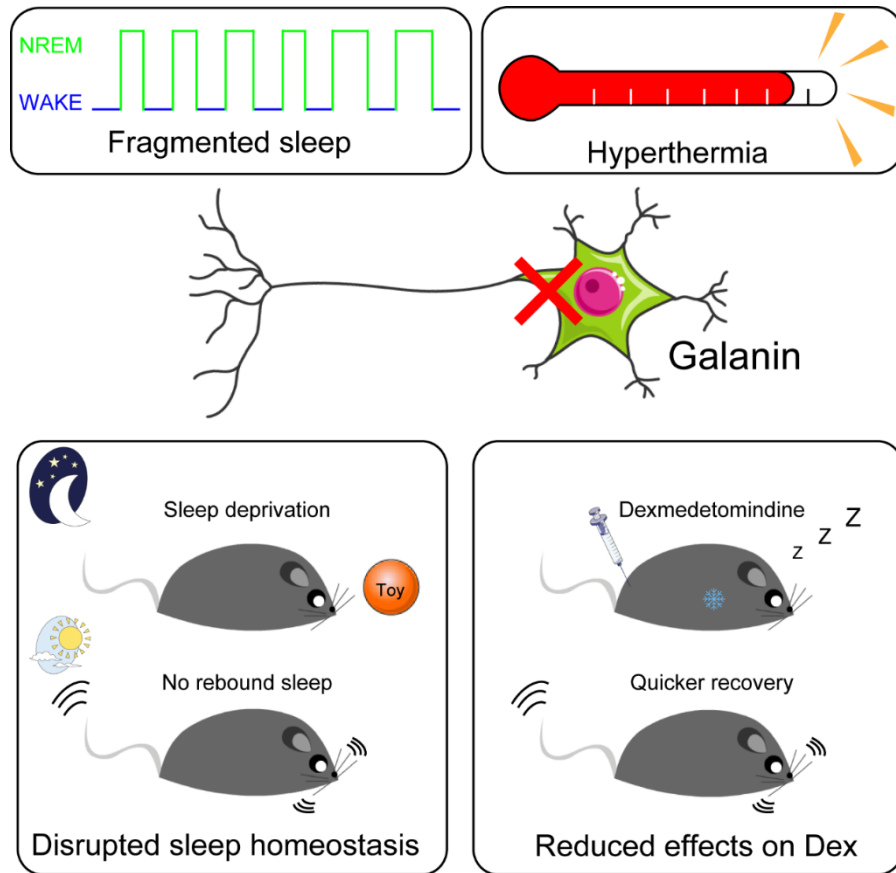
Both the DEX-induced NREM sleep-like state and hypothermia are mediated by the metabotropic α 2A adrenergic receptor[262, 264]. There is increasing evidence implicating that the POA is also involved in the NREM sleep-like and hypothermic effects induced by DEX, other than conventional theory on the LC (see **Introduction**). One idea is that DEX excites POA neurons directly by Gi-mediated inhibition of hyperpolarization-activated cyclic nucleotide-gated cation channels[272], as this mechanism has been shown for the neighbouring neurons of the bed nucleus stria terminalis. Conceptually, the chemogenetic activation of LPO^{Gal} neurons through the CNO-DREADD system (see **Results** in **Chapter 2**) mimics the actions of DEX. Both DEX and CNO induce a NREM sleep-like sedation with increased δ power in EEG along with hypothermia. The difference between the two is the hM₃D_q receptors are restricted in their expression to LPO^{Gal} neurons whereas α 2A receptors are widespread. Indeed, the body cooling triggered by DEX administration in the initial phase still can be observed in the *LPO-ΔGal* mice, probably because DEX works through the α 2A receptors expressed on smooth muscle of peripheral

blood vessels. The injection of DEX will directly promote heat loss through vasodilation of tail veins. Furthermore, the body cooling is initiated by certain central but slower effects, for example, by activation of galanin neurons in the dorsomedial hypothalamus, retroventral lateral medulla and rostral raphe pallidus[175].

Galaninergic POA neurons have various functions and participate in several coordinated regulations, such as parental behaviours (social, motivational, motor) and mating[273, 274], and also sleep and temperature[175, 176]. It cannot be ruled out that one subtype of LPO^{Gal} neurons is responsible for NREM sleep δ power increase, and another subtype regulates chronic cooling. But actually, multiplex *in situ* labelling and single-cell profiling of revealed that there are at least seven subtypes of galanin-expressing neurons, intermingled and dispersed in the mouse POA[249]. A majority of these subtypes are GABAergic and positive for the *Vgat* gene expression, whereas a few are glutamatergic expressing the *Vglut2* gene. One galanin/*Vgat* subtype also expresses the vesicular monoamine transporter and tyrosine hydroxylase (TH)[249]. This would cause the cell to make and possibly release L-DOPA. It is also possible that this type of galanin neuron could locally synthesize and release noradrenaline (if two more genes were expressed that encode aromatic L-amino acid decarboxylase and dopamine beta hydroxylase, but these genes were not reported in the study of Moffitt et al.[249]). It is possible that based on these gene expression results with tyrosine hydroxylase that there could be local monoaminergic regulation by galanin cells in the LPO of sleep and body temperature, and these effects of the endogenous monoamine in the LPO are mimicked by DEX.

The LPO^{Gal} neurons identified for DEX (as well as for sleep homeostasis and chronic body cooling in **Chapter 2**) are possibly GABAergic. Our lab previously demonstrated that deletion of *Vgat* expression in the LPO, which prevents GABA release from GABAergic LPO neurons, diminished the ability of DEX to rapidly induce a NREM sleep-like state, indicating that LPO^{GABA} neurons are crucial for the initial response of DEX[51]. The longer-term effects of DEX on NREM sleep-like state maintenance and cooling body temperature would likely need sustained galanin release from LPO neurons.

Conclusion (Chapter 2 and Chapter 3)



- This is the first identification of a neural type underlying sleep homeostasis.
- Preoptic galanin neurons are essential for sleep homeostasis and chronic body cooling.
- LPO^{Gal} neurons mediate the sedative and hypothermic actions of DEX.
- DEX causes an EEG δ power rebound dependent on galanin neurons.

Based on my genetically selective lesioning results, galaninergic neurons in the LPO are necessary for NREM sleep consolidation, and they mediate both rebound NREM sleep after sleep deprivation linked to body cooling and adrenergic agonist-induced sedation accompanied with sustained hypothermia. Although NREM sleep can still occur in mice with LPO^{Gal} neurons ablated, they are critical for maintaining the normal body temperature by chronic cooling. Galanin neurons are absolutely needed for sleep homeostasis as a similar result has just obtained from zebrafish, suggesting a primordial function of galaninergic POA neurons in sleep homeostasis[275]. Activation of LPO^{Gal} neurons induces higher δ power in EEG, *i.e.* a more synchronized state of neocortical activity, whether through homeostatic sleep following sleep deprivation, or chemogenetic and DEX activation. Work from our lab and others has suggested that the torpor state can be induced by strengthening this sleep/cooling process triggered by e.g. glutamate/NOS1 neurons and galanin neurons in the POA[76, 176]. It is highly possible that DEX over activates the natural homeostatic sleep pathway through LPO^{Gal} neurons, pushing the subject into deep hypothermia, from which there is a δ power rebound in subsequent NREM sleep. This indicates that the sedation induced by DEX is not restorative like natural sleep and it is likely due to extreme cold body temperature of the mice. It would be highly helpful to discover drugs which can cause deep sedation but avoid excessive hypothermia by identifying the molecular substrates of DEX-induced sedative actions.

Future work

To fully understand how all the sleep homeostasis, chronic body cooling and DEX-induced NREM sleep-like state and its accompanied hypothermia are regulated by the LPO^{Gal} neurons and their underlying neuronal circuits, a few further studies are proposed as following:

1. As multiple subtypes of galanin-expressing neurons exist in the POA[249], sing-cell profiling of the LPO neurons before and after LPO^{Gal} ablation with different markers will help resolve the neuroanatomical identity of the LPO neurons responsible for either sleep or thermoregulation.
2. To confirm the expression of $\alpha 2A$ receptors in the LPO^{Gal} neurons, qPCR would be applied before and after LPO^{Gal} ablation.
3. Electrophysiological techniques will provide direct response of LPO^{Gal} neurons for DEX application.
4. To untangle the circuit logic of LPO^{Gal} neurons, intersectional genetics combined with cFos-based activity-tagging could be deployed.
5. Using ChR2-EYFP selectively expressed in LPO^{Gal} neurons, I performed some preliminary anterograde tracing of LPO^{Gal} neurons and found that the LH, PAG and LC receive dense projections from LPO^{Gal} neurons (**Fig. 3.5**). Optogenetic manipulation of downstream terminals and targets will help reveal the neuronal circuits involved.

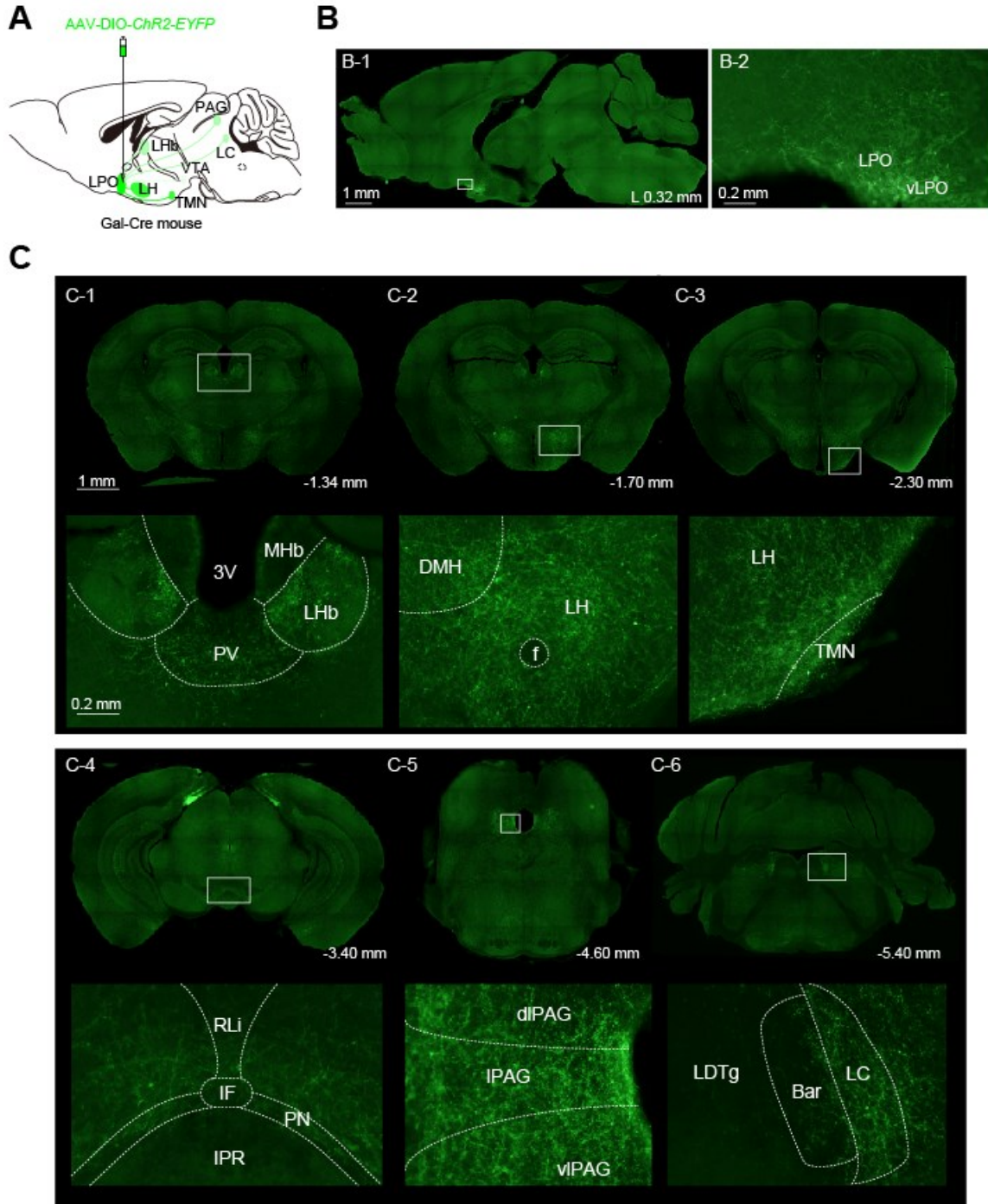


Figure 3.5 Whole brain mapping of axonal projections from LPO^{Gal} neurons. (A) AAV-DIO-ChR2-EYFP was bilaterally injected in the LPO of Gal-Cre mice. (B) Strong viral expression was observed in the LPO area. (C) Projections from LPO^{Gal} neurons were found in several brain regions with strong labellings in the LH and PAG. 3V, the third ventricle; Bar, Barrington's nucleus; dIPAG, dorsolateral periaqueductal gray; DMH, dorsomedial nucleus of hypothalamus; f, fornix; IF, interfascicular nucleus; IPR, interpeduncular nucleus; LC, locus ceruleus; LDTg, laterodorsal

tegmental nucleus; LH, lateral hypothalamus; LHb, lateral habenula; IPAG, lateral periaqueductal gray; LPO, lateral preoptic nucleus; MHb, medial habenular nucleus; PAG, periaqueductal gray; PN, paranigral nucleus; PV, paraventricular thalamic nucleus; RLi, rostral linear nucleus of the raphe; TMN, tuberomammillary nucleus; vLPO, ventrolateral preoptic nucleus; VTA, ventral tegmental area.

Chapter 4

Exploration of whole brain neuronal connections of wake-promoting VTA^{Vglut2} and wake-inhibiting VTA^{Vgat} neurons using chemogenetics and anterograde tracing techniques

Abstract

The ventral tegmental area (VTA) is a group of neurons concentrated with dopamine (DA)-producing cells located on the floor of the midbrain[276]. The VTA^{DA} neurons play important roles in mediating cognitive functions, such as reward-based and associative learning-, motivation-, and addiction and depression-related behaviours. The role(s) of VTA in sleep/wake regulation has only been noticed until recent decade. As shown in the **Preliminary Result Chapter** in **Appendices**, the VTA has different patterns of cFos expression between SD and RS, also implying its importance in sleep/wake behaviours. In addition to VTA^{DA} neurons, the VTA contains relative concentrated GABAergic neurons and a small portion of glutamatergic neurons. Both chemogenetic activation of VTA^{Vglut2} neurons and inhibition of VTA^{Vgat} neuron produce prolonged wakefulness[47], strongly suggesting the involvement of the VTA in regulating sleep/wake behaviours. In this **Chapter**, by utilizing cFos expression, chemogenetics and anterograde tracing techniques, I confirmed during wakefulness, both VTA^{Vglut2} and VTA^{Vgat} neurons showed robust neuronal activity. Anterograde tracing revealed that VTA^{Vglut2} neurons send strong projection to nucleus accumbens (NAc) and ventral pallidum (VP), as well as the lateral hypothalamus (LH) to promote wakefulness[47], whereas VTA^{Vgat} neurons mainly produced local inhibition and partially innervated to the LH. Together with the

behavioural data of chemogenetics[47], the VTA is certainly one of the most powerful sleep/wake-regulating centres in the brain.

The results of this **Chapter** have been published as Yu et al. *Nat Neurosci.*[47].

Introduction

The ventral tegmental area (VTA), also simply known as the ventral tegmentum, or the ventral tegmental area of Tsai, named after the first person who found and defined this structure in the opossum[277], is a group of neurons concentrated with dopamine (DA)-producing cells located on the floor of the midbrain[276]. It is an evolutionary conserved structure in higher-order vertebrates, especially mammals, with a high degree of similarity[278]. However, over the years, there have been difficulties defining the VTA. Firstly, different definitions and terminology exist at the anatomical level for the VTA[279-285]. Secondly, the functions and structures of the VTA and its neighbour, the substantia nigra pars compacta (SNc) overlap and some studies even take the SNc and the VTA as one whole midbrain DA-complex[286-288]. Although a clear anatomical boundary of the VTA is lacking, studies have shown the heterogeneity and neurochemical profile of the VTA make it distinct from the SNc morphologically, developmentally, and functionally[281, 283, 284, 289, 290]. There is a common agreement on five nuclei as being part of the VTA: the parabrachial pigmented nucleus (PBP), located most laterally to all VTA nuclei[284, 291]; the paranigral nucleus (PN), sometimes in combination with the PBP referred to as the lateral VTA[281, 284]; the interfascicular nucleus (IF), located in the medial VTA[292]; and the two components comprising the midline linear raphe nuclei, the rostral linear nucleus (RLi) and the caudal linear nucleus (CLi)[293].

Dopaminergic neuronal circuits serve many cognitive functions, such as motivation, reward-based and associative learning, safety-seeking, addiction and depression, cognitive control in decision-making and memory[276, 294]. As the VTA is one of the DA-

producing centres, it is believed to hold an important role in the neuromodulation of DA related behaviours via dopaminergic pathways. Over the last five decades, intensive research has been focusing on the above functions of VTA DAergic neurons[295-299]. This diversity of functions associated with the VTA may partially be mediated by various subpopulations of VTA neurons. As mentioned above, the VTA has a high heterogeneity in its neurochemical profile. Following the discovery of DA in the VTA[300], which accounts for approximately 65% of VTA neurons, GABAergic (35%) and glutamatergic (3%) neurons were also found to present in the VTA[301, 302]. Like VTA DAergic neurons, both VTA GABAergic and glutamatergic neurons are believed to be involved in the regulation of goal-related and reward-directed and social behaviours. These functions are mediated by VTA GABAergic or glutamatergic neurons co-releasing with VTA DAergic neurons, or even by some subpopulations of VTA GABAergic and glutamatergic neurons only[284]. For example, Stamatakis and his colleagues demonstrated that a population of VTA GABA-releasing neurons, not DA, projecting to the lateral habenula (LHb) can promote reward[303]; Qi *et al.* reported that VTA glutamatergic neurons can excite nucleus accumbens (NAc) GABAergic interneurons having synapses on medium spiny neurons (MSNs) and this circuit sufficiently drives aversive behaviours[304].

These cognitive behaviours require wakefulness. Only in recent decades, researchers started to pay attention to sleep/wake regulation by the VTA. Several studies have focused on VTA DAergic neurons in sleep/wake behaviours and found that VTA DAergic neurons promote wakefulness and activation of these neurons even induces reanimation from general anaesthesia[46, 52, 53]. Indeed, VTA DAergic neurons are active during

wake and REM sleep[46]. This year, our lab has complemented the earlier work on sleep/wake regulation by the VTA, and demonstrated that GABAergic and glutamatergic neurons in the VTA play a central role in regulating sleep/wake behaviours[47], followed by a few works done by other research groups reporting similar results[88, 305]. Like VTA DAergic neurons, VTA glutamatergic neurons are selectively active during wake and REM sleep and strongly promote wakefulness. Our lab found that chemogenetic activation of those neurons produced 100% wakefulness determined by EEG and EMG lasting for 5 hrs [47]. On the contrary, although VTA GABAergic neurons also have their highest activity during wake and REM sleep, selective lesioning of VTA GABAergic neurons produced continuous wakefulness and chemogenetic activation of those neurons induced sustained (80%) NREM sleep for 6 hrs by limiting arousal-promoting circuits[47]. With all the results indicating that mammalian vigilance states can be mediated by VTA DAergic, GABAergic and glutamatergic neurons, the VTA is believed to be a novel hub for sleep/wake regulation.

Aims and objectives

After discovery of the wake-promoting VTA glutamatergic and the wake-inhibiting VTA GABAergic neurons[47], the neuronal circuitry underlying these phenotypes are still unknown. In this **Chapter**, to uncover the circuitry regulating sleep/wake behaviours by VTA glutamatergic and GABAergic neurons, I will

- Use chemogenetic activation/inhibition of VTA glutamatergic/GABAergic neurons to confirm the neuronal activity in the local VTA by cFos protein expression, an immediate early gene representing neuronal activity.
- Examine the neuronal activity by cFos protein expression in the brain regions innervated by VTA glutamatergic/GABAergic neurons after chemogenetic activation/inhibition.
- Map the axonal projections of VTA glutamatergic and GABAergic neurons using channelrhodopsin2, a light-sensitive excitatory channel labelling the axon terminals of neurons containing *Vglut2* or *Vgat*.

Results

Wake-promoting VTA^{Vglut2} neurons induce cFos protein expression in different brain regions followed by chemogenetic activation and send axonal projections to these target areas

In the search for glutamatergic circuitry promoting wakefulness, a 5 hrs of 100% wakefulness was achieved by chemogenetic activation of the VTA^{Vglut2} neurons [47]. Chemogenetic activation was conducted by injecting adeno-associated virus (AAV)-*DIO-hM₃D_q-mCherry* in the VTA of *Vglut2-ires-Cre* mice to express the excitatory hM₃D_q designer receptors exclusively activated by designer drugs (DREADD) receptor in VTA^{Vglut2} neurons (**Fig. 4.1 A**). Immunohistochemistry against hM₃D_q-mCherry showed DREADD receptor was restrictedly expressed in the VTA (**Fig. 4.1 A**). In order to confirm that VTA^{Vglut2} neurons were truly activated to induce this prolonged wakefulness, CNO (1mg/kg, *i.p.*) was injected to VTA^{Vglut2} -*hM₃D_q* mice at ZT0 (the start of “lights-on” period when the mice had strongest desire to sleep). Saline injection was also given to an independent group of VTA^{Vglut2} -*hM₃D_q* mice at the same time as controls. 1 hr after CNO or saline injection, all the mice were transcardially perfused and brains were used for immunohistochemical staining against cFos protein. The cell number expressing cFos protein was significantly elevated in hM₃D_q-expressing VTA^{Vglut2} neurons after chemogenetic activation by CNO (378±36 cells) compared with saline (41±4 cells) injection controls (**Fig. 4.1 B and C**). This elevation of cFos protein expression confirms the excitation of VTA^{Vglut2} neurons by CNO which resulted in prolonged wakefulness [47].

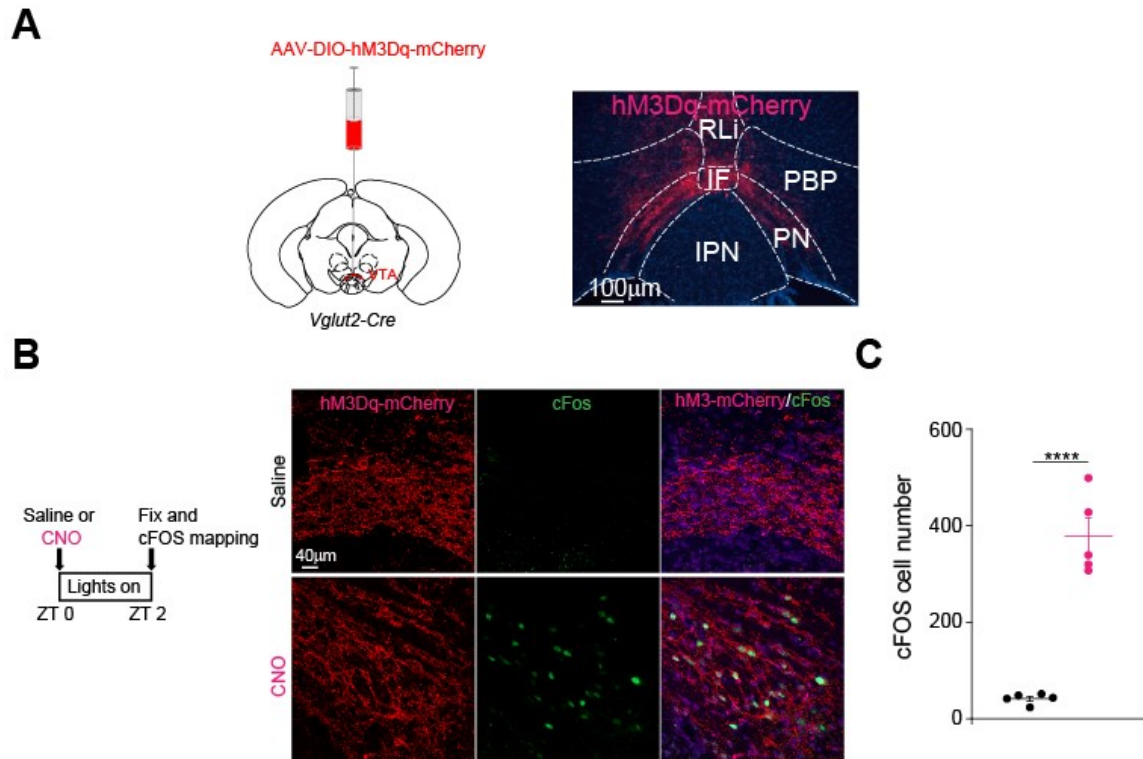


Figure 4.1 Chemogenetic activation of VTA^{Vglut2} neurons induced elevated cFos protein expression in local VTA. **(A)** AAV-DIO-hM₃D_q-mCherry was delivered into the VTA of Vglut2-ires-Cre mice for chemogenetic activation of VTA^{Vglut2} neurons. Immunohistochemistry of hM₃D_q-mCherry was restricted to VTA. **(B)** Immunohistochemistry for cFos protein and hM₃D_q-mCherry expression in the VTA of VTA^{Vglut2} -hM₃D_q mice one hour after CNO (1mg/kg, *i.p.*) or saline injection at ZT0 (the start of “lights-on” period). The magenta staining in the histology figures are the primary fluorescence of the hM₃D_q-mCherry positive axons; and the cFos immunohistochemistry is shown in green. **(C)** The cell number with cFos protein expression in the VTA was significant elevated after activation of VTA^{Vglut2} neurons by CNO injection (red; $n=5$) compared with saline injection (black; $n=5$) (**** $P<0.0001$; unpaired two-tailed *t*-test). IF, interfascicular nucleus; IPN, interpeduncular nucleus; PBP, parabrachial pigmented nucleus; PN, paranigral nucleus; RLi, rostral linear nucleus. Both error bars represented the S.E.M..

To further identify the brain regions involving in the generation of the VTA^{Vglut2}-mediated wakefulness, VTA^{Vglut2}-hM₃D_q mice were used for whole-brain cFos activity mapping. Dense axonal projections of hM₃D_q-mCherry were found in the nucleus accumbens (NAc), ventral pallidum (VP) and lateral hypothalamus (LH) (**Fig. 4.2 A and B**). Several other brain regions also had a few axonal projections of hM₃D_q-mCherry including the prefrontal cortex (PFC), lateral preoptic nucleus (LPO), lateral habenula (LHb), dorsal raphe (DR) and locus cereleus (LC) (**Fig. 4.2 A and B**). VTA^{Vglut2}-hM₃D_q mice received injection of either CNO (1mg/kg, *i.p.*) or saline at ZT0. 2 hrs time was given before the mice were transcardially perfused to allow cFos protein to express in target areas. In the brain areas that had dense axonal projections of hM₃D_q-mCherry, *i.e.* the NAc, VP and LH, significant increases of cell number expressing cFos protein after chemogenetic activation of VTA^{Vglut2} neurons were observed (**Fig. 4.2 B and C**). cFos-positive cells were also found in other hM₃D_q-mCherry projecting areas after CNO injection but the cell number of cFos-positive cells was unchanged compared with saline injection only (**Fig. 4.2 B and C**).

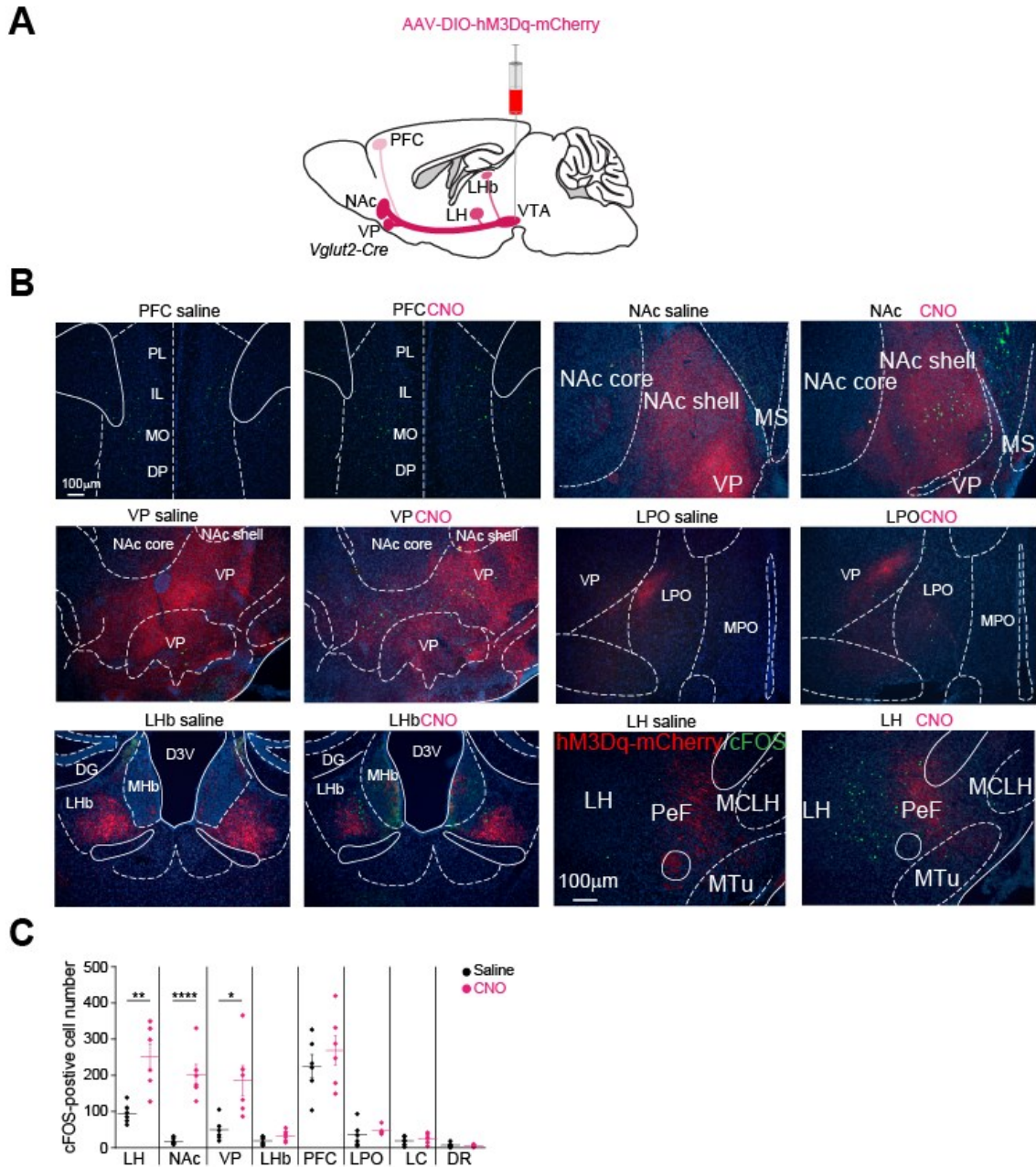


Figure 4.2 cFos-based activity mapping of brain areas after chemogenetic activation of VTA^{Vglut2} neurons. (A) In the VTA^{Vglut2}-hM₃D_q mice, the labelled axons projected to several different brain regions across the whole brain. (B) cFos protein expression in the brain areas that had axonal projections from the VTA of VTA^{Vglut2}-hM₃D_q mice two hours after receiving injection of either CNO (1mg/kg, *i.p.*) to activate VTA^{Vglut2} neurons or saline at ZT0 (the start of “lights-on” period). The magenta staining in the histology figures are the primary fluorescence of the hM₃D_q-mCherry positive axons; and the cFos immunohistochemistry is shown in green. (C) The cell number of cFos

protein expression was significantly elevated in several brain regions including NAc, VP and LH after activation of VTA^{Vglut2} neurons by CNO injection (red; $n=6$) compared with saline injection (black; $n=6$) while the number remained similar in the PFC, LPO, LHb, DR and LC (* $P<0.05$, ** $P<0.01$, *** $P<0.0001$; unpaired two-tailed t -test). D3V, dorsal 3rd ventricle; DG, dentate gyrus; DP, dorsal peduncular cortex; DR, dorsal raphe; IL, infralimbic cortex; LC, locus ceruleus; LH, lateral hypothalamus; LHb, lateral habenula; LPO, lateral preoptic nucleus; MCLH, magnocellular nucleus of lateral hypothalamus; MHb, medial habenular nucleus; MO, medial orbital cortex; MPO, medial preoptic nucleus; MS, medial septal nucleus; MTu, medial tuberal nucleus; NAc, nucleus accumbens; PeF, perifornical nucleus; PFC, prefrontal cortex; PL, paralemniscal nucleus; VP, ventral pallidum; VTA, ventral tegmental area. All error bars represented the S.E.M..

We next conducted circuit mapping of the VTA^{Vglut2} neurons based on channelrhodopsin2 (ChR2). AAV-DIO-ChR2-EYFP was injected to *Vglut2-ires-Cre* mice to generate VTA^{Vglut2} -ChR2 mice (**Fig. 4.3 A**). The neurons containing axon terminals of VTA^{Vglut2} would show EYFP expression. Immunohistochemistry against ChR2-EYFP revealed that ChR2 was restrictedly expressed in the VTA, especially in the medial VTA (**Fig. 4.3 A**) where VTA^{Vglut2} neurons were most concentrated [47]. Whole brain coronal sections were sliced in 50 μ m thickness and used for ChR2-EYFP immunohistochemistry to identify axonal projection of VTA^{Vglut2} neurons. Consistent with the *hM₃D_q-mCherry* projections and cFos activation data in **Figure 4.2**, strong projections from VTA^{Vglut2} neurons were observed in the NAc, VP and LH (**Fig. 4.3 B and C**). Other VTA^{Vglut2} -projecting brain areas included the PFC, LHb, DR and LC (**Fig. 4.3 B and C**). Sagittal brain sections also confirmed axonal projections from VTA^{Vglut2} neurons in above brain regions in a more visualized way (**Fig. 4.3 C**).

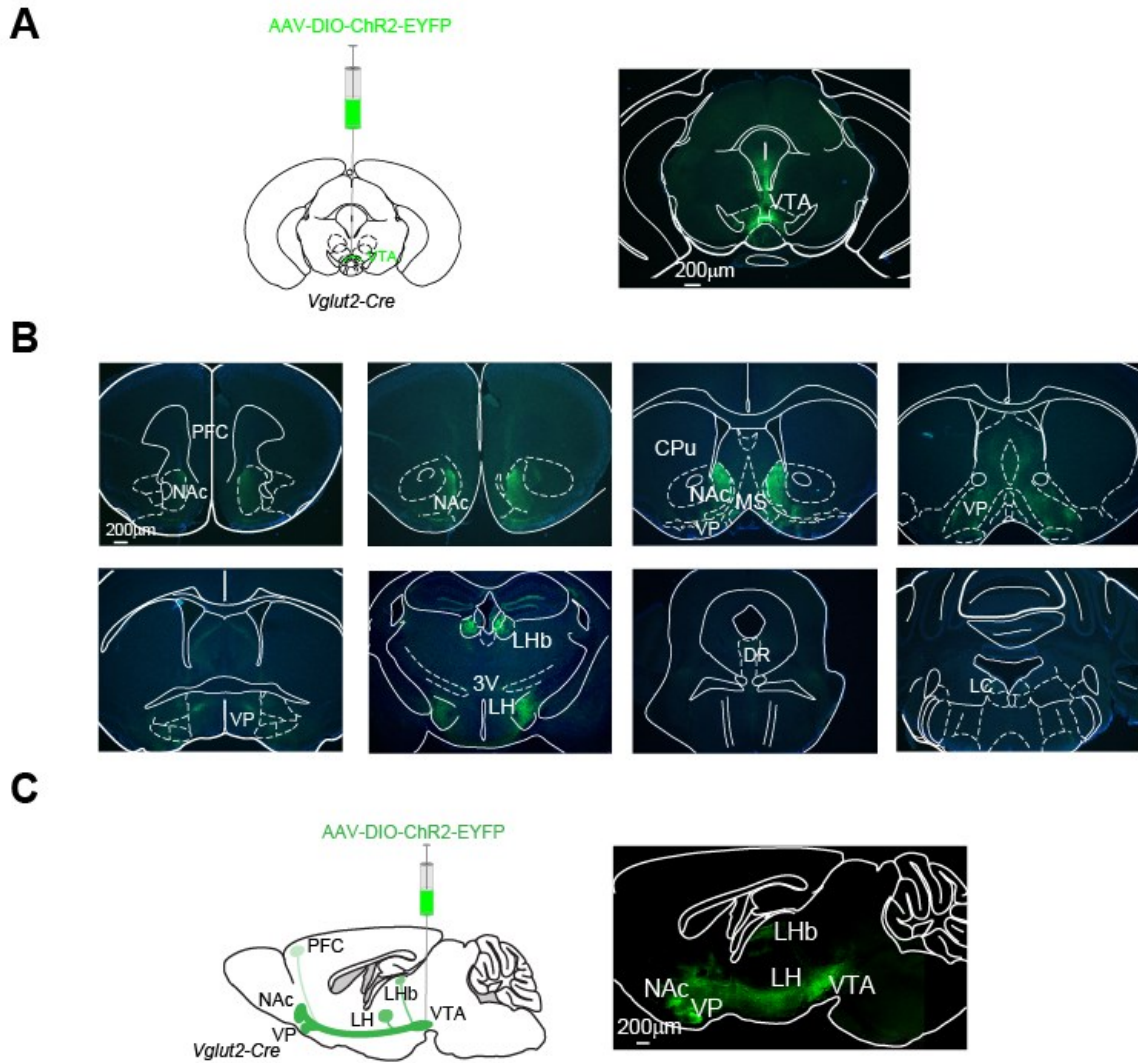


Figure 4.3 Whole brain mapping of axonal projections from VTA^{Vglut2} neurons. (A) AAV-DIO-ChR2-EYFP was injected into the VTA of $Vglut2$ -ires-Cre mice and the injection site was restricted to the medial VTA. (B) Axon projections to several different brain areas across whole brain with the LH and NAc strongly labelled. (C) Sagittal brain sections revealed similar projecting circuitry as coronal mapping. All the experiments were independently repeated four times. 3V, the third ventricle; CPu, striatum; DR, dorsal raphe; LC, locus ceruleus; LH, lateral hypothalamus; LHb, lateral habenula; MS, medial septal nucleus; NAc, nucleus accumbens; PFC, prefrontal cortex; VP, ventral pallidum; VTA, ventral tegmental area;

Wake-inhibiting VTA^{Vgat} neurons induce strong cFos protein expression in the LH and VTA followed by chemogenetic inhibition and send axonal projections to brain areas different with the ones of VTA^{Vglut2} neurons

Besides glutamatergic neurons, a relatively large percentage of GABAergic neurons can also be found in the VTA [294]. These GABAergic neurons can be detected by expression of their vesicular transporter, the vesicular GABA transporter (VGAT). Only few GABAergic neurons express dopamine or glutamate, confirming that *Vgat* gene-expressing neurons were a distinct group of neurons in the VTA [47]. Chemogenetic activation of VTA^{Vgat} neurons induced sustained (80%) NREM sleep for 6h while chemogenetic inhibition of those neurons produced 100% wakefulness for 6 hrs [47]. As VTA^{Vgat} neurons are selectively wake- and REM-active, instead of physiologically triggering NREM sleep, they may contribute to sleep/wake regulation by limiting wakefulness [47]. To explore the role of VTA^{Vgat} neurons in limiting wakefulness, *AAV-DIO-hM₄D_q-mCherry* was delivered into the VTA of *Vgat-ires-Cre* mice to generate *VTA^{Vgat}-hM₄D_q* mice (**Fig. 4.4 A**). In contrast with hM₃D_q DREADD receptor, CNO injection will inhibit hM₄D_q-mCherry expressing neurons. Immunohistochemistry against hM₄D_q-mCherry showed restricted expression of virus in the VTA (**Fig. 4.4 A**). Unlike VTA^{Vglut2} neurons in **Fig. 4.1**, the expression pattern of hM₄D_q-mCherry in VTA^{Vgat} neuron was mostly in the lateral VTA, further confirming VTA^{Vgat} neurons are distinct from VTA^{Vglut2} neurons. *VTA^{Vgat}-hM₄D_q* mice were injected with either CNO (1mg/kg, *i.p.*) to inhibit VTA^{Vgat} neurons or saline at ZT0 (the start of “lights-on” period). As VTA^{Vgat} neurons were hypothesized to work by limiting wakefulness, inhibition of VTA^{Vgat} neurons would produce wakefulness. The phenotype would be most predominant at the beginning of “lights-on” period. 2 hr after injection,

mice were transcardially perfused and 40 μm coronal brain sections covering the VTA were used for immunohistochemistry against cFos protein expression. Dense VTA^{Vgat} fibres were observed in the VTA and cFos protein expression was significantly elevated after inhibition of VTA^{Vgat} neurons by CNO injection (1mg/kg, *i.p.*) compared with saline injection (**Fig. 4.4 B and C**). Immunohistochemical staining also showed there was no overlap of hM₄D_q-mCherry-expressing neurons and cFos-positive neurons, indicating VTA^{Vgat} neurons were indeed silenced and that induction of cFos protein expression in the local VTA by disinhibition of VTA^{Vgat} neurons represented strong local inhibition.

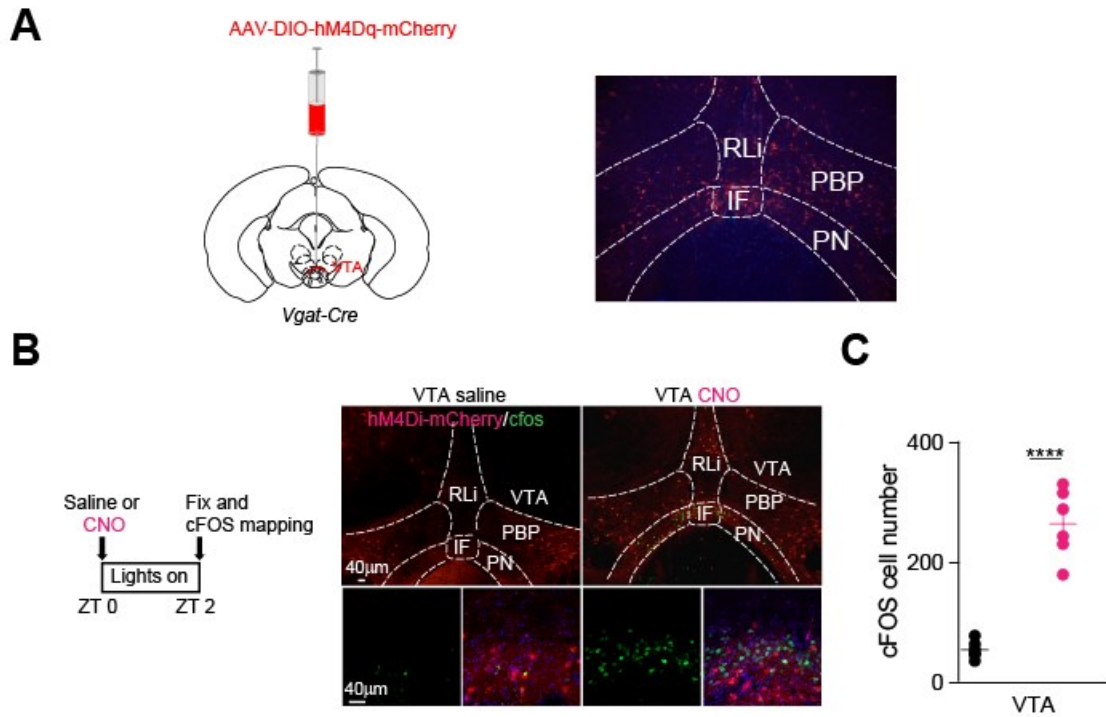


Figure 4.4 Chemogenetic inhibition of VTA^{Vgat} neurons induced elevated cFos protein expression in local VTA. (A) AAV-DIO-hM₄D_q-mCherry was delivered into the VTA of Vgat-ires-Cre mice for chemogenetic inhibition of VTA^{Vgat} neurons. Immunohistochemistry of hM₄D_q-mCherry was restricted to the VTA. **(B)** Immunohistochemistry for cFos protein and hM₄D_q-mCherry expression in the VTA of VTA^{Vgat}-hM₄D_q mice two hours after CNO (1mg/kg, *i.p.*) or saline injection at ZT0 (the start of “lights-on” period). The magenta staining in the histology figures are the primary fluorescence of the hM₄D_q-mCherry positive axons; and the cFos immunohistochemistry is shown in green. **(C)** The cell number with cFos protein expression in the VTA was significant elevated after inhibition of VTA^{Vgat} neurons by CNO injection (red; *n*=6) compared with saline injection (black; *n*=6) (*****P*<0.0001; unpaired two-tailed *t*-test). IF, interfascicular nucleus; PBP, parabrachial pigmented nucleus; PN, paranigral nucleus; RLi, rostral linear nucleus. Both error bars represented the S.E.M..

Apart from the local VTA, immunohistochemistry against hM₄D_q-mCherry across the whole brain of VTA^{Vgat}-hM₄D_q mice showed dense axonal projections to the LH and, to some extent, to the LHb and DG of the hippocampus (**Fig. 4.5 A and B**). A few fibres were also found in the LPO (**Fig. 4.5 A and B**). To test the connections between target brain areas and the VTA, cFos protein activity mapping was conducted by inhibiting VTA^{Vgat} neurons with CNO (1mg/kg, *i.p.*) injection or saline injection at ZT0 (the start of “lights-on”) as control. 2 hrs after injection with CNO, cFos protein expression was strongly induced in the LH which had dense axonal projections from VTA^{Vgat} neurons, as well as some other brain regions including the LPO, LHb and DG (**Fig. 4.5 B and C**), indicating elevated neuronal activity by disinhibition of VTA^{Vgat} neurons in these areas.

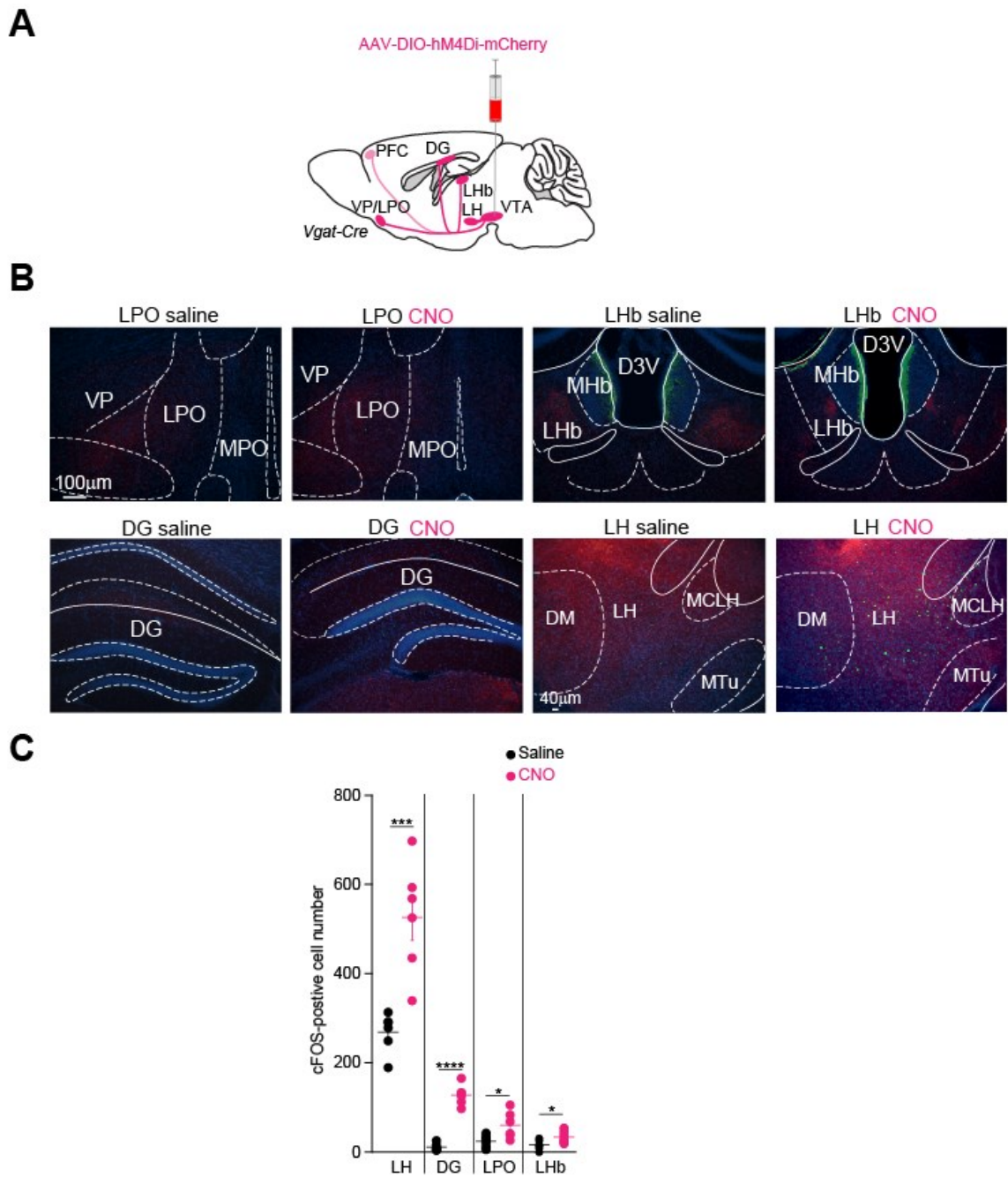


Figure 4.5 cFos-based activity mapping of brain areas after chemogenetic inhibition of VTA^{Vgat} neurons. (A) In the VTA^{Vgat}-hM₄D_q mice, the labelled axons projected to a few brain regions different with the one observed in VTA^{Vgat}-hM₃D_q mice. (B) cFos protein expression in the brain areas that had axonal projections from the VTA of VTA^{Vgat}-hM₄D_q mice two hours after receiving injection of either CNO (1mg/kg, *i.p.*) to inhibit VTA^{Vgat} neurons or saline at ZT0 (the start of “lights-on” period). The magenta staining in the histology figures are the primary fluorescence of the hM₄D_q-mCherry positive axons; and the cFos immunohistochemistry is shown in green. (C) The

cell number of cFos protein expression was significantly elevated in all following brain regions including the LH, LPO, DG, and LHb after inhibition of VTA^{Vgat} neurons by CNO injection (red; $n=6$) compared with saline injection (black; $n=6$) (* $P<0.05$, *** $P<0.001$, **** $P<0.0001$; unpaired two-tailed t -test). D3V, dorsal 3rd ventricle; DG, dentate gyrus; DM, dorsomedial nucleus of hypothalamus; LH, lateral hypothalamus; LHb, lateral habenula; LPO, lateral preoptic nucleus; MCLH, magnocellular nucleus of lateral hypothalamus; MHb, medial habenular nucleus; MPO, medial preoptic nucleus; MTu, medial tuberal nucleus; PFC, prefrontal cortex; VP, ventral pallidum; VTA, ventral tegmental area. All error bars represented the S.E.M..

To further confirm the connections between VTA^{Vgat} neurons and other brain areas, AAV-*DIO-ChR2-EYFP* was injected to the VTA of *Vgat-ires-Cre* mice to generate $VTA^{Vgat-ChR2}$ mice (**Fig. 4.6 A**). Strong expression of ChR2-EYFP was found restrictedly in the VTA. Compared to the expression pattern of ChR2-EYFP in $VTA^{Vglut2-ChR2}$ mice (**Fig 4.3 A**), the one in $VTA^{Vgat-ChR2}$ was distributed laterally (**Fig. 4.6 A**). Consistent with hM_4D_q -mCherry mapping and cFos activity data, dense $VTA^{Vgat-ChR2}$ -expressing fibres were observed in the LH area (**Fig. 4.6 B and C**). The LHb, DG, PFC and LPO also expressed a few $VTA^{Vgat-ChR2}$ -positive fibres (**Fig. 4.6 B and C**). These projections of VTA^{Vgat} neurons can be distinctly visualized in sagittal brain section, particularly those dense projections found in the local VTA and LH (**Fig. 4.6 C**).

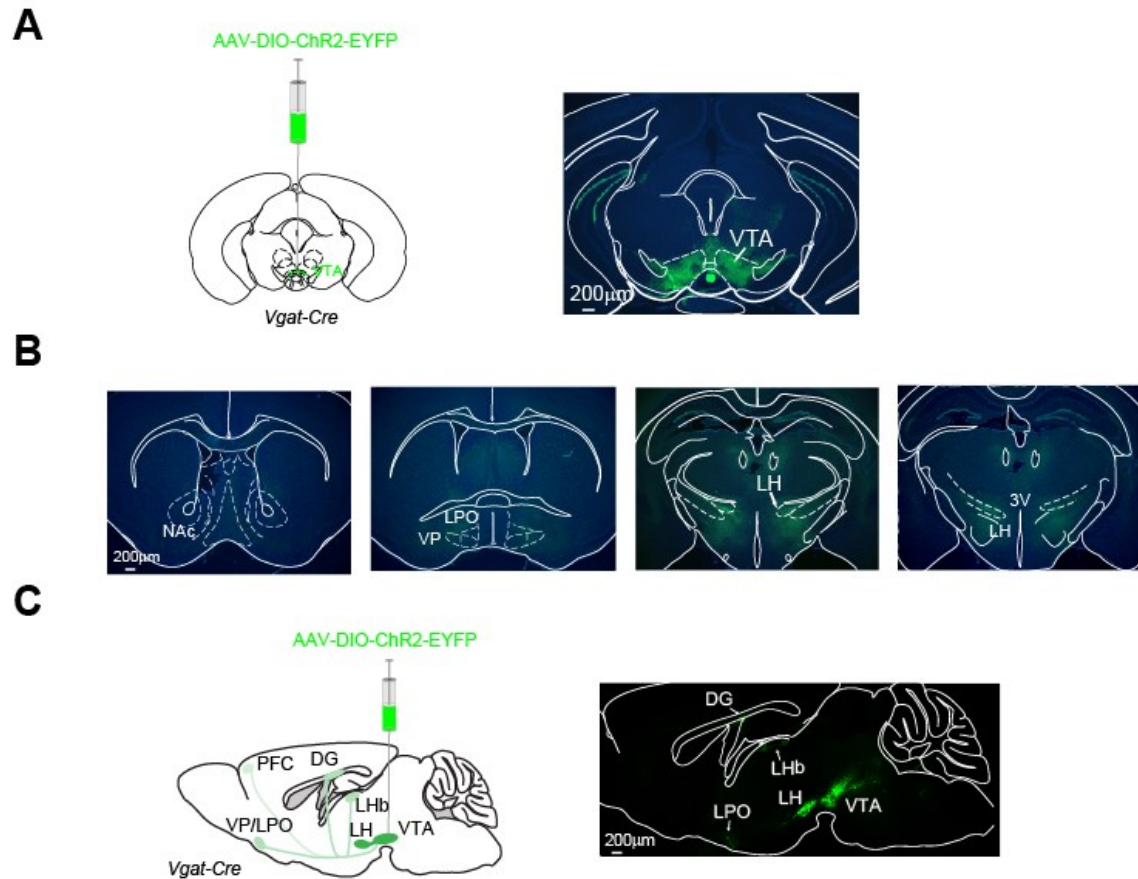


Figure 4.6 Whole brain mapping of axonal projections from VTA^{Vgat} neurons. (A) AAV-DIO-ChR2-EYFP was injected into the VTA of Vgat-ires-Cre mice and the injection site was restricted to the lateral VTA. (B) Axon projections to several different brain areas across whole brain same as the one showed in VTA^{Vgat}-hM₄D_q mice, with the LH strongly labelled. (C) Sagittal brain sections revealed similar projecting circuitry as coronal mapping. All the experiments were independently repeated four times. 3V, the third ventricle; DG, dentate gyrus; LPO, lateral preoptic nucleus; LH, lateral hypothalamus; LHb, lateral habenula; PFC, prefrontal cortex; VTA, ventral tegmental area; VP, ventral pallidum.

Discussion

In this **Chapter**, I examined the neuronal activity induced by chemogenetic activation/inhibition of VTA^{Vglut2} and VTA^{Vgat} neurons, respectively, either locally in the VTA or the brain areas innervated by the axons of VTA^{Vglut2} and VTA^{Vgat} neurons, with cFos protein expression. Meanwhile, I also mapped the axonal projections of VTA^{Vglut2} and VTA^{Vgat} neurons across the whole brain by using channelrhodopsin2.

Prolonged wakefulness can be induced by chemogenetic activation of VTA^{Vglut2} neurons[47]. *Vglut2-ires-Cre* mice were injected with *AAV-DIO-hM₃D_q-mCherry* and the virus was mainly expressed in the midline of the VTA (**Fig. 4.1 A and 4.3 A**) indicating the anatomical distribution of VTA^{Vglut2} neurons. This is consistent with a previous study that found VTA glutamatergic neurons particularly prevalent within midline nuclei, and VTA glutamatergic neurons even outnumber VTA^{DA} neurons in the rostral and medial portions of the VTA [306, 307]. Besides, immunohistochemistry shows the majority of the midline VTA^{Vglut2} neurons expressing nitric oxide synthase 1 (NOS1)[47]. After chemogenetic activation, significant increases of cFos protein were found in the hM_3D_q -expressing VTA^{Vglut2} neurons (**Fig. 4.1 B and C**) demonstrating the wakefulness was indeed due to the activation of VTA^{Vglut2} neurons. A few cFos protein expressing, but not hM_3D_q -expressing, neurons were also present after activation (**Fig. 4.1 B**). Characterization of VTA^{Vglut2} neurons showed VTA glutamatergic neurons formed local synaptic contacts[308] and reward-related behaviour mediated by VTA glutamatergic neurons confirmed this local interaction with DAergic and non-DAergic neurons[309]. It is highly possible that for sleep-wake regulation by VTA^{Vglut2} neurons, there is also local innervation from VTA

Ma, Ying

glutamatergic neurons existing, by activating nearby DAergic neurons to further reinforce wakefulness (Fig. 4.7 A).

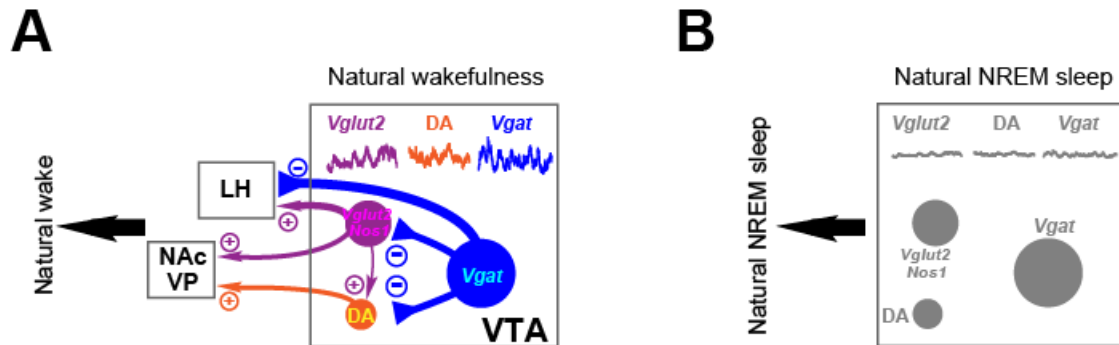


Figure 4.7 Conceptual circuit diagrams illustrating a hypothesis of how VTA^{Vglut2}, VTA^{Vgat} and VTA^{DA} neurons contribute to the natural sleep/wake regulation. (A) In the VTA, VTA^{Vglut2/Nos1}, VTA^{DA} and VTA^{Vgat} neurons are all selectively active during WAKE (and REM sleep). Interactions among these three neurons induce natural wakefulness in mice. **(B)** During nature NREM sleep, all three types of neurons become silent or less active (as indicated by grey shading). Reproduced from [47].

Both axonal projections by AAV-DIO-hM₃D_q-mCherry and AAV-DIO-ChR2-EYFP showed that VTA^{Vglut2} neurons send strong innervations to the NAc and LH along with mild projections to the PFC, VP, LHb, DR and LC (Fig. 4.2 B and 4.3 A, B and C). The wake-promoting effect produced by VTA^{Vglut2} neurons might function in part through the LH and NAc (Fig. 4.7 A). Both the LH and NAc have been suggested in sleep/wake regulation. Wakefulness can be promoted either by exciting GABAergic or orexinergic neurons in the LH[66, 67, 310]. The increased neuronal activities in the LH after chemogenetic activation of VTA^{Vglut2} (Fig. 4.2 B and C) might be induced by excitation of LH^{GABA} and/or LH^{Orexin} by VTA^{Vglut2} terminals in the LH. On the other hand, because lesioning of the NAc increases wakefulness[311, 312], this implies that the NAc GABAergic projections either limit

wakefulness or induce NREM sleep actively. Although evidence showed VTA^{Vglut2/DA} neurons strongly target the NAc[307] and stimulations of either VTA^{DA}[46] or VTA^{Vglut2} neurons produce wakefulness, the wake-promoting effect caused by VTA^{Vglut2} neurons is not blocked by dopamine receptor antagonists[47]. This could be because the wake-promoting effect produced by VTA^{DA} terminals is conducted by inducing glutamate release in the NAc. Similarly, the wake-promoting effect of the paraventricular thalamus (PV) is caused by sending glutamatergic projections to the NAc[89]. The neuronal activity induced by VTA^{Vglut2} terminals (**Fig. 4.2 B and C**) could be the activation of local GABAergic neurons in the NAc, which in turn inhibit the projections from the NREM sleep-inducing GABAergic neurons. The ventral pallidum (VP) is another brain area that has increased neuronal activity after chemogenetic activation of VTA^{Vglut2} neurons (**Fig. 4.2 B and C**). The VP receives inhibitory afferents from the NAc to promote sleep[313]. It is likely that the NAc is activated by VTA^{Vglut2} terminals as mentioned above and then reduces sending inhibitory projections on central arousal brain regions, including the VP. Although VTA^{Vglut2} neurons send axonal projections to some other brain areas (**Fig. 4.2 B and 5.3 B**) as reported in other cases[294], there is no significant change on neuronal activity during the wakefulness induced by chemogenetic activation of VTA^{Vglut2} neurons (**Fig. 4.2 B and C**). These regions may be involved in wakefulness-related cognitive behaviours and need to be investigated for the connections with VTA^{Vglut2} in regulating sleep/wake behaviours for further studies.

Unlike VTA^{Vglut2} neurons mainly located in the medial VTA, VTA^{Vgat} neurons stay laterally in the VTA (**Fig. 4.4 A and 4.5 A**). Before our work, few studies have reported a detailed

subregional mapping of VTA^{Vgat} neurons. Our lab found that chemogenetic inhibition, not activation, of VTA^{Vgat} neurons also induced wakefulness[47] and strongly induced neuronal activity in the local VTA and LH as well as some other brain areas based on cFos protein expression (**Fig. 4.5 B and C**). Immunohistochemistry shows there is no overlap between hM₄D_q-mCherry-positive neurons and cFos-positive neurons (**Fig. 4.4 B**), indicating local neuron excitation increases after inhibition of VTA^{Vgat} neurons. Indeed, VTA GABAergic neurons are known to provide inhibitory connections to VTA^{DA} neurons[314, 315] and our study also directly confirms that VTA^{Vgat} neurons exert inhibition locally[47]. Moreover, we further demonstrate that VTA^{Vgat} neurons use this local inhibition to partially restrict wakefulness[47]. The LH also receives strong axonal projections from VTA^{Vgat} neurons and has increased neuronal activity after chemogenetic inhibition of VTA^{Vgat} neurons (**Fig. 4.5 B and C and 5.6 B**). Approximately 50% of the cFos-positive neurons in the LH are orexinergic[47]. Combining the evidence that lesioning of VTA^{Vgat} neurons causes permanent sleep loss persisting for months and they are selectively wake- and REM-active during normal sleep[47], we propose that VTA^{Vgat} neurons limit wakefulness both by inhibiting local VTA glutamatergic and dopaminergic neurons and sending inhibitory projections to arousal-promoting orexinergic neurons in the LH (**Fig. 4.7 A and B**). Recently, Chowdhury *et al.* found a group of GABAergic neurons in the VTA that has their highest activity during NREM sleep and promotes NREM sleep after chemogenetic activation[88], although its photometry results did not look terribly convincing. One thing that needs to be addressed here is that instead of *Vgat-ires-Cre* mice, they used *Gad67-Cre* mice for their study. As they showed in their study, the *Gad67-*

positive neurons only represent a small portion of Vgat-positive neurons in the VTA[88]. More importantly, the neuroanatomical heterogeneity results in a differential distribution of the cell types along the antero-posterior axis of the VTA and this could play a crucial role in the functional differences observed between different regions of the VTA after local manipulations[316]. There is only around -5.5 mm from the bregma limiting the border of aVTA/pVTA when a study working on the response to cocaine in rats[317]. This limit can be more extreme in mice. Nonetheless, the activity differences between the VTA GABAergic neurons indicate the existence of different subtypes of GABAergic neurons in the VTA regulating sleep/wake behaviours, similar to the VTA GABAergic neurons studied in motivated behaviours[284]. The LPO, DG and LHb also receive axonal projections from VTA^{Vgat} neurons and have an increase of neuronal activity after chemogenetic inhibition of VTA^{Vgat} neurons (**Fig. 4.5 B and C, 4.6 B and C**), but these effects are less dominant compared to the one in the LH. The connections between these brain regions and the VTA require further investigation, for example, using electrophysiology.

Chapter 5

Materials and Methods

Chapter 2 and Chapter 3

Mice

Animal care and experiments were performed under the UK Home Office Animal Procedures Act (1986) and were approved by the Imperial College Ethical Review Committee. I was trained with the Home Office procedures and received a personal license (No. IOF5FF90B) upon successful completion of all trainings. The strain of mice used in **Chapter 2** and **Chapter 3** was as following: *Gal-Cre* mice (Tg(Gal-cre)KI87Gsat/Mmucd) which were generated by The Gene Expression Nervous System Atlas (GENSAT) Project (NINDS Contracts N01NS02331 & HHSN271200723701C to The Rockefeller University, New York)[318] and deposited at the Mutant Mouse Regional Resource Center, stock No. 031060-UCD. Animals were bred on site by crossing male homozygotic animal with C57bl6 females to generate heterozygotes, in which way would avoid unwanted phenotypes caused by high gene dosage or interruption of surrounding gene function in homozygotes. All mice used in the experiments were equally mixed genders and group-housed individually in solid-bottomed cages with environment enrichment and sawdust bedding. They were also available to *ad libitum* food and water and maintained on a reversed 12h: 12h light/dark cycle (“lights-on” hours: 17:00-05:00) at constant temperature (21±2 °C) and humidity (55±10 %). The first stereotaxic surgery was performed when mice were at the age of 10-12 weeks.

AAV transgene plasmids

All AAV transgenes had a flexed reading frame in an inverted orientation (DIO) and therefore could only be activated by Cre recombinase. The pAAV-EF1 α -DIO-taCasp3-TEVp transgene plasmid (plasmid #45580, gift from Nirao Shah)[319], the pAAV-CAG-DIO-GFP (plasmid #28304, gift from Edward Boyden), the pAAV-hSyn-DIO-hM₃D_q-mCherry (plasmid #44361, gift from Bryan Roth)[320] and pAAV-EF1 α -DIO-hChR2(H314R)-EYFP (plasmid #20298, gift from Karl Deisseroth) transgene constructs were purchased from AddGene (Cambridge, USA).

Generation of recombinant AAV particles

Raquel Yustos in our lab generated all the AAVs. All AAV transgenes, together with a mixed AAV serotype 1 capsid plasmid (pH21) and AAV serotype 2 plasmid (pRV1) (1:1 ratio) and the adenovirus helper plasmid (pF Δ 6) were transfected into HEK-293 cells. Packaged virions were then purified from HEK-293 cells in HiTrap heparin columns (Sigma, #5-4836). Detailed steps of virus production were described previously[321].

Genotyping

Genotype of the animal was confirmed by ear tissues taken from the mice during tagging. The samples were stored at 4 °C until DNA extraction using the HotSHOT method[322] with modifications. Generally, the tissues were submerged in 45 μ L of Alkaline Lysis Solution (25 mM NaOH, 0.2 mM EDTA (ethylenediaminetetraacetic acid), pH 12) and heated at 95 °C for 30 mins. An equal volume of Neutralization Solution (40 mM Tris-HCl, pH 5) was added to the sample mixture after it was cool. 5 μ L of the DNA extraction solution was processed by PCR with recommended primers from the Mutant Mouse

Regional Research Centres (Primer Gal F1: 5'-CCA GAC GTG TGC GTG TTG AGG T-3', Primer CreGS R1: 5'-CGG CAA ACG GAC AGA AGC ATT-3'). A total volume of 25 μ L PCR reaction mixer contained 12.5 μ L of GoTaq Green Master mix (Promega, UK), 10 μ M of each primer (2.5 μ L together), 1 μ L of DMSO (dimethyl sulfoxide), 4 μ L of double distilled water as well as the DNA extraction. The standard PCR conditions for DNA amplification was: (1) 95 °C for 5 mins; (2) 95 °C for 1 min for 25 cycles; (3) 65 °C for 1 min; (4) 72 °C for 1 min; (5) 72 °C for 5 mins for a final extension. The final PCR products were stored at 4 °C until resolution with a 1.8% agarose gel containing the DNA gel stain SYBR Safe (Invitrogen, USA) in 1:10000. The agarose gel was prepared in Tris-acetate EDTA (TAE) running buffer which contained 40 mM of Tris-acetate, 1 mM of EDTA, pH ~8.3 (the recipe for a 50x stock was: 242 g/L of Tris Base, 10% v/v 0.5 M of EDTA, and 57.2 mL/L of glacial acetic acid). Agarose gel was run at 75 volts for 35 mins and the DNA bands were visualized using Kodak DC290 camera under UV light together with 535 nm WB50 emission filter.

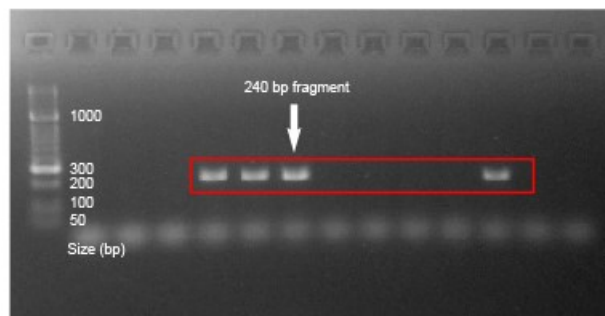


Figure 5.6 An example of *Gal-Cre* genotyping gel of *Gal-Cre* mice. DNA samples were run on 1.8% TAE/agarose gel together with HyperLadder™ 50 bp DNA ladder (Bioline, USA). The DNA fragments were visualized using SYBR® Safe DNA gel stain (Invitrogen, No.2009286). Cre-positive animals had DNA bands presenting at approximately 240 bp position on the gel.

Surgery and Stereotaxic injection of AAV

For all the surgeries, mice received buprenorphine injections before being anesthetized with a concentration of 2.5% vol/vol of isoflurane in O₂ for initiation by inhalation and maintained anesthetized on 2% of isoflurane during surgery mounted on a stereotaxic frame (Angle Two, Leica Microsystems, Milton Keynes, Buckinghamshire, UK). A heat pad was placed under the mice during the whole surgery process to prevent heat loss. For ablating galanin neurons, two AAV viruses, *i.e.* AAV-CAG-DIO-GFP and AAV-EF1A-DIO-*taCasp3-TEVp*, were mixed in a 1:1 ratio prior to the surgery (**Fig. 2.1**). For all the other viral injection surgeries, a single virus type was injected unless otherwise stated. For the parvalbumin quantification experiment in **Fig. 2.3**, AAV-DIO-*mCherry* was used instead of AAV-CAG-DIO-GFP for the ease of experiment. A 10 µL syringe (Hamilton microliter, #701) with a 33-gauge stainless steel needle (Hamilton, point style 3, length 1.5 cm) was used for AAV viral delivery and the injection rate was at 0.1 µL/min. The injection coordinates (bilateral) of the LPO were (relative to Bregma): AP +0.02 mm; ML ±0.75mm; DV -5.8mm (1/2 volume of virus) and -5.6 mm (1/2 volume of virus). A total volume of 0.2-0.5 µL of virus was injected to each hemisphere depending on the titre of the specific virus. The injection needle was left at the injection site for a further 5-10 mins after injection for achieving a better viral diffusion and then pulled out slowly. Mice were placed in a heat box with constant temperature at 32 °C for recovery before being moved back to their home cages.

In vivo EEG and EMG recording and vigilance states scoring

For *in vivo* EEG and EMG recording, mice were instrumented with a cranial implant connected to three stainless steel cranial screws (for EEG recording, two recording channels and one reference channel) and two Teflon-coated stainless-steel wires under the nuchal trapezial muscles (for EMG recording). The skull was exposed and three holes of 1-2 mm deep were drilled with a dental drill using the following coordinates as shown in **Fig. 5.7**: -1.5mm Bregma, +1.5 mm midline --- first recording electrode; +1.5 mm Bregma, -1.5 mm midline --- second recording electrode; -1 mm Lambda, 0 mm midline -- reference electrode. Drill holes were cleaned with saline and screws attached with wires were screwed down into holes and a small amount of superglue was placed on top of the screws for fixation. The two Teflon-coated EEG wires were slide into each side of the midline of the trapezius muscle at the neck with the help of 19-gauge syringe needle. Three EMG wires attached to the screws together with two EEG wires were soldered onto a 7-pin header which was designed to fit with Neurologger 2A[24]. Dental cement mixed with acrylic was used to cover and secure all the screws, wires and the header on the surface of the skull. The open head incision around the protruding head-stage was closed with an absorbable suture. Mice were monitored daily and allowed at least three weeks for recovery in their home cage before fitting with Neurologger 2A and any other subsequent procedures.

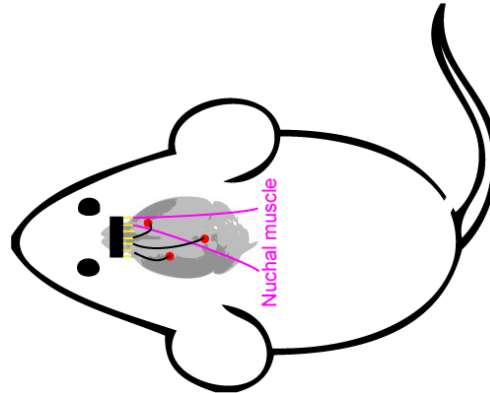


Figure 5.7 Illustration of the head-stage implantation. Mouse was implanted with a head-stage connected to three stainless steel screws on the skull and two Teflon-coated wires inserted into the nuchal trapezial muscles for *in vivo* EEG and EMG recordings by Neurologger 2A.

Once recovered, mice were habituated to wear Neurologger 2A devices for at least 24 hrs before starting recordings. Four data channels (2 of EEG and 2 of EMG) were recorded with four times oversampling at a sampling rate of 200 Hz. The dataset was downloaded and waveforms visualized using Spike2 software (Cambridge Electronic Design, Cambridge, UK). The EEG signals were high-pass filtered (0.5 Hz, -3dB, an FFT size of 512 was the designated time window) using a digital filter and the EMG was band-pass filtered between 5-45 Hz (-3dB). Power in the δ (0.5-4 Hz), θ (6-10 Hz) wave bands and θ to δ ratio were calculated, together with the root mean square (RMS) value of the EMG signal (average over a bin size of 5 s). The peak frequency during NREM epochs were analysed using Fourier transform power spectra to average power spectra over blocks of time. All of these data were used to define the vigilance states of WAKE, NREM and REM by an automated sleep-scoring script. Each vigilance state was screened and confirmed manually based on the scoring criteria showing in **Fig. 5.8**.

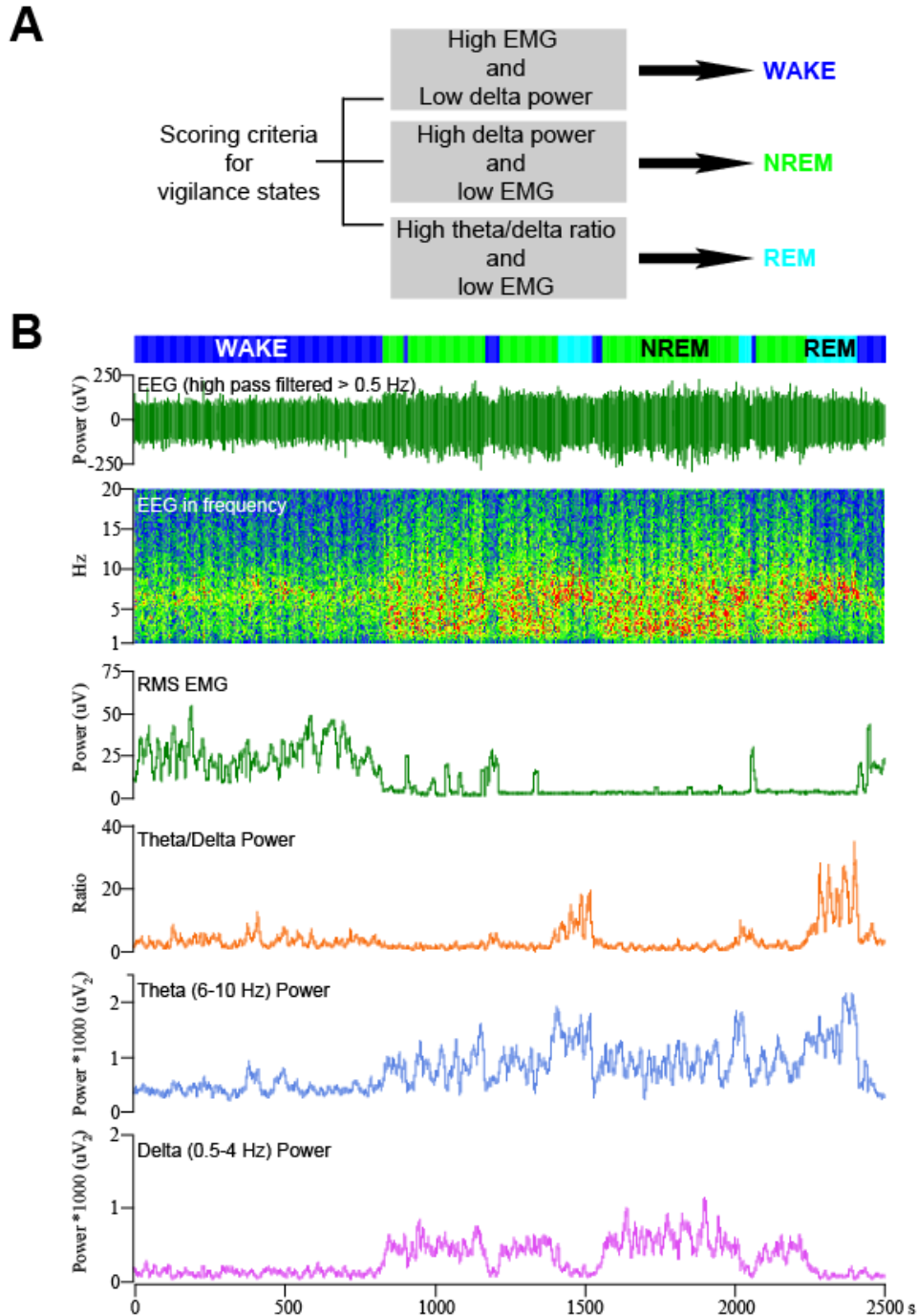


Figure 5.8 Detailed criteria for vigilance states scoring and example of EEG and EMG signals.

(A) Detailed scoring criteria for determining the WAKE, NREM and REM. Periods with high EMG and low δ power were scored as WAKE; periods with high δ power and low EMG were scored as NREM; periods with high θ/δ ratio and very low EMG were scored as REM.

(B) An example of 2,500 seconds segment of EEG and EMG raw data from a *LPO-Gal-GFP* mouse scored using Spike2 software.

Core body temperature recording

Core body temperature of the mice was recorded using a temperature logger (DST nano, Star-Oddi, Herfølge, Denmark) implanted abdominally. A pre-defined program was set to sample the temperature data continuously for an interval of every two minutes both for baseline core body temperature and drug/vehicle administration. At the end of the experiments, the loggers were retrieved, and the data were downloaded and analysed.

Sleep deprivation and recovery sleep

The sleep deprivation used a protocol similar to the one we used previously[51]. Mice were sleep deprived for in total 5 hrs, starting from zeitgeber time zero (ZT0) (17:00), *i.e.* the start of the “lights-on” period when the sleep drive of the mice was at its maximum. 5 mins before “lights-on” period, both SD and RS mice were transferred from their home cages to clean new cages individually. For the subsequent 3 hrs, novel objects were introduced into cages and swapped between cages whenever the mice appeared inactive or drowsy. For the last 2 hrs of sleep deprivation, gentle tapping was applied to keep mice awake and handling was kept to a minimum to avoid causing any stress to the animals. At the end of 5-hr SD, the mice were immediately put back to their home cages and allowed to have undisturbed recovery sleep. EEG and EMG data as well as body temperature were recorded during both 5-hr sleep deprivation and next 19-hr of recovery period to make a whole circadian cycle.

Chemogenetic treatments

For chemogenetic activation of LPO^{Gal} neurons, *LPO-Gal-hM₃D_q* mice were split into random groups that receiving either 1 mg/kg of clozapine-N-oxide (CNO) (dissolved in

saline, Sigma, C0832) or saline injection (*i.p.*) in the same volume for an unambiguous comparison. As pilot experiment showed that chemogenetic activation of LPO^{Gal} neurons would induce NREM sleep, we set the injection time at ZT18 (“lights-off” period) when mice were in their most active phase and highest body temperature. All experiments were carried out in the home cages and EEG and EMG data and core body temperatures were recorded during the experiment.

DEX experiments

Mice were implanted with temperature loggers and fitted with Neurologger 2A prior to experiment. The EEG and EMG data along with core body temperature recordings started at ZT18 (11:00, “lights-off”) in their home cages when the mice were in their most active phase and highest body temperature. 1 hr after baseline recordings of EEG/EMG and body temperature, 50 µg/kg of dexmedetomidine (DEX) (Tocris Bioscience) dissolved in 0.9% v/v saline was injected *i.p.* at ZT19 (12:00, “lights-off”). Animals were placed back to their home cages immediately after injection. A further 5 hrs of EEG/EMG and body temperature data were continuously recorded. The baseline recordings of the natural sleep-wake cycle and body temperature between ZT18-24 (11:00-17:00, “lights-off”) from the exact same mouse were also recorded for parallel comparison with the DEX-injected experiments.

Transcardial perfusion

Accurate injection of virus in the LPO was confirmed by histology. Mice were given a terminal overdose of pentobarbital sodium anaesthetic (Euthatal™) by *i.p.* injection and then were monitored for loss of surgical reflexes. Once the righting reflexes and paw

withdrawal were lost, the animal was transcardially perfused. Generally, the heart was exposed with a thoracotomy and a pump-connecting sterile butterfly needle was inserted into the left ventricle. The top right atrium was lanced with sharp tweezers immediately after the insertion. 20 mL of ice-cold PBS (Sigma, P4417) was perfused via the heart through the body at a flow rate of 3.5 mL/min. Once the liver turned to yellow-grey as a result of ex-sanguination and the perfusate was running clear from the heart, 20 mL of 4% paraformaldehyde (diluted in PBS, Thermo Scientific) was perfused through the body to fix the tissues. Subsequently, the brain was dissected out and post-fixed in 4% paraformaldehyde at 4 °C overnight. The brain was then transferred into 30% (w/v, dissolved in PBS) sucrose and allowed at least 48 hrs to saturate, aiding cryoprotection.

Immunohistochemistry

Preserved brains were mounted onto a Leica VT1000S vibratome and frozen with dry ice. 35 or 50- μ m-thick coronal sections or 50- μ m-thick sagittal sections were sliced and kept as free-floating sections in 1x PBS at 4 °C until immunohistochemistry. All solutions were made with 1x PBS and all washing steps were performed on an orbital shaker (PSU-10i, Grant Instruments) at room temperature (RT) unless specified otherwise. Free-floating sections were washed in 1x PBS three times, each for 5 mins. Sections were then permeabilized in 0.4% Triton™ detergent (Sigma, X100) for 30 mins, blocked by incubation with 5% (v/v) normal goat serum (NGS) (Vector, S-1000) plus 0.2% Triton™ for 1 h. Brain slices were shielded from light with aluminium foil wrap and incubated with primary antibody with 2% NGS overnight at 4 °C on a shaker. The following day, primary antibody incubated sections were washed in 1x PBS three times, each for 10 mins, and

incubated with secondary fluorescent antibody with 2% NGS for 2 hrs, avoiding exposure to light. Subsequently, the secondary antibody was washed off with 1x PBS four times, each for 10 mins.

Primary antibodies used were: rabbit polyclonal GFP (1:1000, Life Technology, #A6455); mouse monoclonal mCherry (1:1000, Clontech, #632543); rabbit polyclonal Parvalbumin (1:1000, Abcam, #ab11427). Secondary antibodies (Molecular Probes) were Alexa Fluor 488 goat anti-rabbit IgG (H+L) (1:1000, #A11034) and Alexa Fluor 594 goat anti-mouse IgG (H+L) (1:1000, #A11005). Sections were analysed using an upright fluorescent microscope (Nikon Eclipse 80i, Nikon) and a Leica SP5 MP confocal microscope (Facility for Imaging by Light Microscopy, Imperial College London) (Images were acquired with Z-scan).

Quantification and statistical analysis

Mice were excluded from the analysis if the histology did not confirm significant AAV transgene expression in the LPO area of the hypothalamus, or if the transgene expression had spread beyond the target region. The investigator was not blind to treatments. Origin 2016, Matlab R2018a and Excel 2016 were used for statistical analyses. Data collection and processing were randomized or performed in a counter-balanced way. The sample sizes and statistical test for each experiment are stated in the figure legends. Data are represented as the mean \pm SEM. For the behavioural tests, two-tailed *t*-tests, or one or two-way ANOVA were performed accordingly. *p* values are shown when they are less than 0.05 (**P*<0.05, ***P*<0.01, ****P*<0.001, *****P*<0.0001). When multiple comparisons were made, the Holm-Bonferroni post-hoc test was applied.

Chapter 4

Mice

The strains of mice used were as following: *Vglut2-ires-Cre: Slc17a6^{tm2(cre)Lowl/J}* (JAX stock 016963) and *Vgat-ires-Cre: Slc32a1tm2(cre)Lowl/J* (JAX stock 016962), both of which were kindly provided by B.B. Lowell. All mice used in the experiments were male and had their first stereotaxic surgery at the age of 8 weeks.

AAV transgene plasmids

All AAV transgenes could only be activated by Cre recombinase as they had a flexed reading frame in an inverted orientation. The pAAV-hSyn-DIO-hM₃D_q-mCherry (plasmid #44361), pAAV-hSyn-DIO-hM₄D_q-mCherry (plasmid #44362, gift from Bryan L. Roth) were purchased from AddGene[320].

Surgery and stereotaxic injections of AAV

The injection coordinates (bilateral) for the VTA relative to Bregma were: AP (-3.3 mm); ML (± 0.35 mm); DV (-4.25 mm). A total volume of 20-50 nL of virus was injected into the VTA depending on the viral titration.

Chemogenetic treatments

For chemogenetic experiments, the protocol was similar to the one in **Chapter 2 and 3**. To test for wake-promoting effects, either CNO or saline was injected to *VTA-Vglut-hM₃D_q* and *VTA-Vgat-hM₄D_q* mice at the start of the “lights-on” period (ZT0) when the mice had their highest sleep drive.

Immunohistochemistry

35 or 50- μ m-thick coronal sections or 50- μ m-thick sagittal sections were sliced for immunohistochemistry. Primary antibodies used were: rabbit polyclonal cFos (1:2000, Millipore); mouse monoclonal mCherry (1:1000, Clontech, #632543); rabbit polyclonal GFP (1:1000, ThermoFisher).

Quantification and statistical analysis

Mice with AAV transgene expression not in the VTA, or when there was no AAV expression, were excluded from statistical analysis. Mice were assigned randomly to the control and experimental groups. When mice were given saline versus CNO, for example, they were given saline or CNO in random order. The cFos quantification was carried out manually. All experimental data were analysed blind and the brain areas were determined according to the mouse brain atlas (The Allen Brain Atlas, <http://www.brain-map.org>).

Preliminary Result Chapter (Appendix)

Mice

Animals used in this **Chapter** were C57bl6 purchased from The Jackson Laboratory. All mice used in the experiments were males.

Sleep deprivation and recovery sleep

The sleep deprivation used a protocol similar to the one in **Chapter 2 and 3** while in this time, at the end of 5-hour sleep deprivation, mice in SD group were killed. Meanwhile mice in RS group were immediately placed back to their home cages after sleep deprivation and allowed another 2 hrs for recovery sleep. At ZT7, mice in RS group were taken out and killed.

Transcardial perfusion

cFos expression in mouse brain was confirmed by histology and followed by transcardial perfusion.

Immunohistochemistry

35- μ m-thick coronal sections were sliced for immunohistochemistry. Primary antibody used was rabbit polyclonal cFos (1:2000, Millipore) and secondary antibody (Molecular Probes) was Alexa Fluor 488 goat anti-rabbit IgG (H+L) (1:1000, #A11034). Sections were mounted on glass slides, embedded in VECTASHIELD[®] (Vector) (with DAPI counterstain), cover-slipped, and analysed using an upright fluorescent microscope (Nikon Eclipse 80i, Nikon) and a Leica SP5 MP confocal microscope (Facility for Imaging by Light Microscopy, Imperial College London).

Quantification and statistical analysis

Four mice were used in both SD and RS group. Examples from one mouse from each group were randomly selected for mapping the whole-brain neuronal activity and sections were matched with the Brain Atlas (<http://www.brain-map.org>). For cFos quantification, 4 brain sections containing the anatomical regions were randomly selected from each mouse. Fiji ImageJ was used for initial quantification. Images were adjusted with contrast and brightness to have a clear view of cFos expression by Adobe Photoshop® before being imported into ImageJ. Images were converted to greyscale (16-bit) before proceeding and then were highlighted with all of the structures needed to be counted by adjusting the threshold. The function of “Analyse Particles” was used count the cell with proper “Size” option. All the counting results then will be manually screened by the investigator to confirm the precision of the cell counting. Origin 2016 and Excel 2016 were used for statistical analyses. For the quantitative analysis, paired two-tailed *t*-tests was performed. Data are represented as the mean ± SEM. *p* values are shown when they are less than 0.05 (**P*<0.05, ***P*<0.01, ****P*<0.001, *****P*<0.0001). The investigator was not blind to treatments.

References

1. Campbell, S.S. and I. Tobler, *Animal sleep: a review of sleep duration across phylogeny*. Neurosci Biobehav Rev, 1984. **8**(3): p. 269-300.
2. Allada, R. and J.M. Siegel, *Unearthing the phylogenetic roots of sleep*. Curr Biol, 2008. **18**(15): p. R670-R679.
3. Rajput, V. and S.M. Bromley, *Chronic insomnia: a practical review*. Am Fam Physician, 1999. **60**(5): p. 1431-8; discussion 1441-2.
4. Wolkove, N., et al., *Sleep and aging: 1. Sleep disorders commonly found in older people*. Canadian Medical Association Journal, 2007. **176**(9): p. 1299-1304.
5. Siegel, J.M., *SLEEP - OPINION Sleep viewed as a state of adaptive inactivity*. Nature Reviews Neuroscience, 2009. **10**(10): p. 747-753.
6. Tobler, I.I. and M. Neuner-Jehle, *24-h variation of vigilance in the cockroach *Blaberus giganteus**. J Sleep Res, 1992. **1**(4): p. 231-239.
7. Sauer, S., et al., *The dynamics of sleep-like behaviour in honey bees*. J Comp Physiol A Neuroethol Sens Neural Behav Physiol, 2003. **189**(8): p. 599-607.
8. Goldshmid, R., et al., *Aeration of corals by sleep-swimming fish*. Limnology and Oceanography, 2004. **49**(5): p. 1832-1839.
9. Raizen, D.M., et al., *Lethargus is a *Caenorhabditis elegans* sleep-like state*. Nature, 2008. **451**(7178): p. 569-72.
10. Cirelli, C. and G. Tononi, *Is sleep essential?* Plos Biology, 2008. **6**(8): p. 1605-1611.
11. Knutson, K.L. and E. Cauter, *Associations between sleep loss and increased risk of obesity and diabetes*. Molecular and Biophysical Mechanisms of Arousal, Alertness, and Attention, 2008. **1129**: p. 287-304.
12. Mullington, J.M., et al., *Cardiovascular, inflammatory, and metabolic consequences of sleep deprivation*. Prog Cardiovasc Dis, 2009. **51**(4): p. 294-302.
13. Montagna, P. and E. Lugaresi, *Agrypnia Excitata: a generalized overactivity syndrome and a useful concept in the neurophysiopathology of sleep*. Clin Neurophysiol, 2002. **113**(4): p. 552-60.
14. Rechtschaffen, A. and B.M. Bergmann, *Sleep deprivation in the rat: an update of the 1989 paper*. Sleep, 2002. **25**(1): p. 18-24.
15. Shaw, P.J., et al., *Stress response genes protect against lethal effects of sleep deprivation in *Drosophila**. Nature, 2002. **417**(6886): p. 287-91.
16. Stephenson, R., K.M. Chu, and J. Lee, *Prolonged deprivation of sleep-like rest raises metabolic rate in the Pacific beetle cockroach, *Diploptera punctata* (Eschscholtz)*. J Exp Biol, 2007. **210**(Pt 14): p. 2540-7.
17. Vyazovskiy, V.V. and K.D. Harris, *Sleep and the single neuron: the role of global slow oscillations in individual cell rest*. Nat Rev Neurosci, 2013. **14**(6): p. 443-51.
18. Gross, M., *The reasons of sleep*. Current Biology, 2019. **29**(16): p. R775-R777.
19. Celesia, G.G., *Alcmaeon of Croton's observations on health, brain, mind, and soul*. J Hist Neurosci, 2012. **21**(4): p. 409-26.
20. von Economo, C., *Sleep as a problem of localization*. J. Nerv. Ment. Dis., 1930. **71**(3): p. 249-259.
21. Berger, H., *Über das Elektrenkephalogramm des Menschen*. Arch. Psychiat. Nervenkr., 1929. **87**: p. 527-570.
22. Wendling, F., et al., *From EEG signals to brain connectivity: a model-based evaluation of interdependence measures*. J Neurosci Methods, 2009. **183**(1): p. 9-18.

23. Ros, T., et al., *Tuning pathological brain oscillations with neurofeedback: a systems neuroscience framework*. Front Hum Neurosci, 2014. **8**: p. 1008.
24. Vyssotski, A.L., et al., *EEG responses to visual landmarks in flying pigeons*. Curr Biol, 2009. **19**(14): p. 1159-66.
25. Loomis, A.L., E.N. Havey, and G.A. Hobart, *Cerebral states during sleep, as studied by human brain potentials*. Journal of Experimental Psychology, 1937. **21**(2): p. 127-144.
26. Aserinsky, E. and N. Kleitman, *Regularly occurring periods of eye motility, and concomitant phenomena, during sleep*. Science, 1953. **118**(3062): p. 273-4.
27. Saper, C.B., T.E. Scammell, and J. Lu, *Hypothalamic regulation of sleep and circadian rhythms*. Nature, 2005. **437**(7063): p. 1257-63.
28. Datta, S., *Cellular and chemical neuroscience of mammalian sleep*. Sleep Med, 2010. **11**(5): p. 431-40.
29. Sirota, A., et al., *Communication between neocortex and hippocampus during sleep in rodents*. Proceedings of the National Academy of Sciences of the United States of America, 2003. **100**(4): p. 2065-2069.
30. De Gennaro, L. and M. Ferrara, *Sleep spindles: an overview*. Sleep Med Rev, 2003. **7**(5): p. 423-40.
31. Gais, S., et al., *Learning-dependent increases in sleep spindle density*. J Neurosci, 2002. **22**(15): p. 6830-4.
32. Fogel, S.M., et al., *Sleep spindles and learning potential*. Behav Neurosci, 2007. **121**(1): p. 1-10.
33. Lafortune, M., et al., *Sleep spindles and rapid eye movement sleep as predictors of next morning cognitive performance in healthy middle-aged and older participants*. Journal of Sleep Research, 2014. **23**(2): p. 159-167.
34. Clawson, B.C., J. Durkin, and S.J. Aton, *Form and Function of Sleep Spindles across the Lifespan*. Neural Plast, 2016. **2016**: p. 6936381.
35. Iranmanesh, S. and E. Rodriguez-Villegas, *An Ultralow-Power Sleep Spindle Detection System on Chip*. IEEE Trans Biomed Circuits Syst, 2017. **11**(4): p. 858-866.
36. Vyazovskiy, V.V., et al., *The dynamics of spindles and EEG slow-wave activity in NREM sleep in mice*. Arch Ital Biol, 2004. **142**(4): p. 511-23.
37. Nolle, M., et al., *REM sleep's unique associations with corticosterone regulation, apoptotic pathways, and behavior in chronic stress in mice*. Proc Natl Acad Sci U S A, 2019. **116**(7): p. 2733-2742.
38. Goldstein, A.N. and M.P. Walker, *The role of sleep in emotional brain function*. Annu Rev Clin Psychol, 2014. **10**: p. 679-708.
39. van der Helm, E., et al., *REM sleep depotentiates amygdala activity to previous emotional experiences*. Curr Biol, 2011. **21**(23): p. 2029-32.
40. Boyce, R., et al., *Causal evidence for the role of REM sleep theta rhythm in contextual memory consolidation*. Science, 2016. **352**(6287): p. 812-6.
41. McCarley, R.W., *Neurobiology of REM and NREM sleep*. Sleep Med, 2007. **8**(4): p. 302-30.
42. Leung, L.C., et al., *Neural signatures of sleep in zebrafish*. Nature, 2019. **571**(7764): p. 198-+.
43. Scammell, T.E., E. Arrigoni, and J.O. Lipton, *Neural Circuitry of Wakefulness and Sleep*. Neuron, 2017. **93**(4): p. 747-765.
44. Moruzzi, G. and H.W. Magoun, *Brain stem reticular formation and activation of the EEG*. Electroencephalogr Clin Neurophysiol, 1949. **1**(4): p. 455-73.
45. Ma, S., et al., *Dual-transmitter systems regulating arousal, attention, learning and memory*. Neurosci Biobehav Rev, 2018. **85**: p. 21-33.

46. Eban-Rothschild, A., et al., *VTA dopaminergic neurons regulate ethologically relevant sleep-wake behaviors*. *Nat Neurosci*, 2016. **19**(10): p. 1356-66.
47. Yu, X., et al., *GABA and glutamate neurons in the VTA regulate sleep and wakefulness*. *Nat Neurosci*, 2019. **22**(1): p. 106-119.
48. Jones, B.E., *From waking to sleeping: neuronal and chemical substrates*. *Trends Pharmacol Sci*, 2005. **26**(11): p. 578-86.
49. Gompf, H.S., et al., *Locus ceruleus and anterior cingulate cortex sustain wakefulness in a novel environment*. *J Neurosci*, 2010. **30**(43): p. 14543-51.
50. Carter, M.E., et al., *Tuning arousal with optogenetic modulation of locus coeruleus neurons*. *Nat Neurosci*, 2010. **13**(12): p. 1526-33.
51. Zhang, Z., et al., *Neuronal ensembles sufficient for recovery sleep and the sedative actions of alpha2 adrenergic agonists*. *Nat Neurosci*, 2015. **18**(4): p. 553-561.
52. Taylor, N.E., et al., *Optogenetic activation of dopamine neurons in the ventral tegmental area induces reanimation from general anesthesia*. *Proc Natl Acad Sci U S A*, 2016. **113**(45): p. 12826-12831.
53. Oishi, Y., et al., *Activation of ventral tegmental area dopamine neurons produces wakefulness through dopamine D2-like receptors in mice*. *Brain Struct Funct*, 2017. **222**(6): p. 2907-2915.
54. Lu, J., T.C. Jhou, and C.B. Saper, *Identification of wake-active dopaminergic neurons in the ventral periaqueductal gray matter*. *J Neurosci*, 2006. **26**(1): p. 193-202.
55. Jacobs, B.L. and C.A. Fornal, *Activity of brain serotonergic neurons in the behaving animal*. *Pharmacol Rev*, 1991. **43**(4): p. 563-78.
56. Oikonomou, G., et al., *The Serotonergic Raphe Promote Sleep in Zebrafish and Mice*. *Neuron*, 2019. **103**(4): p. 686-701 e8.
57. Weissbourd, B., et al., *Presynaptic partners of dorsal raphe serotonergic and GABAergic neurons*. *Neuron*, 2014. **83**(3): p. 645-62.
58. Ito, H., et al., *Analysis of sleep disorders under pain using an optogenetic tool: possible involvement of the activation of dorsal raphe nucleus-serotonergic neurons*. *Molecular Brain*, 2013. **6**.
59. Yu, X., et al., *Wakefulness Is Governed by GABA and Histamine Cotransmission*. *Neuron*, 2015. **87**(1): p. 164-178.
60. Yu, X., et al., *Circadian factor BMAL1 in histaminergic neurons regulates sleep architecture*. *Curr Biol*, 2014. **24**(23): p. 2838-44.
61. Mignot, E., S. Taheri, and S. Nishino, *Sleeping with the hypothalamus: emerging therapeutic targets for sleep disorders*. *Nature Neuroscience*, 2002. **5**: p. 1071-1075.
62. Kroeger, D., et al., *Cholinergic, Glutamatergic, and GABAergic Neurons of the Pedunculopontine Tegmental Nucleus Have Distinct Effects on Sleep/Wake Behavior in Mice*. *Journal of Neuroscience*, 2017. **37**(5): p. 1352-1366.
63. Xu, M., et al., *Basal forebrain circuit for sleep-wake control*. *Nat Neurosci*, 2015. **18**(11): p. 1641-7.
64. Fuller, P.M., et al., *Reassessment of the structural basis of the ascending arousal system*. *J Comp Neurol*, 2011. **519**(5): p. 933-56.
65. Anacleit, C., et al., *Basal forebrain control of wakefulness and cortical rhythms*. *Nat Commun*, 2015. **6**: p. 8744.
66. Herrera, C.G., et al., *Hypothalamic feedforward inhibition of thalamocortical network controls arousal and consciousness*. *Nat Neurosci*, 2016. **19**(2): p. 290-8.
67. Venner, A., et al., *A Novel Population of Wake-Promoting GABAergic Neurons in the Ventral Lateral Hypothalamus*. *Curr Biol*, 2016. **26**(16): p. 2137-43.

68. Chen, L., et al., *Basal Forebrain Cholinergic Neurons Primarily Contribute to Inhibition of Electroencephalogram Delta Activity; Rather Than Inducing Behavioral Wakefulness in Mice*. *Neuropsychopharmacology*, 2016. **41**(8): p. 2133-2146.
69. Schone, C., et al., *Coreleased orexin and glutamate evoke nonredundant spike outputs and computations in histamine neurons*. *Cell Rep*, 2014. **7**(3): p. 697-704.
70. Adamantidis, A.R., et al., *Neural substrates of awakening probed with optogenetic control of hypocretin neurons*. *Nature*, 2007. **450**(7168): p. 420-4.
71. Sasaki, K., et al., *Pharmacogenetic modulation of orexin neurons alters sleep/wakefulness states in mice*. *PLoS One*, 2011. **6**(5): p. e20360.
72. Chemelli, R.M., et al., *Narcolepsy in orexin knockout mice: molecular genetics of sleep regulation*. *Cell*, 1999. **98**(4): p. 437-51.
73. Lin, L., et al., *The sleep disorder canine narcolepsy is caused by a mutation in the hypocretin (orexin) receptor 2 gene*. *Cell*, 1999. **98**(3): p. 365-376.
74. Branch, A.F., et al., *Progressive Loss of the Orexin Neurons Reveals Dual Effects on Wakefulness*. *Sleep*, 2016. **39**(2): p. 369-77.
75. Fogerson, P.M. and J.R. Huguenard, *Tapping the Brakes: Cellular and Synaptic Mechanisms that Regulate Thalamic Oscillations*. *Neuron*, 2016. **92**(4): p. 687-704.
76. Harding, E.C., et al., *A Neuronal Hub Binding Sleep Initiation and Body Cooling in Response to a Warm External Stimulus*. *Curr Biol*, 2018. **28**(14): p. 2263-2273 e4.
77. Gelegen, C., et al., *Excitatory Pathways from the Lateral Habenula Enable Propofol-Induced Sedation*. *Curr Biol*, 2018. **28**(4): p. 580-587 e5.
78. Szymusiak, R. and D. McGinty, *Sleep-related neuronal discharge in the basal forebrain of cats*. *Brain Res*, 1986. **370**(1): p. 82-92.
79. Modirrousta, M., L. Mainville, and B.E. Jones, *Gabaergic neurons with alpha2-adrenergic receptors in basal forebrain and preoptic area express c-Fos during sleep*. *Neuroscience*, 2004. **129**(3): p. 803-10.
80. Sherin, J.E., et al., *Activation of ventrolateral preoptic neurons during sleep*. *Science*, 1996. **271**(5246): p. 216-9.
81. Gong, H., et al., *Activation of c-fos in GABAergic neurones in the preoptic area during sleep and in response to sleep deprivation*. *J Physiol*, 2004. **556**(Pt 3): p. 935-46.
82. Sherin, J.E., et al., *Innervation of histaminergic tuberomammillary neurons by GABAergic and galaninergic neurons in the ventrolateral preoptic nucleus of the rat*. *J Neurosci*, 1998. **18**(12): p. 4705-21.
83. Uschakov, A., et al., *Efferent projections from the median preoptic nucleus to sleep- and arousal-regulatory nuclei in the rat brain*. *Neuroscience*, 2007. **150**(1): p. 104-20.
84. Saito, Y.C., et al., *GABAergic neurons in the preoptic area send direct inhibitory projections to orexin neurons*. *Front Neural Circuits*, 2013. **7**: p. 192.
85. Anacleit, C., et al., *The GABAergic parafacial zone is a medullary slow-wave-sleep promoting center*. *Nat Neurosci*, 2014. **17**(9): p. 1217-1224.
86. Gerashchenko, D., et al., *Identification of a population of sleep-active cerebral cortex neurons*. *Proc Natl Acad Sci U S A*, 2008. **105**(29): p. 10227-32.
87. Morairty, S.R., et al., *A role for cortical nNOS/NK1 neurons in coupling homeostatic sleep drive to EEG slow wave activity*. *Proc Natl Acad Sci U S A*, 2013. **110**(50): p. 20272-7.
88. Chowdhury, S., et al., *GABA neurons in the ventral tegmental area regulate non-rapid eye movement sleep in mice*. *Elife*, 2019. **8**.
89. Ren, S.C., et al., *The paraventricular thalamus is a critical thalamic area for wakefulness*. *Science*, 2018. **362**(6413): p. 429-+.

90. Ma, C., et al., *Sleep Regulation by Neurotensinergic Neurons in a Thalamo-Amygdala Circuit*. *Neuron*, 2019. **103**(2): p. 323-334 e7.
91. Zhang, Z., et al., *An Excitatory Circuit in the Periocolomotor Midbrain for Non-REM Sleep Control*. *Cell*, 2019. **177**(5): p. 1293-1307 e16.
92. Peever, J. and P.M. Fuller, *The Biology of REM Sleep*. *Curr Biol*, 2017. **27**(22): p. R1237-R1248.
93. Clement, O., et al., *Evidence that Neurons of the Sublaterodorsal Tegmental Nucleus Triggering Paradoxical (REM) Sleep Are Glutamatergic*. *Sleep*, 2011. **34**(4): p. 419-423.
94. Datta, S. and D.F. Siwek, *Single cell activity patterns of pedunculopontine tegmentum neurons across the sleep-wake cycle in the freely moving rats*. *J Neurosci Res*, 2002. **70**(4): p. 611-21.
95. Cox, J., L. Pinto, and Y. Dan, *Calcium imaging of sleep-wake related neuronal activity in the dorsal pons*. *Nat Commun*, 2016. **7**: p. 10763.
96. Boucetta, S., et al., *Discharge profiles across the sleep-waking cycle of identified cholinergic, GABAergic, and glutamatergic neurons in the pontomesencephalic tegmentum of the rat*. *J Neurosci*, 2014. **34**(13): p. 4708-27.
97. Van Dort, C.J., et al., *Optogenetic activation of cholinergic neurons in the PPT or LDT induces REM sleep*. *Proc Natl Acad Sci U S A*, 2015. **112**(2): p. 584-9.
98. Hagan, J.J., et al., *Orexin A activates locus coeruleus cell firing and increases arousal in the rat*. *Proc Natl Acad Sci U S A*, 1999. **96**(19): p. 10911-6.
99. Brown, R.E., et al., *Convergent excitation of dorsal raphe serotonin neurons by multiple arousal systems (orexin/hypocretin, histamine and noradrenaline)*. *J Neurosci*, 2002. **22**(20): p. 8850-9.
100. Verret, L., et al., *A role of melanin-concentrating hormone producing neurons in the central regulation of paradoxical sleep*. *BMC Neurosci*, 2003. **4**: p. 19.
101. Hassani, O.K., M.G. Lee, and B.E. Jones, *Melanin-concentrating hormone neurons discharge in a reciprocal manner to orexin neurons across the sleep-wake cycle*. *Proc Natl Acad Sci U S A*, 2009. **106**(7): p. 2418-22.
102. Konadhode, R.R., et al., *Optogenetic stimulation of MCH neurons increases sleep*. *J Neurosci*, 2013. **33**(25): p. 10257-63.
103. Jego, S., et al., *Optogenetic identification of a rapid eye movement sleep modulatory circuit in the hypothalamus*. *Nat Neurosci*, 2013. **16**(11): p. 1637-43.
104. Tsunematsu, T., et al., *Optogenetic manipulation of activity and temporally controlled cell-specific ablation reveal a role for MCH neurons in sleep/wake regulation*. *J Neurosci*, 2014. **34**(20): p. 6896-909.
105. Chen, K.S., et al., *A Hypothalamic Switch for REM and Non-REM Sleep*. *Neuron*, 2018. **97**(5): p. 1168-1176 e4.
106. Lu, J., et al., *Selective activation of the extended ventrolateral preoptic nucleus during rapid eye movement sleep*. *J Neurosci*, 2002. **22**(11): p. 4568-76.
107. Gagnon, J.F., et al., *REM sleep behavior disorder and REM sleep without atonia in Parkinson's disease*. *Neurology*, 2002. **59**(4): p. 585-9.
108. Lu, J., *A putative flip-flop switch for control of REM sleep*. 2006.
109. Nofzinger, E.A., et al., *Forebrain activation in REM sleep: an FDG PET study*. *Brain Res*, 1997. **770**(1-2): p. 192-201.
110. Niwa, Y., et al., *Muscarinic Acetylcholine Receptors Chrm1 and Chrm3 Are Essential for REM Sleep*. *Cell Rep*, 2018. **24**(9): p. 2231-2247 e7.
111. Herice, C., A.A. Patel, and S. Sakata, *Circuit mechanisms and computational models of REM sleep*. *Neurosci Res*, 2019. **140**: p. 77-92.

112. Eban-Rothschild, A., W.J. Giardino, and L. de Lecea, *To sleep or not to sleep: neuronal and ecological insights*. *Curr Opin Neurobiol*, 2017. **44**: p. 132-138.
113. Borbely, A.A., *A two process model of sleep regulation*. *Hum Neurobiol*, 1982. **1**(3): p. 195-204.
114. Borbely, A.A., et al., *Sleep-Deprivation - Effect on Sleep Stages and Eeg Power-Density in Man*. *Electroencephalography and Clinical Neurophysiology*, 1981. **51**(5): p. 483-493.
115. Borbely, A.A., I. Tobler, and M. Hanagasioglu, *Effect of sleep deprivation on sleep and EEG power spectra in the rat*. *Behav Brain Res*, 1984. **14**(3): p. 171-82.
116. Vyazovskiy, V.V., et al., *Cortical firing and sleep homeostasis*. *Neuron*, 2009. **63**(6): p. 865-78.
117. Achermann, P. and A.A. Borbely, *Mathematical models of sleep regulation*. *Front Biosci*, 2003. **8**: p. s683-93.
118. Porkka-Heiskanen, T., et al., *Adenosine: a mediator of the sleep-inducing effects of prolonged wakefulness*. *Science*, 1997. **276**(5316): p. 1265-8.
119. Greene, R.W., T.E. Bjorness, and A. Suzuki, *The adenosine-mediated, neuronal-glia, homeostatic sleep response*. *Curr Opin Neurobiol*, 2017. **44**: p. 236-242.
120. Porkka-Heiskanen, T., *Adenosine in sleep and wakefulness*. *Ann Med*, 1999. **31**(2): p. 125-9.
121. Brown, R.E., et al., *Control of sleep and wakefulness*. *Physiol Rev*, 2012. **92**(3): p. 1087-187.
122. Gallopin, T., et al., *The endogenous somnogen adenosine excites a subset of sleep-promoting neurons via A2A receptors in the ventrolateral preoptic nucleus*. *Neuroscience*, 2005. **134**(4): p. 1377-90.
123. Korkutata, M., et al., *Enhancing endogenous adenosine A2A receptor signaling induces slow-wave sleep without affecting body temperature and cardiovascular function*. *Neuropharmacology*, 2019. **144**: p. 122-132.
124. Leenaars, C.H.C., et al., *Intracerebral Adenosine During Sleep Deprivation: A Meta-Analysis and New Experimental Data*. *J Circadian Rhythms*, 2018. **16**: p. 11.
125. Saper, C.B., et al., *Sleep state switching*. *Neuron*, 2010. **68**(6): p. 1023-42.
126. Liu, S., et al., *Sleep Drive Is Encoded by Neural Plastic Changes in a Dedicated Circuit*. *Cell*, 2016. **165**(6): p. 1347-1360.
127. Szymusiak, R., et al., *Sleep-waking discharge patterns of ventrolateral preoptic/anterior hypothalamic neurons in rats*. *Brain Res*, 1998. **803**(1-2): p. 178-88.
128. Hastings, M.H., E.S. Maywood, and M. Brancaccio, *Generation of circadian rhythms in the suprachiasmatic nucleus*. *Nat Rev Neurosci*, 2018. **19**(8): p. 453-469.
129. Brancaccio, M., et al., *Cell-autonomous clock of astrocytes drives circadian behavior in mammals*. *Science*, 2019. **363**(6423): p. 187-192.
130. Edgar, D.M., W.C. Dement, and C.A. Fuller, *Effect of SCN lesions on sleep in squirrel monkeys: evidence for opponent processes in sleep-wake regulation*. *J Neurosci*, 1993. **13**(3): p. 1065-79.
131. Mistlberger, R.E., *Circadian regulation of sleep in mammals: role of the suprachiasmatic nucleus*. *Brain Res Brain Res Rev*, 2005. **49**(3): p. 429-54.
132. Watts, A.G., L.W. Swanson, and G. Sanchez-Watts, *Efferent projections of the suprachiasmatic nucleus: I. Studies using anterograde transport of Phaseolus vulgaris leucoagglutinin in the rat*. *J. Comp. Neurol*, 1987. **258**: p. 204-229.
133. Deurveilher, S. and K. Semba, *Indirect projections from the suprachiasmatic nucleus to major arousal-promoting cell groups in rat: implications for the circadian control of behavioural state*. *Neuroscience*, 2005. **130**(1): p. 165-83.

134. Morin, L.P., *Neuroanatomy of the extended circadian rhythm system*. Exp Neurol, 2013. **243**: p. 4-20.
135. Lu, J., et al., *Contrasting effects of ibotenate lesions of the paraventricular nucleus and subparaventricular zone on sleep-wake cycle and temperature regulation*. J Neurosci, 2001. **21**(13): p. 4864-74.
136. Chou, T.C., et al., *Critical role of dorsomedial hypothalamic nucleus in a wide range of behavioral circadian rhythms*. J Neurosci, 2003. **23**(33): p. 10691-702.
137. Freedman, M.S., et al., *Regulation of mammalian circadian behavior by non-rod, non-cone, ocular photoreceptors*. Science, 1999. **284**(5413): p. 502-4.
138. Lucas, R.J., et al., *Identifying the photoreceptive inputs to the mammalian circadian system using transgenic and retinally degenerate mice*. Behavioural Brain Research, 2001. **125**(1-2): p. 97-102.
139. Antle, M.C. and R.E. Mistlberger, *Circadian clock resetting by sleep deprivation without exercise in the syrian hamster*. Journal of Neuroscience, 2000. **20**(24): p. 9326-9332.
140. Dijk, D.J. and C.A. Czeisler, *Paradoxical timing of the circadian rhythm of sleep propensity serves to consolidate sleep and wakefulness in humans*. Neurosci Lett, 1994. **166**(1): p. 63-8.
141. Dijk, D.J. and C.A. Czeisler, *Contribution of the circadian pacemaker and the sleep homeostat to sleep propensity, sleep structure, electroencephalographic slow waves, and sleep spindle activity in humans*. J Neurosci, 1995. **15**(5 Pt 1): p. 3526-38.
142. Dijk, D.J. and M. von Schantz, *Timing and consolidation of human sleep, wakefulness, and performance by a symphony of oscillators*. J Biol Rhythms, 2005. **20**(4): p. 279-90.
143. Palchykova, S., T. Deboer, and I. Tobler, *Seasonal aspects of sleep in the Djungarian hamster*. BMC Neurosci, 2003. **4**: p. 9.
144. Rattenborg, N.C., et al., *Migratory sleeplessness in the white-crowned sparrow (*Zonotrichia leucophrys gambelii*)*. PLoS Biol, 2004. **2**(7): p. E212.
145. Nofzinger, E.A., et al., *Functional neuroimaging evidence for hyperarousal in insomnia*. Am J Psychiatry, 2004. **161**(11): p. 2126-8.
146. Winsky-Sommerer, R., B. Boutrel, and L. de Lecea, *Stress and arousal: the corticotrophin-releasing factor/hypocretin circuitry*. Mol Neurobiol, 2005. **32**(3): p. 285-94.
147. Harding, E.C., N.P. Franks, and W. Wisden, *The Temperature Dependence of Sleep*. Front Neurosci, 2019. **13**: p. 336.
148. Morrison, S.F. and K. Nakamura, *Central Mechanisms for Thermoregulation*. Annu Rev Physiol, 2019. **81**: p. 285-308.
149. Schepers, R.J. and M. Ringkamp, *Thermoreceptors and thermosensitive afferents*. Neuroscience and Biobehavioral Reviews, 2009. **33**(3): p. 205-212.
150. McKemy, D.D., W.M. Neuhauser, and D. Julius, *Identification of a cold receptor reveals a general role for TRP channels in thermosensation*. Nature, 2002. **416**(6876): p. 52-8.
151. Peier, A.M., et al., *A TRP channel that senses cold stimuli and menthol*. Cell, 2002. **108**(5): p. 705-715.
152. Yarmolinsky, D.A., et al., *Coding and Plasticity in the Mammalian Thermosensory System*. Neuron, 2016. **92**(5): p. 1079-1092.
153. Almeida, M.C., et al., *Pharmacological blockade of the cold receptor TRPM8 attenuates autonomic and behavioral cold defenses and decreases deep body temperature*. J Neurosci, 2012. **32**(6): p. 2086-99.
154. Gava, N.R., et al., *Transient receptor potential melastatin 8 (TRPM8) channels are involved in body temperature regulation*. Mol Pain, 2012. **8**: p. 36.

155. Romanovsky, A.A., et al., *The Transient Receptor Potential Vanilloid-1 Channel in Thermoregulation: A Thermosensor It Is Not*. Pharmacological Reviews, 2009. **61**(3): p. 228-261.
156. Hori, T., *Capsaicin and central control of thermoregulation*. Pharmacol Ther, 1984. **26**(3): p. 389-416.
157. Gavva, N.R., et al., *The vanilloid receptor TRPV1 is tonically activated in vivo and involved in body temperature regulation*. Journal of Neuroscience, 2007. **27**(13): p. 3366-3374.
158. Steiner, A.A., et al., *Nonthermal activation of transient receptor potential vanilloid-1 channels in abdominal viscera tonically inhibits autonomic cold-defense effectors*. J Neurosci, 2007. **27**(28): p. 7459-68.
159. Gavva, N.R., *Body-temperature maintenance as the predominant function of the vanilloid receptor TRPV1*. Trends in Pharmacological Sciences, 2008. **29**(11): p. 550-557.
160. Caterina, M.J., et al., *Impaired nociception and pain sensation in mice lacking the capsaicin receptor*. Science, 2000. **288**(5464): p. 306-13.
161. Iida, T., et al., *Attenuated fever response in mice lacking TRPV1*. Neurosci Lett, 2005. **378**(1): p. 28-33.
162. Szelenyi, Z., et al., *Daily body temperature rhythm and heat tolerance in TRPV1 knockout and capsaicin pretreated mice*. Eur J Neurosci, 2004. **19**(5): p. 1421-4.
163. Takashima, Y., et al., *Diversity in the neural circuitry of cold sensing revealed by genetic axonal labeling of transient receptor potential melastatin 8 neurons*. J Neurosci, 2007. **27**(51): p. 14147-57.
164. Tominaga, M., et al., *The cloned capsaicin receptor integrates multiple pain-producing stimuli*. Neuron, 1998. **21**(3): p. 531-43.
165. Nakamura, K. and S.F. Morrison, *A thermosensory pathway mediating heat-defense responses*. Proc Natl Acad Sci U S A, 2010. **107**(19): p. 8848-53.
166. Magoun, H.W., et al., *Activation of heat loss mechanisms by local heating of the brain*. J. Neurophysiol, 1938. **1**: p. 101-114.
167. Nakayama, T., J.S. Eisenman, and J.D. Hardy, *Single unit activity of anterior hypothalamus during local heating*. Science, 1961. **134**(3478): p. 560-1.
168. Hermann, D.M., et al., *Afferent projections to the rat nuclei raphe magnus, raphe pallidus and reticularis gigantocellularis pars alpha demonstrated by iontophoretic application of cholera toxin (subunit b)*. J Chem Neuroanat, 1997. **13**(1): p. 1-21.
169. Hosoya, Y., et al., *Direct Projection from the Dorsal Hypothalamic Area to the Nucleus Raphe Pallidus - a Study Using Anterograde Transport with Phaseolus-Vulgaris Leucoagglutinin in the Rat*. Experimental Brain Research, 1989. **75**(1): p. 40-46.
170. Almeida, M.C., R.C. Vizin, and D.C. Carrettiero, *Current understanding on the neurophysiology of behavioral thermoregulation*. Temperature (Austin), 2015. **2**(4): p. 483-90.
171. Baldwin, B.A. and D.L. Ingram, *Effect of heating & cooling the hypothalamus on behavioral thermoregulation in the pig*. J Physiol, 1967. **191**(2): p. 375-92.
172. Carlisle, H.J. and M.L. Laudenslager, *Observations on the thermoregulatory effects of preoptic warming in rats*. Physiol Behav, 1979. **23**(4): p. 723-32.
173. Satinoff, E., *Behavioral Thermoregulation in Response to Local Cooling of the Rat Brain*. Am J Physiol, 1964. **206**: p. 1389-94.
174. Tan, C.L., et al., *Warm-Sensitive Neurons that Control Body Temperature*. Cell, 2016. **167**(1): p. 47-59 e15.
175. Zhao, Z.D., et al., *A hypothalamic circuit that controls body temperature*. Proc Natl Acad Sci U S A, 2017. **114**(8): p. 2042-2047.

176. Kroeger, D., et al., *Galanin neurons in the ventrolateral preoptic area promote sleep and heat loss in mice*. Nat Commun, 2018. **9**(1): p. 4129.
177. Ma, Y., et al., *Galanin Neurons Unite Sleep Homeostasis and alpha2-Adrenergic Sedation*. Curr Biol, 2019.
178. Horne, J.A. and A.J. Reid, *Night-time sleep EEG changes following body heating in a warm bath*. Electroencephalogr Clin Neurophysiol, 1985. **60**(2): p. 154-7.
179. Parmeggiani, P.L., *Interaction between Sleep and Thermoregulation - an Aspect of the Control of Behavioral States*. Sleep, 1987. **10**(5): p. 426-435.
180. Bunnell, D.E., et al., *Passive body heating and sleep: influence of proximity to sleep*. Sleep, 1988. **11**(2): p. 210-9.
181. Krueger, J.M. and S. Takahashi, *Thermoregulation and sleep. Closely linked but separable*. Ann N Y Acad Sci, 1997. **813**: p. 281-6.
182. Gordon, C.J., P. Becker, and J.S. Ali, *Behavioral thermoregulatory responses of single- and group-housed mice*. Physiol Behav, 1998. **65**(2): p. 255-62.
183. Gaskill, B.N., et al., *Heat or Insulation: Behavioral Titration of Mouse Preference for Warmth or Access to a Nest*. Plos One, 2012. **7**(3).
184. Morairty, S.R., et al., *Selective increases in non-rapid eye movement sleep following whole body heating in rats*. Brain Res, 1993. **617**(1): p. 10-6.
185. Szymusiak, R., J. Danowski, and D. McGinty, *Exposure to heat restores sleep in cats with preoptic/anterior hypothalamic cell loss*. Brain Res, 1991. **541**(1): p. 134-8.
186. McGinty, D., R. Szymusiak, and D. Thomson, *Preoptic-Anterior Hypothalamic Warming Increases Eeg Delta-Frequency Activity within Non-Rapid Eye-Movement Sleep*. Brain Research, 1994. **667**(2): p. 273-277.
187. Krilowicz, B.L., R. Szymusiak, and D. McGinty, *Regulation of posterior lateral hypothalamic arousal related neuronal discharge by preoptic anterior hypothalamic warming*. Brain Res, 1994. **668**(1-2): p. 30-8.
188. Guzman-Marin, R., et al., *Discharge modulation of rat dorsal raphe neurons during sleep and waking: effects of preoptic/basal forebrain warming*. Brain Res, 2000. **875**(1-2): p. 23-34.
189. Everson, C.A., B.M. Bergmann, and A. Rechtschaffen, *Sleep deprivation in the rat: III. Total sleep deprivation*. Sleep, 1989. **12**(1): p. 13-21.
190. Prete, F.R., et al., *Sleep deprivation in the rat: XII. Effect on ambient temperature choice*. Sleep, 1991. **14**(2): p. 109-15.
191. Szentirmai, E. and L. Kapas, *Intact brown adipose tissue thermogenesis is required for restorative sleep responses after sleep loss*. European Journal of Neuroscience, 2014. **39**(6): p. 984-998.
192. Franks, N.P., *General anaesthesia: from molecular targets to neuronal pathways of sleep and arousal*. Nat Rev Neurosci, 2008. **9**(5): p. 370-86.
193. Yu, X., N.P. Franks, and W. Wisden, *Sleep and Sedative States Induced by Targeting the Histamine and Noradrenergic Systems*. Front Neural Circuits, 2018. **12**: p. 4.
194. Franks, N.P. and A.Y. Zecharia, *Sleep and general anesthesia*. Can J Anaesth, 2011. **58**(2): p. 139-48.
195. Macdonald, R.L. and J.L. Barker, *Different Actions of Anticonvulsant and Anesthetic Barbiturates Revealed by Use of Cultured Mammalian Neurons*. Science, 1978. **200**(4343): p. 775-777.
196. Nicoll, R.A., *Pentobarbital: differential postsynaptic actions on sympathetic ganglion cells*. Science, 1978. **199**(4327): p. 451-2.

197. Leeb-Lundberg, F., A. Snowman, and R.W. Olsen, *Barbiturate receptor sites are coupled to benzodiazepine receptors*. Proc Natl Acad Sci U S A, 1980. **77**(12): p. 7468-72.
198. Mihic, S.J., et al., *Sites of alcohol and volatile anaesthetic action on GABA(A) and glycine receptors*. Nature, 1997. **389**(6649): p. 385-9.
199. Krasowski, M.D. and N.L. Harrison, *The actions of ether, alcohol and alkane general anaesthetics on GABA(A) and glycine receptors and the effects of TM2 and TM3 mutations*. British Journal of Pharmacology, 2000. **129**(4): p. 731-743.
200. Nishikawa, K., et al., *Volatile anesthetic actions on the GABAA receptors: contrasting effects of alpha 1(S270) and beta 2(N265) point mutations*. Neuropharmacology, 2002. **42**(3): p. 337-45.
201. Koltchine, V.V., et al., *Agonist gating and isoflurane potentiation in the human gamma-aminobutyric acid type A receptor determined by the volume of a second transmembrane domain residue*. Mol Pharmacol, 1999. **56**(5): p. 1087-93.
202. Patel, A.J., et al., *Inhalational anesthetics activate two-pore-domain background K+ channels*. Nat Neurosci, 1999. **2**(5): p. 422-6.
203. Ogata, J., et al., *Effects of anesthetics on mutant N-methyl-D-aspartate receptors expressed in Xenopus oocytes*. J Pharmacol Exp Ther, 2006. **318**(1): p. 434-43.
204. Nutt, D.J. and S.M. Stahl, *Searching for perfect sleep: the continuing evolution of GABAA receptor modulators as hypnotics*. J Psychopharmacol, 2010. **24**(11): p. 1601-12.
205. Greenblatt, D.J. and T. Roth, *Zolpidem for insomnia*. Expert Opin Pharmacother, 2012. **13**(6): p. 879-93.
206. Wisden, W., X. Yu, and N.P. Franks, *GABA Receptors and the Pharmacology of Sleep*. Handb Exp Pharmacol, 2017.
207. Uygun, D.S., et al., *Bottom-Up versus Top-Down Induction of Sleep by Zolpidem Acting on Histaminergic and Neocortex Neurons*. J Neurosci, 2016. **36**(44): p. 11171-11184.
208. Huupponen, E., et al., *Electroencephalogram spindle activity during dexmedetomidine sedation and physiological sleep*. Acta Anaesthesiol Scand, 2008. **52**(2): p. 289-94.
209. Mason, K.P., et al., *Effects of dexmedetomidine sedation on the EEG in children*. Paediatr Anaesth, 2009. **19**(12): p. 1175-83.
210. Akeju, O. and E.N. Brown, *Neural oscillations demonstrate that general anesthesia and sedative states are neurophysiologically distinct from sleep*. Curr Opin Neurobiol, 2017. **44**: p. 178-185.
211. Seidel, W.F., et al., *Alpha-2 adrenergic modulation of sleep: time-of-day-dependent pharmacodynamic profiles of dexmedetomidine and clonidine in the rat*. J Pharmacol Exp Ther, 1995. **275**(1): p. 263-73.
212. Bol, C., et al., *Pharmacokinetic-pharmacodynamic characterization of the cardiovascular, hypnotic, EEG and ventilatory responses to dexmedetomidine in the rat*. J Pharmacol Exp Ther, 1997. **283**(3): p. 1051-8.
213. Gelegen, C., et al., *Staying awake--a genetic region that hinders alpha2 adrenergic receptor agonist-induced sleep*. Eur J Neurosci, 2014. **40**(1): p. 2311-9.
214. Borbely, A.A., et al., *The two-process model of sleep regulation: a reappraisal*. J Sleep Res, 2016. **25**(2): p. 131-43.
215. Porkka-Heiskanen, T., *Sleep homeostasis*. Curr Opin Neurobiol, 2013. **23**(5): p. 799-805.
216. Franken, P., D. Chollet, and M. Tafti, *The homeostatic regulation of sleep need is under genetic control*. Journal of Neuroscience, 2001. **21**(8): p. 2610-2621.
217. Funato, H., et al., *Forward-genetics analysis of sleep in randomly mutagenized mice*. Nature, 2016. **539**(7629): p. 378-383.

218. Holst, S.C., et al., *Cerebral mGluR5 availability contributes to elevated sleep need and behavioral adjustment after sleep deprivation*. *Elife*, 2017. **6**.
219. Bjorness, T.E., et al., *Control and function of the homeostatic sleep response by adenosine A1 receptors*. *J Neurosci*, 2009. **29**(5): p. 1267-76.
220. Franken, P., *A role for clock genes in sleep homeostasis*. *Curr Opin Neurobiol*, 2013. **23**(5): p. 864-72.
221. Mang, G.M., et al., *Altered Sleep Homeostasis in Rev-erbalpha Knockout Mice*. *Sleep*, 2016. **39**(3): p. 589-601.
222. Hasan, S., et al., *A human sleep homeostasis phenotype in mice expressing a primate-specific PER3 variable-number tandem-repeat coding-region polymorphism*. *FASEB J*, 2014. **28**(6): p. 2441-54.
223. Halassa, M.M., et al., *Astrocytic modulation of sleep homeostasis and cognitive consequences of sleep loss*. *Neuron*, 2009. **61**(2): p. 213-9.
224. Wang, Z., et al., *Quantitative phosphoproteomic analysis of the molecular substrates of sleep need*. *Nature*, 2018. **558**(7710): p. 435-439.
225. Nelson, L.E., et al., *The alpha2-adrenoceptor agonist dexmedetomidine converges on an endogenous sleep-promoting pathway to exert its sedative effects*. *Anesthesiology*, 2003. **98**(2): p. 428-36.
226. McGinty, D. and R. Szymusiak, *Keeping cool: a hypothesis about the mechanisms and functions of slow-wave sleep*. *Trends Neurosci*, 1990. **13**(12): p. 480-7.
227. Hoekstra, M.M., et al., *Cold-inducible RNA-binding protein (CIRBP) adjusts clock-gene expression and REM-sleep recovery following sleep deprivation*. *Elife*, 2019. **8**.
228. McAlpine, C.S., et al., *Sleep modulates haematopoiesis and protects against atherosclerosis*. *Nature*, 2019. **566**(7744): p. 383-387.
229. de Vivo, L., et al., *Ultrastructural evidence for synaptic scaling across the wake/sleep cycle*. *Science*, 2017. **355**(6324): p. 507-510.
230. Diering, G.H., et al., *Homer1a drives homeostatic scaling-down of excitatory synapses during sleep*. *Science*, 2017. **355**(6324): p. 511-515.
231. Xie, L., et al., *Sleep drives metabolite clearance from the adult brain*. *Science*, 2013. **342**(6156): p. 373-7.
232. Diessler, S., et al., *A systems genetics resource and analysis of sleep regulation in the mouse*. *PLoS Biol*, 2018. **16**(8): p. e2005750.
233. Archer, S.N., et al., *Mistimed sleep disrupts circadian regulation of the human transcriptome*. *Proc Natl Acad Sci U S A*, 2014. **111**(6): p. E682-91.
234. Davies, S.K., et al., *Effect of sleep deprivation on the human metabolome*. *Proc Natl Acad Sci U S A*, 2014. **111**(29): p. 10761-6.
235. Ehlen, J.C., et al., *Bmal1 function in skeletal muscle regulates sleep*. *Elife*, 2017. **6**.
236. Szymusiak, R., I. Gvilia, and D. McGinty, *Hypothalamic control of sleep*. *Sleep Med*, 2007. **8**(4): p. 291-301.
237. Alam, M.A., et al., *Neuronal activity in the preoptic hypothalamus during sleep deprivation and recovery sleep*. *J Neurophysiol*, 2014. **111**(2): p. 287-99.
238. Gvilia, I., et al., *Homeostatic regulation of sleep: a role for preoptic area neurons*. *J Neurosci*, 2006. **26**(37): p. 9426-33.
239. Siemens, J. and G.B. Kamm, *Cellular populations and thermosensing mechanisms of the hypothalamic thermoregulatory center*. *Pflugers Arch*, 2018. **470**(5): p. 809-822.
240. Nakamura, K. and S.F. Morrison, *A thermosensory pathway that controls body temperature*. *Nat Neurosci*, 2008. **11**(1): p. 62-71.

241. Tan, C.L. and Z.A. Knight, *Regulation of Body Temperature by the Nervous System*. Neuron, 2018. **98**(1): p. 31-48.
242. Franken, P., I. Tobler, and A.A. Borbely, *Cortical temperature and EEG slow-wave activity in the rat: analysis of vigilance state related changes*. Pflugers Arch, 1992. **420**(5-6): p. 500-7.
243. Alfoldi, P., et al., *Brain and core temperatures and peripheral vasomotion during sleep and wakefulness at various ambient temperatures in the rat*. Pflugers Arch, 1990. **417**(3): p. 336-41.
244. Gaus, S.E., et al., *Ventrolateral preoptic nucleus contains sleep-active, galaninergic neurons in multiple mammalian species*. Neuroscience, 2002. **115**(1): p. 285-94.
245. Tatemoto, K., et al., *Galanin - a novel biologically active peptide from porcine intestine*. FEBS Lett, 1983. **164**(1): p. 124-8.
246. Lu, J., et al., *Effect of lesions of the ventrolateral preoptic nucleus on NREM and REM sleep*. J Neurosci, 2000. **20**(10): p. 3830-42.
247. Vetrivelan, R., C.B. Saper, and P.M. Fuller, *Armodafinil-induced wakefulness in animals with ventrolateral preoptic lesions*. Nat Sci Sleep, 2014. **6**: p. 57-63.
248. Lim, A.S., et al., *Sleep is related to neuron numbers in the ventrolateral preoptic/intermediate nucleus in older adults with and without Alzheimer's disease*. Brain, 2014. **137**(Pt 10): p. 2847-61.
249. Moffitt, J.R., et al., *Molecular, spatial, and functional single-cell profiling of the hypothalamic preoptic region*. Science, 2018. **362**(6416).
250. Chung, S., et al., *Identification of preoptic sleep neurons using retrograde labelling and gene profiling*. Nature, 2017. **545**(7655): p. 477-481.
251. Huber, R., T. Deboer, and I. Tobler, *Effects of sleep deprivation on sleep and sleep EEG in three mouse strains: empirical data and simulations*. Brain Res, 2000. **857**(1-2): p. 8-19.
252. Pimentel, D., et al., *Operation of a homeostatic sleep switch*. Nature, 2016. **536**(7616): p. 333-337.
253. Song, K., et al., *The TRPM2 channel is a hypothalamic heat sensor that limits fever and can drive hypothermia*. Science, 2016. **353**(6306): p. 1393-1398.
254. Campbell, S.S. and R.J. Broughton, *Rapid decline in body temperature before sleep: fluffing the physiological pillow?* Chronobiol Int, 1994. **11**(2): p. 126-31.
255. Schonrock, B., D. Busselberg, and H.L. Haas, *Properties of tuberomammillary histamine neurones and their response to galanin*. Agents Actions, 1991. **33**(1-2): p. 135-7.
256. Reichert, S., *The neuropeptide galanin is required for homeostatic rebound sleep*. Neuron, 2019.
257. Baker, R., et al., *Altered activity in the central medial thalamus precedes changes in the neocortex during transitions into both sleep and propofol anesthesia*. J Neurosci, 2014. **34**(40): p. 13326-35.
258. Adams, R., et al., *Efficacy of dexmedetomidine compared with midazolam for sedation in adult intensive care patients: a systematic review*. Br J Anaesth, 2013. **111**(5): p. 703-10.
259. Ramsay, M.A., et al., *Controlled sedation with alphaxalone-alphadolone*. Br Med J, 1974. **2**(5920): p. 656-9.
260. Akeju, O., et al., *Dexmedetomidine promotes biomimetic non-rapid eye movement stage 3 sleep in humans: A pilot study*. Clin Neurophysiol, 2018. **129**(1): p. 69-78.
261. Akeju, O., et al., *Spatiotemporal Dynamics of Dexmedetomidine-Induced Electroencephalogram Oscillations*. PLoS One, 2016. **11**(10): p. e0163431.

262. Hunter, J.C., et al., *Assessment of the role of alpha2-adrenoceptor subtypes in the antinociceptive, sedative and hypothermic action of dexmedetomidine in transgenic mice.* Br J Pharmacol, 1997. **122**(7): p. 1339-44.
263. Malmberg, A.B., et al., *Contribution of alpha(2) receptor subtypes to nerve injury-induced pain and its regulation by dexmedetomidine.* Br J Pharmacol, 2001. **132**(8): p. 1827-36.
264. Lakhiani, P.P., et al., *Substitution of a mutant alpha2a-adrenergic receptor via "hit and run" gene targeting reveals the role of this subtype in sedative, analgesic, and anesthetic-sparing responses in vivo.* Proc Natl Acad Sci U S A, 1997. **94**(18): p. 9950-5.
265. Correa-Sales, C., B.C. Rabin, and M. Maze, *A hypnotic response to dexmedetomidine, an alpha 2 agonist, is mediated in the locus coeruleus in rats.* Anesthesiology, 1992. **76**(6): p. 948-52.
266. Sanders, R.D. and M. Maze, *Noradrenergic trespass in anesthetic and sedative states.* Anesthesiology, 2012. **117**(5): p. 945-7.
267. Hu, F.Y., et al., *Hypnotic hypersensitivity to volatile anesthetics and dexmedetomidine in dopamine beta-hydroxylase knockout mice.* Anesthesiology, 2012. **117**(5): p. 1006-17.
268. Quan, N., et al., *Preoptic norepinephrine-induced hypothermia is mediated by alpha 2-adrenoceptors.* Am J Physiol, 1992. **262**(3 Pt 2): p. R407-11.
269. Alam, M.N. and B.N. Mallick, *Role of lateral preoptic area alpha-1 and alpha-2 adrenoceptors in sleep-wakefulness and body temperature regulation.* Brain Research Bulletin, 1994. **35**(2): p. 171-177.
270. Daan, S., B.M. Barnes, and A.M. Strijkstra, *Warming up for sleep? Ground squirrels sleep during arousals from hibernation.* Neurosci Lett, 1991. **128**(2): p. 265-8.
271. Trachsel, L., D.M. Edgar, and H.C. Heller, *Are ground squirrels sleep deprived during hibernation?* Am J Physiol, 1991. **260**(6 Pt 2): p. R1123-9.
272. Harris, N.A., et al., *Dorsal BNST alpha2A-Adrenergic Receptors Produce HCN-Dependent Excitatory Actions That Initiate Anxiogenic Behaviors.* J Neurosci, 2018. **38**(42): p. 8922-8942.
273. Kohl, J., et al., *Functional circuit architecture underlying parental behaviour.* Nature, 2018. **556**(7701): p. 326-331.
274. Wu, Z., et al., *Galanin neurons in the medial preoptic area govern parental behaviour.* Nature, 2014. **509**(7500): p. 325-30.
275. Reichert, S., O.P. Arocas, and J. Rihel, *Neuronal activity drives homeostatic sleep through engagement of the hypothalamic neuropeptide galanin.* bioRxiv, 2018.
276. Trutti, A.C., et al., *Functional neuroanatomical review of the ventral tegmental area.* Neuroimage, 2019. **191**: p. 258-268.
277. Tsai, C., *The optic tracts and centers of the opossum. Didelphis virginiana.* The Journal of Comparative Neurology, 1925. **39**(2): p. 173-216.
278. Holly, E.N. and K.A. Miczek, *Ventral tegmental area dopamine revisited: effects of acute and repeated stress.* Psychopharmacology (Berl), 2016. **233**(2): p. 163-86.
279. Ding, S.L., et al., *Comprehensive cellular-resolution atlas of the adult human brain.* J Comp Neurol, 2016. **524**(16): p. 3127-481.
280. Hall, H., et al., *Hippocampal Lewy pathology and cholinergic dysfunction are associated with dementia in Parkinson's disease.* Brain, 2014. **137**(Pt 9): p. 2493-508.
281. Halliday, G.M. and I. Tork, *Comparative anatomy of the ventromedial mesencephalic tegmentum in the rat, cat, monkey and human.* J Comp Neurol, 1986. **252**(4): p. 423-45.
282. Hasirci, A.S., et al., *Cellular GABAergic Neuroactive Steroid (3alpha,5alpha)-3-Hydroxy-Pregnan-20-One (3alpha,5alpha-THP) Immunostaining Levels Are Increased in the Ventral*

- Tegmental Area of Human Alcohol Use Disorder Patients: A Postmortem Study*. Alcohol Clin Exp Res, 2017. **41**(2): p. 299-311.
283. McRitchie, D.A., C.D. Hardman, and G.M. Halliday, *Cytoarchitectural distribution of calcium binding proteins in midbrain dopaminergic regions of rats and humans*. J Comp Neurol, 1996. **364**(1): p. 121-50.
 284. Morales, M. and E.B. Margolis, *Ventral tegmental area: cellular heterogeneity, connectivity and behaviour*. Nat Rev Neurosci, 2017. **18**(2): p. 73-85.
 285. Swanson, L.W., *The projections of the ventral tegmental area and adjacent regions: a combined fluorescent retrograde tracer and immunofluorescence study in the rat*. Brain Res Bull, 1982. **9**(1-6): p. 321-53.
 286. D'Ardenne, K., et al., *Role of prefrontal cortex and the midbrain dopamine system in working memory updating*. Proc Natl Acad Sci U S A, 2012. **109**(49): p. 19900-9.
 287. Duzel, E., et al., *NOvelty-related motivation of anticipation and exploration by dopamine (NOMAD): implications for healthy aging*. Neurosci Biobehav Rev, 2010. **34**(5): p. 660-9.
 288. Krebs, R.M., B.H. Schott, and E. Duzel, *Personality traits are differentially associated with patterns of reward and novelty processing in the human substantia nigra/ventral tegmental area*. Biol Psychiatry, 2009. **65**(2): p. 103-10.
 289. Fu, Y., et al., *The substantia nigra and ventral tegmental dopaminergic neurons from development to degeneration*. J Chem Neuroanat, 2016. **76**(Pt B): p. 98-107.
 290. van Domburg, P. and H. ten Donkelaar, *The human substantia nigra and ventral tegmental area: a neuroanatomical study with notes on ageing and ageing disease*. Adv. Anat. Embryol. Cell Biol., 1991. **121**: p. 1-132.
 291. Zhang, T.A., A.N. Placzek, and J.A. Dani, *In vitro identification and electrophysiological characterization of dopamine neurons in the ventral tegmental area*. Neuropharmacology, 2010. **59**(6): p. 431-6.
 292. Aransay, A., et al., *Long-range projection neurons of the mouse ventral tegmental area: a single-cell axon tracing analysis*. Front Neuroanat, 2015. **9**: p. 59.
 293. Poirier, L.J., M. Giguere, and R. Marchand, *Comparative morphology of the substantia nigra and ventral tegmental area in the monkey, cat and rat*. Brain Res Bull, 1983. **11**(3): p. 371-97.
 294. Barker, D.J., et al., *Multiplexed neurochemical signaling by neurons of the ventral tegmental area*. J Chem Neuroanat, 2016. **73**: p. 33-42.
 295. Salamone, J.D. and M. Correa, *Motivational views of reinforcement: implications for understanding the behavioral functions of nucleus accumbens dopamine*. Behav Brain Res, 2002. **137**(1-2): p. 3-25.
 296. Hennigan, K., K. D'Ardenne, and S.M. McClure, *Distinct midbrain and habenula pathways are involved in processing aversive events in humans*. J Neurosci, 2015. **35**(1): p. 198-208.
 297. Brown, M.T., et al., *Ventral tegmental area GABA projections pause accumbal cholinergic interneurons to enhance associative learning*. Nature, 2012. **492**(7429): p. 452-6.
 298. Horvitz, J.C., *Mesolimbocortical and nigrostriatal dopamine responses to salient non-reward events*. Neuroscience, 2000. **96**(4): p. 651-6.
 299. Bromberg-Martin, E.S., M. Matsumoto, and O. Hikosaka, *Dopamine in motivational control: rewarding, aversive, and alerting*. Neuron, 2010. **68**(5): p. 815-34.
 300. Carlsson, A., B. Falck, and N.A. Hillarp, *Cellular localization of brain monoamines*. Acta Physiol Scand Suppl, 1962. **56**(196): p. 1-28.
 301. Nair-Roberts, R.G., et al., *Stereological estimates of dopaminergic, GABAergic and glutamatergic neurons in the ventral tegmental area, substantia nigra and retrorubral field in the rat*. Neuroscience, 2008. **152**(4): p. 1024-31.

302. Sesack, S.R. and A.A. Grace, *Cortico-Basal Ganglia reward network: microcircuitry*. Neuropsychopharmacology, 2010. **35**(1): p. 27-47.
303. Stamatakis, A.M., et al., *A unique population of ventral tegmental area neurons inhibits the lateral habenula to promote reward*. Neuron, 2013. **80**(4): p. 1039-53.
304. Qi, J., et al., *VTA glutamatergic inputs to nucleus accumbens drive aversion by acting on GABAergic interneurons*. Nat Neurosci, 2016. **19**(5): p. 725-733.
305. Takata, Y., et al., *Sleep and Wakefulness Are Controlled by Ventral Medial Midbrain/Pons GABAergic Neurons in Mice*. J Neurosci, 2018. **38**(47): p. 10080-10092.
306. Yamaguchi, T., W. Sheen, and M. Morales, *Glutamatergic neurons are present in the rat ventral tegmental area*. Eur J Neurosci, 2007. **25**(1): p. 106-18.
307. Yamaguchi, T., et al., *Mesocorticolimbic glutamatergic pathway*. J Neurosci, 2011. **31**(23): p. 8476-90.
308. Dobi, A., et al., *Glutamatergic and nonglutamatergic neurons of the ventral tegmental area establish local synaptic contacts with dopaminergic and nondopaminergic neurons*. J Neurosci, 2010. **30**(1): p. 218-29.
309. Wang, H.L., et al., *Rewarding Effects of Optical Stimulation of Ventral Tegmental Area Glutamatergic Neurons*. J Neurosci, 2015. **35**(48): p. 15948-54.
310. Sakurai, T., M. Mieda, and N. Tsujino, *The orexin system: roles in sleep/wake regulation*. Ann N Y Acad Sci, 2010. **1200**: p. 149-61.
311. Qiu, M.H., et al., *Basal ganglia control of sleep-wake behavior and cortical activation*. Eur J Neurosci, 2010. **31**(3): p. 499-507.
312. Qiu, M.H., et al., *The Role of Nucleus Accumbens Core/Shell in Sleep-Wake Regulation and their Involvement in Modafinil-Induced Arousal*. Plos One, 2012. **7**(9).
313. Lazarus, M., et al., *How do the basal ganglia regulate sleep-wake behavior?* Trends in Neurosciences, 2012. **35**(12): p. 723-732.
314. Johnson, S.W. and R.A. North, *Opioids excite dopamine neurons by hyperpolarization of local interneurons*. J Neurosci, 1992. **12**(2): p. 483-8.
315. Omelchenko, N. and S.R. Sesack, *Ultrastructural analysis of local collaterals of rat ventral tegmental area neurons: GABA phenotype and synapses onto dopamine and GABA cells*. Synapse, 2009. **63**(10): p. 895-906.
316. Sanchez-Catalan, M.J., et al., *The antero-posterior heterogeneity of the ventral tegmental area*. Neuroscience, 2014. **282**: p. 198-216.
317. Olson, V.G., et al., *Regulation of drug reward by cAMP response element-binding protein: evidence for two functionally distinct subregions of the ventral tegmental area*. J Neurosci, 2005. **25**(23): p. 5553-62.
318. Schmidt, E.F., et al., *BAC transgenic mice and the GENSAT database of engineered mouse strains*. Cold Spring Harb Protoc, 2013. **2013**(3).
319. Yang, C.F., et al., *Sexually dimorphic neurons in the ventromedial hypothalamus govern mating in both sexes and aggression in males*. Cell, 2013. **153**(4): p. 896-909.
320. Krashes, M.J., et al., *Rapid, reversible activation of AgRP neurons drives feeding behavior in mice*. J Clin Invest, 2011. **121**(4): p. 1424-8.
321. Klugmann, M., et al., *AAV-mediated hippocampal expression of short and long Homer 1 proteins differentially affect cognition and seizure activity in adult rats*. Mol Cell Neurosci, 2005. **28**(2): p. 347-60.
322. Truett, G.E., et al., *Preparation of PCR-quality mouse genomic DNA with hot sodium hydroxide and tris (HotSHOT)*. Biotechniques, 2000. **29**(1): p. 52, 54.

323. Tononi, G. and C. Cirelli, *Modulation of brain gene expression during sleep and wakefulness: a review of recent findings*. *Neuropsychopharmacology*, 2001. **25**(5 Suppl): p. S28-35.
324. Terao, A., et al., *Region-specific changes in immediate early gene expression in response to sleep deprivation and recovery sleep in the mouse brain*. *Neuroscience*, 2003. **120**(4): p. 1115-24.
325. Wisden, W., et al., *Differential expression of immediate early genes in the hippocampus and spinal cord*. *Neuron*, 1990. **4**(4): p. 603-14.
326. Hunt, S.P., A. Pini, and G. Evan, *Induction of c-fos-like protein in spinal cord neurons following sensory stimulation*. *Nature*, 1987. **328**(6131): p. 632-4.
327. Morgan, J.I. and T. Curran, *Role of ion flux in the control of c-fos expression*. *Nature*, 1986. **322**(6079): p. 552-5.
328. Morgan, J.I., et al., *Mapping patterns of c-fos expression in the central nervous system after seizure*. *Science*, 1987. **237**(4811): p. 192-7.
329. Rusak, B., et al., *Light-Pulses That Shift Rhythms Induce Gene-Expression in the Suprachiasmatic Nucleus*. *Science*, 1990. **248**(4960): p. 1237-1240.
330. Jacobson, L., F.R. Sharp, and M.F. Dallman, *Induction of fos-like immunoreactivity in hypothalamic corticotropin-releasing factor neurons after adrenalectomy in the rat*. *Endocrinology*, 1990. **126**(3): p. 1709-19.
331. Pompeiano, M., C. Cirelli, and G. Tononi, *Immediate-early genes in spontaneous wakefulness and sleep: expression of c-fos and NGFI-A mRNA and protein*. *J Sleep Res*, 1994. **3**(2): p. 80-96.
332. O'Hara, B.F., et al., *Immediate early gene expression in brain during sleep deprivation: preliminary observations*. *Sleep*, 1993. **16**(1): p. 1-7.
333. Lee, E.H. and S.L. Huang, *Role of lateral habenula in the regulation of exploratory behavior and its relationship to stress in rats*. *Behav Brain Res*, 1988. **30**(3): p. 265-71.
334. Menard, J. and D. Treit, *Lateral and medial septal lesions reduce anxiety in the plus-maze and probe-burying tests*. *Physiol Behav*, 1996. **60**(3): p. 845-53.
335. Swanson, L.W. and W.M. Cowan, *The connections of the septal region in the rat*. *J Comp Neurol*, 1979. **186**(4): p. 621-55.
336. Henn, V., R.W. Baloh, and K. Hepp, *The sleep-wake transition in the oculomotor system*. *Exp Brain Res*, 1984. **54**(1): p. 166-76.
337. Chase, M.H., et al., *Intracellular potential of medullary reticular neurons during sleep and wakefulness*. *Exp Neurol*, 1981. **71**(1): p. 226-33.
338. Vertes, R.P., *Selective firing of rat pontine gigantocellular neurons during movement and REM sleep*. *Brain Res*, 1977. **128**(1): p. 146-52.
339. Jones, B.E., *Elimination of paradoxical sleep by lesions of the pontine gigantocellular tegmental field in the cat*. *Neurosci Lett*, 1979. **13**(3): p. 285-93.
340. Chan, S.H. and J.Y. Chan, *Correlated effects of clonidine on single-neuron activities in the gigantocellular reticular nucleus, arterial pressure and heart rate in the cat*. *Neurosci Lett*, 1983. **40**(2): p. 139-43.
341. Scammell, T.E., et al., *An adenosine A2a agonist increases sleep and induces Fos in ventrolateral preoptic neurons*. *Neuroscience*, 2001. **107**(4): p. 653-63.
342. Moruzzi, G., *The sleep-waking cycle*. *Ergeb Physiol*, 1972. **64**: p. 1-165.

Appendices

Preliminary Result Chapter: Exploration of brain regions regulating sleep/wake behaviours by expression of immediate early gene, cFos

Abstract

The Immediate-early genes (IEGs) have been widely used as a marker for neuronal activities. Previous studies have shown that the expression of IEGs is tightly associated with vigilance states[323], especially its gene member, cFos, whose expression can be strongly induced by sleep deprivation[324]. In this **Chapter**, I examined the expression of cFos in mouse brain following short-term (5 hr) sleep deprivation (SD) and 2 hr recovery sleep (RS) after SD to search for any novel brain regions that might be involved in sleep/wake regulation. cFos expression across whole-brain was revealed by immunohistochemistry and then quantified in brain regions that had a statistical difference. SD induced strong expression of cFos in mouse brain and levels of cFos expression were elevated during SD in all five main brain regions, *i.e.* cerebral cortex, hypothalamus, thalamus, cerebellum and pons. The only exception I found in this study is the lateral preoptic nucleus (LPO) of the hypothalamus, which had lesser cFos expression during SD but higher level of expression during RS. Most of the brain regions showing the differences of cFos expression between SD and RS have been reported to be

involved in sleep/wake regulation or its related behaviours. However, there are still a few regions that might need further attention regarding to their roles in sleep/wake regulation, for example, the septal nuclei, bed nucleus of the stria terminalis (BNST), ventral tegmental area (VTA), gigantocellular nuclei, and reticular formation in the brainstem. Based on previous study from our lab[51], I focused on the LPO (**Chapter 2 & 3**) and VTA (**Chapter 4**) for further investigation of their functions in sleep/wake behaviours.

Introduction

Immediate-early genes (IEGs) have been used as a powerful tool for the identification of activated neurons in the mammalian brain[325-328], and after its initial description, cFos mapping was soon applied to studies of vigilance states and circadian timing[80, 127, 329]. IEGs are named because their rapid transcription induced by different extracellular stimulation, not only in neurons but in a wide range of non-neuronal cell types. One of their best-known gene members is c-fos, which shows increased levels of mRNA quickly after a short-time stimulation and the rapid synthesis of its protein product, Fos, can be detected several hours after stimulation. Therefore, the expression of cFos has been used in numerous neuroscientific researches served as a functional marker of brain activity.

The expression of cFos can be induced by environmental, physiological and pharmacological stimulation. There are several advantages of the use of cFos as a functional anatomical marker in the central nervous system for activated neurons: under basal conditions, the expression of cFos is at low level[330]; its response to extracellular stimuli is transient[325]; it is relative easy to detect the expression of c-fos, either by c-fos mRNA or cFos protein; and more importantly, the detection of cFos can be combined with various different markers, such as neuropeptides and anti- and/or retro-grade tracers. As a result, for the neuroendocrine systems, the cFos-based mapping technique can contribute to gather valuable details regarding cellular targets, neuronal pathways and molecular mechanisms through which stimuli to neurosecretory cells are processed.

The idea of homeostatic regulation of sleep is supported by numerous studies of sleep deprivation conducted in both human and animals. Periods of wakefulness trigger a

homeostatic response of increased sleep duration and intensity (δ power, slow wave activity), known as “recovery sleep” that is proportional to the duration of prior wakefulness, both spontaneous and induced by sleep deprivation[115, 116]. It is highly possible that the mechanisms of homeostatic regulation and functional consequences of sleep and wakefulness are linked with molecular changes in related brain areas. For example, it could be that short-term sleep deprivation results in compensatory changes in neuronal gene expression that rise the possibility of subsequent sleep.

A downside of cFos expression is that the temporal resolution is poor, in the order of minutes (for transcripts) to hours (for the protein), so its expression cannot be locked precisely to a vigilance state, unless, for example, there is a consolidated block of NREM sleep after sleep deprivation. Nevertheless, a practical use of cFos expression is that if a novel brain region is found to be cFos positive during e.g. sleep deprivation/recovery sleep, the cFos promoter allows the use of genetic activity tagging[51]. By reactivating tagged cells, this method can be used to explore the sufficiency of tagged cell types for e.g. inducing sleep.

The goal of this **Chapter** is to search for any brain regions activated during sleep and wakefulness which have not been fully studied before. A whole-brain cFos mapping was conducted in forced sleep-deprived and sleep-recovered animals. In addition to neuronal marker of brain activity, cFos also served as a transcriptional regulator and therefore may regulate the transcription of numerous downstream genes that could be associated with the homeostatic regulation and the cellular functions of sleep.

Aims and objectives

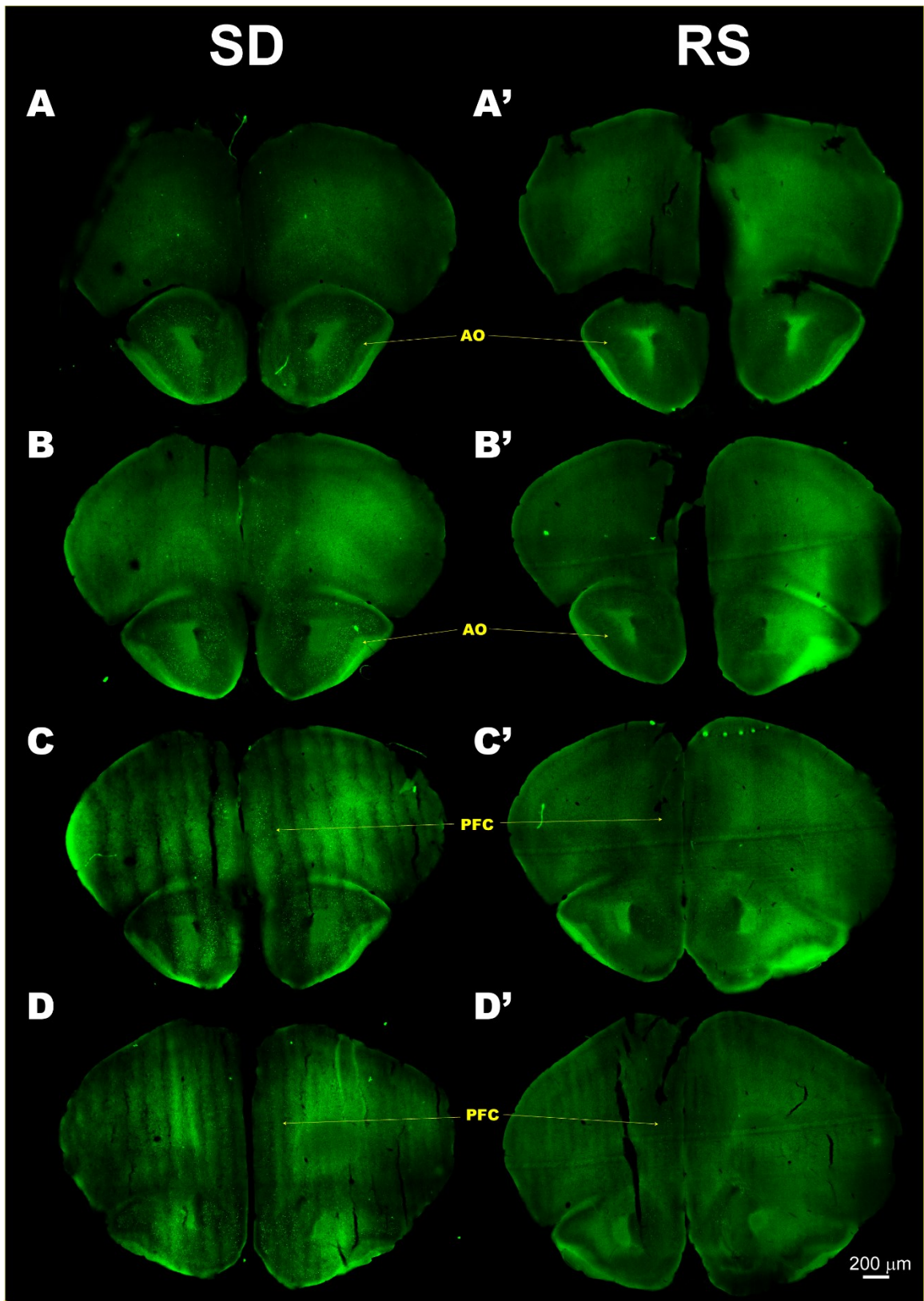
The brain activities in the waking state are different from that in sleep state. To further understand the homeostatic regulation of sleep and its functional consequences, in this

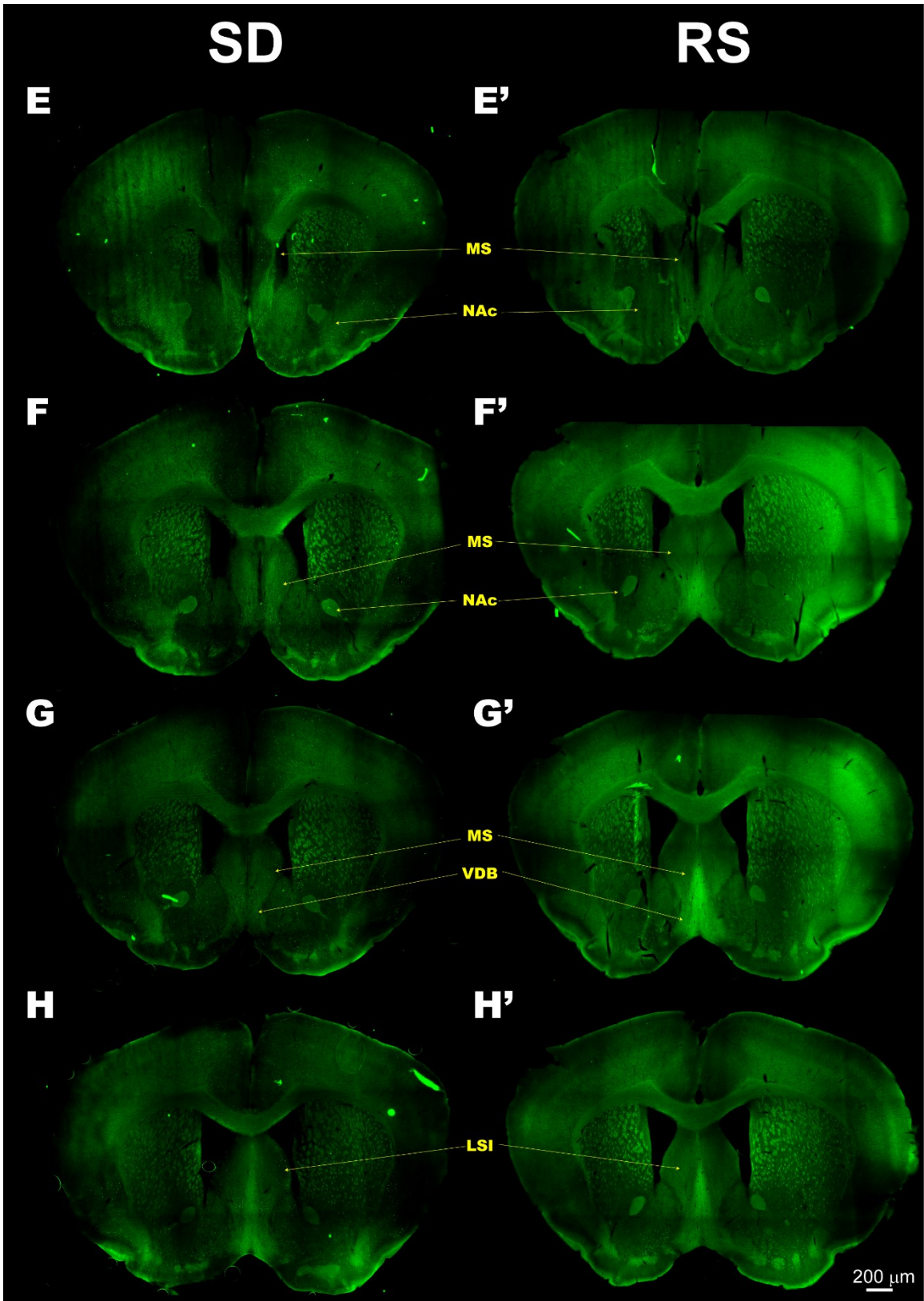
Chapter, I will

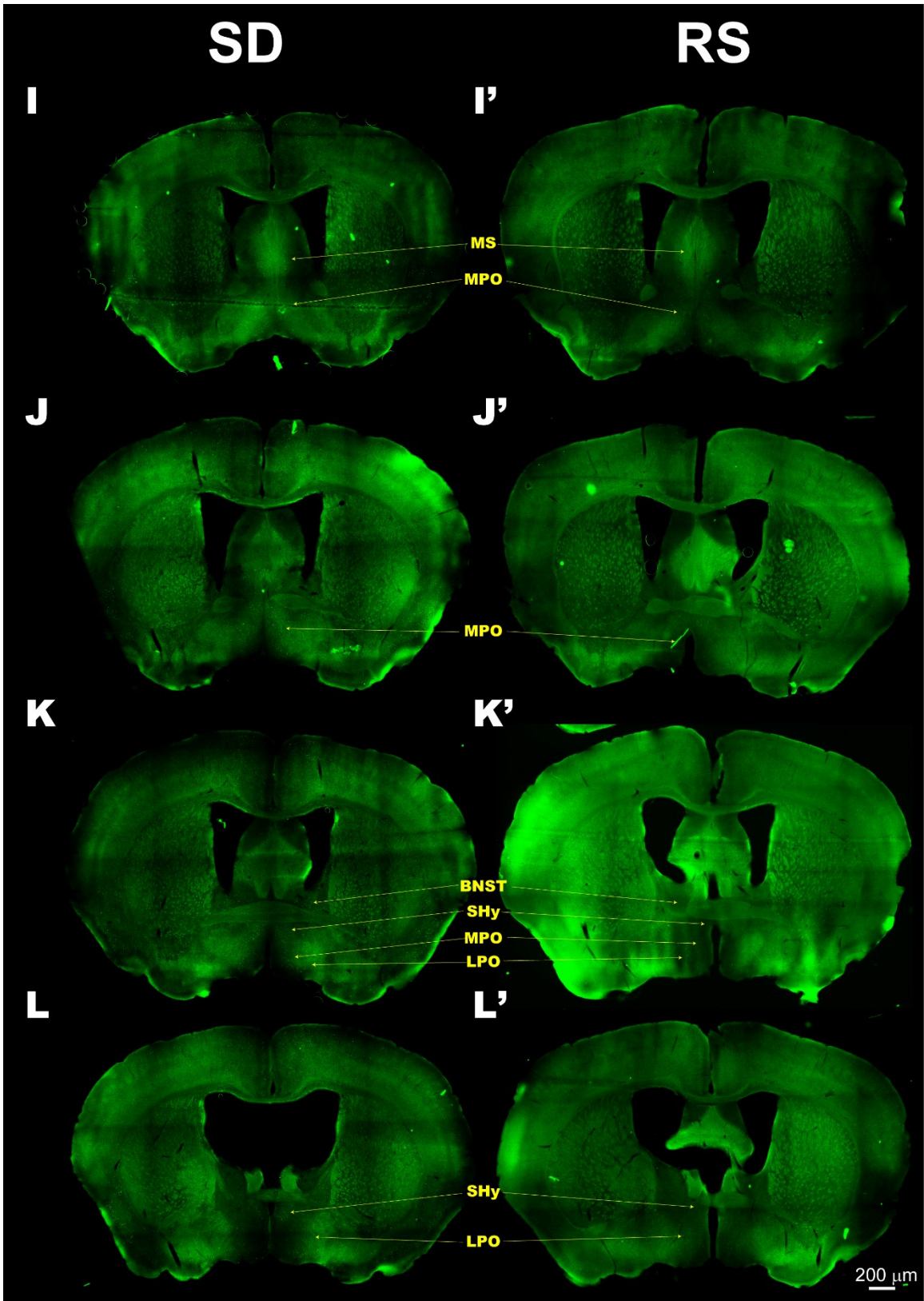
- Map whole-brain activity of both sleep-deprived mice and sleep-recovered mice by the expression of cFos.
- Search for novel brain regions regulating sleep/wake states.

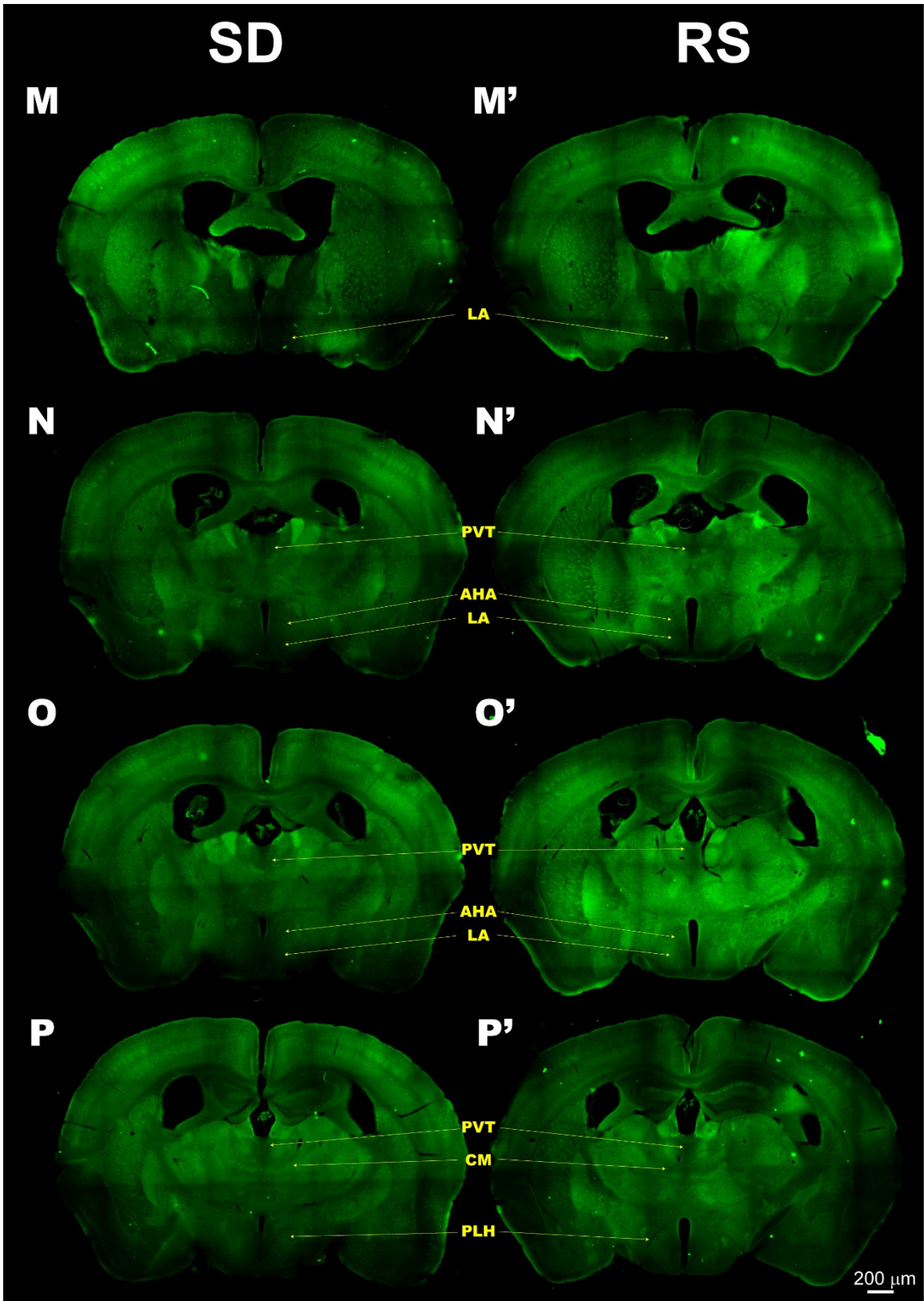
Results

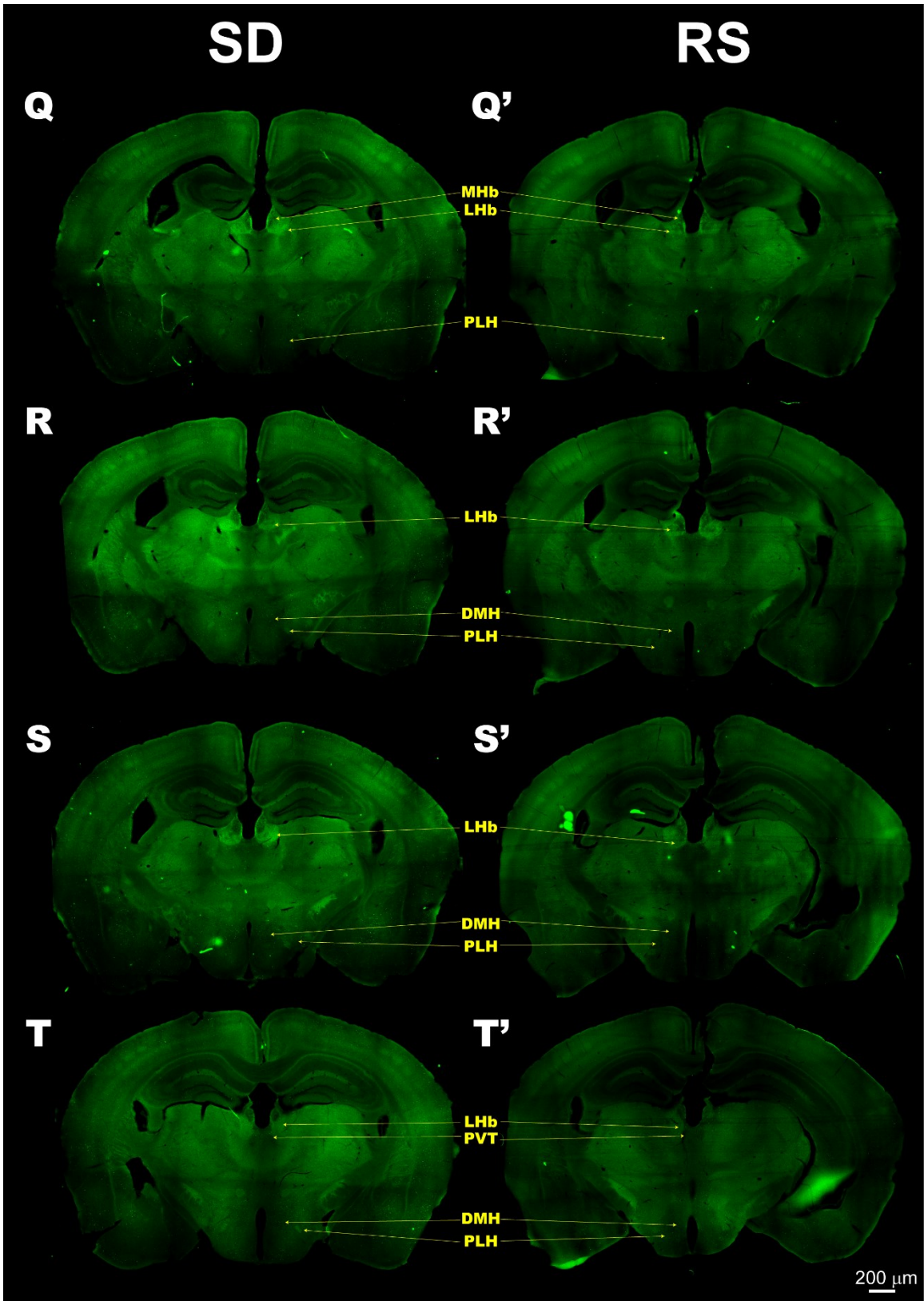
Previous studies have shown that behavioural states can modulate the expression of cFos. In this **Chapter**, in the sleep deprivation (SD) group, mice underwent 5-hour sleep deprivation from ZT0 (the start of the “lights-on” period when the mice have the highest sleep drive) by introducing novel objects or gentle tapping on the cages. At the end of the sleep deprivation (ZT5), mice in SD group were killed and their brains were removed for subsequent immunohistochemistry. In addition to the 5-hour sleep deprivation, mice in recovery sleep (RS) group received a further 2-hour recovery sleep in their home cages. A different group of mice that have the Neurologger 2A on underwent the 5-hour SD and 2-hour RS at the same time as a parallel experiment. Data from the Neurologger 2A showed that mice spent most of the time in sleep during recovery sleep period (data not shown here but detailed EEG results regarding sleep deprivation and recovery sleep have been shown in **Chapter 2**). At the end of the 2-hour recovery sleep (ZT7, 5-hour sleep deprivation plus 2-hour recovery sleep) periods, RS mice were killed and their brains were taken. 40- μ m thick brain sections were sliced across the whole brain and sections from Bregma 2.58 to -7.32 were used for immunohistochemistry against cFos protein. **Figure 5.1** presents representative results from cFos expression in these two experimental conditions for selected brain sections. In SD mice, cFos expression levels were relatively high in most of the brain regions whereas in RS mice, the expression of cFos was low or absent. In general, the cFos expression was more marked in all five main brain regions in SD mice with respect to RS mice, including the cortex, thalamus, hypothalamus, cerebellum, and pons (**Fig. 5.1**).

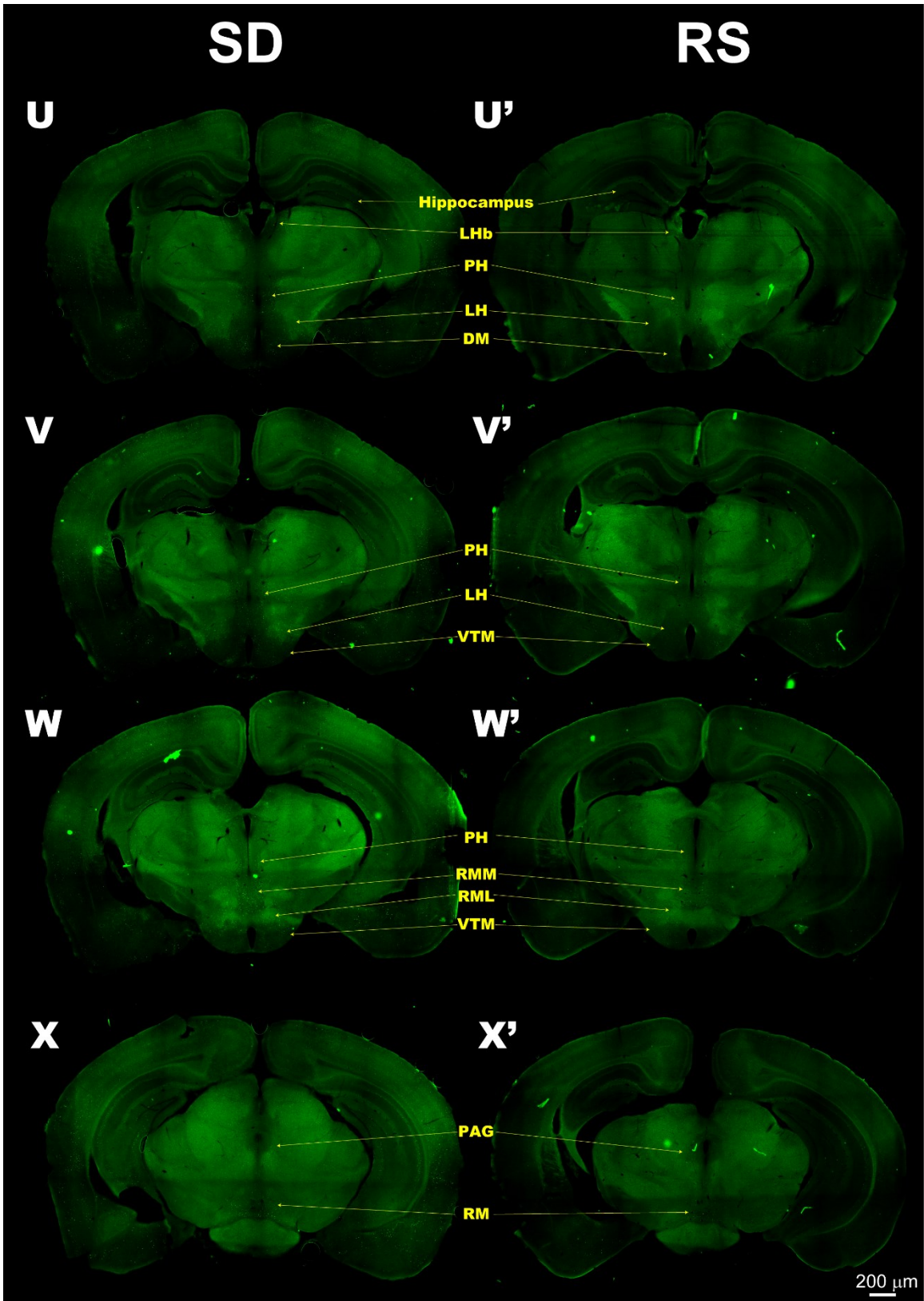


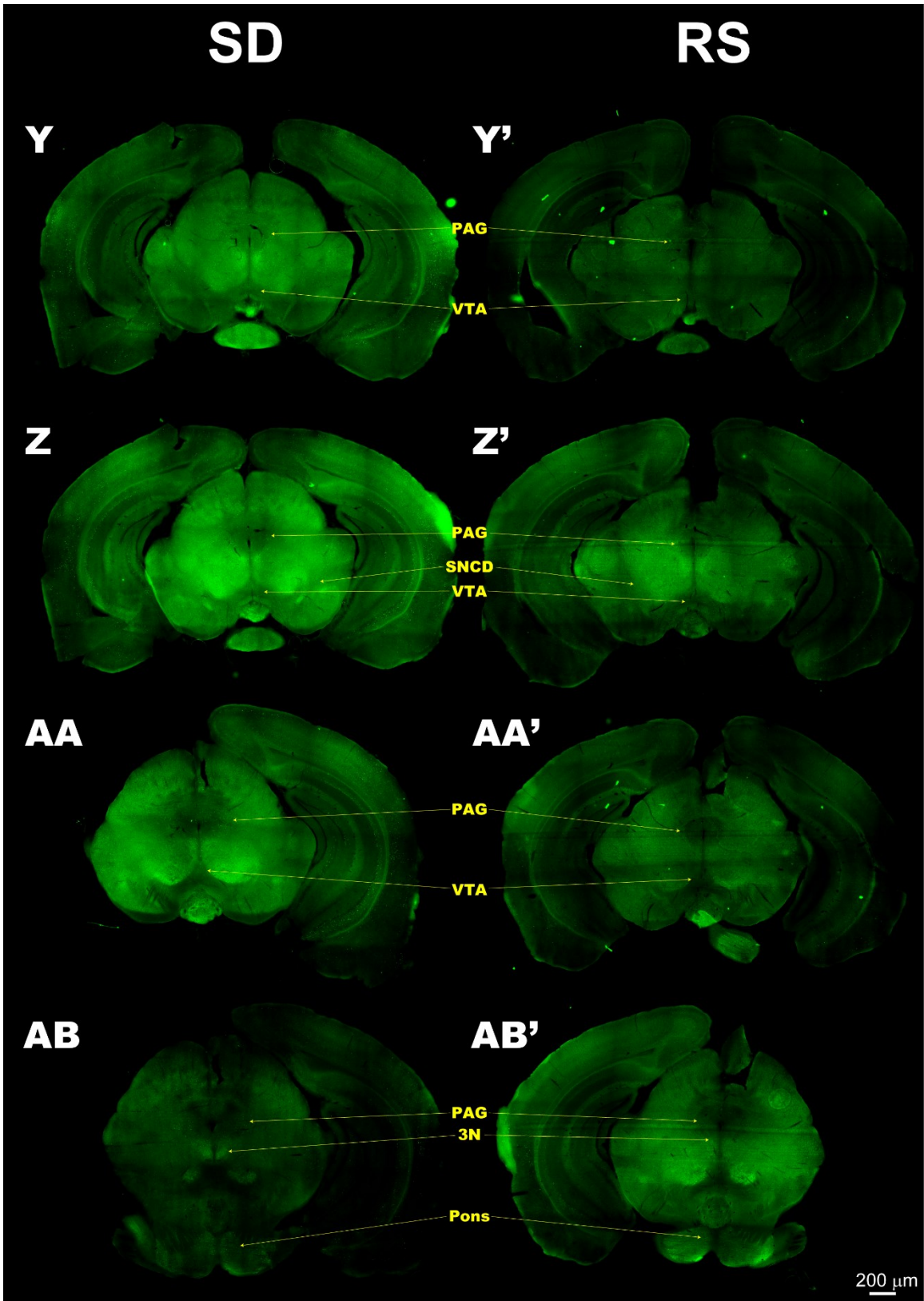


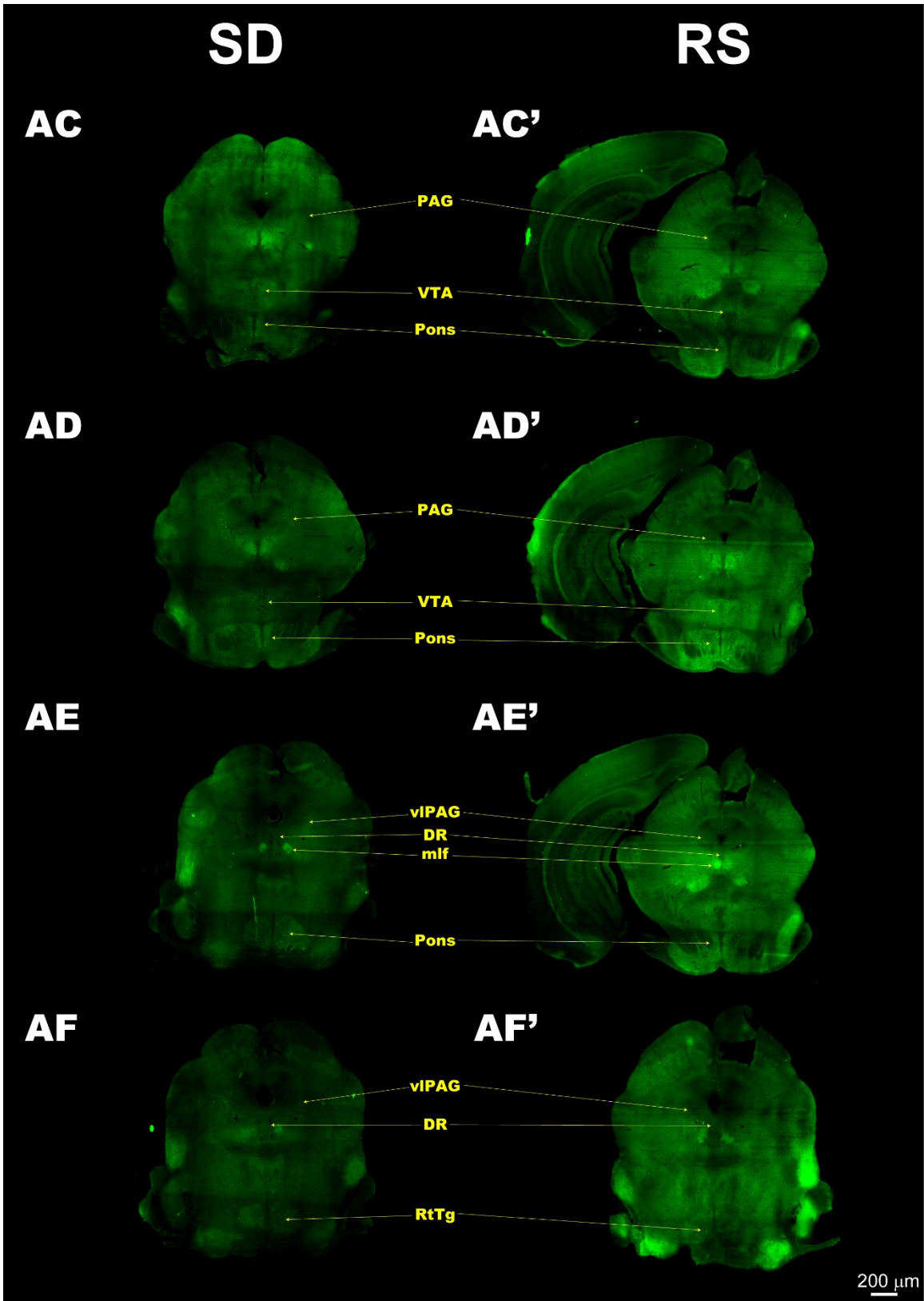


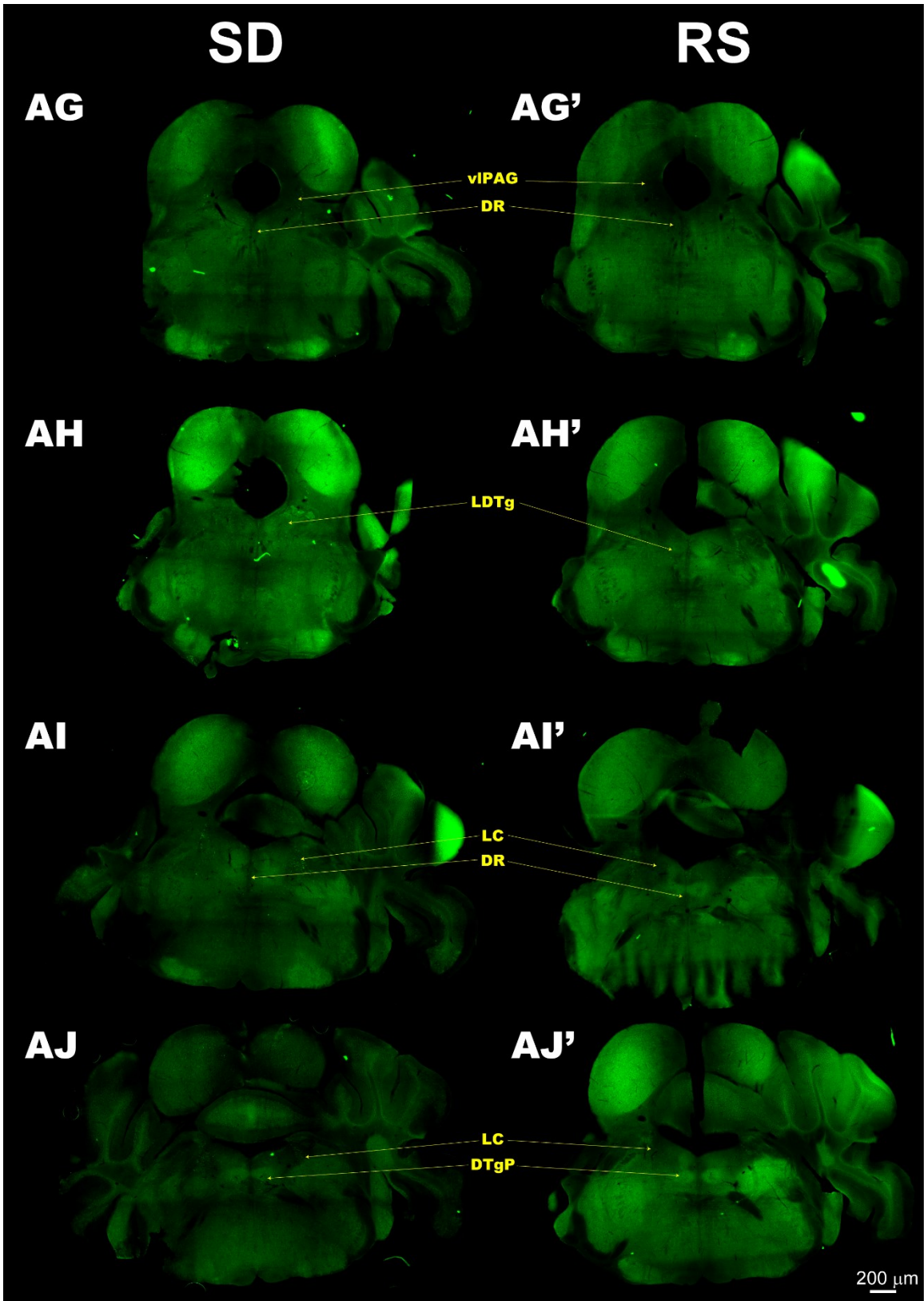












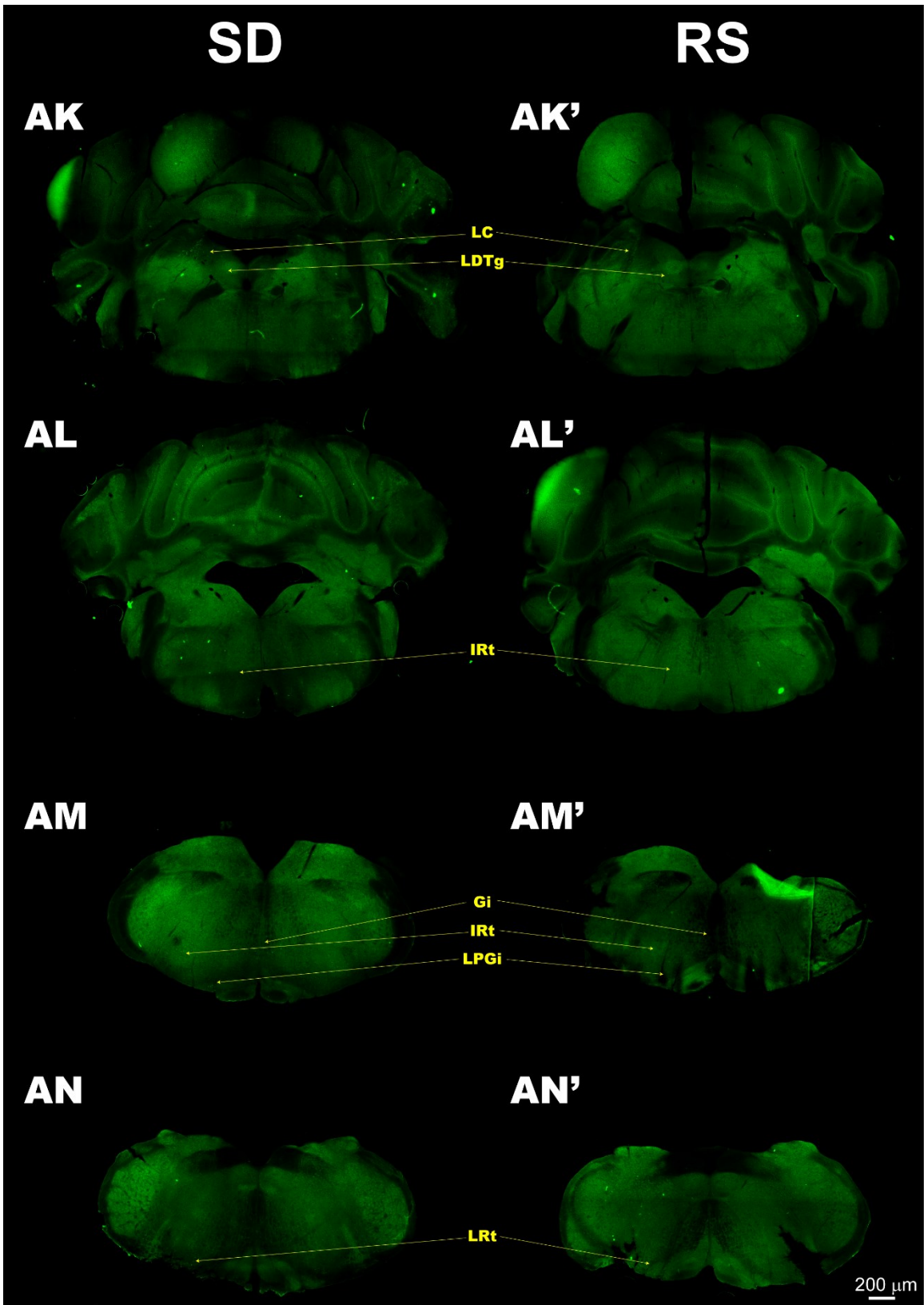
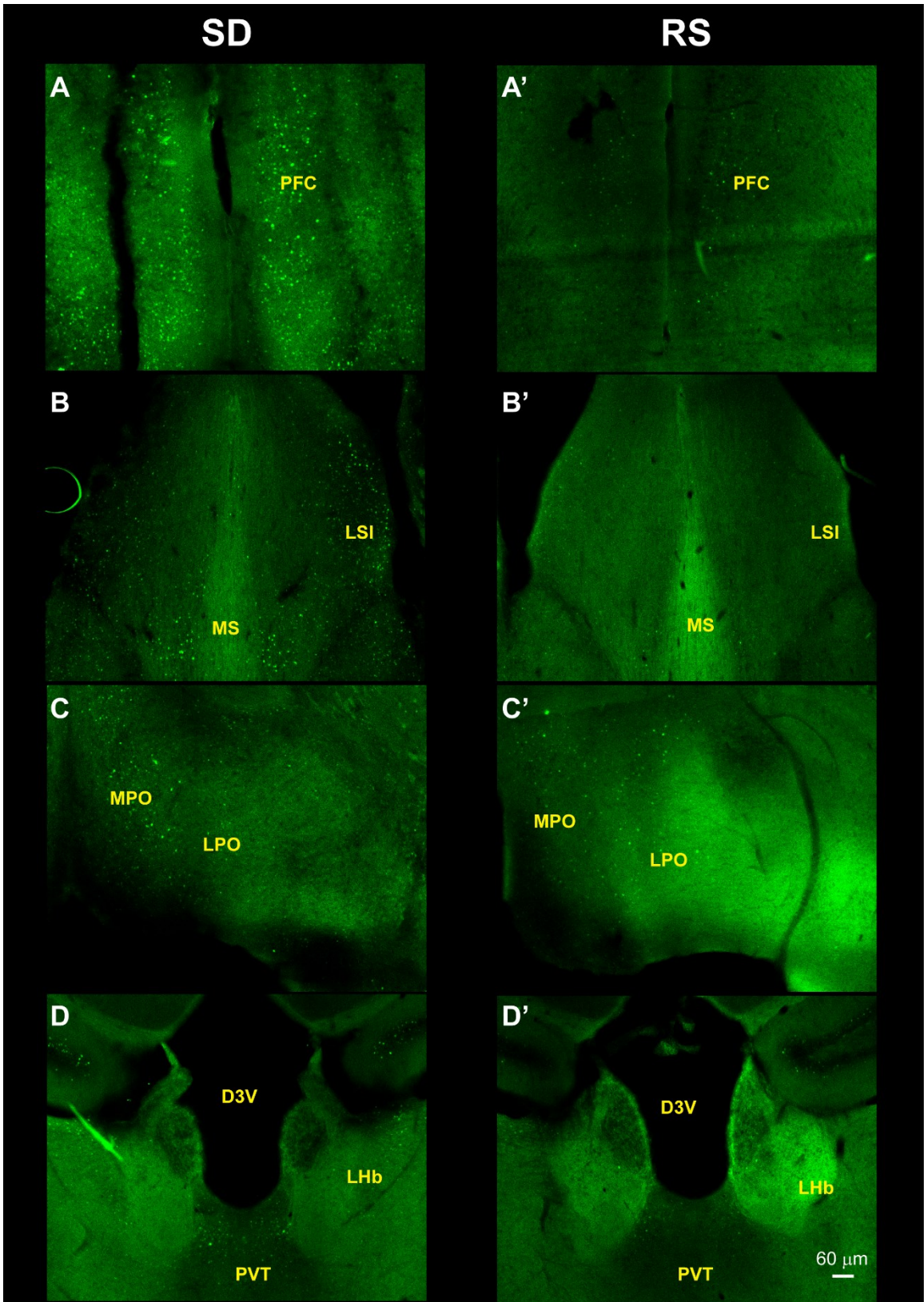


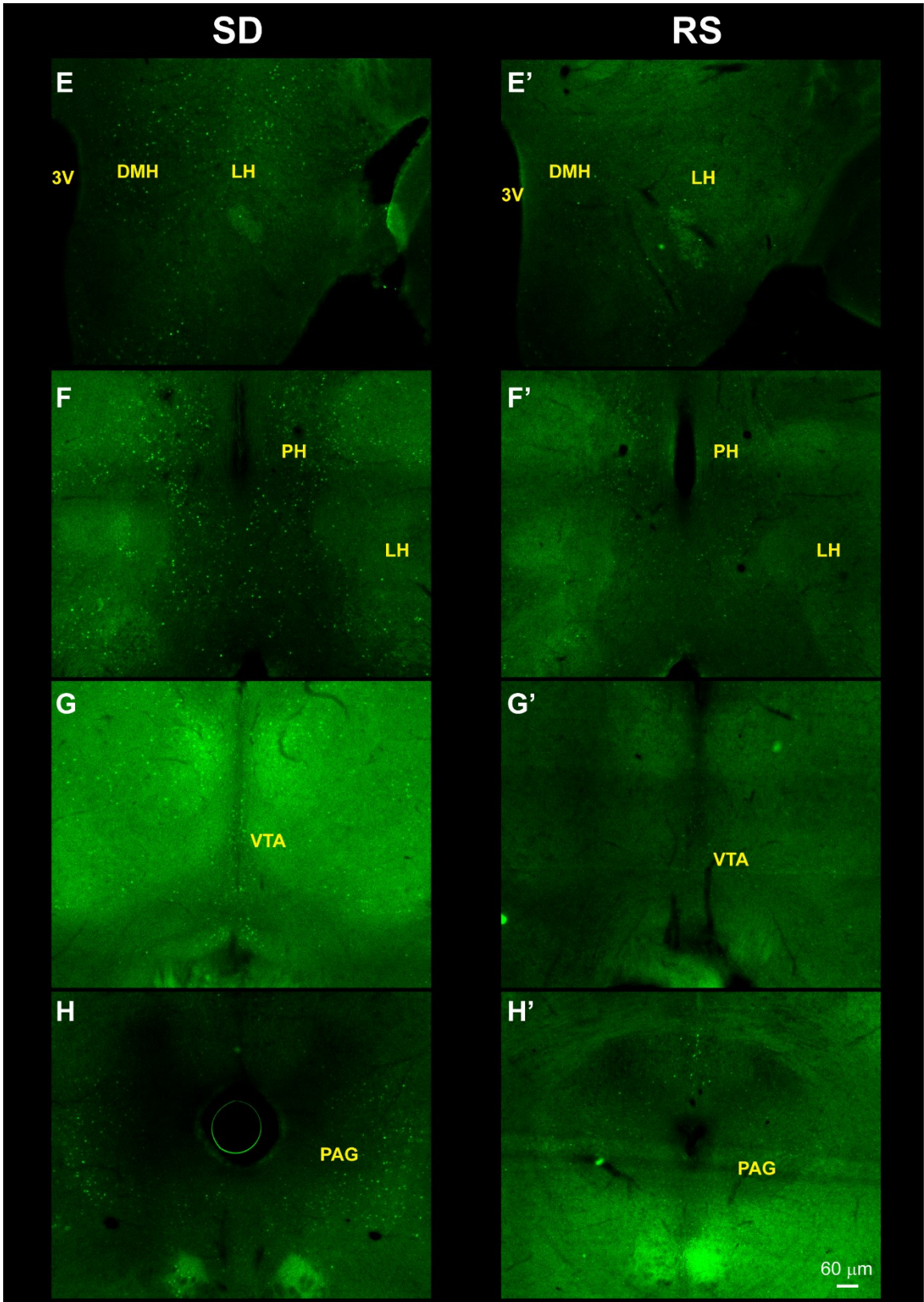
Figure 5.1 Examples of whole-brain cFos expression mapping of 5-hour sleep deprived mice and 2-hour sleep recovered (after 5-hour SD) mice. Immunohistochemistry shows the differential expression of cFos expression in brain sections of a mouse killed after 5-hour sleep deprivation (A-AN) and of a mouse killed after 2-hour recovery sleep following 5-hour sleep deprivation (A'-AN'). In general, all five main brain regions (the cortex, thalamus, hypothalamus, cerebellum, pons) showed strong cFos expression in the SD mice in respect to the RS mice. 3N, oculomotor nuclear complex; AHA, anterior hypothalamic area; AO, anterior olfactory nucleus; BNST, bed nucleus of the stria terminalis; CM, central medial nucleus; DM, dorsomedial nucleus of hypothalamus; DMH, dorsomedial hypothalamus; DR, dorsal raphe; DTgP, dorsal tegmental nucleus; Gi, gigantocellular nucleus; IRt, intermediate reticular nucleus; LA, lateranterior hypothalamic nucleus; LC, locus ceruleus; LDTg, laterodorsal tegmental nucleus; LH, lateral hypothalamus; LHb, lateral habenular nucleus; LPGi, lateral paragigantocellular nucleus; LPO, lateral preoptic nucleus; LRt, lateral reticular nucleus; LSI, lateral septal nucleus; MHb, medial habenular nucleus; MPO, medial preoptic nucleus; MS, medial septal nucleus; NAc, nucleus accumbens; PAG, periaqueductal gray; PFC, prefrontal cortex; PH, posterior hypothalamic area; PLH, posterolateral hypothalamus; PVT, paraventricular thalamic nucleus; RM, retromammillary nucleus; RMM, retromammillary nucleus medial; RML, retromammillary nucleus lateral; sHy, septohypothalamic nucleus; SNCD, s nigra, compact, dors tier; VDB, nucleus of the verticle limb of the diagonal band; vIPAG, ventrolateral periaqueductal gray; VTA, ventral tegmental area; VTM, ventral tuberomammillary nucleus.

Next, I narrowed down to precise brain regions that had statistical differences of the number of cFos-expressing neurons between SD mice and RS mice. A number of brain regions were found to show different patterns of cFos expression between SD and RS mice, most of which had previously been reported to be related with the regulation of sleep-wake cycle. **Figure 5.2** shows representative immunohistochemical images of cFos expression of SD mice (**A-J**) and corresponding images of RS mice (**A'-J'**) and **Figure 5.2 K** summarizes the anatomical brain regions that had statistical significance in cell numbers of cFos positive neurons between SD and RS mice. Red colour indicates animals were subjected to sleep deprivation (SD) and grey indicates animals were allowed to have recovery sleep (RS). In the prefrontal cortex and anterior part of the brain such as medial septal nucleus (MS) and lateral septal nucleus (LSI), there were robust of cFos expression in SD mice (**Fig. 5.2 A, A', B and B'**) and the number of cFos positive neurons in PFC nearly tripled in SD mice (~1,400) compared with RS mice (~550) (**Fig. 5.2 K**). The hypothalamus had several nuclei that showed strong responses to vigilance states in terms of cFos expression, including the medial preoptic nucleus (MPO), dorsomedial hypothalamus (DMH), lateral hypothalamus (LH), and posterior hypothalamic area (PH). All these regions had much stronger cFos expression (**Fig. 5.2 C, C', E, E, F and F'**) and more cFos positive neurons in SD mice compared with RS mice (**Fig. 5.2 K**). However, the only brain region observed to have higher level of cFos expression in RS mice is the lateral preoptic nucleus (LPO) of the hypothalamus, next to the MPO (**Fig. 5.2 C and C'**). The number of cFos positive neurons in the LPO slightly but still significantly increased in the brains of RS mice (~700) in respect to the one of SD mice (~400). Stronger cFos expression was also found

in thalamic and epithalamic area in SD mice. The paraventricular thalamic area (PVT) and its neighbouring lateral habenula (LHb) had elevated level of cFos expression in SD mice (**Fig. 5.2 D and D'**). A large increase in cFos expression of SD mice was also found in brain regions located in the posterior part and brainstem, such as the ventral tegmental area (VTA) (~290 vs. ~80), periaqueductal gray (PAG) (~650 vs, ~150), dorsal raphe (DR) (~300 vs. ~100), locus ceruleus (LC) (~600 vs. ~150), reticular formation (Rt) and paragigantocellular reticular nucleus (Gi) (**Fig. 5.2 G-J, and G'-J'**).

This quantification analysis of cFos expression not only highlighted well-known areas of sleep regulation, but also identified many others of interest. For example, the PVT had a strong cFos expression during SD (~350) but not RS (~100), and later was shown to be important in sleep/wake regulation[89]; the VTA also showed significant differences of cFos expression between SD (~300) and RS (~50) and has been demonstrated to be involved in vigilance state regulation[47, 88, 305] (a detailed discussion has been presented in **Chapter 4**). Nearly all brain regions had higher level of cFos expression in SD mice, with the exception of the LPO of the hypothalamus. The number of cFos positive neurons increased in RS mice. The LPO plays a crucial role in sleep-wake cycle, especially in sleep homeostasis, as well as thermoregulation (a detailed discussion has been presented in **Chapter 2 and 3**).





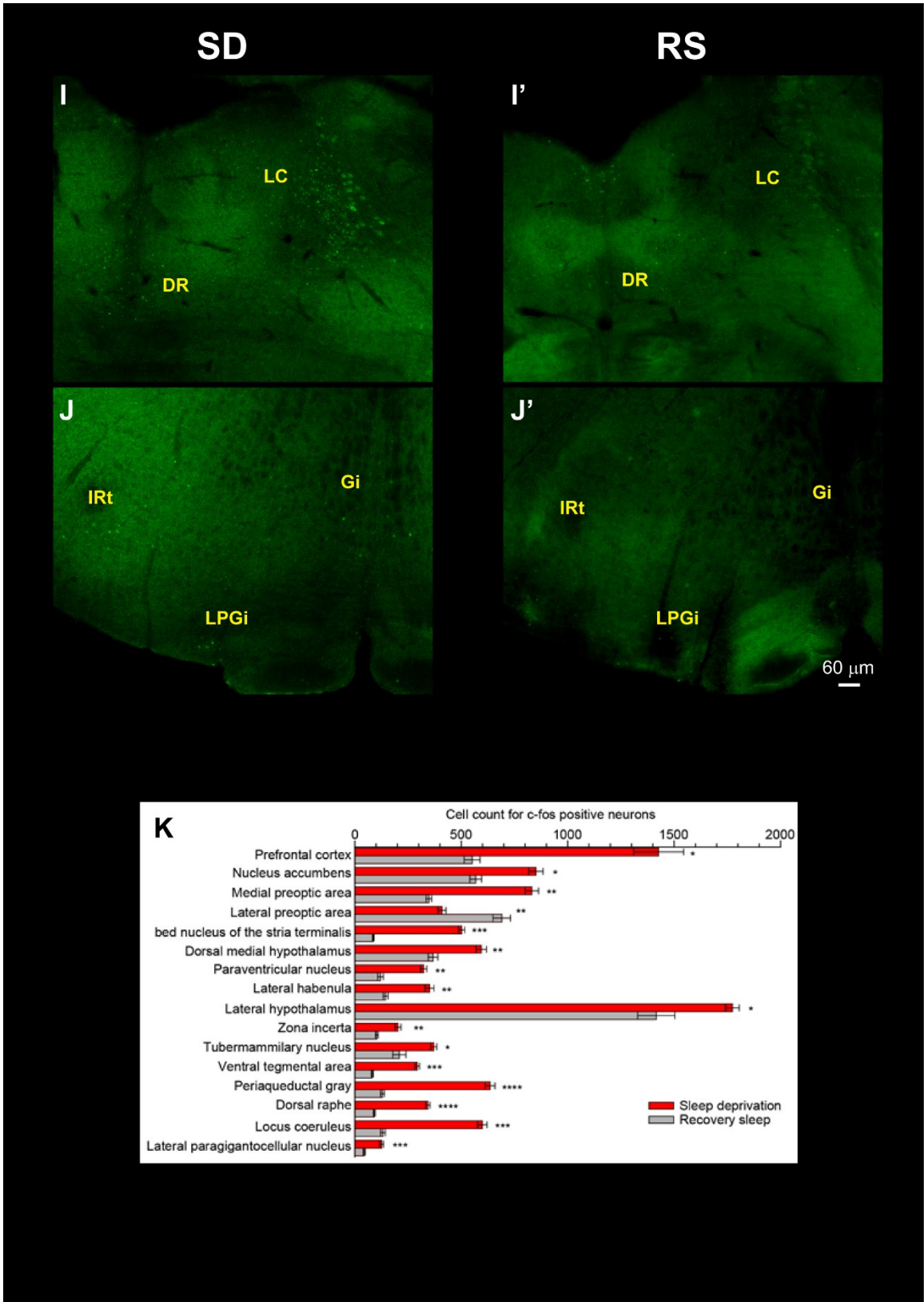


Figure 5.2 Robust expression of cFos has been found in the brain of SD mice compared with the one of RS mice, except for the LPO of the hypothalamus. (A-J and A'-J') Representative immunohistochemistry images of cFos expression in SD mice (A-J) and RS mice (A'-J'). **(K)** Quantification of cFos-positive neurons in anatomical regions with cell count differences in SD and RS mice. Paired two-tailed *t*-test. **P*<0.05, ***P*<0.01, ****P*<0.001, *****P*<0.0001. 3V, the third ventricle; D3V, dorsal 3rd ventricle; DMH, dorsomedial hypothalamus; DR, dorsal raphe; IRt, intermediate reticular nucleus; Gi, gigantocellular nucleus; LC, locus ceruleus; LH, lateral hypothalamus; LHb, lateral habenular nucleus; LPGi, lateral paragigantocellular nucleus; LPO, lateral preoptic nucleus; LSI, lateral septal nucleus; MPO, medial preoptic nucleus; MS, medial septal nucleus; PAG, periaqueductal gray; PFC, prefrontal cortex; PH, posterior hypothalamic area; PVT, paraventricular thalamic nucleus; VTA, ventral tegmental area. All error bars represent the S.E.M..

Discussion

In this **Chapter**, the goal was to search for novel brain regions involving in sleep/wake regulation for further investigation. With the use of the IEG, cFos, I have completed the whole-brain mapping of brain activity in mouse brain after 5-hour sleep deprivation (SD) and SD followed by 2-hour recovery sleep, as well as a detailed quantitative analysis of brain regions with statistical significance of cell number of cFos expression between SD and RS mice.

Results indicate that during SD, there is a widespread activation of cFos expression. The elevated level of cFos in the cerebral cortex, hypothalamus and thalamus are consistent with previous research in both mouse and rat[324, 331]. By contrast, limited changes in cFos expression occurred during RS compared to the widespread activation of cFos during SD. Among the anatomical areas examined, the PFC, LH, VTA, PAG, DR and LC appear to be the most sensitive brain regions to SD, in terms of both the magnitude of the responses and the number of cFos induced. Induction of cFos was greatest in the PAG and DR followed by the VTA, LC and BNST and then the LPGi, consistent with previous observation in both mouse and rat brain after short-term sleep deprivation[324, 332]. Expression of cFos in the lateral hypothalamic area, including the DMH, LH, and PH, also shows strong elevation during SD, implying the role of hypocretin/orexin neurons[310] or arousal promoting GABA neurons[67] in promoting wakefulness. A few other brain regions, such the septal nuclei in the anterior part and the reticular formation and the gigantocellular reticular nuclei in the brainstem, are also found to have higher level of cFos expression in the brains of SD mice in this study. The septal nuclei, which send strong projections to the

LHb, has been demonstrated to be involved in social behaviours and is considered as a pleasure zone in animals[333, 334]. Meanwhile, the septum also projects to the LPO and LH[335], suggesting a potential role in sleep/wake regulation. The reticular formation[336, 337] and gigantocellular reticular nuclei[338, 339] have both been found to associated with sleep/wake behaviours previously, but their neuronal circuitry has not been fully elicited in the molecular level. Apart from sleep/wake regulation, the gigantocellular reticular nuclei also play a role in mediating expiration[340].

The LPO is the only region in which elevated level of cFos expression is found during RS. This observation is consistent with previous studies indicating that the LPO area containing the vLPO is an important sleep generation centre[80, 246]. GABAergic neurons in the LPO send inhibitory projections to the wake-promoting cortex and LH to promote sleep[82].

Both the PVT and VTA show different patterns of cFos expression during SD and RS. They have stronger cFos expression in SD when compared with that during RS, implying a role in possibly promoting wakefulness. Both regions are confirmed to be intensively involved in sleep/wake cycle by our group[47] and other groups[88, 89, 305]. Another brain region of interest is the BNST, which is located just above the PO, not only expressed strong cFos signal in SD mice, as also found by Zhang et al.[51], but also has elevated level of cFos expression after administration of the adenosine α 2a agonist[341], indicating a potential target for further sleep research.

In addition to providing a detailed whole-brain map of neuronal activation regarding sleep deprivation and recovery sleep, other important implications can be revealed from the demonstration of significant changes in cFos expression during such vigilance states. cFos together with other IEGs may involve in gene expression as third messengers following its induction by neuronal activity. It is possible that sleep/wakefulness-related changes in cFos expression might induce modifications of downstream gene expression subsequently. cFos induction in brain regions previously suggested in sleep/wake regulation may indicate a correlation in the homeostatic regulation of sleep[332]; and in other areas like cortex and hippocampus, elevated level of cFos induction by sleep deprivation may promote molecular changes crucial for restorative functions of sleep[342]. Besides cFos expression, various genes change their expression level in the brain in response to sleep deprivation and sleep. As a result, apart from behaviours, neuronal activity and metabolism, wakefulness and sleep also differ in brain gene expression. Most of the genes unregulated after prolonged wakefulness are demonstrated to be involved in transporters, neurotransmitter receptors, immediate early genes/transcription factors, energy metabolism and others[323], suggesting the arousal state can affect several basic cellular functions of the animal.

However, there are limitations for using cFos as markers of neuronal activation. First, there is slow time course (see **Introduction**). Second, there might be neuronal activation occurring without induction of cFos; or chronically activated neurons do not express markers of neuronal activation. Some brain regions highly involving in sleep/wake regulation are not revealed by current cFos mapping, like the newly discovery PIII nucleus.

Apart from these limitations, cFos mapping still can be used as an extremely powerful technique. Nevertheless, although a few regions appear to be potentially involved in sleep/wake regulation as showing in **Results** section, the LPO shows its unique feature that has more cFos expression during recovery sleep. Besides, previous study from our lab has demonstrated that the LPO is involved in both sleep homeostasis and $\alpha 2$ adrenergic agonist-mediated sedation[51], therefore, I chose to focus on the function of the LPO in sleep/wake regulation and look at neuronal cell types in the LPO in the **Chapter 2 and 3**. Also, in **Chapter 4**, I had briefly investigated the newly found target, the VTA, based on the results of this **Chapter**, on its role(s) in sleep/wake regulation.

List of publications

- **Ma Y**, Miracca G, Yu X, Harding EC, Miao A, Yustos R, Vyssotski AL, Franks NP, William W. (2019) Galanin neurons unite sleep homeostasis, torpor and alpha2 adrenergic sedation. **Current Biology**, Vol: 29, pages: 1-8
- Yu X, Ba W, Zhao GC, **Ma Y**, Harding EC, Yin L, Wang D, Shi YR, Vyssotski AL, Dong HL, Franks NP, William W. (2019) Dysfunction of ventral tegmental area GABA neurons causes mania-like behavior. **Molecular Psychiatry**. (In review).
- Yu X, **Ma Y**, Harding EC, Yustos R, Vyssotski AL, Franks NP, William W. (2019) Genetic lesioning of histamine neurons increases sleep-wake fragmentation and reveals their contribution to modafinil-induced wakefulness. **Sleep**, Vol: 42(5), zsz031.
- Yu X*, Li W*, **Ma Y**, Tossell K, Harris JJ, Harding EC, Ba W, Miracca G, Wang D, Li L, Guo J, Chen M, Li YQ, Yustos R, Vyssotski AL, Burdakov D, Yang QZ, Dong HL, Franks NP, William W. (2018) GABA and Glutamate Neurons in the VTA Are Major Determinants Governing Vigilance State. **Nature Neuroscience**, Vol: 22(1), pages: 106-119.
- Harding EC, Yu X, Miao A, Andrews N, **Ma Y**, Ye Z, Lignos L, Miracca G, Ba W, Yustos R, Vyssotski AL, Wisden W, Franks NP. (2018) A Neuronal Hub Binding Sleep Initiation and Body Cooling in Response to a Warm External Stimulus, **Current Biology**, Vol: 28, pages: 2263-2273.e4
- Yu X, Ye Z, Houston CM, Zecharia AY, **Ma Y**, Zhang Z, Uygun DS, Parker S, Vyssotski AL, Yustos R, Franks NP, Brickley SG, Wisden W. (2015) Wakefulness Is Governed by GABA and Histamine Cotransmission, **Neuron**, Vol: 87, pages: 164-178.
- Yu X, Zecharia A, Zhang Z, Yang Q, Yustos R, Jager P, Vyssotski AL, Maywood ES, Chesham JE, **Ma Y**, Brickley SG, Hastings MH, Franks NP, Wisden W. (2014) Circadian Factor BMAL1 in Histaminergic Neurons Regulates Sleep Architecture, **Current Biology**, Vol: 24, pages: 2838-2844.